The University of Edinburgh

College of Science and Engineering

School of Chemistry

Combinatorial Polymer Synthesis and Inkjet Printing for Cellular Control and Manipulation

By

Albert Ryszard Liberski

Thesis for the degree of Doctor of Philosophy

February 2009

University of Edinburgh; College of Science and Engineering

AIM OF THE THESIS

Combinatorial Polymer Synthesis and Inkjet Printing for Cellular Control and Manipulation

By Albert Liberski

The opening aim of this thesis was to optimize parameters for the utilisation of inkjet printing in the generation of polymer microarrays. After this was achieved, inkjet printing was used for fabrication of polymer microarrays for high-throughput screening of small molecule polymorphism. In particular, inkjet printing was used for polymer deposition in a microarray format and for the dispensing of small molecules in solution. Crystals formed on polymer spots were screened to record the polymorphism. **(Chapter 1)** Moreover, inkjet printing was applied to perform high-throughput polymerisation. In the *in situ* nanolitre scale polymerisation the homo- and copolymers were fabricated directly in microarray format. **(Chapter 2)** Polymer microarray screening was used to develop a platform for human cornea epithelial cell transfer. In this case, 252 polymers (polyurethanes and polyacrylates) were screened in a culture of cells. A transfer experiment was performed to prove the ability of cells to migrate from the cultivation surface to the target surface. The best polymer was then used to construct a platform suitable for medical use. **(Chapter 3)** Moreover, polymer microarrays were screened to identify polymers suitable for mouse embryonic stem cell adhesion and growth. **(Chapter 4)** Finally, to advance cell patterning in various non-microarray formats a strategy based on preferential cell binding on collagen was applied. Collagen was dispensed by inkjet printing in patterns laid-down by a bitmap converter. The second strategy to advance cell patterning was based on a simple masking process. A laser printer was used to generate a non-binding surface on glass. This simple concept delivered excellent results. **(Chapter 5)**

Declaration of Authorship

The research described in this thesis was carried out by the author under the supervision of Prof. Mark Bradley at the University of Edinburgh between March 2005 and March 2008. No part of this thesis has been previously submitted at this or any other university for any other degree or a professional qualification. Part of this work has been published in the scientific literature and part of it is protected under patent:

Patent:

Copolymers Suitable for Use in Corneal Bandages –WO 2008/047169 A2

Articles:

Liberski, A.; Tizzard, G. J.; Diaz-Mochon, J. J.; Hursthouse, M. B.; Milnes, P.; Bradley, M. *J. Comb. Chem.* **2008**, 24-27.

Zhang, R.; Liberski, A.; Khan, F.; Diaz-Mochon, J. J.; Bradley, M. *Chem. Commun.*, **2008**, 1317-1319

Liberski, A.; Zhang, R.;Bradley, M. *Chem. Commun.*, **2009**, *334-336*

Liberski, A.; Zhang, R.;Bradley, M. *JALA.*, **2009**, *In Press, Accepted Manuscript: JALA-D-09-00005R1*

Signed: ....[redacted]....

Date: 27.05.2009

Acknowledgements

Firstly, I would like to thank Professor Mark Bradley for the trust he placed in me throughout my research project and for granting me the independence to explore my own scientific ideas. I would also like to thank Ilika Technologies and the Engineering and Physical Sciences Research Council who sponsored my research.

Also, I would like to thank members of the ASL laboratory in Southampton (Dr. Hitoshi Mizomoto, Dr. Jeff Thaburet), for the synthesis of many of the polymers that I have used. I thank collaborators who have supported us in developing polymer microarrys for small molecule polymorphism studies; in Southampton, Dr. Graham Tizzard and Prof. Mike Hursthouse. Special thanks are due to Dr. Pallavi Deshpande and Prof. Sheila MacNeil for fruitful collaboration in developing polymeric platforms for use in corneal bandages. In Edinburgh, I would particularly like to thank Dr. Meng Li who personally trained me in the culture of embryonic stem cells and allowed me to use her facilities.

I would like to thank everybody in the Bradley Group, and in particular Dr. Guilhem Tourniaire who answered complicated technical questions and trained me, Dr. Rong Zhang for friendship and for being the best collaborator ever. These acknowledgments would not be completed without thanking Lois Alexander, Adam Belsom, Graham Henderson, Frank Bowler who participated in improving the quality of this thesis by providing language corrections.

I would like to thank all my friends back home, from Poznań and Edinburgh who shared with me moments of broken spirits and moments of glory. Especially, I would like to thank friends and colleagues from the Edinburgh University Amateur Boxing Club and the Leith Victoria Amateur Boxing Club for sharing the second passion of my life (after Chemistry) and Edinburgh Tango Society for sharing the third one.

I would like to thank my family (Mum, Sister and parents-in-law) for their support throughout my education and specially for helping to take care of my affairs back home. Finally, I would like to thank my lovely wife Aleksandra (Ola), for her enormous support and absolutely crucial help until the very end of this thesis.

Contents

Figures

Tables

Abbreviations

AFM	atomic force microscope
AIBN	2,2'-azobis(2-methylpropionitrile)
BSA	bovine serum albumin
BSE	bovine spongiform encephalitis
CBM	carbamazepine
cDNA	complementary deoxyribonucleic acid
Coll1	collagen type I
Cy	cyanine
DMEM	dubelcco's modified Eagle's medium
DMSO	dimethyl sulfoxide
DoE	design of experiment
EC	extracellular
FACS	fluorescence-activated cell sorting
FBS	fetal bovine serum
FN	fibronectin
GMEM	glasgow's modified Eagle's medium
HCEC	human cornea epithelial cells
HT	high-throughput
LIF	leukaemia inhibitor factor
MALDI	matrix assisted laser desorption/ionisation-mass spectrometry
M-EPI	epithelial cell media
mESC	mouse embryonic stem cells
mRNA	messenger ribonucleic acid
MS	mass spectrometry
PEG	poly(ethylene glycol)
PET	poly(ethylene terephthalate)
PMDS	polydimethylsiloxane
PXRD	powder X-ray diffraction
RAFT	reversible addition–fragmentation chain transfer
ROP	ring opening polymerisation
ROY	2-[(2-nitrophenyl)amino]-3-thiophenecarbonitrile
SD	standard deviation
SEC	size exclusion chromatograph
SMA	sulfamethaxazole
SNP	single nucleotide polymorphisms
TCP	tissue culture plastic
TFCS	(tridecafluoro-1,1,2,2-tetrahydrooctyl)dimethylchlorosilane

General introduction

The projects presented in this thesis are all based on microarray format surface modification by the development and application of a variety of printing techniques. The employed printing techniques included inkjet printing, contact printing and heat transfer printing.

Inkjet printing relies on technology commonly used in desktop printers, where small drops of a solution are deposited without contact between the dispensing device and the substrate. The advantages of this system over contact printing and heat transfer printing are the control of the quantities of liquid delivered, gentle deposition (enabling printing on soft substrates) and the fact that a wide range of spot sizes can be obtained. The piezo jet is based on rapid dimensional change of a piezoelectric material which generates a pressure wave to eject a droplet from the nozzle. In this system, liquid delivery can be performed, generating several hundred spots in one second, due to the unique capabilities of this piezo material. The size of the spot generated is related to the diameter of the nozzle and substrate properties; it can be increased by delivering several drops in the same position. In **Chapter 1**, inkjet printing was used for hydrophobic patterning of glass slides followed by polymer deposition in a microarray format and the dispensing of small molecules in solution. Hydrophobic patterning has been developed *via* inkjet mediated dispensing of sucrose solution onto glass slides into the grids. After drying, sucrose was used as a mask during hydrophobic glass surface modification and subsequently removed. The polymer solutions were inkjet printed into the hydrophilic features using carefully optimised printing parameters. Prepared polymer microarrays have been used for screening crystal polymorphism by inkjet mediated imprinting of solutions of small molecules onto the polymer features. This method allowed three different small molecule compounds to be screened (in triplicate) with 128 polymers and required just milligram quantities of compound and 27 μg of each polymer per array, while generating large numbers of polymorphic forms.

In **Chapter 2**, inkjet printing was also used for the direct fabrication of polymer microarrays, consisting of either discrete features or a matrix of inter-crossed lines. In this approach, the individual monomers and initiator solutions in organic solvents were inkjet printed through a film of oil, thereby allowing the rapid generation of a broad range of co-polymers, while solving the problem of selective monomer evaporation. Both polymer microarray and polymer grids were used to identify polymers suitable for cell binding and growth.

Moreover, inkjet printing was also utilized in **Chapter 5** as a method for advanced biomaterials and cellular patterning. A desired image (picture) was converted from an image file into a coordinate file for printing in this defined pattern,. The printer was used to ink different solutions and print them at the required positions with high accuracy. HeLa and mouse embryonic stem cells (mES-Oct4) both adhered and proliferated only on the patterned areas of the slides. To further evaluate this method, cellular gradients were produced that showed a constant decrease in cellular attachment proportional to the amount of collagen printed. These findings improve upon those previously reported, indicating that the precision of biomolecular deposition using this approach has been greatly advanced.

In the contact printing technique the solution is deposited onto the substrate by contact from a transfer device (pin) and this is where the technique has gained its name. Contact printing requires a high precision X-Y-Z robot that holds one or more pins. The factors affecting this printing are a combination of the chemical and physical properties of the solution(s), pin(s), the printing parameters of the robot (number of depositions and speed) and the substrate type. In **Chapter 3** and **Chapter 4**, contact printing was used for the fabrication of polymer microarrays with density up to 512 polymer features per slide. Polymer microarrays were subsequently used for cellular screening. Automatic analyses of the microarrays allowed for quick identification of polymers that facilitate growth of human cornea epithelial cells **(Chapter 3)** and mouse embryonic stem cells **(Chapter 4)**. Subsequently the polymers that supported cellular adhesion were spin coated onto coverslips in order to perform scale up experiments and validate results of the microarray analysis. Finally, in **Chapter 3** active polymers were coated onto a

coverslip by spin coating and human corneal epithelial cells were cultivated on them. Coverslips were inverted and placed onto limbal- imitate surfaces, the coverslips were then removed and cells which were left on limbal-mimicking surfaces were counted. The polymer that facilitated transfer of the largest amount of cells was used to develop a platform for cell transfer.

The final section of **Chapter 4** involved the flow cytometric analysis of mouse embryonic stem cells harvested from a coverslip, to investigate cell polymer interactions.

Heat transfer printing is the main printing technique for printing coloured images, *e.g.* words on T-shirts, caps, bags, ski boards, etc. It is the process used to transfer ink from a carrier (PET foil) to the receiving surface (glass). The ink is transferred when heat and pressure is applied to the carrier. The advantage of heat transfer printing methods over the other methods reported in this thesis is that this utilises widely available tools, such as laser printers and hot plates. In **Chapter 5** the heat transfer printing technique was applied to the patterning of glass slides with cytophobic polymers; this was subsequently used for cell patterning with resolution down to 25 nm. In the first phase the desired pattern was printed onto a colour laser transparency (the carrier) using a standard office based laser printer. The patterns on the carrier were transferred to the glass via heating. In the second phase the patterned glass slide was used for cell patterning. Seeded cells were observed to be successfully restricted on the unmasked glass surface; in this way, cell patterning was performed. Increasing the incubation time of the patterned cells allowed the formation of shaped stem cell continuums that were detached from the patterned glass substrate. Moreover, this free standing cell film, placed on tissue culture plastic with medium, attached to the bottom of the dish and the cells proliferated.

Chapter 1 : Screening for small molecule polymorphs on polymer microarrays

1.1 Polymorphism

The way in which compounds crystallise has been the subject of study for many centuries, the classic example being tartaric acid. Tartaric acid has been known since ancient times as a natural by-product of grape juice fermentation and is found as a deposit of white crystals inside wine barrels.[1] Early in the nineteenth century the French scientist Jean Baptiste Biot discovered that crystals of the tartaric acid could rotate the plane of polarised light.[2] It was also found that *natural* tartaric acid could rotate the plane of polarized light, but not when prepared synthetically. Pasteur explained this behaviour when he manually separated the L and D crystals forms (this phenomena was later named "chirality" by Lord Kelvin in 1873).[2]

Polymorphism has been enunciated by McCorne[3] "as a solid crystalline phase of a given compound resulting from the possibility of at least two different arrangements of the molecules of that compound in the solid state".

The phenomenon of polymorphism is a very old issue in chemistry. In the nineteenth century (before the development of spectroscopic and X-ray crystallographic methods) the properties of solids were a crucial aspect for the identification of materials and crystallisations were performed with great attention to detail in order to obtain characteristic morphologies and physical properties such as interfacial angle, colour, melting point, indices of refraction and taste (*e.g.* Schorlemmer 1874,[4] Senechal 1990,[5] Kahr and McBride 1992).[6] The huge amount of information about crystallisation protocols also included polymorphism and between 1906-1919 Groth published a five-volume compendium about crystallisation and solid properties which covered more than 10000 compounds.[7] For example Groth reported two different types of crystals of 4-methyl benzophenone. His discovery was based on the different melting ranges of 58-59 °C and 54-55 °C, which he had measured for two different crystal habits of this compound (crystal morphology such as needle, prism). Polymorphism of 4-methyl

benzophenone was confirmed by Kutze in 1996 by X-ray diffraction methods.[8] Examples of well-known compounds for which new polymorphic forms have been discovered, after many years of work, include maleic acid (120 years after it was first crystallised)[9] and aspirin,[10] confirming McCrone's often quoted pronouncement "the number of forms known for a given compound is proportional to the time and money spent in research on that compound."[11]

Statements by Findlay (1951) "polymorphism is now recognized as a very frequent occurrence indeed",[12] Buerger and Bloom (1937) "polymorphism is an inherent property of the solid state and that it fails to appear only under special conditions",[13] and Sirota (1982)" polymorphism is now believed to be characteristic of all substances, its actual non-occurrence arising from the fact that a polymorphic transition lies above the melting point of the substance or in the area of yet unattainable values of external equilibrium factors or other conditions providing for the transition"[14] indicate that polymorphism is not the exception, but the rule. In fact instances of polymorphism must always be considered when solid materials are developed and manufactured into products under conditions that may vary (sometimes unintentionally).[15] That means that polymorphism of many products (or components of the products) is in general out of control. This issue is also important when growing crystals of proteins.[16]

The phenomenon of polymorphism is a current focal point in the area of crystallisation. This arises because of two main considerations; firstly in terms of patent law, new crystal forms of a solid compound can be considered as innovations and can be protected as intellectual property (this crucial issue has promoted the intense search for new polymorphs). Secondly, and of more practical consideration, is the fact that specific crystal forms can alter the dissolution rate of a compound[17] and thus, the pharmacokinetics of any drug are partially determined by the specific crystal form, an issue that also supports the patentability of a polymorph.[15,18]

"One high profile case of polymorphism was ritonavir, a peptidomimetic drug used to treat HIV-1 infection and introduced in 1996. In 1998, a lower energy, more stable polymorph (form II) appeared, causing slowed dissolution of the marketed dosage form

and compromising the oral bioavailability of the drug. This event forced the removal of the oral capsule formulation from the market."[15]

Traditional methods of discovery and selection of polymorphic forms usually involve the variation of crystallisation parameters such as temperature and solvent[19] and current high-throughput screens generally rely on variation of these parameters. For example, Cima reported a polymorph screen consisting of 2,000 experiments carried out with just 2 g of the active pharmaceutical ingredient.[54] However, most of documented cases of polymorphism have been discovered by accident rather than through systematic research. This opens a large field of new systematic methods for developing conditions which trigger polymorphism. Common awareness among chemists of the phenomenon of polymorphism does not change the fact that conditions and methods are required to generate the various polymorphic forms and the properties they will exhibit are still a challenge for researchers.

Recently, fewer than 5% of compounds in the Cambridge Structural Database were reported to be polymorphic.[20] Therefore new developments in high-throughput platforms for primary polymorph screening would be a valuable tool for the discovery of, as yet, uncharacterized forms. The substrates upon which crystals grow play a pivotal role in allowing selective growth. For example, calcium carbonate crystal growth can be easily "tuned" by interaction with different surfaces,[21-24] allowing a range of specific structures to be generated. (**Figure 1.1**)

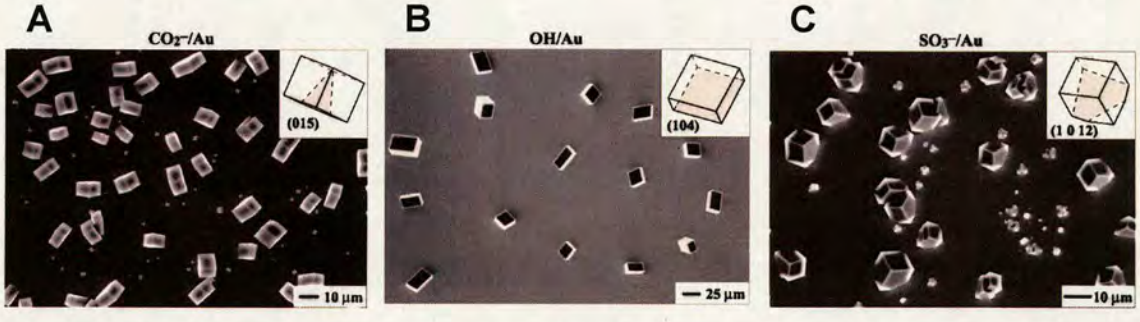

Figure 1.1 *Scanning electron micrographs showing the face-selective nucleation of calcium carbonate crystals mediated by self assembly monolayers (HS-X-R) supported on gold: (A) R=CO_2^-/Au; (B) R=OH/Au; (C) R=SO_3^-/Au.*[21]
Reproduced with permission (copyright ACS, 1999).

Organic compounds, however, are often difficult to tune because their "packing" is much more temperamental than inorganic compounds.[19,25]

The ability to control nucleation of crystal growth in biological[26] and synthetic[27] environments by structured organic surfaces has driven a number of studies on oriented crystallisation of organic and inorganic materials using functionalized polymer surfaces.[28-30]

Growth of a given polymorph is expected to depend on the complementarity between the heteronucleating surface and the crystal nucleus. Employing a library of surfaces is aimed at diversification of the functional groups and spacing of these groups. This hypothesis was confirmed by experiments in which a library of heteronuclear centres was drawn from polymers in order to control polymorphism of acetaminophen and carbamazepine.[19,25] In the case of polymer-assisted heteronucleation however, it is not known whether the polymer itself acts as the heteronuclear centre or whether the polymer acts solely as a scaffold which orders the way heteronuclear centres grow on one another.[31]

In the approach presented here, control over specific factors involved in the crystallisation processes such as concentration and temperature were used, but the main variable was the surface upon which crystallisation occurred. It is widely recognized that the majority of crystallisations occurring on a laboratory scale are the result of heterogeneous nucleation.[32] The nature of the interactions between the polymer and the compound under investigation are not understood and it is not possible to predict the specific polymorphic form generated by crystallisation on any specific polymeric support. The technique developed here provides a tool to better understand these types of interactions, as well as reducing the amount of material needed to carry out a "full polymorphic screen". The approach developed used polymer microarrays onto which solutions of small-molecules were applied and allowed to crystallise and which, because of the size of the arrays, required only tiny amounts of solution. The resultant crystals underwent direct characterization on the microarray by optical and Raman microspectroscopy (Raman spectroscopy has been proven to be a valid tool to differentiate between polymorphic forms).[19] It should be noted that even though

different crystal habit forms were found within the array these did not always correspond to different polymorphic forms according to Raman shifts. In general, organic materials tend to crystallise in less symmetric space groups than inorganic materials, a phenomenon which makes crystal habit a less efficient indicator of different polymorphic forms for organic materials than it is for inorganic materials. For example, the crystallisation of acetaminophen on different polymeric surfaces allowed the generation of many different crystal habits. However Raman spectroscopies revealed that all of them were in fact, the same polymorph. (**Figure 1.2**)

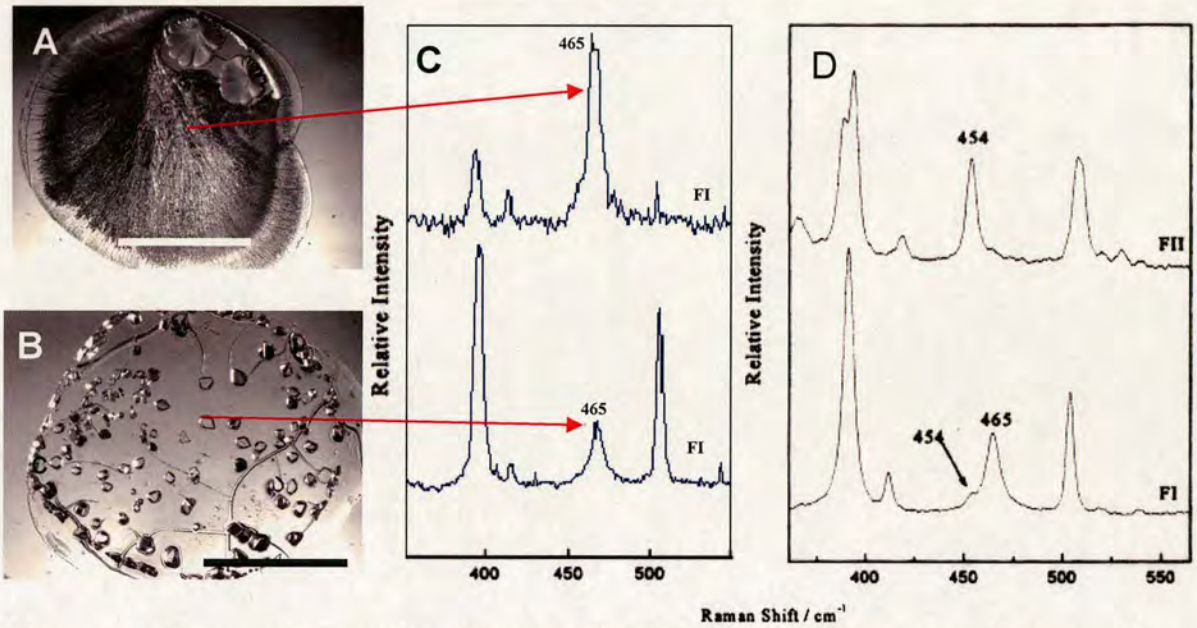

Figure 1.2 *Images of acetaminophen crystals. Crystal habits are a poor indicator of polymorphism in acetaminophen crystals: (A) needles of paracetamol obtained on N-vinylpyrrolidone/vinyl acetate copolymer; (B) prisms of paracetamol obtained on Poly(4,4'-dipropoxy-2,2'-diphenyl propane fumarate); (A) and (B) both represent form I (FI) of paracetamol (scale bars 0.7 mm); (C) Raman shifts observed for crystals; (D) partial Raman spectra of monoclinic (FI) (bottom) and orthorhombic (FII) (top) paracetamol reference samples. Figure "D" is reproduced with permission[33] (copyright Elsevier, 2002).*

So called diagnostic peaks (**Figure 1.2 D**) are chosen with great care since they must allow polymorphisms to be distinguished independently of variations in crystal habits. It was demonstrated that crystal habit can influence the relative intensities of certain peaks.[33] Moreover commonly the assignment of frequencies of the main Raman shift to

a particular stretch is very difficult. In the case of acetaminophen the C–N amide stretching peaks are assigned to frequencies 1566 and 1507 cm^{-1}, the C–C aromatic stretching peaks to1614, 1507, 1442. But, also frequencies corresponding to inter- or intra-molecular interactions at 806, 682 and 1228 cm^{-1} can be distinguished. However, the origin of diagnostic peaks (454 for FII and 465 for FI) is not clear but could be associated with the aromatic system.[33]

1.2 Polymer microarray preparation

The first step in the process consisted fabrication of the polymer microarrays. This approach consisted of hydrophobic patterning of a glass slide into grids, each consisting of 8x16 hydrophilic "features". Slide patterning presented in **Figure 1.3** was performed according to the following protocol. Glass slides were rinsed in solvents to remove manufacturing grease and residues. The glass slides were then etched using oxygen plasma (Europlasma NV Junior System, Frequency: 50 Hz, R_f Power: 100 W). A 30% w/v sucrose masking solution was prepared by dissolving sucrose in water, which was printed on the glass surface using an Autodrop inkjet printing system (Microdrop Technology, Norderstedt, Germany). This consisted of an automated XYZ stage and a stroboscopic video camera. The diameter of the nozzle used was 100 μm. To achieve homogenous patterning the printing parameters needed to be established. The printing voltage identified was 120 V, as a voltage greater than this resulted in drops breaking up to produce satellite drops. A printing voltage lower than 120 V was insufficient for drops to be generated by the printing nozzle. After printing, sucrose masked slides were dried at 60 °C for 1 h and coated with tridecafluoro-1,1,2,2-tetrahydrooctyl)-dimethylchlorosilane (TFCS). Finally, the slides were washed to remove the mask and excess TFCS and dried under a stream of nitrogen.

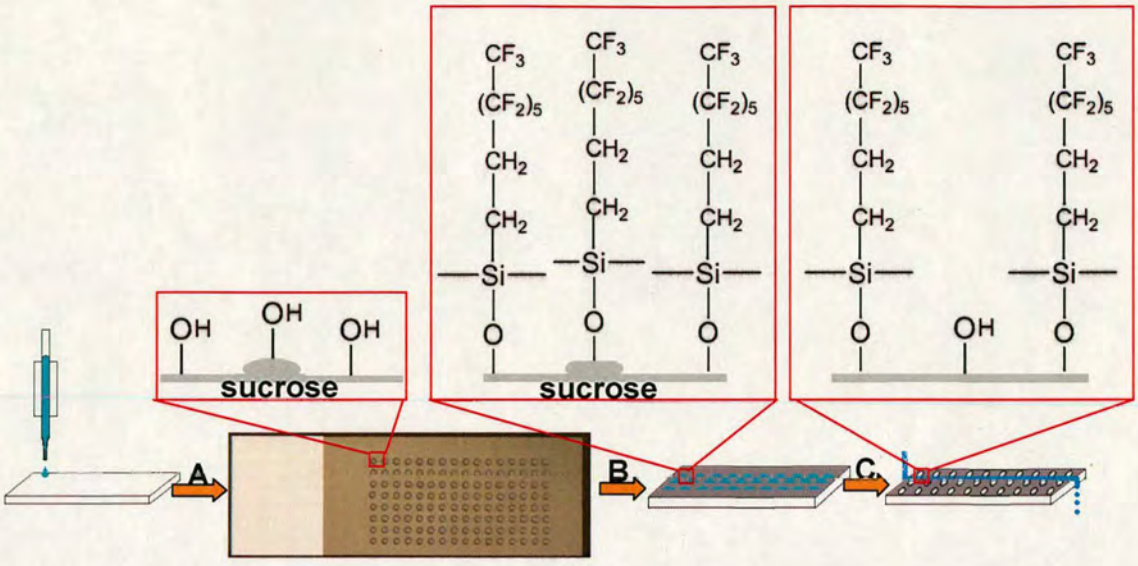

Figure 1.3 *Slide patterning: (A) sucrose mask printing; (B) glass surface modification by tridecafluoro-1,1,2,2-tetrahydrooctyl)dimethylchlorosilane; (C) mask dissolution.*

These modifications allowed the production of hydrophobic surfaces patterned with hydrophilic areas. The use of these patterned surfaces was essential to keep all the polymers within the desired area of the slide.

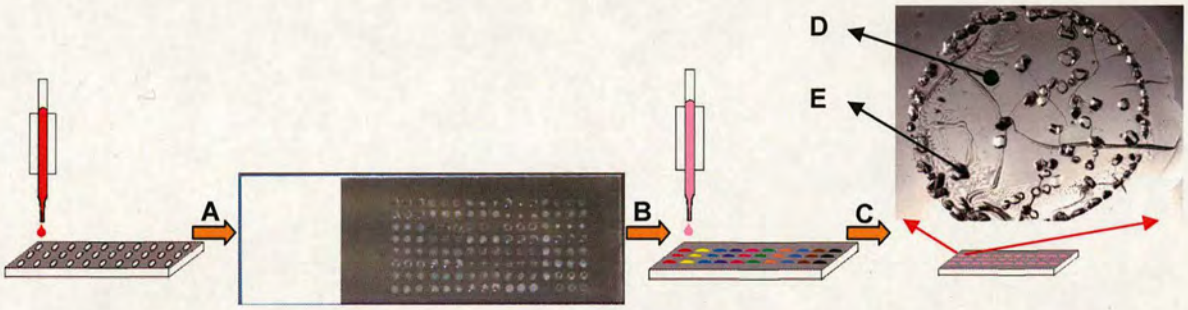

Figure 1.4 *Polymer printing and deposition of small-molecule solutions onto the polymer spots: (A) polymer printing; (B) small molecule solution printing; (C) drying and crystallisation; (D) polymer surface; (E) crystal.*

A specific polymer was deposited by piezo jet-printing 800 drops of each of the polymer solutions onto a defined hydrophilic feature (each drop was ~30 µm in diameter and therefore, ~0.9 µL of a 1% polymer solution was deposited, equating to approximately 9 µg of polymer per spot). (**Figure 1.4**) The polymers used in this study were synthesized or obtained commercially (see sections 6.2.3, 6.2.4 and 6.2.5.). Two

solvents were predominantly used for inkjet printing: NMP and toluene. NMP was the matrix solvent used because it efficiently dissolved the majority of the library of polymers, whereas toluene was used for the more hydrophobic polymers (see section 6.2.5). Each slide thus contained an 8x16 grid giving a total of 128 polymer spots, with the area of each being spot approximately 1.76 mm^2. (**Figure 1.5**)

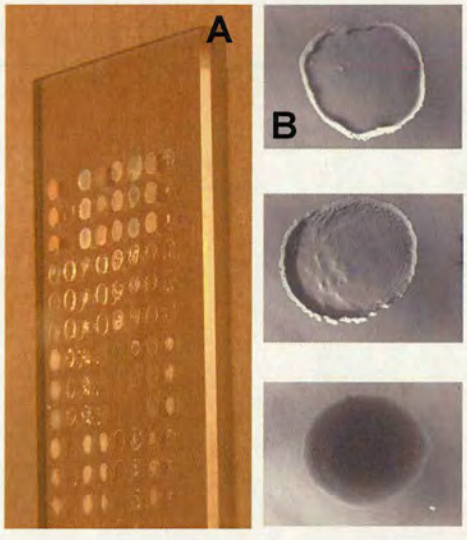

Figure 1.5 *Optical image of a polymer microarray: (A) printed on a masked 27x75 mm glass slide, used for polymorph seeding; (B) images of a single polymer features (~1.5 mm in diameter).*

1.3 Small molecule choices

Three well-known and broadly studied small molecules were used in this study: carbamazepine,[34-38] sulfamethoxazole[39-43] and 2-[(2-nitrophenyl)amino]-3-thiophenecarbonitrile[44-48] (often termed ROY (red/orange/yellow) from the well-known colours of the different polymorphic forms).[49] This choice was the result of the large number of polymorphic studies previously carried out on these compounds, which allowed us to compare our approaches to previous reports.[19,50,51] The literature data for these molecules, showing crystal form and Raman spectra, are provided in **Figures 1.6- 1.8**.

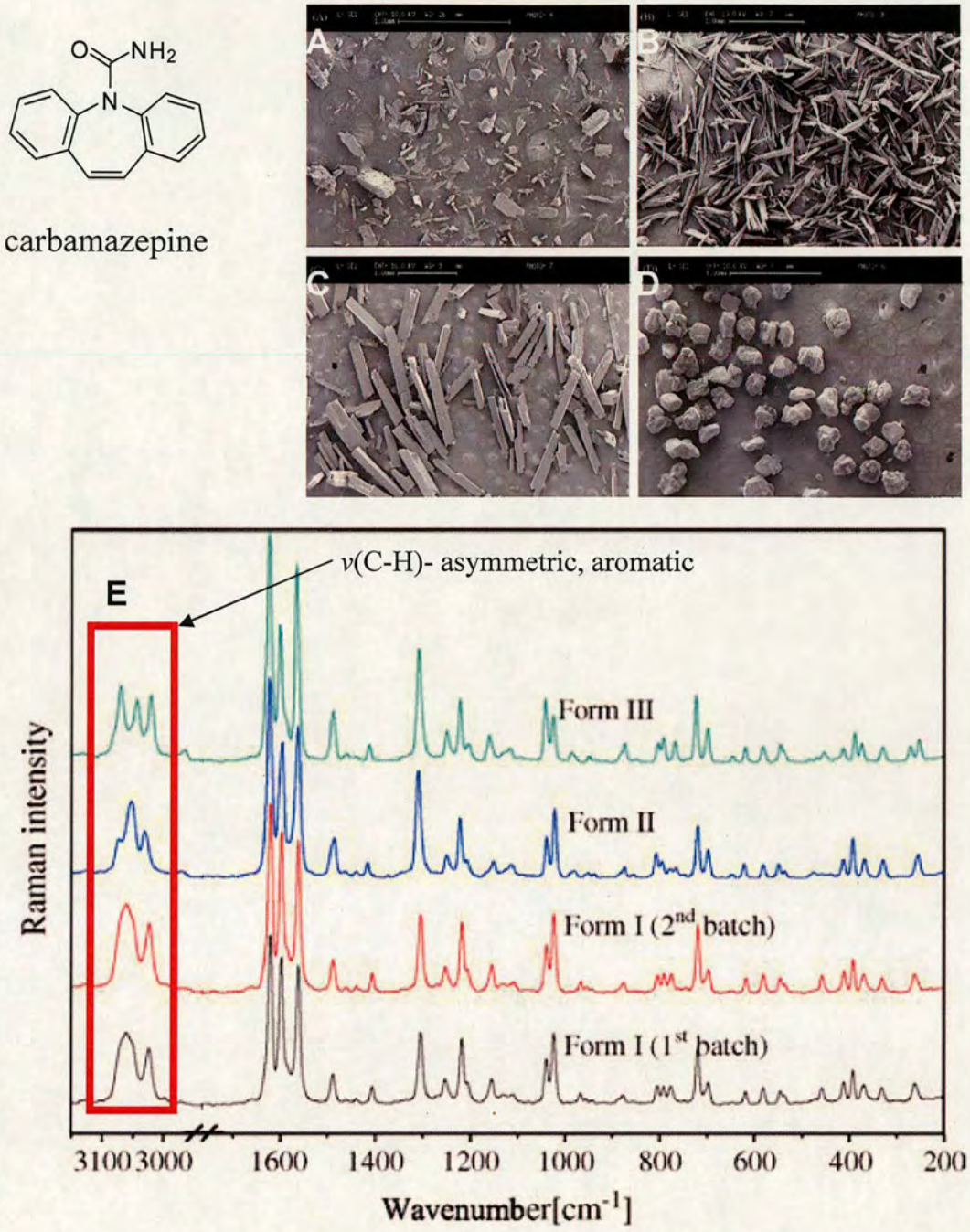

Figure 1.6 *SEM micrographs of carbamazepine polymorphs: (A) and (B) form I; (C) form II; (D) form III (horizontal scale bars: 1.00 mm); (E) Raman spectra of the carbamazepine polymorphs. The red rectangle shows areas of spectral differences between the samples. Reproduced with permission*[51] *(copyright AAPS, 2007).*

Form III	Form I	Approximate description of vibrational mode	Form III	Form I	Approximate description of vibrational mode
3071w		ν(CH) asymmetric, aromatic	874w	876w	ν(C—N—C)
	3061m	ν(CH) aromatic	853vw	853vw	Amide V/δ(C—H) aromatic
3043w		ν(CH) aromatic	723m	720m	ν(C—N—C) 3° amide
3020w	3024m	ν(CH) non-aromatic	691mw	699w	δ aromatic, in-plane/C—H wag *cis*
1624s	1621s	ν(C=C) non-aromatic	646vw	646vw	δ(O—C—N) ring/δ(C=O)
1600ms	1598s	δ(N—H) amide II	620vw	620w	δ(O—C—N) ring
1588m sh		ν(C=C) aromatic	582w	582w	δ(O—C—N)
1565s	1563s	ν(C=C) aromatic	559w		δ aromatic, out-of-plane
1489m	1489m	ν(C=C) symmetric, aromatic/ν(C—N) amide III	546w	546w	δ aromatic, out-of-plane
1460vw	1461vw	δ(CH) aromatic, in-plane	538w sh	537w	δ aromatic, out-of-plane
1439vw	1440vw	ν(C—C) aromatic	486vw	481w sh	
1412w	1406w	ν(C=C)/δ(CH)	469vw	473vw	
1309ms	1305ms	δ(CH) in-plane, non-aromatic	454w	458w	
1273vw	1271w	ν(C=C)	413w	413w	Lattice vibration
1250mw	1253mw	ν(C—N) amide III 1° amide	390m	394mw	Lattice vibration
1221m	1218m	ν(C—N) amide III	375mw	371w	Lattice vibration
1204w	1206w sh	ν(C—C) ring	330w	332w	Lattice vibration
1160w	1155w	ν(C—C) ring/(C—N—C) asymmetric	272w	263w	Lattice vibration
1130w	1133w	ρ(NH_2)	253mw		Lattice vibration
1116w	1110w	ρ(NH_2)	227vw		Lattice vibration
1042m	1040m	δ(C—H) aromatic, in-lane	182ms		Lattice vibration
1025m	1025ms	δ(C—H) aromatic, in-plane	170s	172s	Torsion
987w	968w	ν(C—N)	120s	116vs	Lattice vibration
949w	955vw	δ(C—H) aromatic, out-of-plane	105s		Lattice vibration
936vw	943vw	δ(C—H) aromatic, out-of-plane			
884vw sh	888vw sh	ν(C—N—C) ring, symmetric			

ν: Sretch, δ: bend, ρ: rocking, s: strong, m: medium, w: weak, v: very, sh: shoulder.

Table 1.1 *Assignment of FT-Raman bands to molecular vibration for carbamazepine. Reproduced with permission[51] (copyright AAPS, 2007).*

The most prominent spectral features in the FT-Raman spectra of sulfamethoxazole includes following assignment. The bands that appeared between 800 – 950 cm^{-1} region, could correspond to S–N stretching and C–S out of plane bending. The strong band located within the region 1100–1200 cm^{-1} corresponds to the symmetric SO_2 stretching. In this zone the C–N stretching of the arylamine and C–H in-plane bending of the aromatic ring can also be found. The stretching modes of N–C in the heterocycle ring and C–N between sulfonamide group and heterocycle ring appear in the zone of 1500–1550 cm^{-1}. In the 1550–1650 cm^{-1} region, the NH_2 bending and C=C aromatic ring stretching can be found. Finally, between 3000 and 3100 cm^{-1}, bands due to C–H stretching appear. The specific bands of sulfamethoxazole, corresponding to the methylisoxazole group, are weak bands and, in general, appeared at similar zones to the common bands of sulfonamides. The band observed at 2930 cm^{-1} is assigned to the CH_3 stretch of methylisoxazole, and 841 cm^{-1} can be due to the N–O stretching vibration.[19]

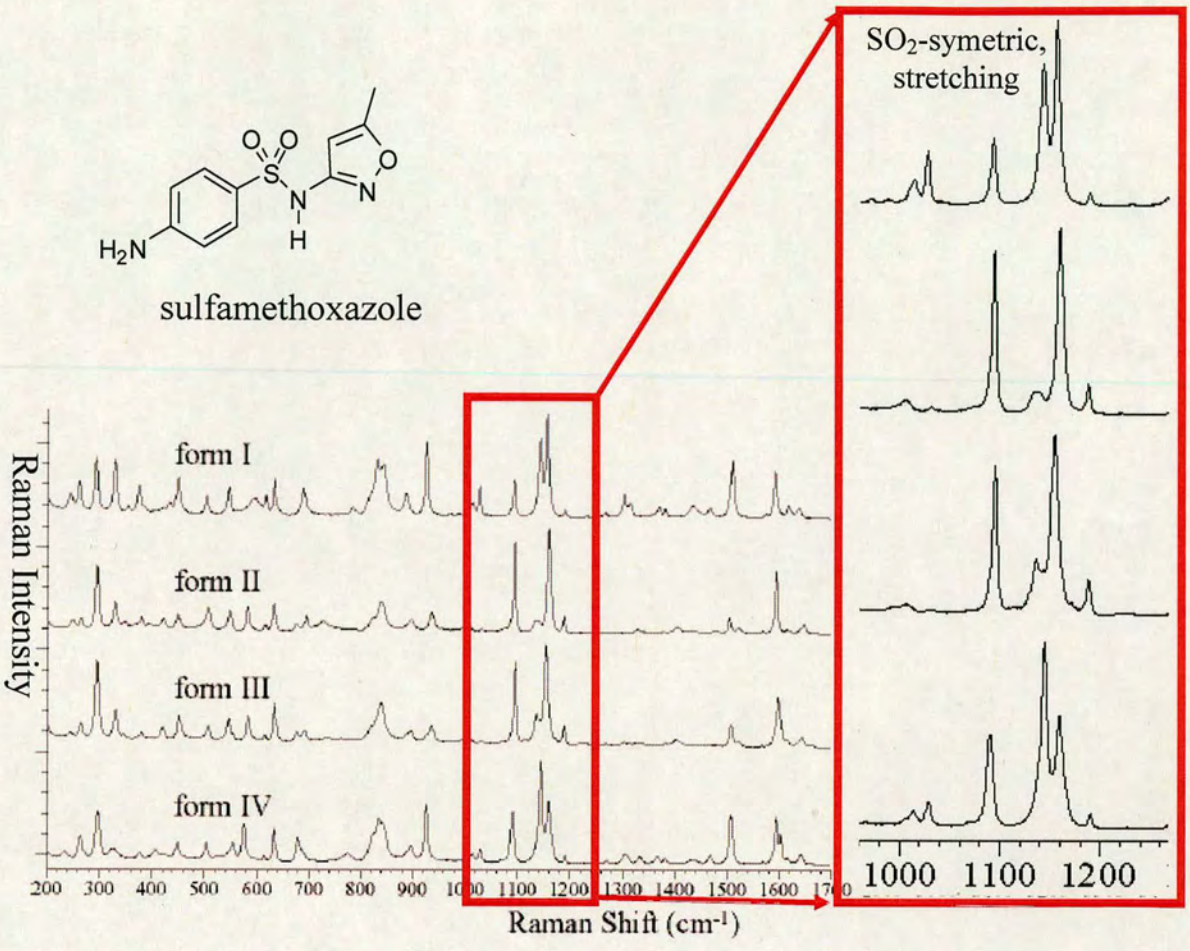

Figure 1.7 *Raman spectra of the sulfamethaxazole polymorphs. The red rectangle shows areas of spectral differences between the samples.*[19] *Reproduced with permission (copyright ACS, 2005).*

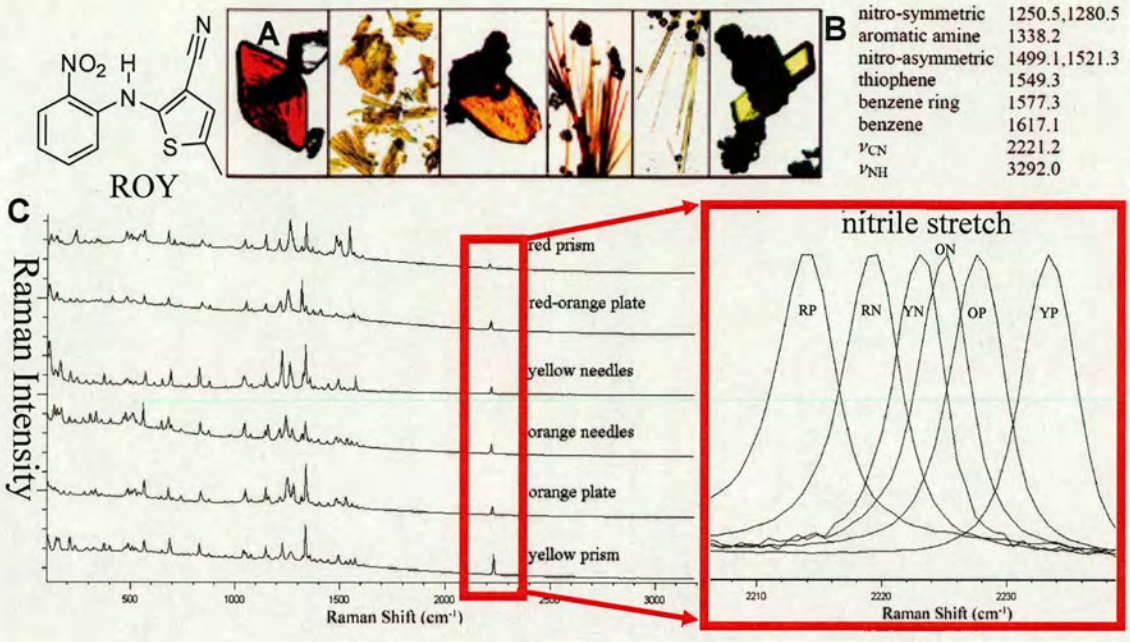

Figure 1.8 *Photomicrographs of ROY: (A) polymorphs produced in the presence of polymers; (From left to right) red prisms, orange-red plates, orange plats, orange needles, yellow needles and yellow prisms; (B) selected vibration frequencies (cm^{-1}) for ROY; (C) Raman spectra of the ROY polymorphs. The red rectangle shows areas of spectral differences between the samples.*[19] *Reproduced with permission (copyright ACS, 2005).*

1.4 Crystal analysis

Mother liquors of the small molecules were printed onto the polymer features (again 800 drops per spot, 0.9 μL, taking 1.5 s) and after solvent evaporation, the crystals remaining on the polymer spots were analysed, initially by optical microscopy. (**Figure 1.9**) Solvent can play many roles, passively acting as a carrier for the small molecule. It can also play more of a role by co-dissolving the polymer. Here solvent choice also dictates the evaporation rate, which influences crystallisation.

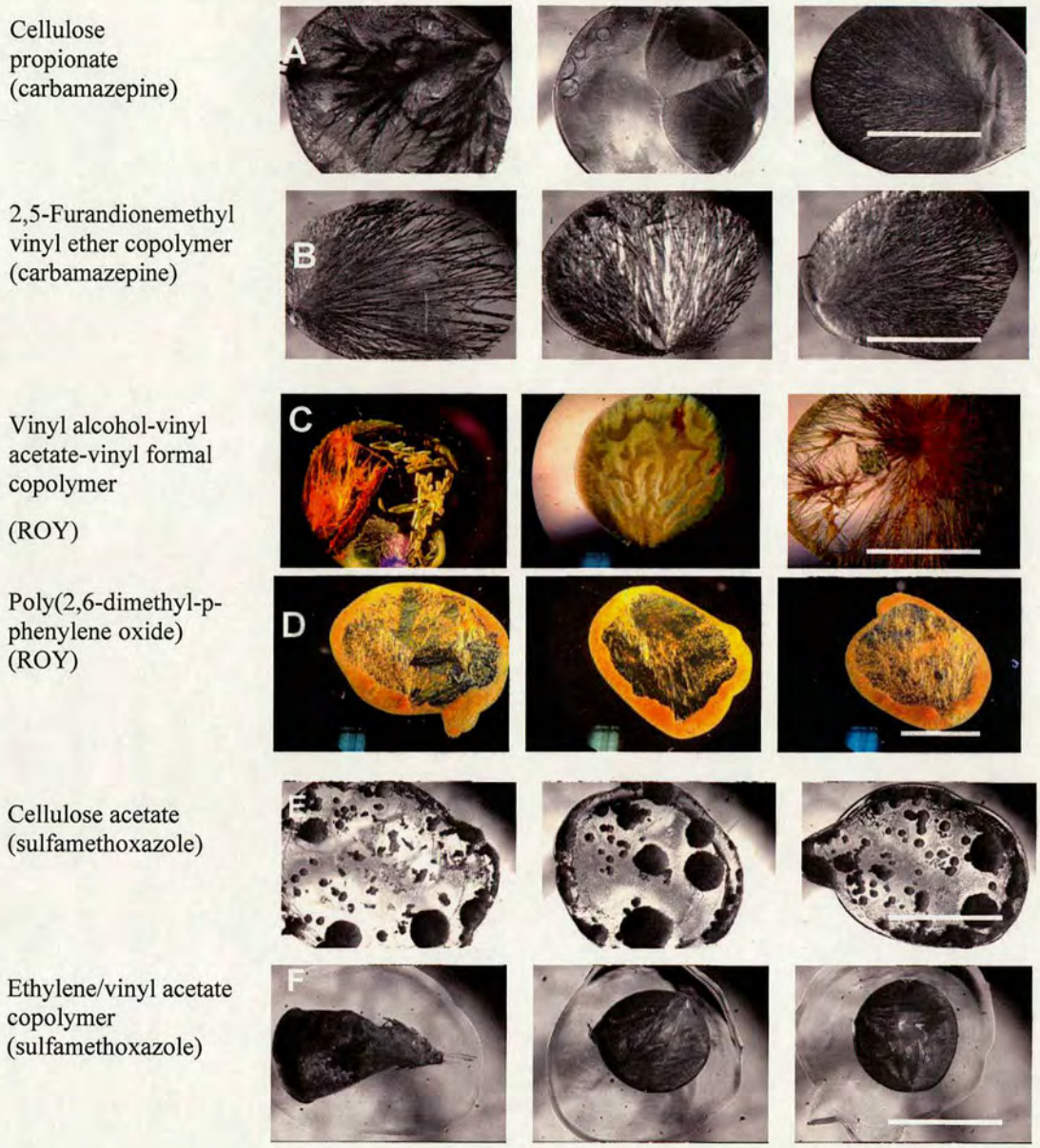

Figure 1.9 *Results of optical microscopy analysis: (A) crystals of carbamazepine on cellulose propionate – no repeatable crystal habits; (B) crystals of carbamazepine on 2,5-Furandionemethyl vinyl ether copolymer – repeatable crystal habits; (C) crystals of ROY on poly(vinyl formal) – no repeatable crystal habits; (D) crystals of ROY on poly(2,6-dimethyl-pphenylene oxide) – repeatable crystal habits; (E) and (F) crystals of sulfamethoxazole on cellulose acetate and on spots of ethylene/vinyl acetate copolymer-both repeatable crystal habits. Scale bars 0.7 mm.*

The preliminary screening (*via* microscopy) identified polymers giving "3 times repeatable crystal habits" which were then analysed by Raman Spectroscopy. Spectra were typically collected using an Olympus SLM Plan100 objective and a 150 μm slit in either extended scan mode with a range of 300-3500 cm^{-1} or a static scan mode centred at 1350 cm^{-1} for SMA and 2200 cm^{-1} for ROY.

The spectra were acquired from at least 10 places on each polymer spot (x3) on the polymer microarray. (**Figure 1.10**)

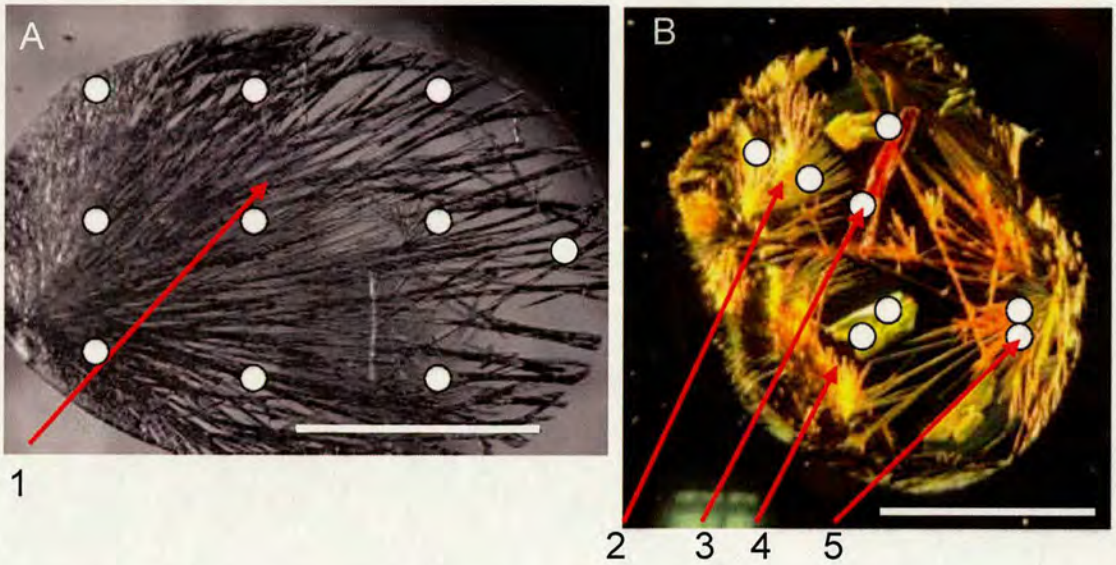

Figure 1.10 *Images of crystals: (A) carbamazepine on 2,5-Furandionemethyl vinyl ether copolymer; (1) characteristic repeatable crystal form II; (B) ROY on Poly(vinyl formal); multiple crystal forms on a single polymer; (2) yellow needles; (3) red prism; (4) yellow prism; (5) orange needles. Scale bars 0.7 mm. o = laser beam irradiation for Raman analysis.*

10 Raman spectra were collected with 16 scans per spectrum for each of the 3 spots to ensure reproducibility. (**Figure 1.10**) For ROY, ten polymers were identified to be of interest. At least 10 Raman spectra were recorded for each spot, in triplicate, of features so that a total of 300 spectra were generated for ROY. For Sulfamethoxazole, 23 polymers were identified and again 10 Raman spectra for each spot in triplicate were taken to produce a total of 690 spectra. For carbamazepine 15 polymers were identified, 10 Raman spectra for each spot in a triplicate of features were recorded to produce a total of 450 spectra. (**Figure 1.11**)

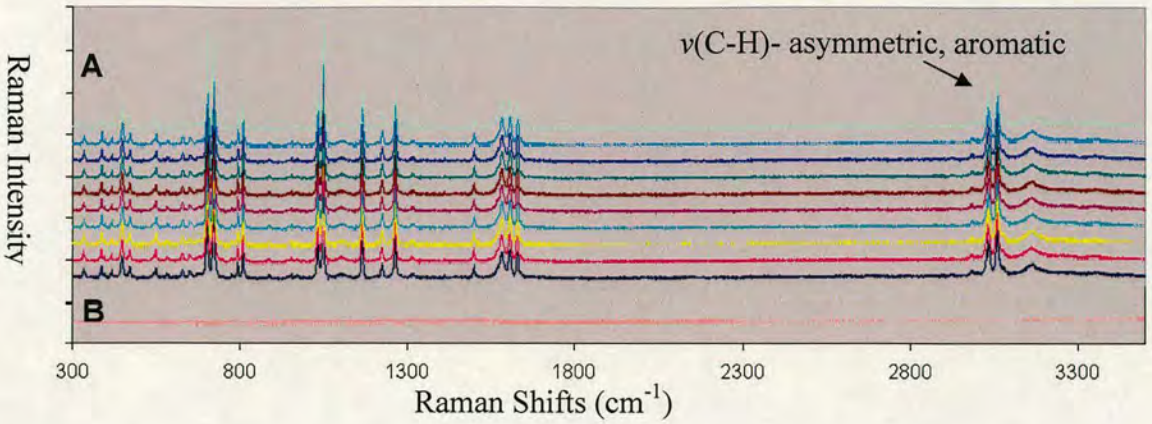

Figure 1.11 *Raman spectra for crystals and polymeric background: (A) stack of 10 Raman spectra (16 scans per spectra) recorded for single polymer feature (form II of carbamazepine) on 2,5-furandione-methyl vinyl ether copolymer; (B) background signal (from polymer itself).*

1.5 Carbamazepine

The first compound analysed was carbamazepine. There are four known polymorphic forms of carbamazepine reported in the Cambridge Structural Database, although to our knowledge, form IV of carbamazepine has not been characterized by Raman spectroscopy.[51,52] Following the protocol described above, polymer spots containing specific and repeatable crystal habit forms were identified using Raman spectroscopy. (**Figures 1.12**)

In the case of carbamazepine (printed in DMSO), most of the polymers supported specifically polymorphic form I, for example poly-*n*-butyl methacrylate. Vinyl chloride-acrylic acid copolymer and 2,5-furandione-methyl vinyl ether copolymer supported selectively and specifically form II. Additional characterization of the crystals obtained was undertaken using thermomicroscopy with analysis of the crystals on a hot-stage, while heating at 10 °C/min and confirmed the interpretation of the Raman spectra and matched previous reports.[50]

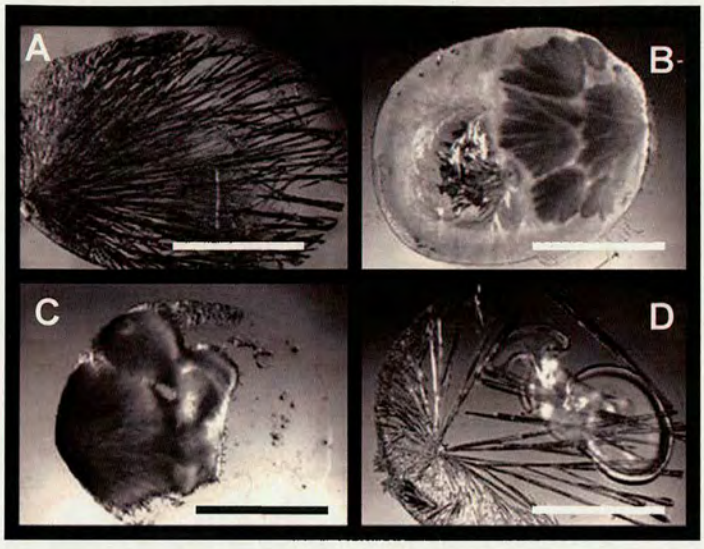

E

Polymer name	frequency/ Raman Shifts cm^{-1}	Postulated polymorphic form
2,5-furandione-methyl vinyl ether copolymer	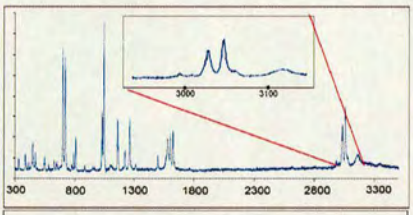	Carbamazepine FormII, ν = 3075 cm^{-1} 3054 cm^{-1} 3031 cm^{-1}
poly(vinyl butyral)	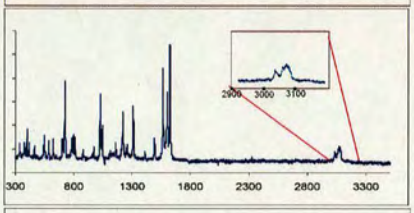	Carbamazepine Form I 3061 cm^{-1} 3024 cm^{-1}
poly(*n*-butyl methacrylate)	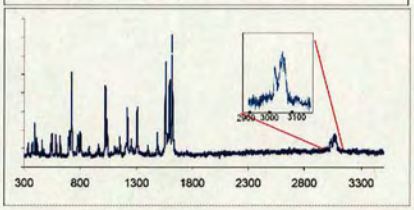	Carbamazepine Form I 3061 cm^{-1} 3024 cm^{-1}
vinyl chloride-acrylic acid copolymer	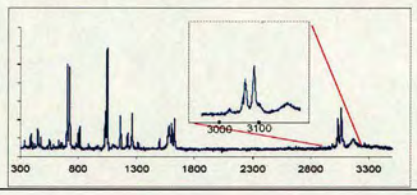	Carbamazepine Form II 3075 cm^{-1} 3054 cm^{-1} 3031 cm^{-1}

Figure 1.12 *Images of carbamazepine crystals generated on different polymer feature. (A) Form II on 2,5-furandione-methyl vinyl ether copolymer; (B) form I on poly(vinyl butyral); (C) form I on poly(n-butyl methacrylate); (D) form II on vinyl chloride-acrylic acid copolymer. Scale bars 0.7 mm; (E) Raman Shifts/frequency table of Carbamazepine.*

Thermomicroscopy for crystals collected from polymeric spots of 2,5-furandione-methyl vinyl ether copolymer, poly(vinyl butyral), poly(n-butyl methacrylate) and vinyl chloride-acrylic acid copolymer were performed with a Mettler Toledo FP82HT hot stage connected to an FP 90 control processor and viewed with a Leica DME microscope (work carried out by Dr. Graham Tizzard, University of Southampton). Samples of each of the four polymorphs were heated from 45 to 200 °C at a rate of 10 °C/min for initial observations. From comparison with references,[50] it was concluded that carbamazepine on polymer 2,5-furandione-methyl vinyl ether copolymer and carbamazepine on polymer vinyl chloride-acrylic acid copolymer were form II with melting temperature range 188 and 192 °C. Furthermore carbamazepine on polymer poly(vinyl butyral), and carbamazepine on polymer poly(n-butyl methacrylate) were form I with melting point 193.5 °C.

These results confirmed the interpretation of the Raman spectra and matched those previously reported.[50] However in our studies, only 27 μg of each polymer and 6.5 mg of carbamazepine were used, with two different polymorphic forms detected.

1.6 Sulfamethoxazole

According to the Cambridge Structural Database, four forms of sulfamethoxazole have been discovered to date and all of them have characteristic Raman shifts.[9] In this case, the 128 polymers were screened in triplicate under two different experimental conditions (ethanol or methanol) giving rise to 768 crystallisation experiments! With ethanol as a solvent, excellent control of crystal habit could be achieved. **(Figures 1.13)**

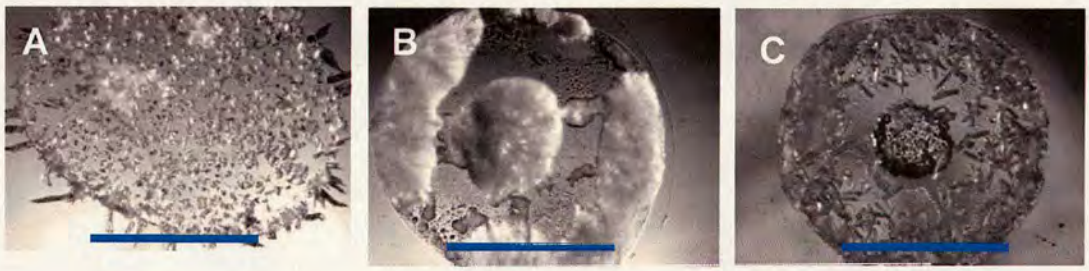

Figure 1.13 *Images of sulfamethoxazole crystallized from ethanol on different polymer features: (A) poly(diallyl phthalate); (B) poly(vinyl butyral); (C) ethylene/vinyl acetate copolymer. Different morphologies but the same polymorphs were identified (form I of sulfamethoxazole). Scale bars 1.4 mm.*

However, closer analysis by Raman spectroscopy revealed all of the crystals were polymorphic form I, again confirming that in the case of organic compounds, crystal habit is often not correlated with polymorphic form. (**Figures 1.14**)

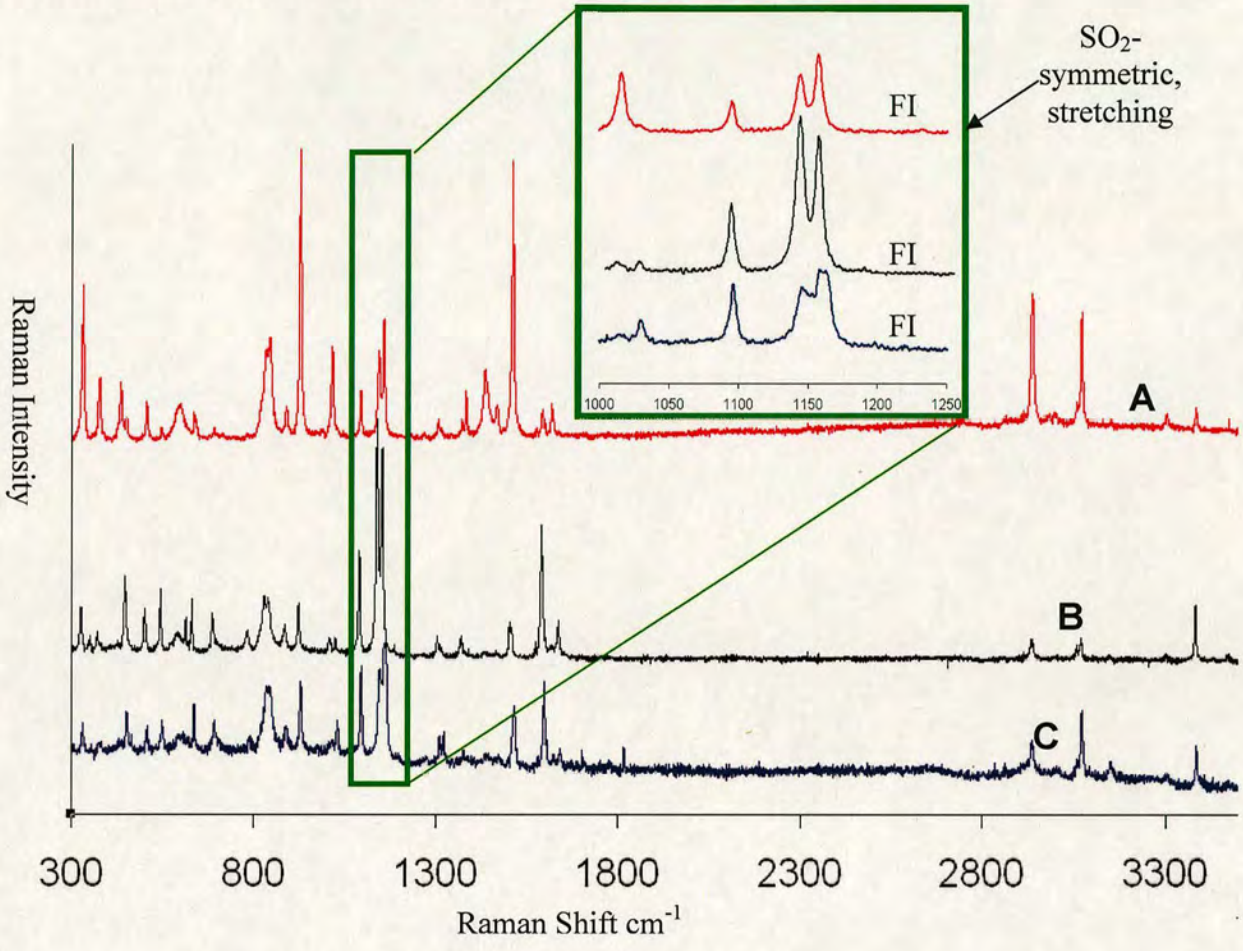

Figure 1.14 *Raman spectrum of sulfamethoxazole crystallized from ethanol - crystals generated on different polymer features: (A) poly(diallyl phthalate); (B) poly(vinyl butyral); (C) ethylene/vinyl acetate copolymer. Different morphology but the same polymorphism (form I of sulfamethoxazole).*

If methanol was used, the results were significantly different. Raman measurements showed that on most polymers, mixtures of form I and II were present.

However, ethyl cellulose supported specifically form II of sulfamethoxazole, while on hydroxybutyl methyl cellulose most of the spot area was occupied by polymorphic form II, but with form I appearing on the polymer edge. Butyl methacrylate/isobutyl

methacrylate copolymer and Zein[53] supported the formation of only form I. (**Figures 1.15, 1.16**)

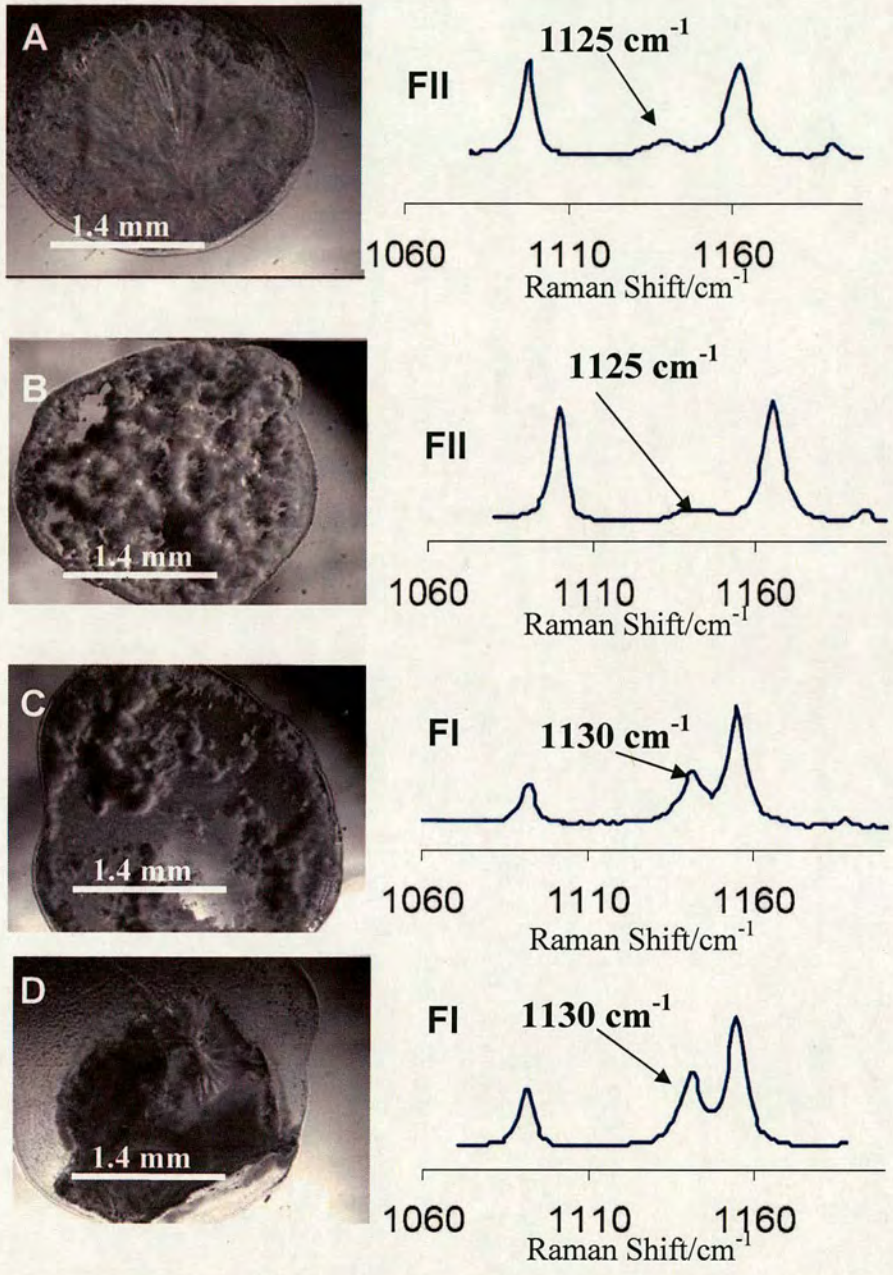

Figure 1.15 *Images of sulfamethoxazole crystallized from methanol - crystals generated on different polymer features (left), analytical bands in the Raman spectrum (right): (A) ethyl cellulose (Form II); (B) hydroxybutyl methyl cellulose (Form II); (C) Butyl methacrylate/isobutyl methacrylate copolymer (Form I); (D) Zein, purified (Form I).*

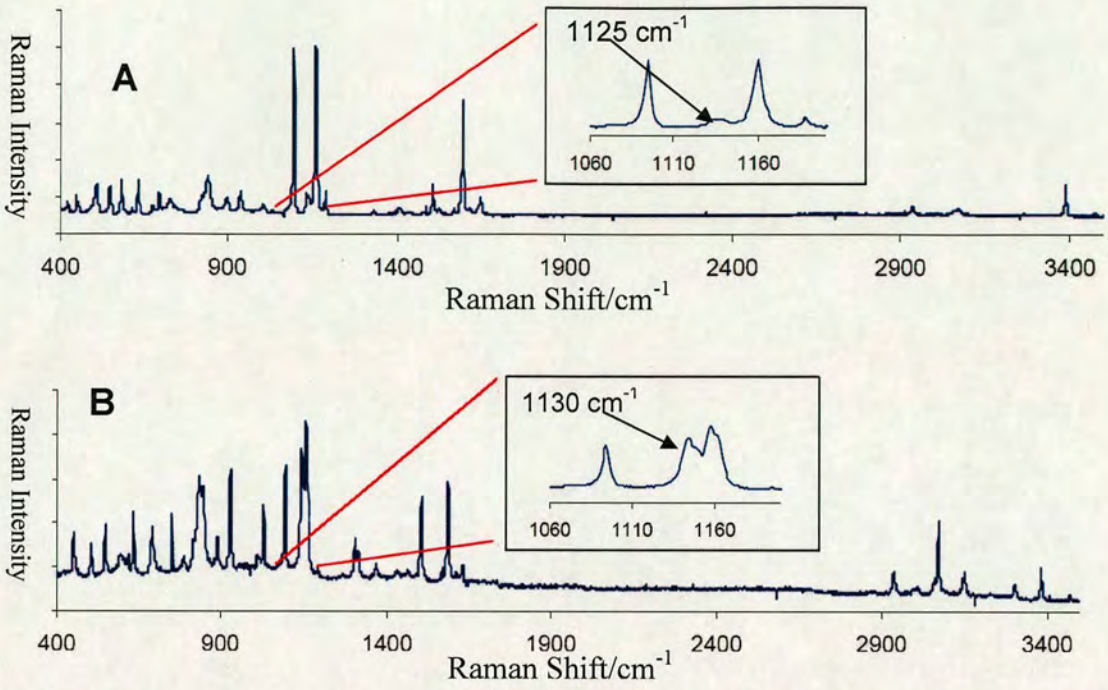

Figure 1.16 *Examples of full Raman spectra of sulfamethoxazole - with analytical region 1000-1200 cm $^{-1}$ expanded: (A) crystals generated on hydroxybutyl methyl cellulose (Form II - 1125 cm $^{-1}$); (B) crystals generated on ethylene/ethyl acrylate copolymer (Form I - 1130 cm $^{-1}$).*

1.7 ROY

Finally, a challenging small-molecule from a polymorphic study point of view, 5-methyl-2-[(2-nitrophenyl)amino]-3-thiophenecarbo-nitrile (ROY), was analysed. According to the Cambridge Structural Database, six forms of ROY have been reported to date, all of which have characteristic Raman shifts.[19] After a solution of ROY (in NMP/acetone) was printed onto the polymer array, polymorphic forms could be readily detected by bright field microscopy because the different forms of ROY have different colours. From the six known polymorphic forms, four of them were found within the array, yellow needles (YN), yellow prisms (YP), red prisms (RP) and orange needles (ON). (**Figures 1.17 and 1.18)**

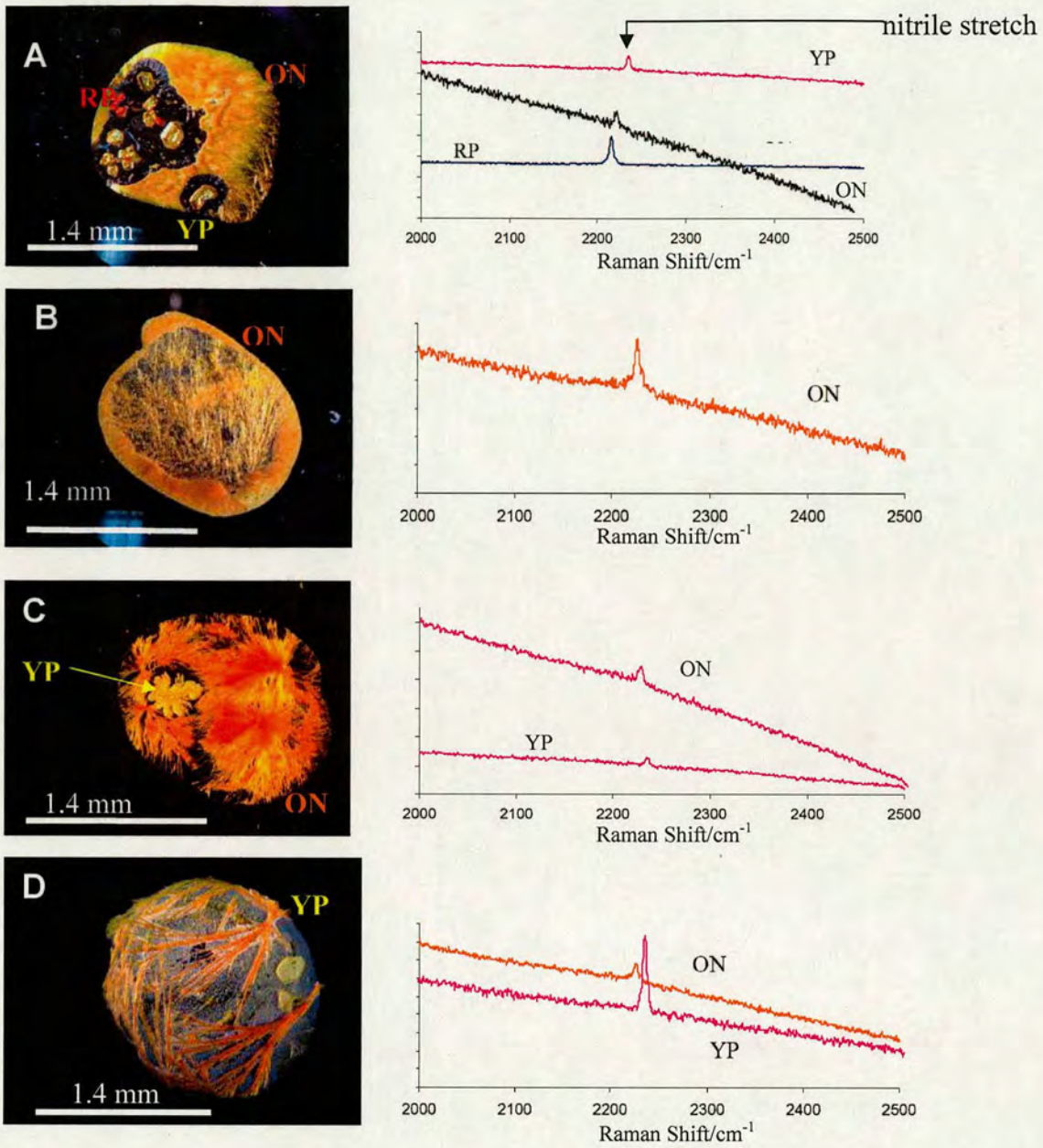

Figure 1.17 *Images of ROY crystals generated on different polymers: (A) three polymorphic forms, red prisms (2214 cm^{-1}), yellow prisms (2233 cm^{-1}), and orange needles (2225 cm^{-1}) on ethylene/acrylic acid copolymer; (B) a single polymorph, orange needles (2225 cm^{-1}) on poly(2,6-dimethyl-p-phenylene oxide); (C) two polymorphic forms, orange needles (2225 cm^{-1}) and yellow prisms (2233 cm^{-1}) on polyacrylamide, carboxyl-modified low carboxyl content; (D) two polymorphic forms, orange needles (2225 cm^{-1}) and yellow prisms (2233 cm^{-1}) on poly(isobutyl methacrylate).*

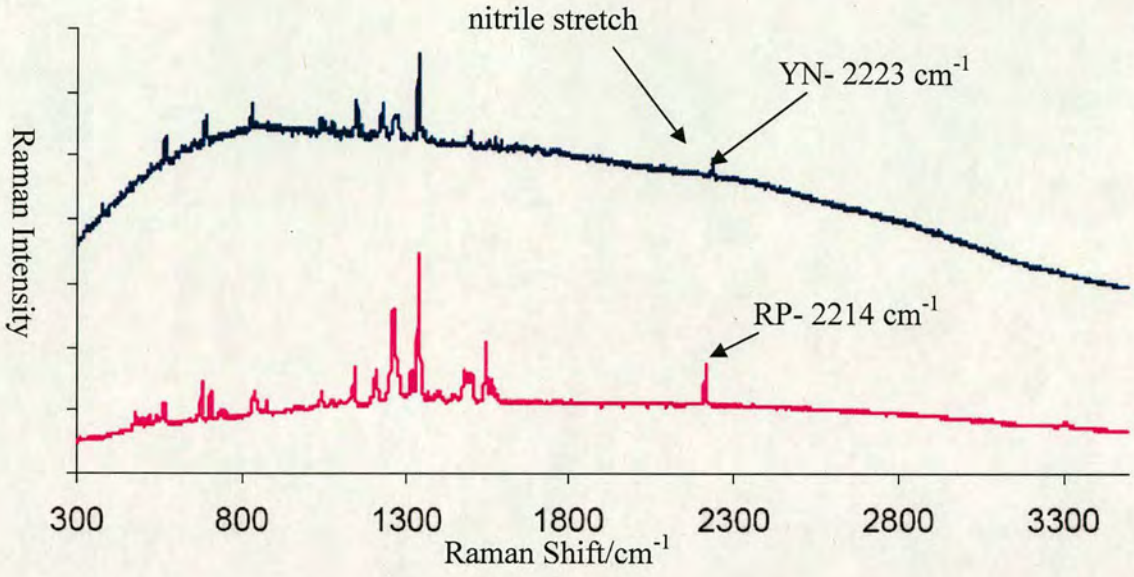

Figure 1.18 *Examples of full Raman spectra of ROY - with analytical region 2000-2500 cm^{-1}. Crystal generated on hydroxypropyl cellulose (YN-yellow needles and RP-red prisms).*

Acrylic acid-ethene copolymer and cellulose hydroxypropyl ether supported four polymorphic forms. Other polymers gave three types of crystal, thus poly(ethyl methacrylate) gave yellow prisms, red prisms and orange needles. Selectivity, in the case of polyacrylamide carboxyl, was better with just two forms (yellow prisms and orange needles). More selective polymers were also discovered. Thus, poly(isobutyl methacrylate) supported almost exclusively orange needle generation, but in small regions perfectly shaped yellow prisms were detected, confirming that polymer impact was rather subtle. (**Figure 1.17 D**) One of the most selective polymers was poly(2,6-dimethyl-*p*-phenylene oxide), which supported the growth of only orange needles. These results were confirmed by Raman spectroscopy.

1.8 Powder X-ray diffraction analysis

Attempts were made to characterize each of the samples using powder X-ray diffraction (PXRD), but because of the scale of the method, the PXRD response was found to be inadequate. (**Figure 1.19**)

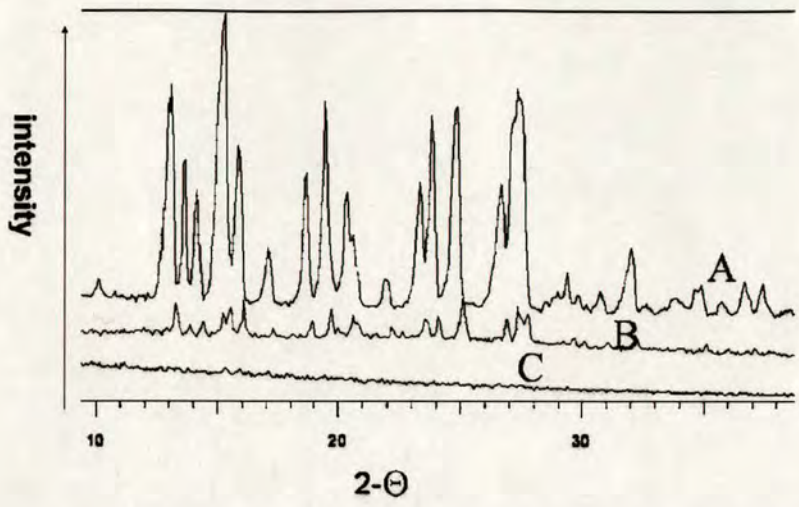

Figure 1.19 *PXRD signals for carbamazepine (data collection time 3 min): (A) 12 mm spot diameter; (B) 6 mm spot diameter; (C) 2 mm spot diameter (polymer microarray feature size).*

1.9 Conclusions

In conclusion, a high-throughput method for studying polymorphism in small molecules has been presented. This approach uses arrays of polymers to generate or trigger different polymorphic forms. The crystal habit forms of the small molecule solids were found to be a poor indicator of polymorphic form, but Raman spectroscopy was a very successful technique that could be used to characterize different polymorphic forms. PXRD was not suitable because of the small scale of the high-throughput method. The hydrophilic glass surface (control) yielded just amorphic forms in all three of the compounds studied. Many of the polymers were selective in terms of triggering specific polymorphic forms and a few were very selective and specific, demonstrating the role of polymers in the crystallisation process. The method is clearly an attractive alternative to the screening processes previously reported.[54] This method allowed three different small molecule compounds to be screened (in triplicate) with 128 polymers and required just milligram quantities of compound and 27 μg of each polymer per array, while generating large numbers of polymorphic forms. Polymers triggered different polymorphic forms of small molecules in a very subtle manner and although the materials on which crystals grow are important, as demonstrated here, there are many other influences such as solvent type and control of evaporation.[55]

Chapter 2 : Inkjet fabrication of polymer microarrays and grids - solving the evaporation problem

2.1 Polymer patterning on surfaces[56]

As stated previously[56] the possible applications of polymer-patterned surfaces can be sorted into 4 main categories: (1) medicinal research including tissue engineering and the study of cell/substrate behaviour[57-59] and less important for this thesis (2) the generation of light-emitting displays, plastic electronics and semiconductor microelectronics[60-62], (3) the generation of templates and masks[63,64] and (4) the production of optical components such as photonic crystals or gratings.[65,66]

The two most important techniques for patterning polymers are photolithography and printing techniques.

2.1.1 Photolithography[56]

In photolithographic methods two basic steps can be distinguished. The first step is the site-specific exposure of an oligomer, monomer, or polymer-coated surface to photoirradiation which causes local reaction (photopolymerisation, photocrosslinking, functionalisation and decomposition reactions, or induces phase separation). The second step involves removing non-irradiated areas of the substrate through dissolution in an appropriate solvent. Site-specific exposure is performed by irradiation through a mask or by optical interference techniques[67] and is suitable for large-area surface patterning with good control over the topography and resolution of patterns (micrometers to nanometers). (**Figure 2.1**)

Using non-conventional masks *e.g.* block co-polymer lithography,[64] new photoactive polymers,[68] irradiation at short wavelengths[69] and high resolution patterning can be achieved.

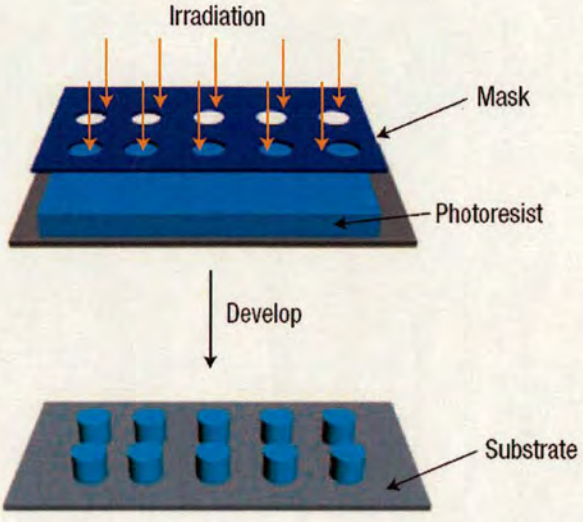

Figure 2.1 *Scheme of polymer patterning via photolithography. Reproduced with permission*[56] *(copyright NAS, 2006).*

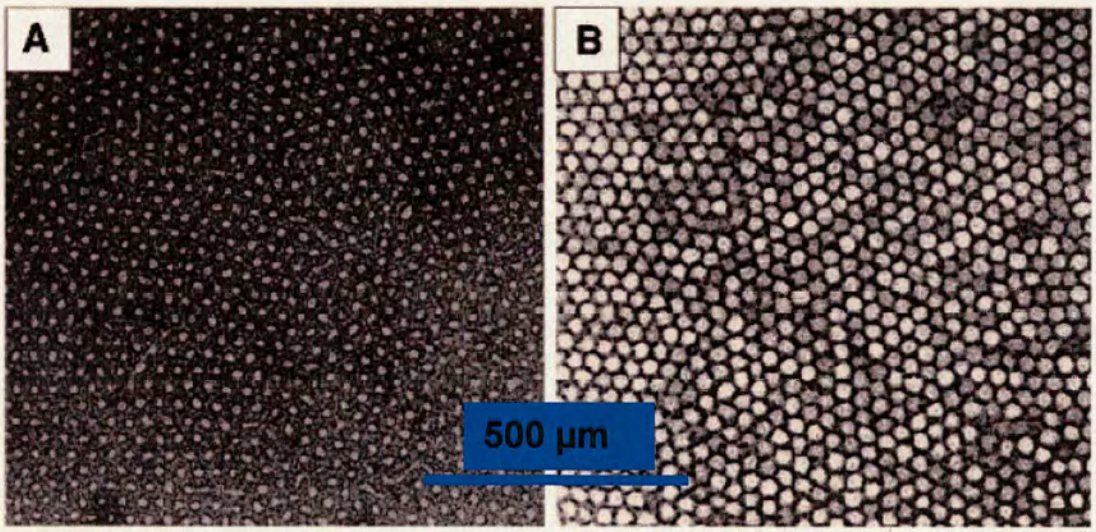

Figure 2.2 *Block co-polymer lithography: (A) polystyrene - polybutadiene layer; lighter regions are polybutadiene domains (that were removed by ozonolysis), darker background is polystyrene; (B) hexagonally ordered arrays of holes in silicon nitride obtained after ozonolysis and reactive ion etching.*
Reproduced with permission (copyright AAAS, 1997).[64.]

Adamson, for example, reported fabrication of masks consisting of periodic arrays of holes with density of 10^{11} holes per cm^2, *via* fabrication on a silicon nitride–coated

silicon wafer, where spin-coated diblock copolymer thin films with well-ordered spherical microdomains were employed as the templates.[64]In thin layers of diblock co-polymers (such as polystyrene-polybutadiene), a very specific orientation of the polymeric chains results and the polybutadiene forms spheres (20 nm diameter) within the polystyrene matrix. **(Figure 2.2)** Ozonolysis selectively degrades polybutadiene and generates 20 nm holes in the polystyrene. Reactive ion etching[70] of the silicon nitride (underneath the polystyrene layer) produces holes 15 nm-deep.

2.1.2 Printing techniques[56]

Modern printing methods can be classified into two groups: (1) Methods in which a material is transferred to the substrate without direct contact with the surface (*e.g.* inkjet printing and robotic deposition) and; (2) Techniques involving the contact of a writing head or a stamp with a substrate, *e.g.* nanoimprinting, microcontact printing and scanning probe microscopy-based methods.

2.1.2.1 Nanoimprint lithography[56]

In nanoimprint lithography the patterning of polymers is performed *via* pressing a mold against a liquid polymer precursor or a softened thermoplastic polymer and trapping the pattern in the solid state by either UV initiated curing of the polymer precursor or by cooling the molded material. These methods have demonstrated to givehigh as 5 nm horizontal patterning resolution.[71,72] UV mediated nanoimprinting is quicker, requires lower imprinting pressures and allow simpler fabrication of multilevel topographic patterns in comparison to thermally mediated nanoimprinting. (**Figure 2.3**)

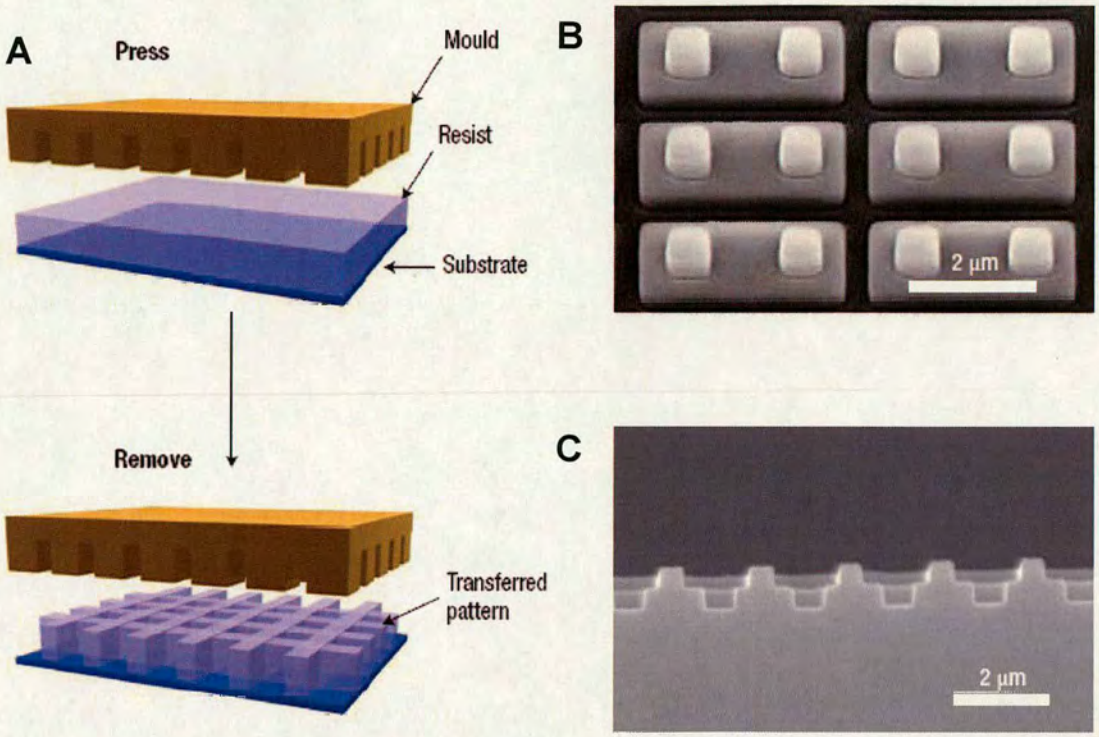

Figure 2.3 *Scheme of the nanoimprinting: (A) scheme of polymer patterning; (B) SEM images of template (DuPont Photomasks, Inc.)[73] (C) cross section of a polymeric pattern (T8- EPOXY).[73] Reproduced with permission[56] (copyright NAS, 2006).*

2.1.2.2 Microcontact printing[56]

Microcontact printing allows patterning of large surface areas with resolution down to the submicrometer range.[75] In microcontact printing, a stamp with features is used to transfer material to a receiving substrate. High-quality microcontact printing patterns are fabricated through avoiding contamination, deformation of the stamps and diffusion of the ink out of the desired region of the stamping.[75-77] (**Figure 2.4 B**) Microcontact printing becomes extremely useful in patterning surfaces with thin films and polymer monolayers and can be performed using a direct and indirect mode.

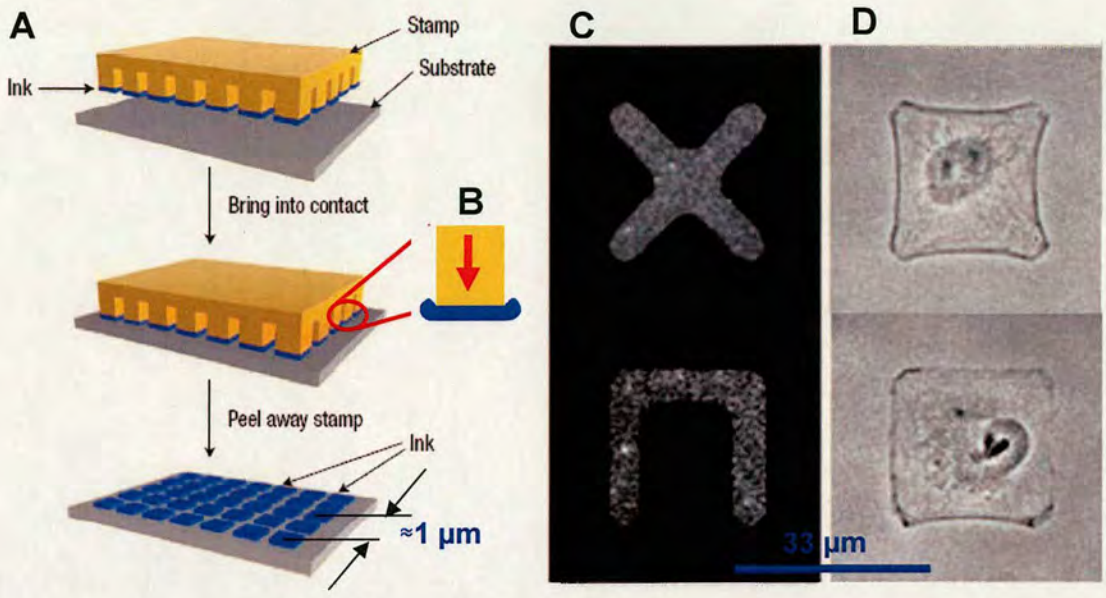

Figure 2.4 *Scheme of polymer patterning via microcontact printing: (A) process of microcontact printing; (B) the diffusion of the ink out of desire region of the stamping; (C) fibronectin pattern surrounded with PEG (left) produced by microcontact printing the protein onto a PEG coated surface; (D) phase-contrast microscopy images of single RPE1 cell plated on a fibronectin micropattern. Reproduced with permission (copyrights ACS, 2006)[78] and (copright NAS, 2006)[56].*

2.1.2.2.1 Direct microcontact printing[56]

In direct microcontact printing, a stamp transfers a polymer solution to the surface. Polymers that strongly interact with the surface give increased resolution of patterning. For instance, electrostatic interactions between a cationic poly(allylamine-hydrochloride)-coated substrate and an anionic polymer such as poly(acrylic acid) enabled patterning with a resolution of 80 nm.[79] Another technique, which gives high resolution patterning, is reactive contact printing.[80] For example, patterning of poly(ethylene imine) onto surfaces comprised of carboxylic anhydride groups generated structures with an edge resolution of 500 nm.[80]

2.1.2.2.2 Indirect microcontact printing[56]

In indirect microcontact printing, selective deposition of a monomer to the pre-patterned surface is followed by surface-initiated polymerisation or site-specific electropolymerisation.[81-83]

In indirect contact printing, atom-transfer radical polymerisation was utilized to pattern surfaces with layers of polymer brushes of polyacrylates. Anchoring an initiator to a pre-patterned surface allows site-specific polymerisation to pattern a surface with polymeric brushes with high density (5–50 nm thick).[71]

Both synthetic and natural polymers were patterned *via* microcontact printing to enable precise immobilization of biological molecules and control of cell adhesion on various substrates. For example, site-specific immobilization of fibroblasts, proteins, or microvascular endothelial cells was conducted by selectively coating the "adhesive" surface with a poly(oligoethyleneglycol methacrylate)-based polymer thus creating protein-resistant areas.[84,85] (**Figure 2.4 B**) shows cells grown on cell adhesive material (fibronectin) islands surrounded with cell resistant areas (PEG).[78]

2.1.2.3 Direct writing[56]

Patterning by direct writing is conducted by delivering chemical reagents from a probe tip or a nozzle to desired regions of the substrate. Pattern geometry can be generated by the computer-controlled motion of the tip or the nozzle along the surface. Two groups of direct writing techniques can be distinguished: (1) Scanning probe microscopy-based methods and (2) Ejection methods such as robotic deposition and inkjet printing.

2.1.2.3.1 Scanning probe microscopy lithography

The tip of an atomic force microscope (AFM) or a scanning tunnelling microscope is used for selective covering of the underlying substrate with the patterning material, or removing the underlying substrate by heating, applying mechanical force or an electric field.[86,87] Advantages of the scanning probe microscopy methods are the extremely high (several nanometres) resolution patterning combined with *in situ* imaging of the patterns.[87] Dip-pen nanolithography relies on translating an ink-coated AFM tip above the surface. The liquid meniscus formed between the tip and substrate allows deposition of the ink molecules from the tip to the underlying substrate.[88] The resolution of patterning depends on the type of ink, the scanning

speed, the volume of meniscus, the temperature, the surface chemistry and the humidity.[88] (**Figure 2.5**)

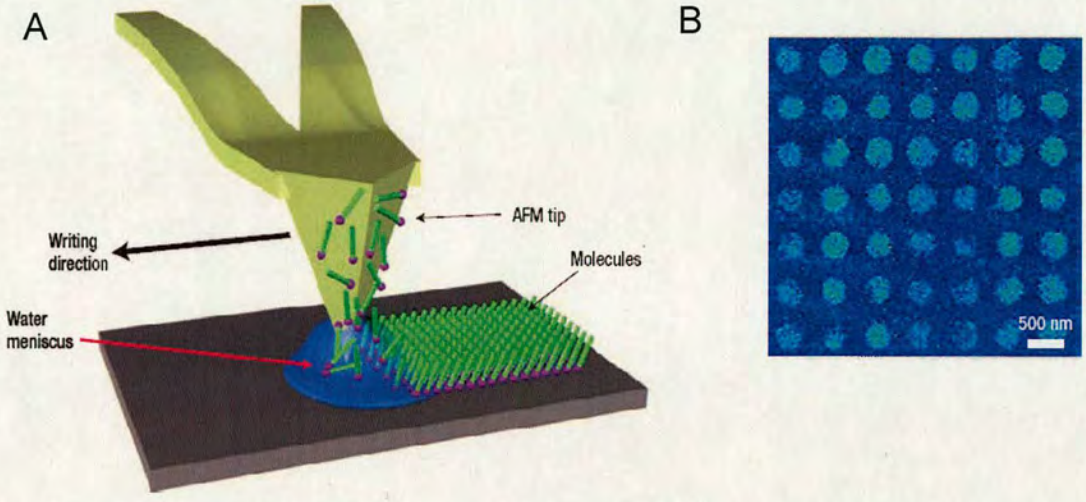

Figure 2.5 *Scheme of dip-pen nanolithography: (A) scheme of dip-pen printing; (B) fluorescently labelled human immunoglobulin nanoarray. Reproduced with permission (copright NAS, 2006)[56] and (AAAS, 1999).[88]*

2.1.2.3.2 Robotic deposition[56]

In robotic deposition, the deposited material is continuously extruded from a nozzle onto a substrate to yield 2D or 3D patterns. Complex 3D structures can be fabricated by a computer-aided layer-on-layer sequential build-up process. Robotic deposition has been used for patterning reactive pre-polymers, conductive polymers, melts, solutions and polyelectrolytes with a resolution of hundreds of nanometers[56]. (**Figure 2.6 B)** The patterning process is possible after optimization of the viscosity and viscoelasticity of the deposited material and the hardening of the material after extrusion from the nozzle. The technique is extremely useful for the patterning of biocompatible polymers and biopolymers. Precise geometries were fabricated by robotic patterning of poly(ethylene glycol terephthalate-*b*-butylene terephthalate),[89] poly-L-lactic acid, polycaprolactone,[90] poly(D-L-lactide-*co*-glycolide),[91] agarose, chitosan,[92] gelatin[93] and polyelectrolytes.[94]

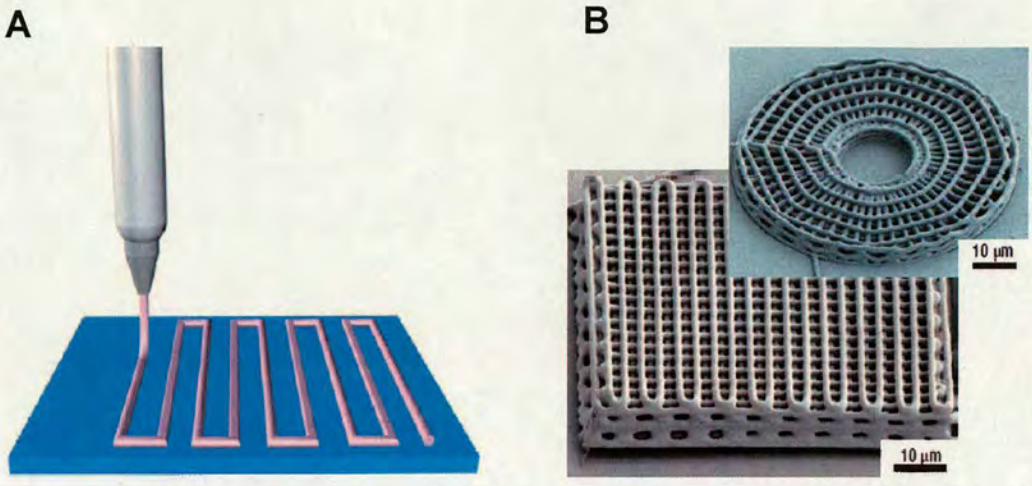

Figure 2.6 *Scheme of polymer robotic deposition: (A) scheme of patterning; (B) 3D periodic structure of polymer blend containing: polyacrylic acid and polyethylenimine(1:1 w/w) Reproduced with permission' (copyright NAS, 2006)*[56] *and (copyrights NAS, 2004)*[94].

Besides applications in the production of photonic crystals, microfluidic devices and templates for biomimetic mineralization,[95-97] the most promising application of polymer patterns generated by robotic deposition are the fabrication of scaffolds for tissue engineering.[98] Polymer scaffolds with well-defined porosity, geometry and mechanical properties that are appropriate for biological applications were used for cell organization into tissue-like structures.[59] Bovine articular chondrocytes seeded and cultured on poly(ethylene glycol terephthalate-*b*-butylene terephthalate) scaffolds were used for the regeneration of bone tissue and cartilage.[89]

2.1.2.3.3 Inkjet printing

In inkjet printing, droplets of a polymer solution are deposited onto a surface to form a dried pattern after solvent evaporation. Polymer patterning can be performed by depositing onto a polymer substrate, a solvent or a reactive material that etches the substrate polymer.[99,100] The droplet size determines the resolution of the method. Electrohydrodynamic and acoustic inkjetting or printing on pre-patterned surfaces improve resolution.[60,99,101,102] Inkjet printing has been used to pattern conjugated polymers, photoresist, polyelectrolytes, photocurable oligomers and monomers and

biopolymers[56]. The rheological properties, surface tension and solvent volatility of polymer solutions designed for inkjet printing need to be well-defined.[103] The non-Newtonian nature of polymer solutions complicates the break-up of jets and makes droplet formation difficult and sometimes impossible.[103] The viscosity of polymer solutions is controlled by tuning the polymer concentration and by selecting polymers with appropriate architectures and molecular weights. Patterning of polymers by inkjet printing has been applied in the fabrication of micro-lense arrays, waveguides,[100] sensors[104] and arrays of proteins and cells.[105] An example of an advanced application of this technique is the production of polymer transistor circuits and organic LEDs (plastic electronics). In this area the challenge is to achieve reproducible and precise patterning with resolutions less than 10 μm while preserving polymer stability against the dissolution of inner layers in multilayer systems.

2.1.3 Functional polymer patterning for new material development

It is a time of intensive development in the field of functional polymeric materials. To develop new polymers that can be patterned with high resolution and reliability, without compromising polymer properties, is an important challenge. These methods are especially important in planning new and optimizing existing formulations for research and discovery applications. Flexibly patterning tens or hundreds of different polymers on a substrate for polymer-screening is a more complex undertaking and a number of micro-scale direct printing approaches have been developed.

The most relevant approaches to polymer patterning (to this thesis) have been reported by Langer and Schubert. Langer first published the work on polymer microarrays for studying cell-polymer interactions while Schubert's works on inkjet printing deposition inspired methods for performing in situ nanolitre polymerisation

2.1.3.1 Langer's approach towards polymer microarray fabrication and screening

In 2004, Langer reported the nanolitre-scale synthesis of arrayed biomaterials and developed arrays for applications with human embryonic stem cells (hES).[106] The first step was the choice of a relevant class of biomaterials. Polyacrylates were chosen due to the number of commercially available monomers and a variety of already existing applications of acrylate-based polymers (in tissue engineering and drug delivery) and because acrylates can be polymerized quickly using a photo activated initiator. 576 different combinations of 25 different acrylate monomers (with a radical initiator) were deposited on poly(hydroxyethyl methacrylate) coated slides, which allowed fabrication of 1,728 individual polymer spots.

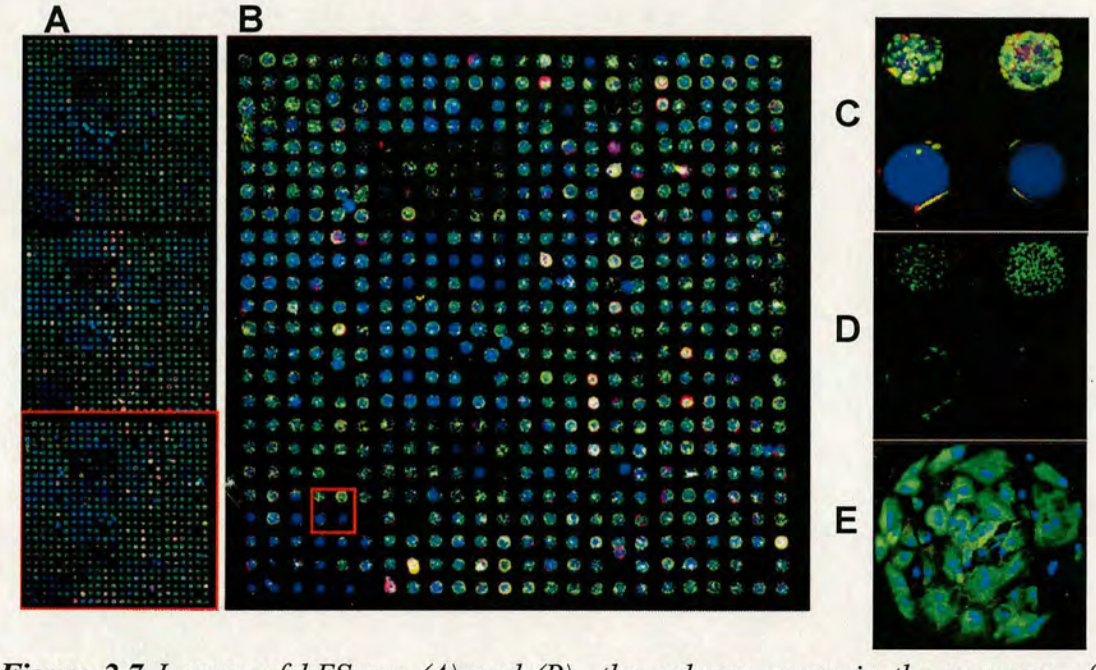

Figure 2.7 *Images of hES on: (A) and (B) the polymer array in the presence of retinoic acid for 6 days and then stained for vimentin (red), and cytokeratin 7 (green); (C) polymer spots can be identified by blue fluorescence (bottom); (D) stained nuclei (green); (E) Cytokeratin 7 positive spot on one of the polymers. Reproduced with permission (copyright NAS, 2004).*[106]

The format of the slide allowed for rapid staining and four-color fluorescence imaging. These biomaterial microarrays were tested for their effects on hES differentiation and cell growth. In general most of the polymers showed an ability to

support cell growth. Only a few polymers inhibited hES cell attachment and spreading. It was also shown that the majority of polymers triggered hES differentiation into cytokeratin-positive cells (which are useful in tissue engineering and cell therapy). (**Figure 2.7**)

Langer's proof-of-principle study allowed for varying levels of hES cell attachment and spreading and also for cell-type specific growth and growth factor-specific proliferation. Testing biopolymer microarrays with an embryonic muscle cell line (C2C12), Langer showed that unlike hES cells the C2C12 cells can grow only on polymers containing more than 70% of the m-phenylene diacrylate monomer. Identification of materials that selectively support the growth of specific cell types is useful for the development of complex tissue engineered scaffolds.

An important part of Langer's papers was related to the equipment used for polymer synthesis and the fabrication of microarrays. Langer discussed in details the problems and solutions of fluid handling in a highly miniaturised manner. For example the deposition of diverse acrylate monomers to produce a uniform polymer microarray required significant modification of existing robotic technology. Firstly, viscous acrylate monomers affect fluid ejection (during monomer formulation *via* liquid handling equipment) and printing and pin washing (during monomer contact-printing). Another problem is oxygen mediated inhibition of radical polymerisation which is particularly significant at small volumes. Consequently, printing was performed in an atmosphere of humid argon. Next, a very important problem noticed by Langer was that some monomers spread instantly after deposition, forming irregular polymer spots, whereas others started to evaporate after a few minutes![106]

In 2005, in research concerning the rapid, microscale screening of polymer–cell interactions, Langer used biomaterial microarrays to simultaneously characterise over 3456 human mesenchymal stem cell (hMSC)–biomaterial composite interactions.[107] This allowed identification of biomaterials that induce optimal gene expression (tested *via* reverse transcription *in situ* PCR) with appropriate levels of cellular attachment. The biomaterials were generated by blending 24 different polymers in various proportions giving, in total, 1152 polymer blends. [107]

2.1.3.2 Bradley's approach towards polymer microarray fabrication and screening

In 2006, Bradley presented[108] new methods of microarray fabrication by contact printing pre-formed polymer solutions from a polymer library onto agarose coated glass slides. In the same year, Bradley and co-workers developed new substrates for phagocytosis assays.[109] The polymer microarrays were screened in order to search for polymers capable of binding bone marrow dendritic cells whilst allowing them to stay in an immature stage. In the same publication, the authors described protocols for validation of microarray screening results, including scale-up.[110] The polymers selected after microarray screening were coated on coverslips and again showed affinity for bone marrow dendritic cells. Tourniaire used polymer microarrays for screening polymers for selective leucocytes separation and also for triggering mouse embryonic stem cell mES differentiation.[108] In 2008, polymer microarrays were used to develop polymers capable of mouse fibroblast cell (L929) attachment and controlling specific L929 cell morphology.[111] It was discovered that some specific polyurethanes triggered a linear morphology of the cells while other polymers triggered a "triangular cell" morphology. Pernagallo also reported the discovery of a polymer capable of binding suspension cells. Microarray screening was this time followed by a DNA microarray approach for biomaterial/genetic investigation, deducing how the attachment process affected the cells by detailed genetic analysis of suspended cells vs attached cells.[112]

The Bradley group formulated a new challenge in the field by the concept of increasing experiment efficiency by fabricating polymer microarrays *via in situ* nanolitre scale polymerisation. The first attempt to realise this idea was performed by Hitoshi Mizomoto in 2004.[113] The polymerisation on a glass slide was performed using 36 different monomer solutions. NMP was chosen as a solvent due to its high boiling point and high solubility of monomers. The solution was contact-printed using a Genetix Q Array mini arrayer. Polymerisation was initiated by AIBN (pre-mixed with monomers) and was carried out at 40 °C overnight. Mizomoto reported that polymer spots were not uniform and polymerisation on the slides was "very

difficult". However, Mizomoto successfully utilized several analytical techniques (microscope IR, TOF-SIMS) in order to analyse polymeric features directly on slides. To overcome problems reported by Mizomoto, new types of liquid handling device were introduced. Piezo inkjet printing allows dispension of pico-litres of material at highly defined positions.

2.1.3.3 Schubert's approach towards inkjet mediated material deposition

Schubert is a leader in inkjet printing for research applications. His works have been valuable and inspiring. Schubert's interest in inkjet printing techniques arose from the search for new screening methods and from an interest in using this technology for "plastic electronics". In 2004, Schubert published a review dedicated to inkjet printing, described by him as a "key technology in the field of defined polymer deposition". [114] This article provides examples of polymer inkjet printing applications such as, three-dimensional printing, manufacturing of polymer electronics, multicolour polymer light-emitting diode displays and polymers for tuning drug release. Importantly, the review presents general information about the relation between inkjet printability and polymer structure, molar mass, solvents and concentration. Indeed matters of printability especially material properties and behaviour during printing became a focal point of some of Shubert's publications. For example, he optimized micropipettes for a variety of polymer solutions and he noticed that printability of polymer solutions decreases when the polymer concentration and molecular weight increase. He additionally reported the "elastic stresses originating from elongational flow in the pipette nozzle, later named the "tail effect".[115] In the same year, Schubert published an article about challenges involved in printing well-defined polymer structures from dilute solutions.[117] In this paper, Schubert demonstrated how to produce uniform polymeric features using non-volatile (acetophenone-based) inks and the importance of the surface upon which printing is performed. He also demonstrated how to utilize inkjet printing for polymer film fabrication[117] and the advantage of using solvent mixtures over single solvents for printing uniform features. Parameters such as the effect of solvent mass

ratio, dot spacing printing method and print head velocity were optimized to obtain homogeneous polymer films. In 2005 Schubert investigated the relationship between polymer structure and printability. Visual examination of drops generated using solutions of linear and star polymers was used to describe filament formation on the nozzle (the tail effect). But the most important output of this particular publication was the demonstration of how important a tool drop visualisation is. In fact stroboscopic cameras (typically used for imaging drop formation) not only allowed controlled drop formation but were an extremely important analytical tool.[118] In two articles, Schubert directed his attention toward applications of inkjet printing in the field of electronics, the development of solar cells[119] and light emitting devices constructed *via* inkjet printing of luminescent ruthenium- and iridium-containing polymers.[120] In 2007, Schubert reported using inkjet printing for fabrication of conductive silver paths. In order to increase conductivity of silver deposited onto the substrate, Schubert merged the material using microwaves.[121] Schubert used inkjet printing to advance surface architecture. To demonstrate the principals of the method, n-butylacetate (or isopropylacetate) was printed using a 30 μm micropipette onto a layer of polybenzylmethacrylate (or polystyrene). The effect of the deposited material was three dimensional fabrication canals and wells (1 μm deep).[122] In general, Schubert's research covers a very wide spectrum of inkjet printing applications.

2.1.3.4 Bradley's approach towards inkjet mediated material deposition

The power of inkjet printing was demonstrated by Cull in 2007. Cull utilised inkjet printing to produce liquid crystal libraries and also presented a high-throughput technique for analysis of the generated libraries.[123] Libraries were produced using three liquid crystals which were *in situ* mixed in ratios controlled *via* the number of drops deposited by the nozzle at each position on the matrix. 231 different liquid crystal formulations were fabricated on a 30x30 mm substrate with a 1.9 mm spacing between spots (100 drop per spot). Cull showed that fabrication of the 250-member library of liquid crystals would have required

~750 steps to be entered using a single-step manual interface. To overcome this limitation he designed an application in Microsoft Visual Basic 6 that was compatible with inkjet printer control software. Therefore, Cull defined the number of drops for dispensation at each fixed XY position on the substrate for each of the three liquid crystals in a single rapid step. The format of the library allowed for rapid screening of the phase transition temperature and selection of optimal liquid crystal formulae.[123]

The challenge of nano-scale polymer synthesis was successfully approached by Zhang *et al.* (Bradley group) in 2008. The strategy included *in situ* fabrication through pico to nano litre scale mixing of inkjet printed water soluble monomers and initiators that were deposited onto a slide under conditions of high humidity (to prevent monomer evaporation). This approach, allowing over 1800 polymer features to be generated on a single microscope glass slide, was restricted to hydrogels and water compatible polymerisations.[124]

In this chapter, I present an inkjet printing approach that broadens considerably the monomers that can be used for rapid biomaterial development and allows a much broader range of polymers to be generated, as well as using inkjet printing to generate a new type of microarray composed of a matrix of inter-crossed polymer lines.

2.2 Inkjet printing for high-throughput polymerisation

This section will focus on inkjet printing methods used in high throughput polymerisation. Piezo inkjet printing avoids sample heating during dispensing, which can be destructive for many types of ink, while maintaining good control over the amount of material deposited. Ink is deposited onto substrates as a drop, with no contact between the print head and the substrate,[125] while stroboscopic cameras can be used to monitor droplet formation.[126] This allows accurate control of the volume of the deposited materials by simply varying the number of drops printed in any specific location. Inkjet printers can be controlled to print any desired pattern using

virtually whatever material desired, while giving a reproducibility of nozzle reposition of +/-1 μm, accurate enough for spot-on-spot printing.[125]

An ink's formulation is a crucial aspect of material deposition for inkjet printing and solvent type and material concentration must be carefully optimized to achieve printability, an optimization process that must be performed individually for all deposited materials.[118] An illustration of system optimization prior to printing is shown in **Figure 2.8**.

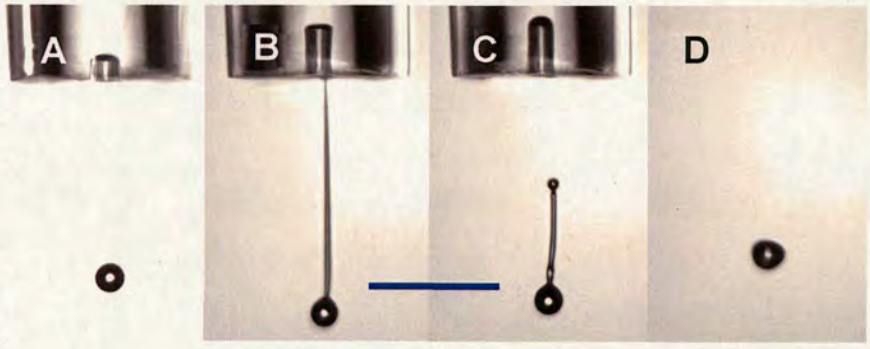

Figure 2.8 *Optimization of ink "printability": (A) correct drop morphology (solvent = NMP) (130 μs after impulse); (B) tail effect for a 1.5% solution of styrene/maleic anhydride copolymer in NMP. The drop is not printable because the tail does not detach from the nozzle (150 μs after impulse); (C) tail effect for a 0.5% solution of styrene/maleic anhydride copolymer (solvent = NMP); printable because tail detached from nozzle and the drop is reconstructed (150 μs after impulse); (D) drop of a 0.5% solution of styrene/maleic anhydride copolymer (solvent = NMP), 300 μs after impulse. Scale bar 500 μm. Printing parameters: voltage 140 V, impulse length 30 μs, frequency 100 Hz.*

Other factors which determine drop quality are voltage, impulse length and frequency. All these parameters are related to the piezo actuators (ceramic material) responsible for generating the force which pushes drops of fluid out of the nozzle. (**Figure 2.9**)

The core of the microdrop dispensing pipette is a glass capillary surrounded by a tubular piezo actuator. The capillary terminates in a nozzle (diameter 70 μm). Voltage pulses applied to the piezo actuator generate a pressure wave, (**Figure 2.9 B**) which flows through the glass into the liquid. Once the wave reaches the nozzle

region the pressure pushes a small liquid column out of the nozzle, which forms a droplet which flies freely through the air. (**Figure 2.9 D**)

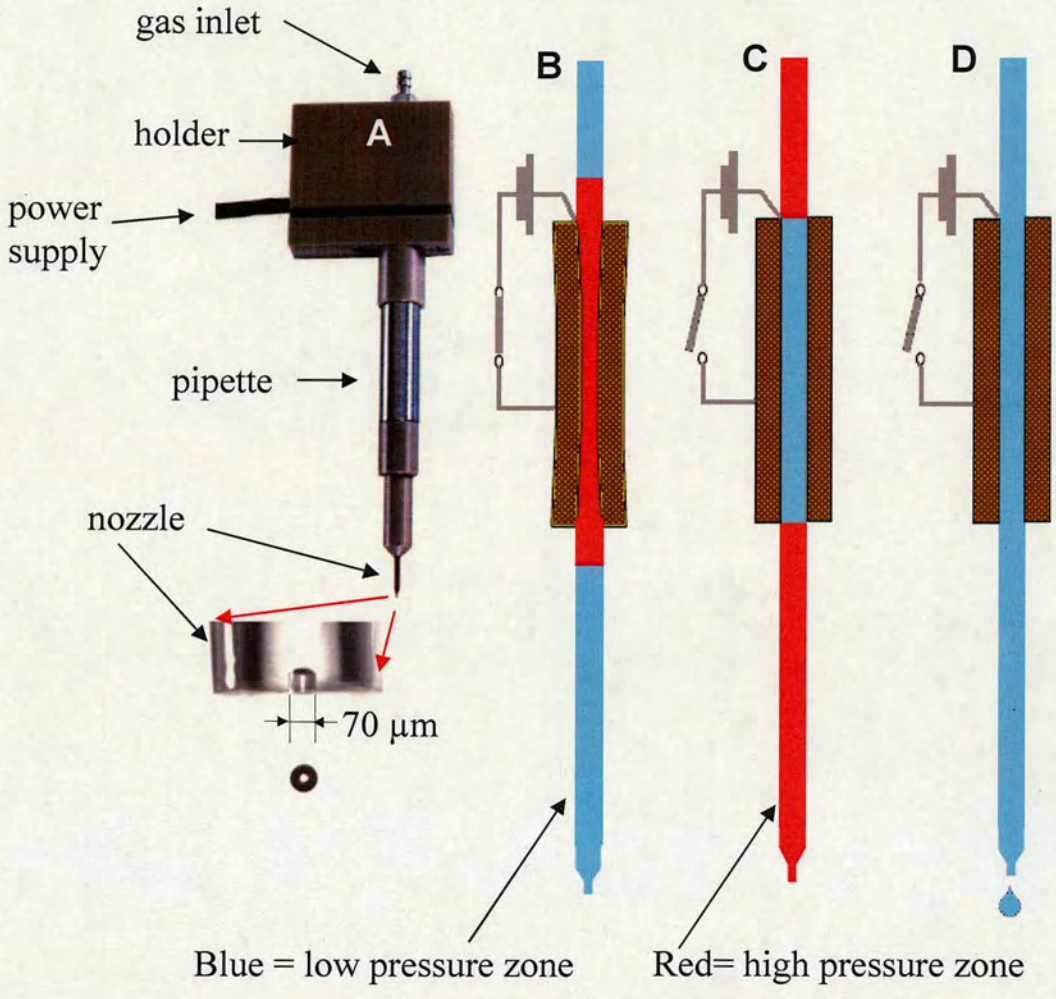

Figure 2.9 *Pipette for inkjet printing: (A) pipette and holder of a Microdrop inkjet printer; (B) power is applied to the piezo, generating an impulse and pressure wave flows through the glass into the liquid; (C) pressure wave flows through the glass capillary; (D) pressure wave reaches the nozzle and a drop is pushed out of the nozzle.*

If the voltage is too high, satellite drops are generated and if it is too low the voltage does not push liquid out of the nozzle. Values of impulse length indicate how long the voltage is applied to the piezo actuator. Too short an impulse causes insufficient piezo actuator contraction, while too long an impulse can disturb the relaxation

process before the next impulse. Frequency (*e.g.* 100 Hz) describes the number of drops generated per second, which can be changed up to 500 Hz without impacting on drop morphology when the voltage and impulse length are properly optimized. Most of the monomers used were printed as 50% w/v solutions in NMP. Printing parameters used for monomers in this work were 98 V, 29 μs and 200 Hz.

2.3 Choice of surface for high-throughput polymerisation

Another parameter which determines print quality, *e.g.* repeatability of spot shape, is the substrate upon which the drop is deposited. The advantages and disadvantages of glass (obtained from Menzel-Glaser), aminoalkylsilane glass (obtained from Sigma-Aldrich,), agarose coated (prepared in-house), hydrophobic surfaces (prepared *via* coating with TFCS, see section 6.2.1) and hydrophobic patterned slides (prepared *via* sucrose masking, see section 6.2.1) are discussed below.

Unmodified glass slides could not be used for printing most of the inks (polymers and monomers) because the spot shape was not uniform. (**Figure 2.10**) A second disadvantage was that glass was a "universal" cell binder.

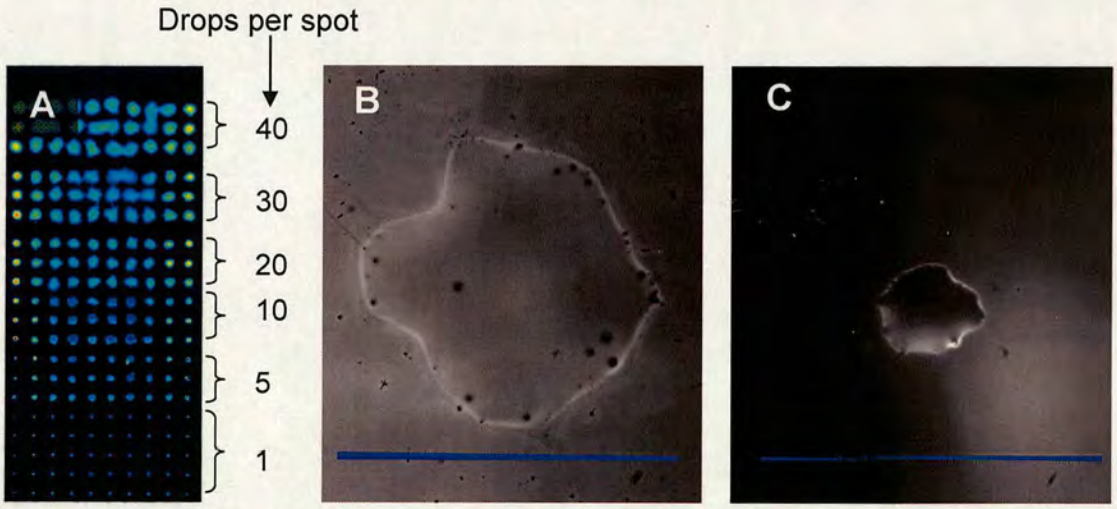

Figure 2.10 *Fluorescent scan of a microarray, 15 min after printing: (A) onto unmodified glass slide fluorescein in NMP (0.5% w/v); (B) expanded image of one of the features; 30 drops printed per position; (C) 1 drop printed per position (scale bars 1 mm).*

Aminoalkylsilane functionalized slides allowed much better shape/reproducibility. (**Figure 2.11**)

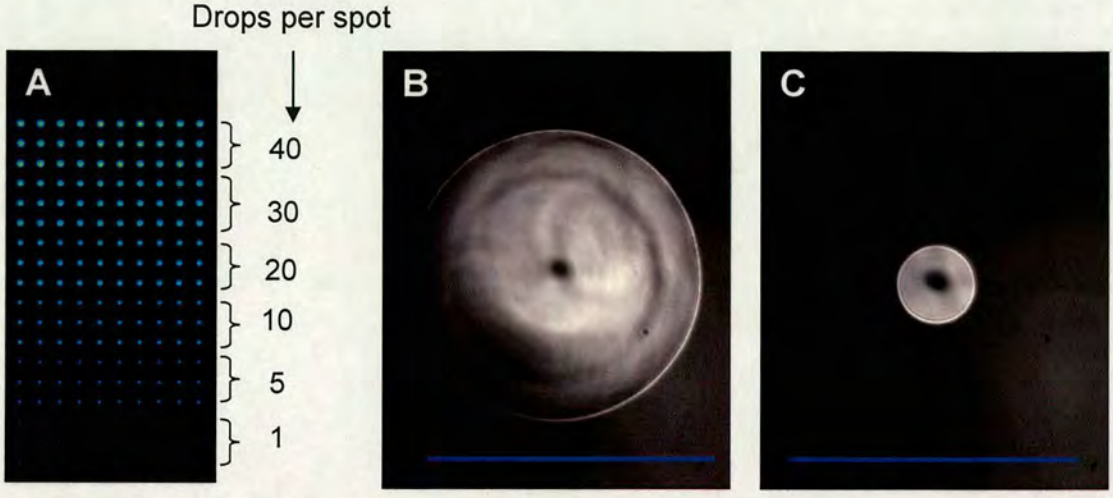

Figure 2.11 *Fluorescent scan of a microarray, 15 min after printing: (A) onto an aminoalkylsilane slide fluorescein in NMP (0.5% w/v); (B) expanded image of one of the features; 10 drops printed per position; (C) 1 drop printed per position (scale bars 350 μm).*

Glass slides covered with a thin layer of agarose are not toxic to cells, yet do not allow cellular adhesion[108], while agarose is able to absorb "ink" into its porous structure thus giving good spot repeatability and polymer immobilization. (**Figure 2.12**)

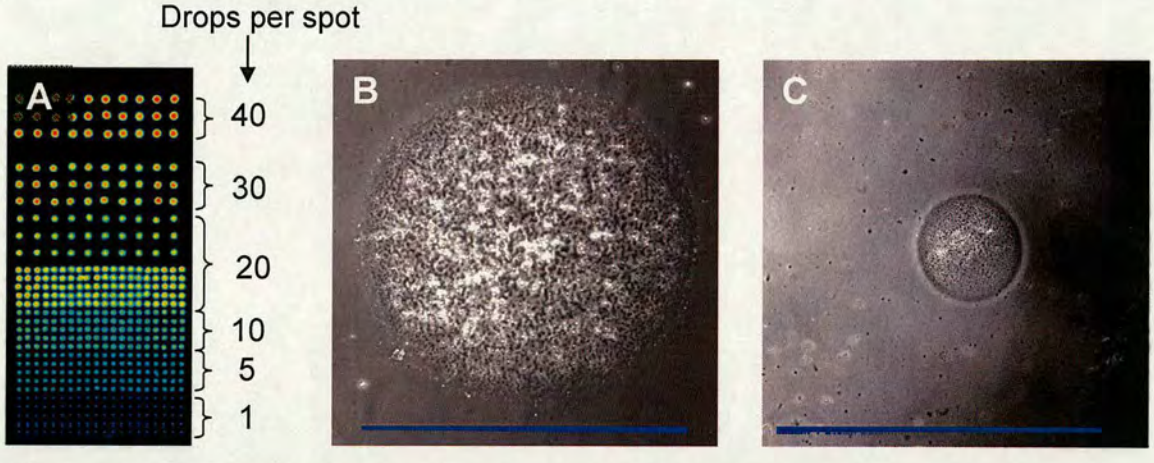

Figure 2.12 *Fluorescent scan of a microarray, 15 min after printing: (A) onto an agarose coated slide fluorescein in NMP (0.5% w/v); (B) expanded image of one of the features; 40 drops printed per position; (C) 1 drop printed per position (scale bars 1 mm).*

Glass slides coated with tridecafluoro-1,1,2,2-tetrahydroocctyl)dimethylchlorosilane (TFCS) become highly hydrophobic and allowed the generation of spots smaller than 200 μm. The interaction between the ink and the substrate was, however, weak so during evaporation the spots became smaller. This did not occur for other types of slide due to the much stronger interactions between the ink and the substrate, which is why the spot maintains its shape throughout the evaporation process at the region of adhesion in those cases. (**Figure 2.13**)

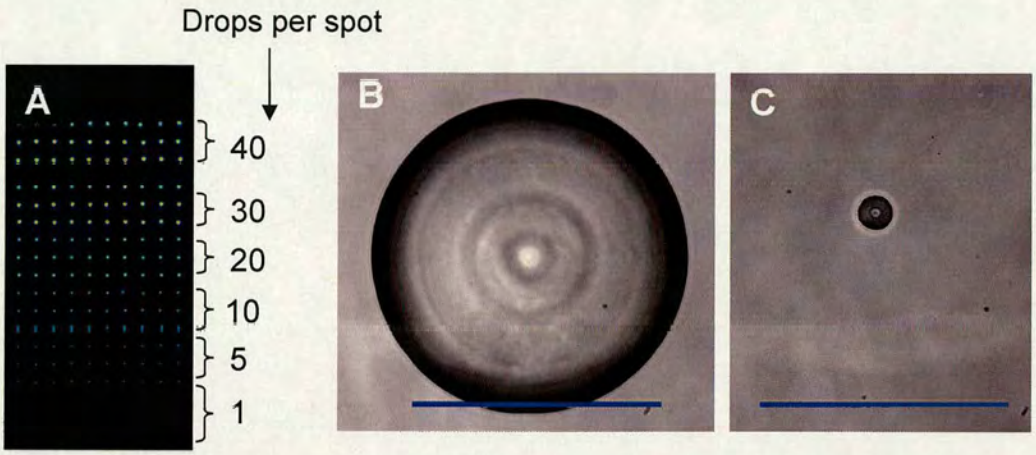

Figure 2.13 *Fluorescent scan of a microarray, 15 min after printing: (A) onto a hydrophobic slide fluorescein in NMP (0.5% w/v); (B) expanded image of one of the features; 30 drops printed per position; (C) 1 drop printed per position (scale bars 350 μm).*

Slides patterned with a sucrose mask (see section 3.6), treated with TFCS and then washed with water allowed good spot control. Hydrophilic areas surrounded by a hydrophobic frame allowed the ink to be kept in specific areas without flowing away from the site of deposition. (**Figure 2.14**)

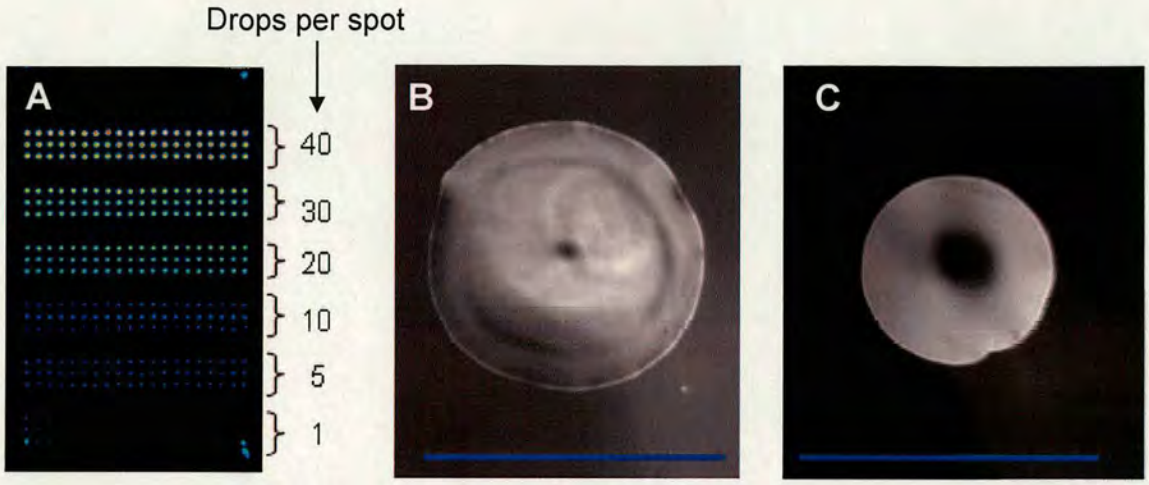

Figure 2.14 *Fluorescent scan of a microarray, 15 min after printing: (A) onto a hydrophobic patterned slide fluorescein in NMP (0.5% w/v); (B) expanded image of one of the features; 20 drops printed per position; (C) 10 drops printed per position (scale bars 350 μm).*

Spot size could be controlled by varying the number of drops deposited per spot. The relationship between the number of drops and the size of the resulting spot must be considered during microarray design. For example if the spots are deposited close to one another they can merge to form one bigger feature, thus a careful study of the relationship between the spot size and the number of drops per spot was essential. Another important factor was the number of spots on a given chip that is allowed for a given diameter of each spot. This issue is especially apparent in polymer synthesis on the surface of the chip, since (on one hand) it is beneficial to increase the number of individual figures per chip due to the fact that it increases the experiment efficiency for the chip, but on the other hand exceeding a certain number of drops in a spot leads to the aforementioned merging.

The smallest spots were generated when the ink was printed onto hydrophobic slides. Agarose coated and unmodified glass give similar spot morphologies but on agarose coated slides the spots were much more uniform. (**Figure 2.15**)

In conclusion, the choice of substrate for high throughput polymer synthesis depends on the desired final application of the microarray. In the work described in this part of the chapter, microarrays were used for screening for mES adhesion. Use of

agarose coated slides as a substrate provided excellent polymer adherence during polymerisation and prevented non-specific cell binding during cellular screening applications. Therefore, agarose coated glass slides were optimal for performing high throughput *in situ* polymerisations.

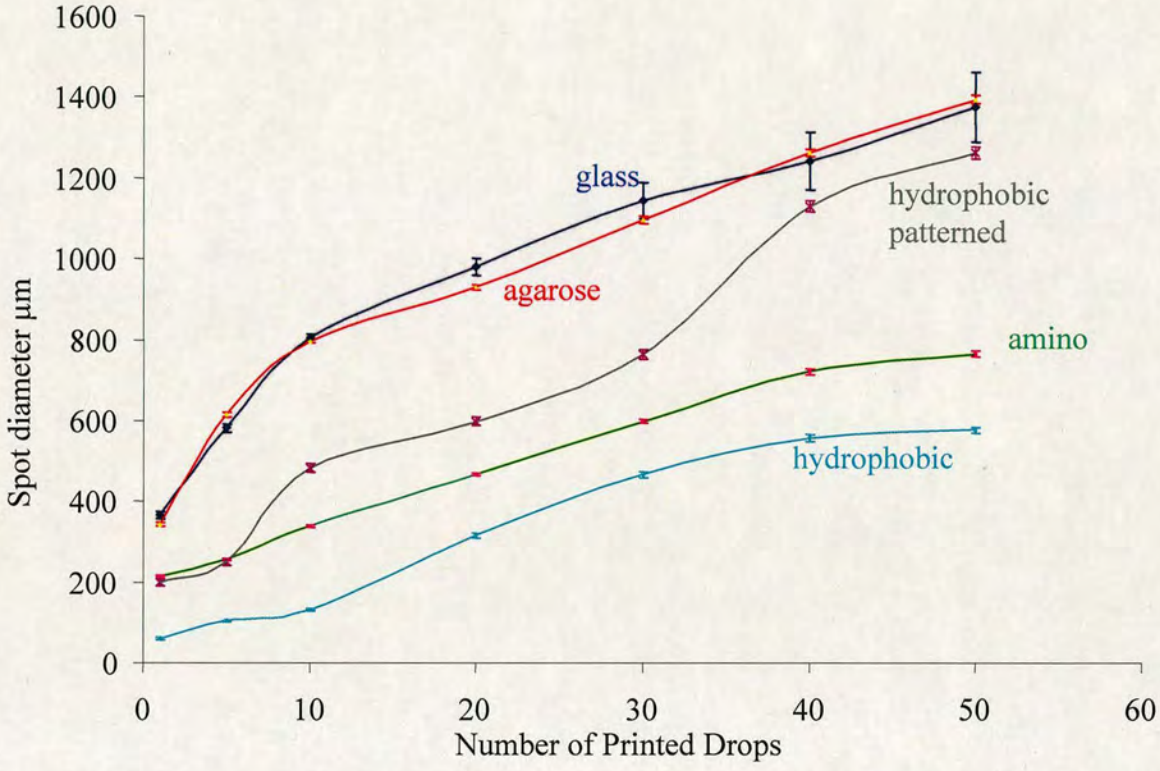

Figure 2.15 *Plot of spot diameter versus the number of printed drops. Blue line = glass surface, red line = agarose surface, grey line = hydrophobic patterned surface, green line = amino slide and cyan line = hydrophobic slide.*

2.4 High-throughput polymerisation – solving the evaporation problem

In liquid handling systems that operate on a microscale (such as inkjet printing) the evaporation of deposited material is an important and challenging issue. Firstly, evaporation determines the final morphology of deposited material[122] and morphology can trigger specific properties such as peptide and protein absorption or cellular adhesion. A high boiling point solvent[108] and high humidity[124] are applied to

ensure slower evaporation and better (more uniform) features. Secondly, performing chemical reactions on a gram-scale or a nano-gram scale requires the prevention of evaporation. On a gram-scale, the problem is resolved by using a reflux condensation system or simply by sealing the reaction vial. This approach is not achievable on a nano- or micro- scale, where the materials are printed on unsealed slides. In order to overcome this problem, Zhang *et al.* performed *in situ* nanolitre-scale polymerisation *via* inkjet printing using high (50%) humidity in order to prevent evaporation.[124] This approach limits the range of used monomers because only those resistant to the presence of water during polymerisation can be used. Langer *et al* reported using UV initiated radical polymerisation directly in a microarray format. In this case the monomers were pre-mixed in 364 well plates prior to deposition on the slide. Langer used high molecular weight monomers in order to overcome evaporation problems, the range of monomers used was thus limited.[106] In order to prevent evaporation a new method was developed here.

Co-polymerisation on an array requires mixing of two or more monomers. The time between spotting the first and the second monomer could vary between 1 to 40 min (if a large library of compounds is being generated). Volatile monomers would thus evaporate from the substrates before the second monomer could be printed. To prevent evaporation, over 20 different approaches were evaluated. One approach was to use a calorimetric bomb in order to increase the pressure in the reacting system. Another approach was to synthesize polymers in confined volumes, which was achieved in pipette tips and also in 364 well plates. In order to confine the volume, an approach in which monomers were printed onto a glass slide which was then covered by another slide was tested. The most successful strategy was to use paraffin oil to prevent evaporation. (**Figure 2.16**)

Paraffin oil was placed onto a microscope glass slide (thickness of the oil = 150 μm) and drops of monomer printed. These "sank" due to their density and after UV initiated polymerisation (oil is transparent to UV radiation) slides were washed to remove the oil from the slide. The efficiency of this process was confirmed experimentally. Thus, 100 spots of ink (water) were printed and analysed over 15

min on slides with and without an oil layer. With oil, the printed array could be stored for more than 3 h without any mass loss. (**Figure 2.17**)

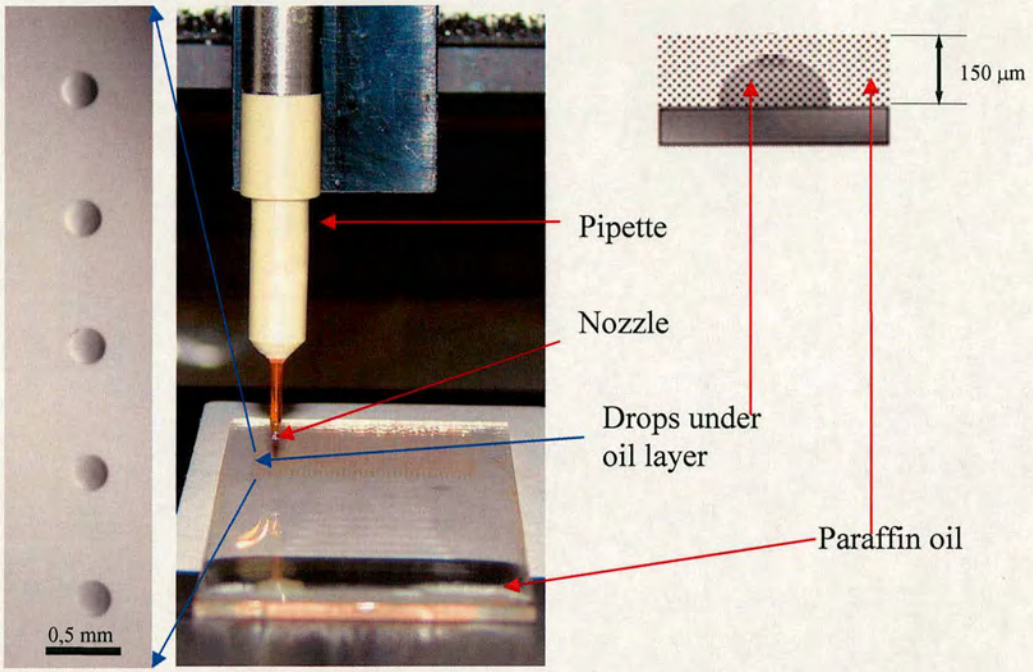

Figure 2.16 *Paraffin oil as evaporation protector during monomer inkjet printing and polymerisation.*

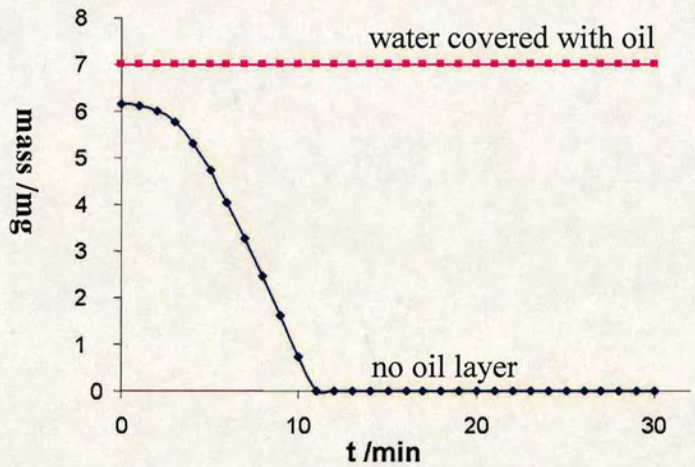

Figure 2.17 *Evaporation of water droplet printed on a microscope slide via inkjet printing.*

Thus, an oil layer prevented evaporation and allowed polymerisation on a nano-litre scale regime using a broad range of monomers.

2.5 Inkjet fabrication of polymer microarrays and grids

Polymer microarrays consisting of spots or a matrix of inter-crossed lines were fabricated by *in situ* inkjet printing of monomers and initiator solutions in organic solvents through an oil film, allowing the rapid generation of a broad range of co-polymers without issues of selective monomer evaporation. In all experiments a layer of oil was used which covered the whole slide (0.3 mL/slide – 150 μm thick). The thickness was important for a number of reasons. The path of a drop travelling through the oil should be as short as possible so that minimal diffusion takes place, while the oil layer has to be thick enough to cover the whole slide uniformly. The inkjet based approach allowed the rapid preparation of patterned polyacrylates as either inter-crossed matrices of polymers or a series of features on agarose coated glass slides using *in situ* nL/pL scale polymerisation. (**Figure 2.18**)

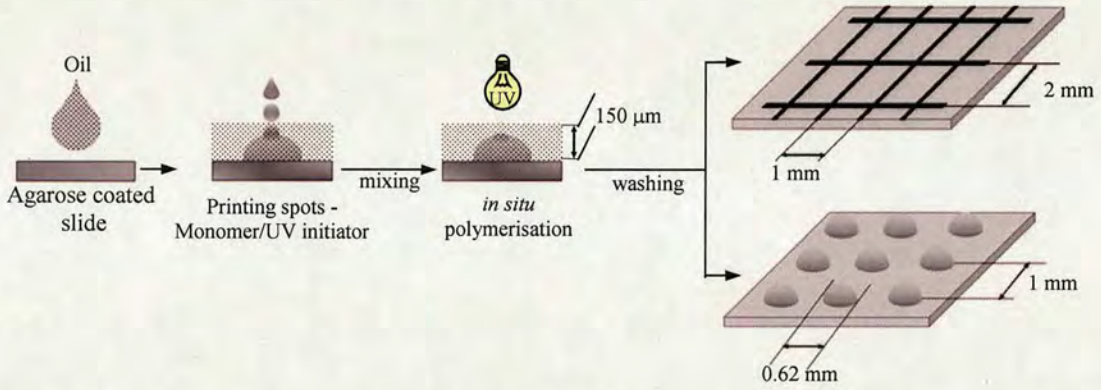

Figure 2.18 *The two approaches used to prepare the in situ co-polyacrylate patterns. An oil film was used to prevent evaporation of the nanolitres of monomer solutions while maintaining the pattern on the glass surface. Following UV photopolymerisation and removal of the oil film the polyacrylate library remained on the agarose slide.*

The oil film did not just prevent solvent evaporation but it also allowed *in situ* polymerisation upon UV irradiation and provided excellent spot morphology after removal of the oil film. (**Figure 2.19**) The drops of monomer solutions sank and settled down on the agarose layer due to the fact that the density of the monomer

solution was greater than that of the oil. For this reason a robust microarray is formed. (see section 6.3.2)

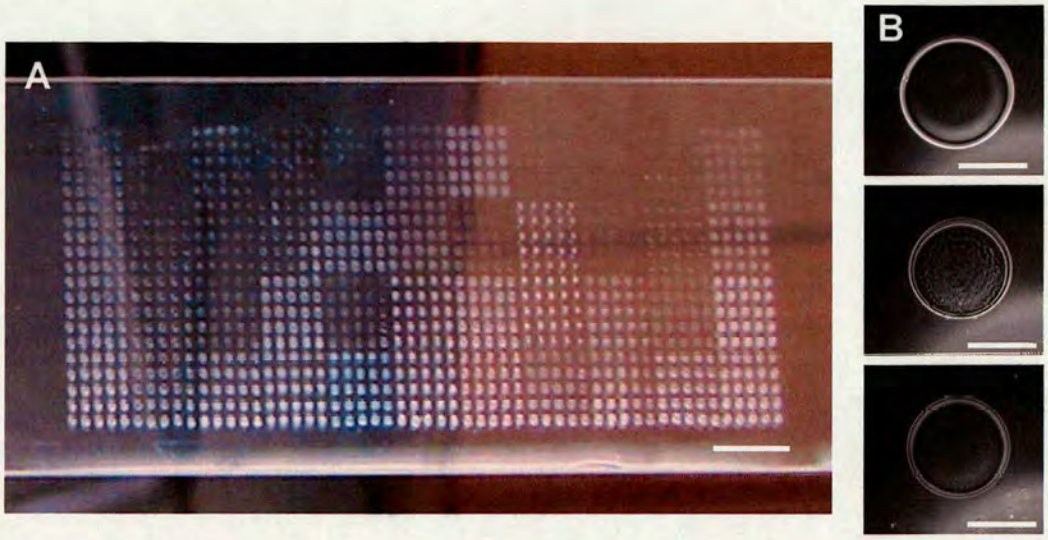

Figure 2.19 *Image of (A) microarray containing 44 (x25) co-polyacrylates synthesised in situ following removal of the oil film. 16 identical spots of each co-polymer were printed (scale bar 5 mm); (B) phase contrast microscopy images of polymer features: 2-(methylthio)ethyl methacrylate (top), DVB (middle), 2-methoxyethyl methacrylate (bottom). Scale bar 0.5 mm.*

The inkjet printer was used to rapidly print monomer solutions pre-mixed with a UV initiator (2,2-dimethoxy-2-phenylacetophenone) onto slides with specific numbers of drops of the desired monomer printed in any defined position on the grid or array. The use of agarose coated slides as a substrate, provided excellent polymer adherence during polymerisation and prevented non-specific cell binding during cellular screening applications and the oil layer could be removed subsequently by washing with ethanol. Polymer microarrays were fabricated by printing 50 drops (per feature) of each monomer solution (**Table 2.1**) with a 1 mm pitch between spots. Co-polymers were fabricated by printing 25 drops of each monomer.

Using this approach polymers were synthesised with feature sizes of 0.62 mm with a density of 100 spots/cm^2. (**Figure 2.19**)

Most of the polymers prepared *via* this microarray approach had identical molecular weights to those prepared using more conventional conditions (50% w/v monomer solutions with 5% (w/w) initiator mixed and polymerised in a glass vial with UV

initiation for 30 min (see section 6.3.4) as analysed by GPC, **(Table 6.7)** except 2-vinylpyridine which had a much higher molecular weight when prepared using the inkjet printing approach (82 kDa versus 17 kDa); while 2-hydroxylethyl methacrylate gave the opposite result (11 kDa on the array versus 48 kDa conventionally).

Line number	Monomer[a]	Line number	Monomer[a]
1	butyl methacrylate	13	glycidyl methacrylate
2	ethyl methacrylate	14	ethoxyethyl methacrylate
3	N,N-diethylacrylamide	15	methyl methacrylate
4	4-vinylpyridine	16	N-isopropylacrylamide
5	2-vinylpyridine	17	N-tert-Butylacrylamide
6	2-(methylthio)ethyl methacrylate	18	3-(trimethoxysilyl)propyl methacrylate
7	benzyl methacrylate	19	*tert*-butyl methacrylate
8	2-methoxyethyl methacrylate	20	N,N-dimethylacrylamide
9	2-hydroxyethyl acrylate	21	4-hydroxybutyl acrylate
10	divinylbenzene	22	methyl acrylate
11	styrene	23	ethylene glycol methacrylate
12	poly(ethylene glycol) monomethacrylate – Mn 360	24	4-bromostyrene

[a]*Each solution contained 50% w/v monomer in NMP and 5% w/v UV initiator.*

***Table 2.1** Monomers used for the fabrication of the polyacrylate arrays and grids.*

The same oil coating technique was used to prepare grids of polyacrylates. Grids were fabricated through printing and polymerisation of the 24 solutions of the monomers in NMP. (**Table 2.1**) Monomers were deposited in a grid pattern, so that lines contained homopolymers, (**Figure 2.20 A**) whereas nodes contained copolymers. (**Figure 2.20 B**) Lines were generated by printing drops onto a slide with movement of the pipette along a linear path at a constant velocity (10 mm/s) and a constant printing frequency (100Hz). To illustrate the presence of gradients at the cross points, some monomers were mixed with fluorescein (0.5% w/v) so that the concentration changes along the lines were clearly visible. (**Figure 2.20**)

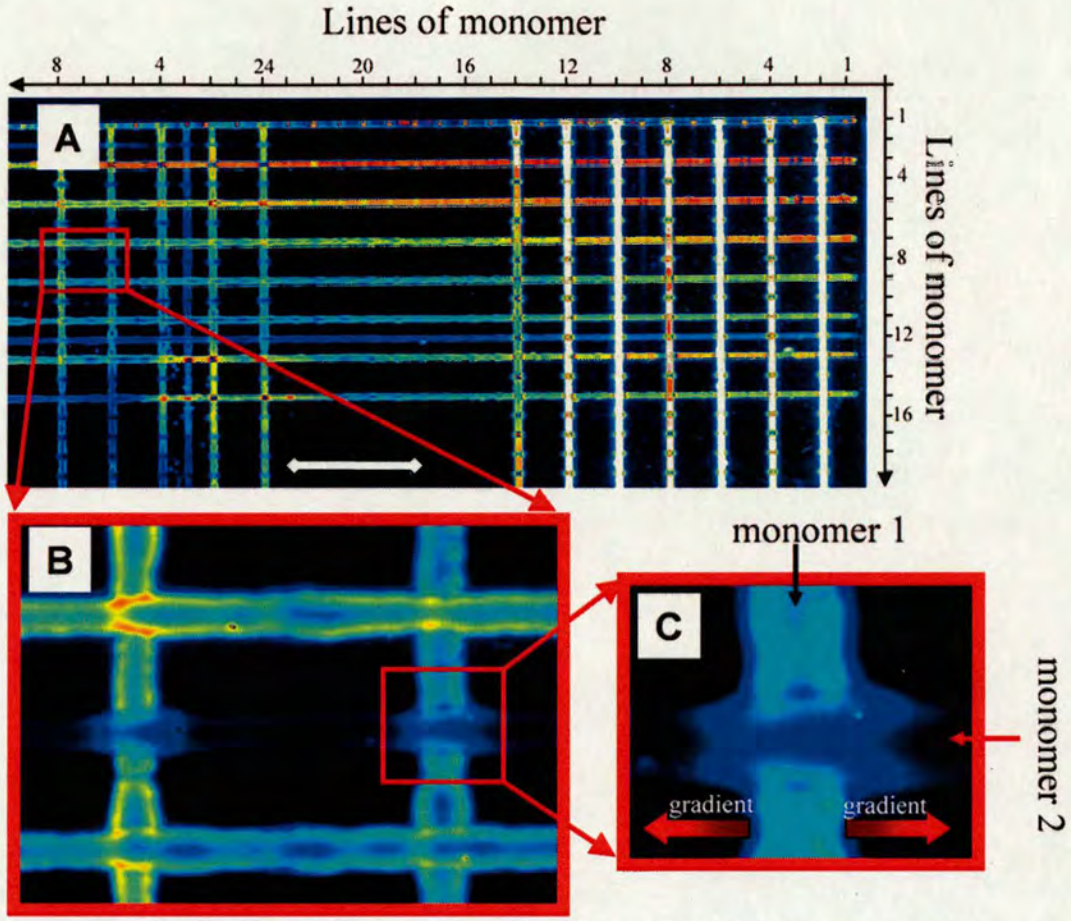

Figure 2.20 *Fluorescent images of a polyacrylate grid fabricated in situ. Fluorescein was used as a dye to image the generated grid: (A) grid generated by inkjet printing 24 monomers in horizontal and vertical lines, the numbers on the axis corresponds to the monomers listed in Table 4.1 (scale bar 5mm); (B) six nodes showing the diffusion effect between high and low concentration of fluorescein as a indicator of monomer gradients (scale bar 1 mm); (C) a single node.*

In conclusion, the fabrication of the polyacrylates in both a microaray and a grid-based format using inkjet printing through oil (to prevent monomer loss) with UV initiation is reported. This allowed rapid fabrication of arrays of co-polyacrylates and now allows access to a broad range of new polymers in both a highly miniaturized and highly productive manner, which can then be screened for a number of physical/ biological properties.[127]

2.6 Screening for mES adhesion on microarrays and grids prepared *via in situ* polymerisation

Polymer microarrays (4 replicates) and polymer grids (4 replicates) were used for cellular screening of mES-Oct4 cells. Cells were seeded onto a slide ($7x10^5$ cells per slide) and incubated in a four well-rectangular plate (Nunc, Denmark) for 48 h in medium supplemented with leukemia inhibitory factor (LIF). Cells attached on the slides were fixed with formaldehyde and stained with Hoescht 33342.

Poly 2-(methylthio)ethyl methacrylate and poly(divinylbenzene) showed high mES cell binding. The cells attached on these polymers were uniformly spread over the polymer features. Poly(ethyl methacrylate), benzyl methacrylate /divinylbenzene co-polymer (1:1 weight ratio) did not show good affinity for mES cells. However, this type of polymer and mES cells interaction (3D cellular structures) has been observed previously when mES cells were cultivated on collagen type I (see section 4.3). Collagen is a well known universal cellular binder, widely applied in cell culture,[115] therefore low affinity for mES cells was rather unexpected. Explanation of such specific cell-polymer interactions was found in the principles of cellular adhesion. Typically mES cells are cultivated using gelatine and tissue culture plastic. Thus a sudden change of adhesive surface shocks mES cells which may result in the appearance of 3D cellular structures rather than cellular monolayers. (**Figure 2.21**)

mES cell cultivation on grids resulted in patterned cells aligned to polymeric lines. (**Figure 2.22**) Importantly, in terms of reproducibility and comparability of the two platforms the mES cells grew on identical polymers on both the "grid" and "spot" based microarrays. In summary microarray screenings allowed the selection of two polymers as substrates for mES-Oct4 cell proliferation experiments. (see section 2.7)

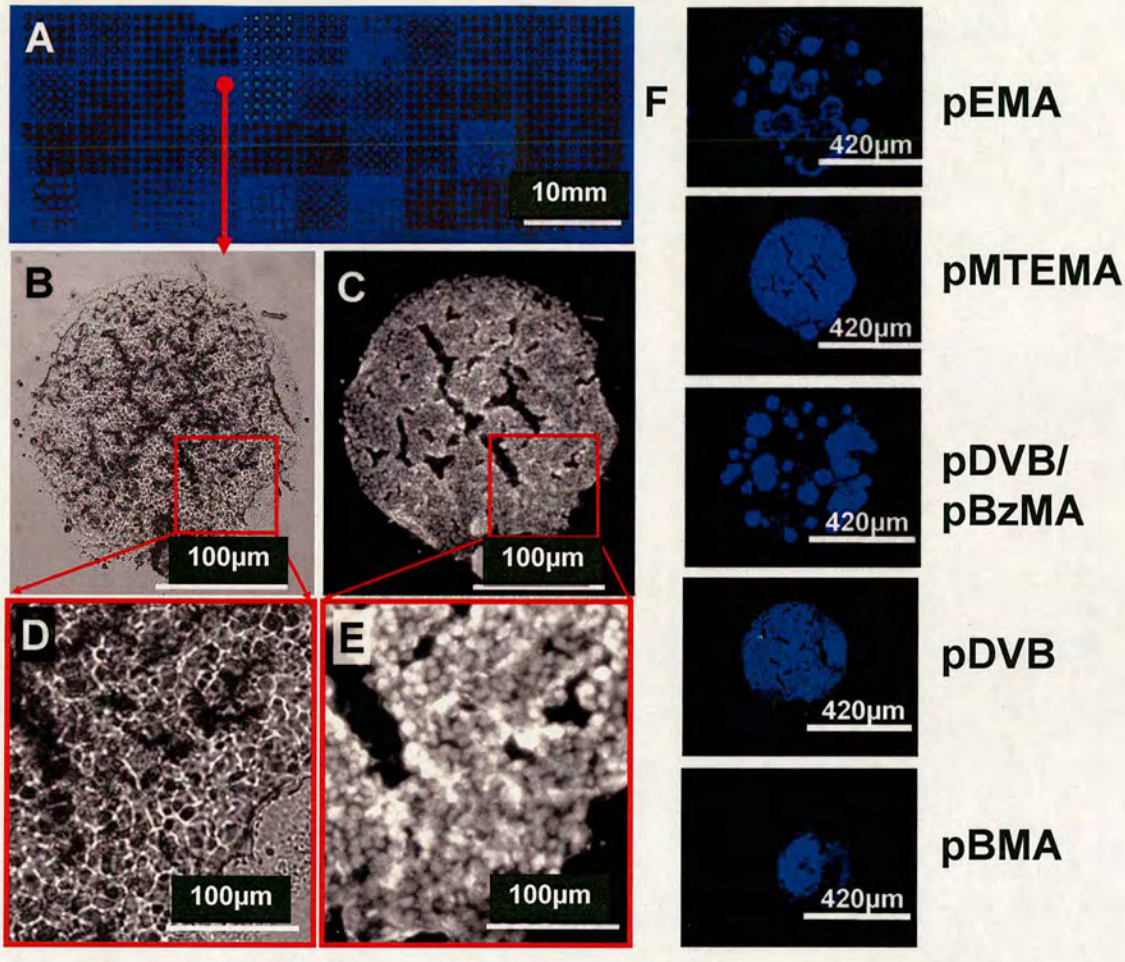

Figure 2.21 *Images of mES cells grown for 48 h on an in situ fabricated polymer microarray. Cells were treated with* Hoescht *33342 (a nuclei stain). Fluorescent images were obtained using 350 nm excitation and 460 nm emision filters. (A) Fluorescence image of the whole slide; (B) and (D) bright field images of mES cells on poly 2-(methylthio)ethyl methacrylate; (C) and (E) are fluorescent images; (F) mES-Oct4 cells on polymer spots from top: poly ethyl methacrylate, poly-2-(methylthio)ethyl methacrylate, benzyl methacrylate /divinylbenzene co-polymer (1:1 weight ratio), poly divinylbenzene, poly benzyl methacrylate.*

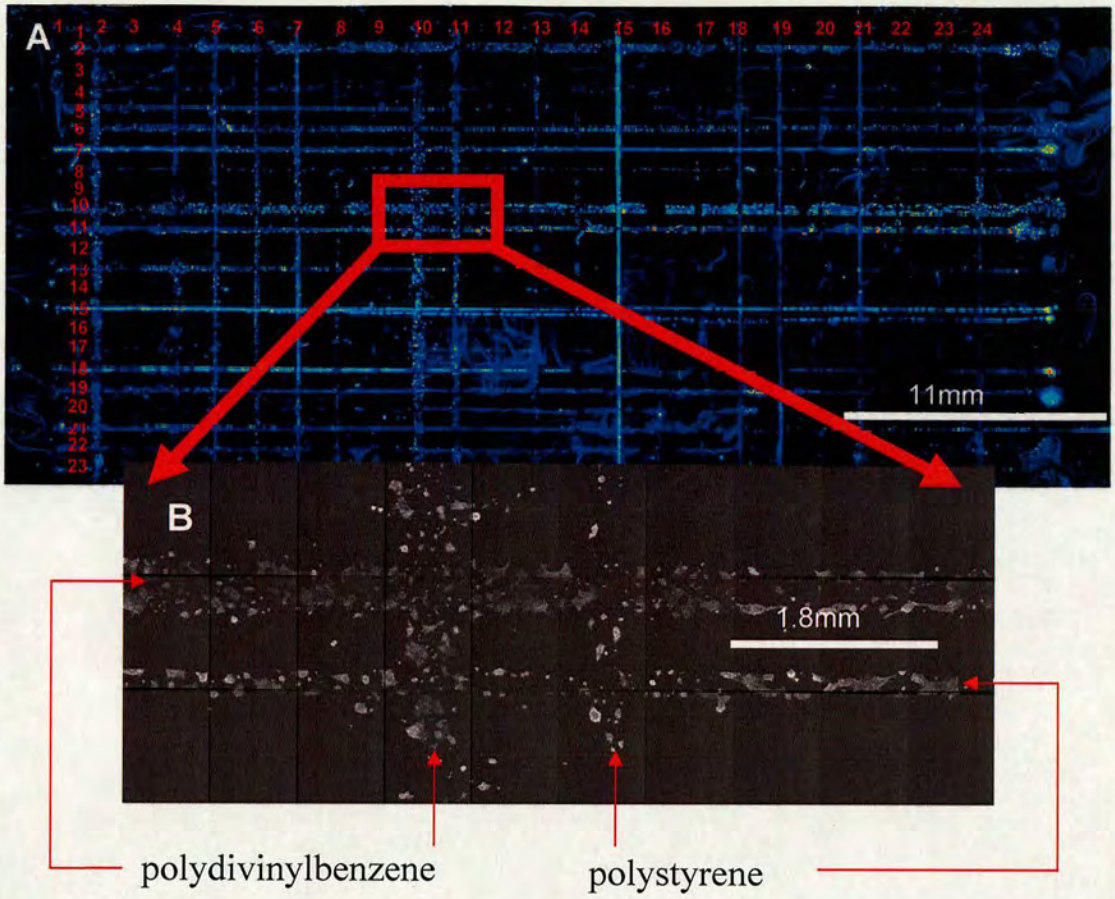

Figure 2.22 *The screening results of mES cell adhesion on grids prepared via high throughput polymerisation: (A) mES cells bound on polymer grids on an agarose coated glass slide, fixed with formaldehyde (4% wt) and stained with Hoechst 33342 (nuclei stain). The image (scale bar 10 mm) was taken with a "low resolution (30 μm)" BioAnalyzer scanner (LaVision Bio Tech); (B) mES cells grown on the polymeric lines.*

2.7 Coverslip experiments

The capacity of polymers for cellular attachment established by an initial microarray screening had to be confirmed by scale-up experiments on cover slips.

On the coverslips the binding surfaces are significantly larger than the analogous polymer areas on the microarray (the diameter of cell binding polymeric spots varied between 0.4 to 0.7 mm). The larger available area for cells meant that experiments investigating proliferation could be carried out, allowing observation of the growth rates of cells and cell morphology. Another benefit of using a larger binding area was

that cells could be attached to surfaces and incubated independently. **(Figure 2.23)** Poly (2-(methylthio)ethyl methacrylate) was deposited onto coverslips (13 mm diameter) as a thin uniform layer. In order to spread polymer onto coverslips, the polymer was dissolved in a low boiling point solvent (THF). Solvent evaporated quickly after the polymer solution had been dispersed by spin coating and coverage of the slide was formed on the coverslip. Due to lack of solubility of poly(divinylbenzene) (a cross linked polymer) 100 μL of divinylbenzene solution (50% w/v in NMP) containing 0.5% of 2,2-dimethoxy-2-phenylacetophenone (UV initiator) was placed on the coverslip and UV photo-polymerized. Cells were grown on the coverslips (see section 6.1.9) for 8 days. **(Figure 2.23)** As a reference, a disc of the tissue culture plastic (13 mm diameter) coated with 0.1% gelatine solution was used.

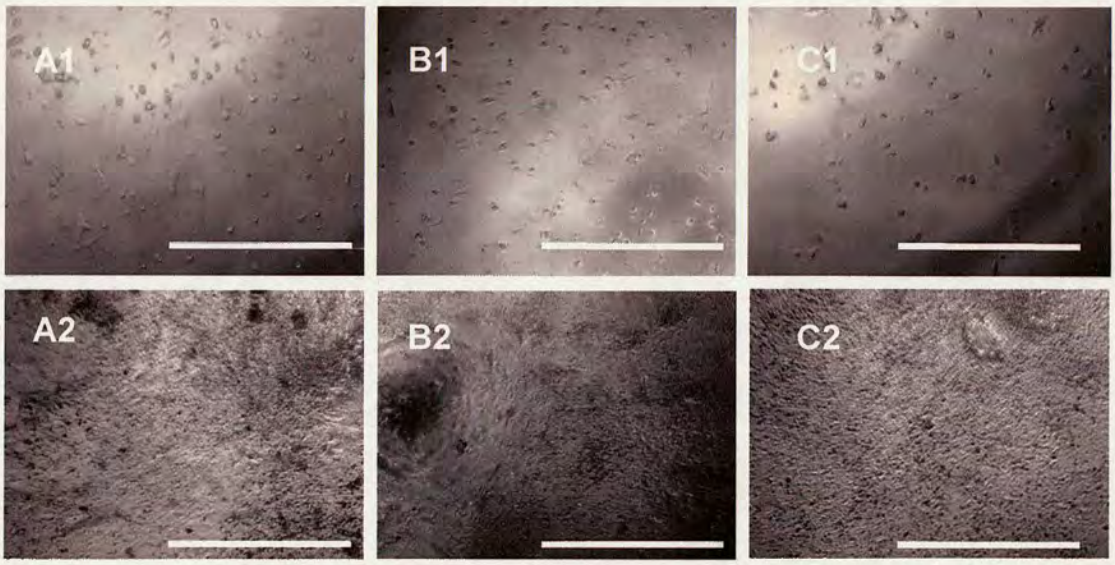

Figure 2.23 *Images of mES-Oct4 cells growing on: (A) a standard tissue culture plastic (disc 13 mm diameter, coated with 0.1% gelatine; (B) poly 2-(methylthio)ethyl methacrylate coated coverslip (C) poly divinylbenzene coated coverslip; (A1, B1, C1) bright field image of living cells after 24 h incubation; (A2,B2,C2) 7 days incubation showing a layer of cells on polymeric surfaces (Scale bars 0.25 mm). Images were taken with a Leica microscope using a 5x/0.12 objective.*

Cells were harvested (using trypsin) from the polymer surfaces and analysed by flow cytometry in order to calculate cell numbers and look at changes in fluorescence.

mES-Oct4 cells have the gene for GFP fused to Oct. Oct4 is present in immature undifferentiated cells only,[128] meaning that analysis of GFP allows easy recognition of differentiated and non-differentiated cells (by flow cytometry). (**Figure 2.24**) Four independent experiments were run.

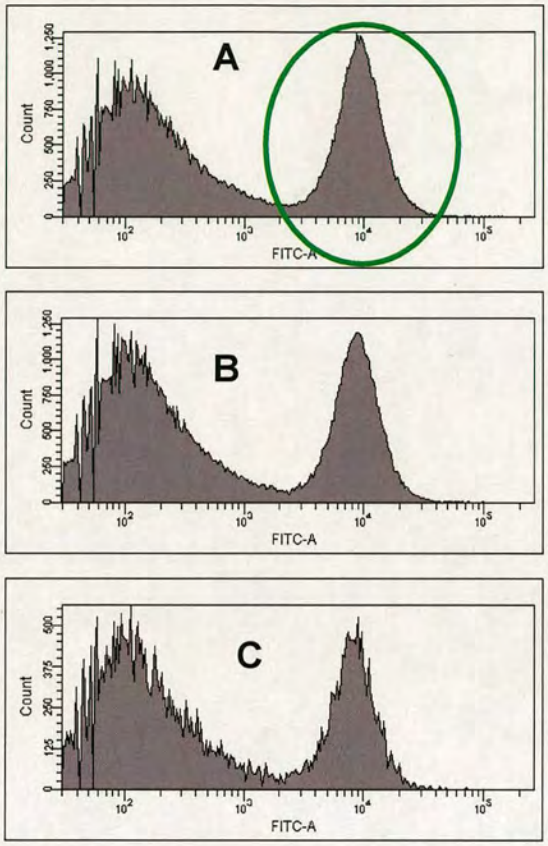

Figure 2.24 *Flow Cytometry results of mES-Oct4 cells. Cells harvested from the mES cell population incubated after 8 days (A) on tissue culture plastic coated with 0.1% gelatine; (B) poly divinylbenzene; (C) poly 2-(methylthio)ethyl methacrylate. Green circles indicate the fluorescent population of non differentiated cells.*

All samples analysed by flow cytometry were prepared according to the same procedure (see section 6.1.10). The procedure allowed for evaluation of number of cells present on the coverslip. (**Table 2.2**)

Results from analysis by flow cytometry of cells attached to coverslips covered with polymers showed that as found previously, the tissue culture plastic covered with gelatine provided the highest protection from cell differentiation. Gelatine provided a culture surface that allowed 55% of cells to remain in undifferentiated state. In

contrast, polymer poly 2-(methylthio)ethyl methacrylate promoted the undifferentiated state of only 30% of cells. However poly (divinylbenzene) was almost as good at preventing differentiation as gelatine. The crucial advantage of artificial polymers is that they are free of bio-contamination.

Coverslip coated with	**cells/coverslip** [a] **/10^6**	S.D. n=4 **/10^6**	Undifferentiated cells (%)	S.D. n=4
TCP [b], gelatine,	1.14	±0.13	54	±7.5
pDVB [c]	2.01	±0.46	40	±8.6
pMTEMA [d]	0.83	±0.25	29	±2.7

Notes: a) Average number of cells attached on coverslip; b) TCP = tissue culture plastic flask; c) pDVB = poly divinylbenzene; d) pMTEA = poly 2-(methylthio)ethyl methacrylate.

Table 2.2 *FACS results of the differentiation of mES cells under different conditions.*

2.8 Conclusions

In conclusion, the fabrication of arrays of polymers generated either as spot-based microarrays or as grids, *via* inkjet printing through oil, has been demonstrated allowing the generation of large arrays of co-polymers in a highly miniaturized, automated and highly reproducible manner, giving polymers with excellent spot morphology (on the micro-array platform). These arrays of polymers were used to identify polymers for selective mES cells binding. Polymer microarrays prepared by high-throughput polymerisation have proven to be useful tools for the selection of cell binding polymers. Screening of microarrays with mES cells allowed the selection of 2 polymers which were later tested on coverslips for comparison of their ability of mES cell cultivation compared to traditional substrates used for mES cultivation. The most important achievement was increasing the experimental efficiency by the preparation of polymer microarrays by *in situ* polymerisation instead of traditional gram scale polymer synthesis.[127]

Chapter 3 : Identification of polymers for human corneal epithelial cells (HCEC) growth and transfer

3.1 Corneal epithelium-structure, maintenance and treatment

The corneal epithelium is composed of regenerating multiple cellular layers. (**Figures 3.1** and **3.2**)

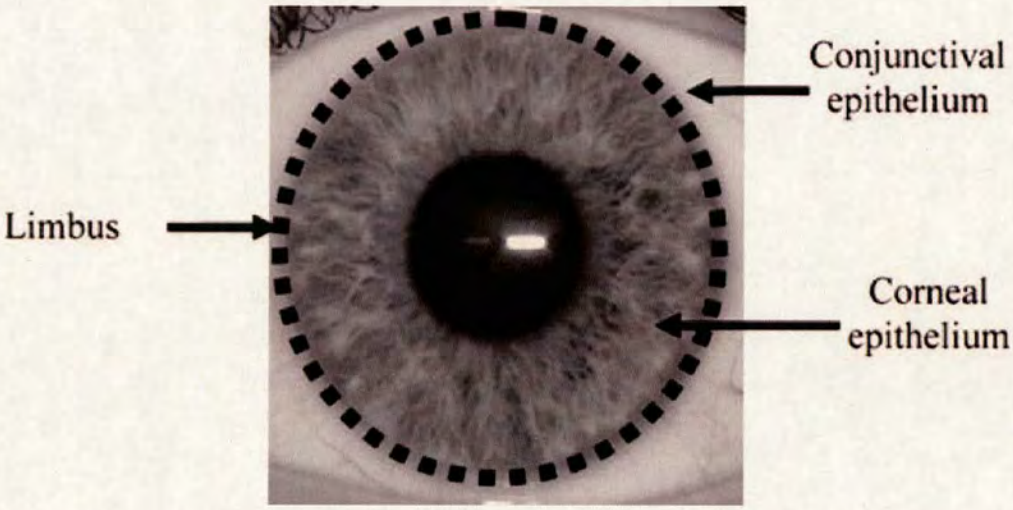

Figure 3.1 *Image of human eye. Limbal epithelial stem cells reside in the limbus along the dashed line. This figure is reproduced with permission (copyright Springer, 2007).*[129]

Under normal conditions and following injury, the maintenance of the corneal epithelial cell mass is possible thanks to the unipotent stem cells present inside the top layer of the limbus.[130-133]

Corneal epithelium failure

Limbal epithelial stem cell failure leads to loss of vision and great discomfort and since the eye is not able to repair itself in other, ways, ultimately blindness will follow. Patients with partial limbal epithelial stem cell disorder[134] could be treated by the application of bandage contact lenses that could serve as an artificial epithelium and protect the patient from complications, such as stromal melting[134] or persistent epithelial

defects.[134] In cases of extensive limbal epithelial stem cell failure, a population of limbal epithelial stem cells must be supplied in order to restore corneal epithelium.

Corneal epithelium surgical treatment

Surgical procedures for corneal epithelium treatment include the transplantation of limbal tissue.[135-137] Transplantations of corneas have high success rates, although the post-transplantation cornea can exhibit functional and structural changes in terms of endothelial cell morphology and gradient of the density of the cells in the epithelium.[138] Cornea transplantation operations, which require transplantation of the whole cornea (a full-thickness, 360°), often result in complete removal of nerve supply to the transplanted tissue[139,140] so hypoesthesia (a loss of sensitivity to sensory stimuli) persists for several years after initial surgery.

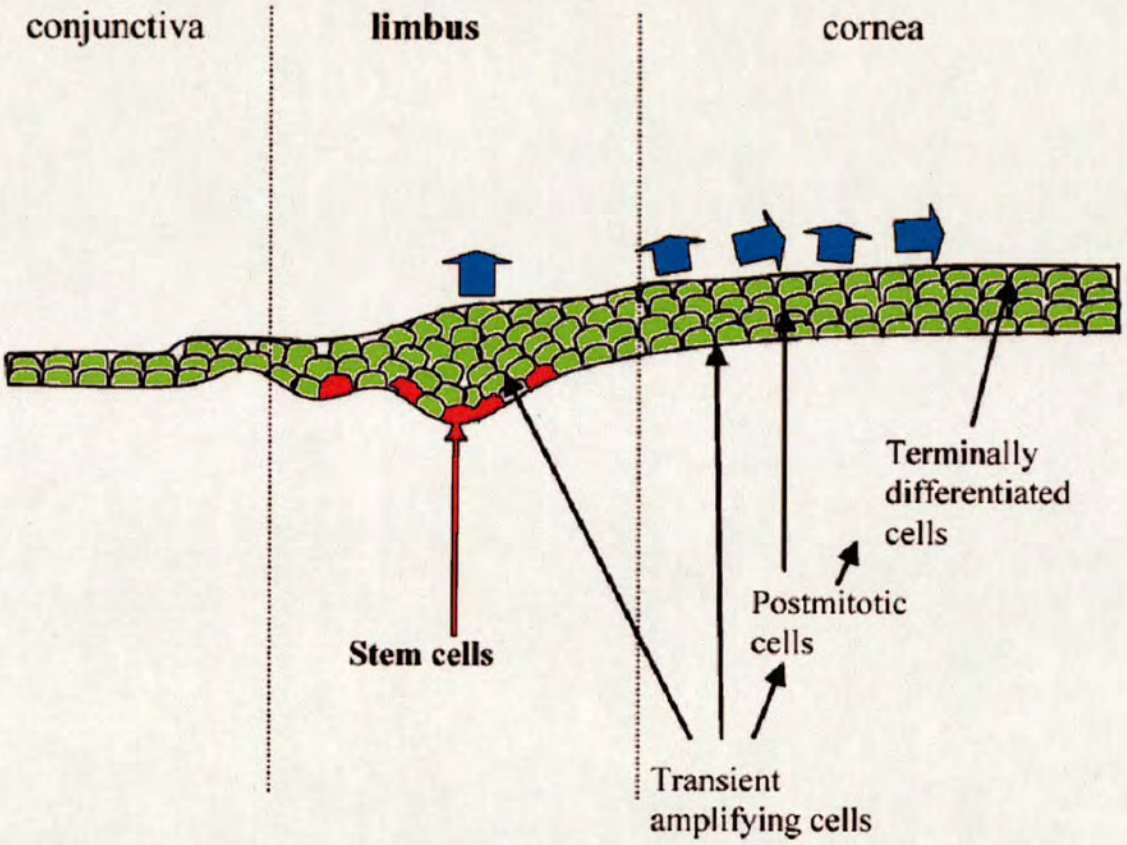

Figure 3.2 *Scheme of human eye epithelium. Limbal epithelial stem cells (red) give rise to transient amplifying cells (blue arrows), which migrate towards the superficial layer of the corneal area ultimately forming the terminally differentiated corneal ephitelium (green). This figure is reproduced with permission (copyright Springer, 2007).*[129]

Corneal epithelium alternative treatments

The alternative to cornea transplantation is the technique of *ex-vivo* expansion and transplantation of limbal epithelial stem cells from the cornea which was first described by Pellegrini *et al.*[141] The cell culture technique used was based upon that developed for the cultivation of epidermal keratinocytes.[142] Briefly, limbal tissues (2x2 mm^2) are harvested from a healthy eye. Limbal epithelial stem cells are isolated and cultured to give a sheet of cultured limbal epithelium suitable for transplantation. After surgical removal of the abnormal epithelium and limbus, the cultured cells are transplanted onto the eye of the patient. The advantage of this technique over conventional treatments is that small numbers of cells are required for starting *ex-vivo* cellular expansion and the necessary limbal epithelial stem cells can be isolated from healthy areas of the patient's eye. In this way, risk of rejection is reduced because the donor of the cells is also the acceptor of the cells.

Recent techniques for the fabrication of sheets containing limbal epithelial stem cell for transplantation

Two methodologies have been used to produce epithelial sheets containing limbal epithelial stem cell for transplantation; the suspension culture system and the explant culture.

Suspension culture system

The suspension culture system involves separating the epithelial cells from the stroma and then using trypsin (for separating the epithelial cells from one another) prior to seeding[141, 143-145] either onto a plastic tissue culture dish containing a feeder layer of growth-arrested 3T3 fibroblasts[147] or onto an amniotic membrane[148]. Culture medium is added and the cells are incubated for up to 3 weeks. Confluent epithelial sheets can be transferred to the ocular surface using a fibrin gel,[146] collagen shield[143] or contact lens.[141,143]

Explant culture

The explant culture procedure is performed using human amniotic membrane as both a substrate for growth of limbal epithelial stem cell and also as a carrier. A fragment of the limbal tissue (biopsy) is adhered to the amnion. Limbal epithelial cells migrate out of the

biopsy and proliferate on the amnion.[149] The disadvantages of using amniotic membrane are the unpredictable biological variability between donor tissues, limited tissue availability and the risk of viral disease transmission and costly donor screening.

New approaches to the fabrication of limbal epithelial stem cell sheets

Limited number of attempts have been made to overcome the problems mentioned above and to develop a technique more effective and appropriate for a greater number of patients.

For example, the culture and delivery of limbal epithelial cells using a fibrin substrate has been described.[141] Another approach is based on temperature-sensitive polymers.[150] In this system, limbal epithelial cells are cultivated on a surface and changing the temperature results in cell sheet detachment and the sheet of cells can be grafted onto the eye.

The development of polymeric platforms for human cornea transplantation under full synthetic control were the aims of this research. The crucial properties of the polymer had to include allowing the cells to attach and proliferate and also allowing the cells to efficiently transfer (detachment from the polymer to the eye). In the first set of experiments, a series of polyurethanes[151] and polyacrylates[113,152] (252 polymers in total) were screened for cell adhesion. Selected active polymers were then experimentally tested for cell transfer. Finally, the development of a surface-engineered cell transfer system for human corneal epithelial cells for the treatment of the cornea was performed. The summary of the experiments described is presented in **Figure 3.3**.

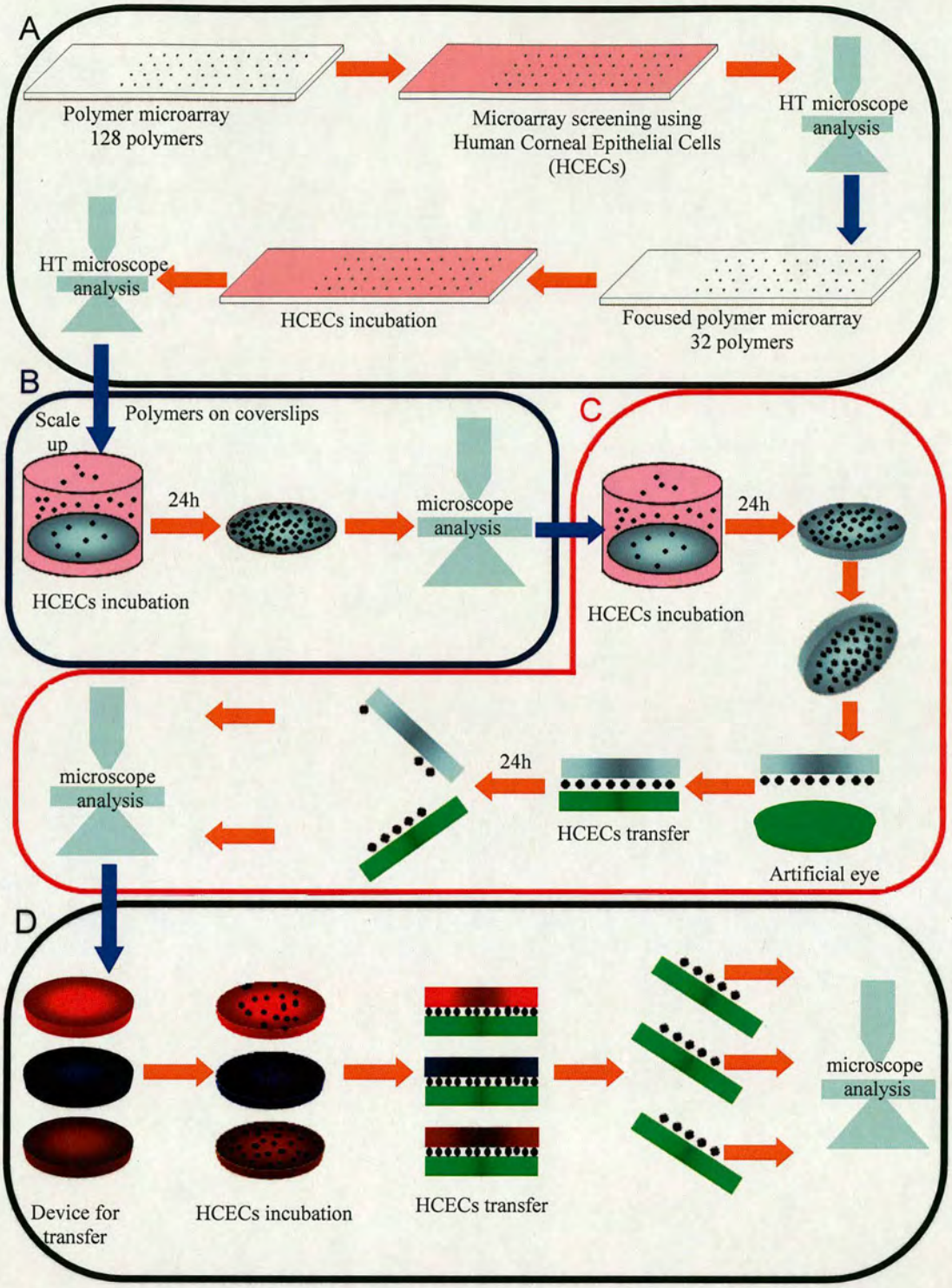

Figure 3.3 *Summary of experiments: (A) microarray screening; (B) scale-up; (C) cell transfer; (D) systems for cell transfer.*

3.2 Polymer screening for HCEC adhesion

125 polyurethanes[151] and 128 polyacrylates[113,152] were printed by contact printing in a microarray format on an agarose coated slide. Each polymer was printed in quadruplicate to give the primary microarrays, while sixteen copies of each polymer were printed to give the focused library microarrays (250 μm diameter spot). The Human Corneal Epithelial Cells (HCEC) suspended in media were introduced onto a printed slide. The homogeneity of this mixture of cells and media determine the quality of the screening. The basic consideration in the screening of microarrays is that all polymeric spots have the same chance to be approached and occupied by cells. While this condition is completed, only the cell-polymer interactions can define cell attachment. The incubation was carried out for 24 h then cells were fixed with formaldehyde. In order to perform analysis of microarrayed cells, the nuclei were stained with dye (Hoechst 33342). This fluorescent dye binds strongly to DNA and cells can be easily distinguished.

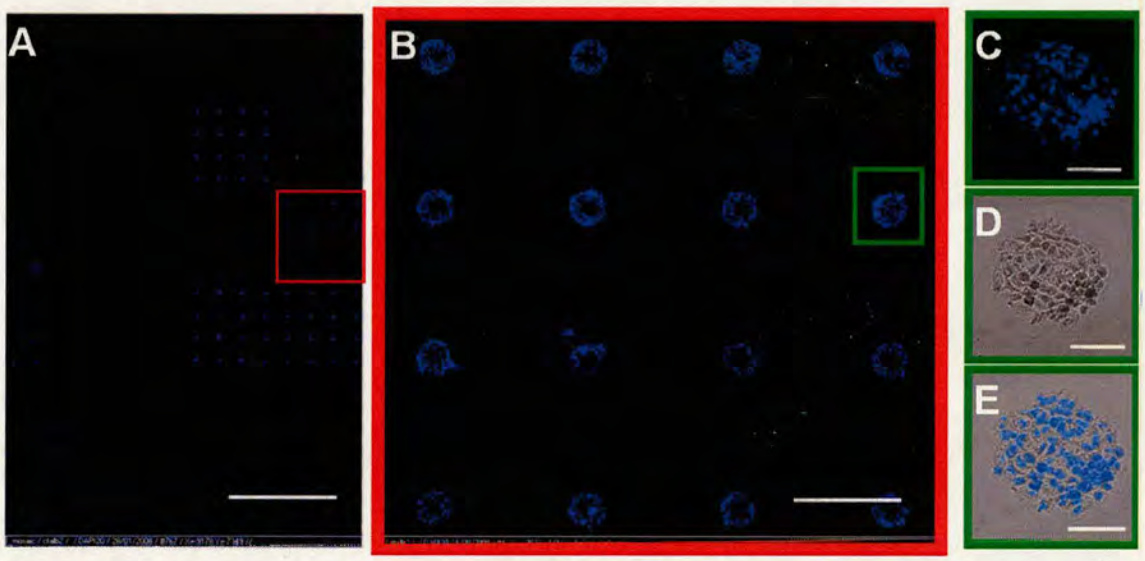

Figure 3.4 *Images of human corneal epithelial cells binding on a polymer microarray: (A) cells on an microarray containing 24 polymers each printed as 16 replicate spots (scale bar 6mm); (B) nucleus stained with Hoechst 33342 (16 spots of the same polymer (scale bar 0.8 mm)); (C) nucleus stained with Hoechst 33342 on single spot (scale bar 0.2 mm); (D) brightfield image of cells on single spot (scale bar 0.2 mm); (E) composite image of (C) and (D) (scale bar 0.2 mm). Fluorescent images were obtained using 350 nm excitation, 460 nm emision filters (DAPI).*

The prepared slides were analysed using a high resolution scanner (Imstar) using a 20x/0.30 objective and a DAPI filter set to give a mosaic of images. An example of a mosaic of focused library (16 copies of each polymer) is showed on **Figure 3.4**.

Images (DAPI filter) gave qualitative identification of cell binding polymers. The Imstar software allowed the number of cells per unit area of the polymer to be determined. Results are shown in **Figure 3.5**. (The polymer symbols are defined in sections 6.4.8. and 6.4.9)

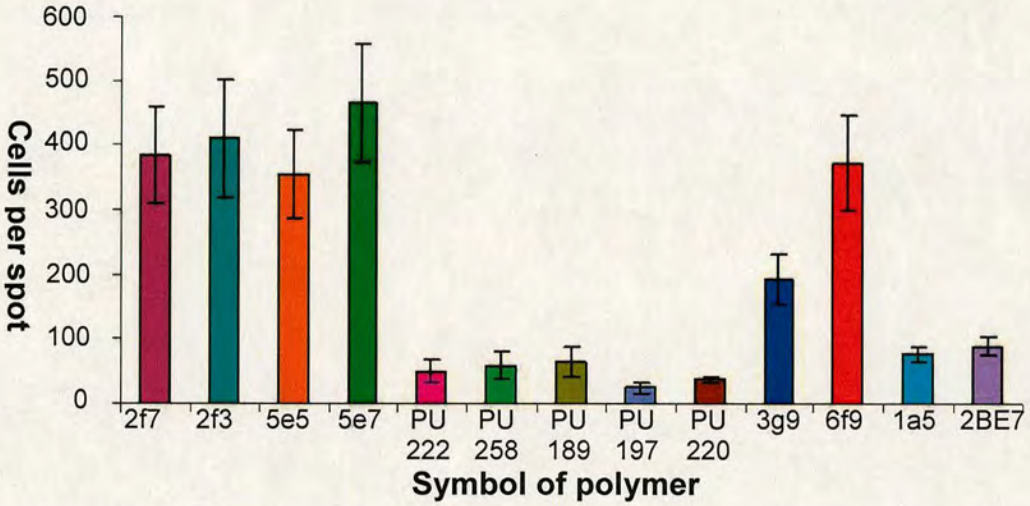

Figure 3.5 *Number of cells per polymer spot (average from 16 spots of same polymer) vs. polymer type.*

PU-	Polymer structure				ratio (mol)		
	Diol	Mn	DIS	Extender	mon (1)	mon (2)	x
222	PHNAD	900	BICH	OFHD	0.25	0.52	0.23
258	PTMG	1000	BICH	OFHD	0.17	0.52	0.33
220	PHNAD	900	MDI	DMAPD	0.25	0.52	0.23
197	PTMG	650	BICH	DHM	0.25	0.52	0.23
189	PPG	1000	BICH	OFHD	0.17	0.52	0.33
Polyacrylates symbol;monomer 1/monomer 2 (molar ratio%)							
2f7; MMA/DMAEMA(70/30)				6f9; HPMA/DMAEMA(90/10)			
2f3; MMA/DMAEMA(30/70)				1a5; St/DEAA(50/50)			
5e5; HEMA/DEAEMA(50/50)				2BE7; MMA/AAG-H(70/30)			
5e7; HEMA/DEAEMA(70/30)							

Table 3.1 *Symbol definition of HCE cell binding polymer.*

List of monomers used for polymer synthesis

PHNAD:	poly[1,6-hexanediol/neopentyl glycol-*alt*-(adiptic acid)]diol
PPG:	poly(propylene glycol)
PTMG:	poly(tetramethylene glycol)
BICH:	1,3-bis(isocyananatomethyl)cyclohexane
MDI:	4,4'-methylenebis(phenylisocyanate)
OFHD:	2,2,3,3,4,4,5,5-octafluoro-1,6-hexanediol
DMAPD:	3-dimethylamino-1,2-propanediol
DHM:	diethyl bis(hydroxymethyl)malonate
MMA:	methyl methacrylate
DMAEMA:	2-(dimethylamino)ethyl methacrylate
DEAEMA:	2-(diethylamino)ethyl methacrylate
HEMA:	2-hydroxyethylmethacrylate
HPMA:	hydroxypropylmethacrylate
DEAA:	diethylacrylamide
St	styrene
AAG-H:	2-acrylamidoglycolic acid

Generally, the polyurethanes did not show significant affinity for human corneal cell attachment. The best of the polyurethanes such a PU 189, attached less than 100 cells per single spot, which is less than the weakest polyacrylate binder. The lack of polyurethane binding activity was unexpected. Many of the polyurethanes present on the microarray (PU 190, PU206, PU214, PU159, PU166 and PU174) during the screening with human corneal epithelial cells showed significant affinity for cell attachment in case of mouse embryonic stem cells, mesenchymal stromal cell and bone marrow dendritic cells.[153] However, thanks to the high throughput approach polyacrylates, 5e5 and 5e7 were discovered which were able to attach up to 500 cells per spot. These polymers were constructed with the monomers 2-hydroxyethylmethacrylate (HEMA) and 2-(diethylamino)ethyl methacrylate (DEAEMA) with the molar percentage of the monomers 50% HEMA/50% DEAEMA and 70% HEMA/ 30% DEAEMA respectively. Although poly(HEMA) is used for the prevention of cell adhesion[106] the high molar percentage of HEMA in polymer 5e7 seems to be crucial for high binding affinity of this polymer. Slight reduction in HEMA monomer participation results (from 70% (5e7) to 50% (5e5) in reduction of the number of human corneal epithelial cells from 500 down to 400 cells per spot. These results and others confirm the observation that changes in

monomer ratio can be correlated with the properties of the final polymer in particular polymer affinity for cellular attachment.

For confirmation of polymer activity the polymers were coated on a coverslip by spin coating and cultivated with human corneal epithelial cells. The numbers of cells on the polymer were recorded. (**Figure 3.6**)

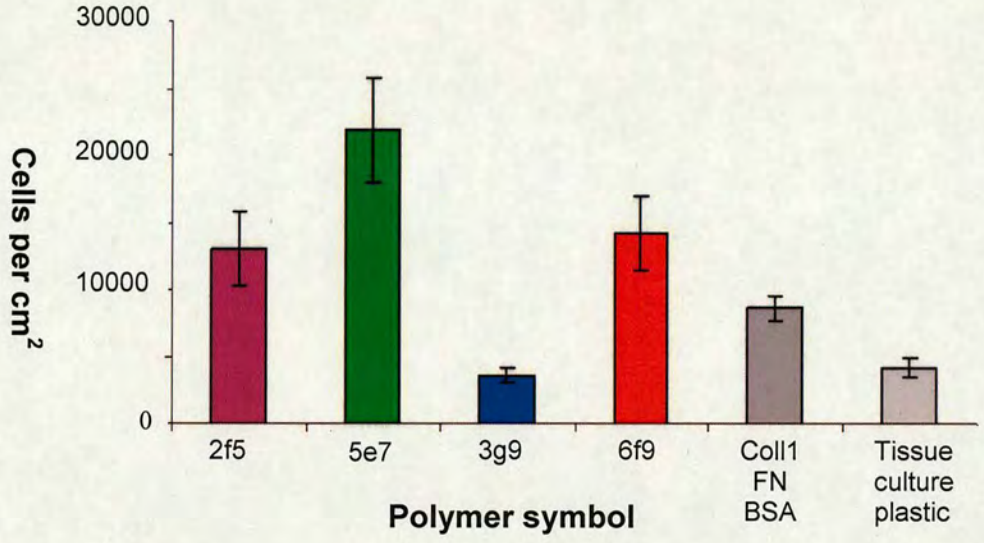

Figure 3.6 *Number of cells per cm^2. Control: dark grey bar = coverslip covered with Collagen type 1, fibronectin and bovine serum albumin; light grey bar = polystyrene tissue culture plastic.*

It was shown that polymers 5e7 and 6f9 had higher affinities for cell attachment than polystyrene tissue culture plastic and coverslips coated with a mixture of Collagen type 1, Fibronectin and bovine serum albumin. Potentially, using this type of synthetic polymeric surface in place of the traditional natural product based substrates could result in reduction the of time necessary for *ex-vivo* cell growth and reduce the risk of viral cell contamination.

Polymer 6f9 consist of 90% hydroxypropylmethacrylate (HPMA) and 2-(dimethylamino)ethyl methacrylate (DMAEMA) while 5e7 consists of 70% hydroxyethylmethacrylate (HEMA). Probably the longer distance between the hydroxyl groups and methacrylate groups of HPMA in comparison to HEMA is responsible for the slightly worse cell attachment of 6f9 than in the case of 5e7. Because in this

particular project the ability of polymers for cellular attachment must parallel the ability of polymers for transferring, the weaker cell binder was used in the next stage of the project.

3.3 Cell transfer experiment

Active polymers were coated onto a coverslip by spin coating and Human Corneal Epithelial Cells were cultivated on them for 24 h. Coverslips were inverted and placed onto limbal- imitate surfaces (polystyrene cultivation dish covered with collagen type IV, fibronectin and bovine serum albumin (Coll1/FN/BSA), tissue culture plastic and polystyrene cultivation dish covered with matrigel.

After 24 h, coverslips were removed and cells which were left on limbal-mimicking surfaces were fixed, stained and counted. (**Figure 3.7 A**) Human Corneal Epithelial Cells remaining on the coverslips were also counted. Results are presented in **Figure 3.7 B**.

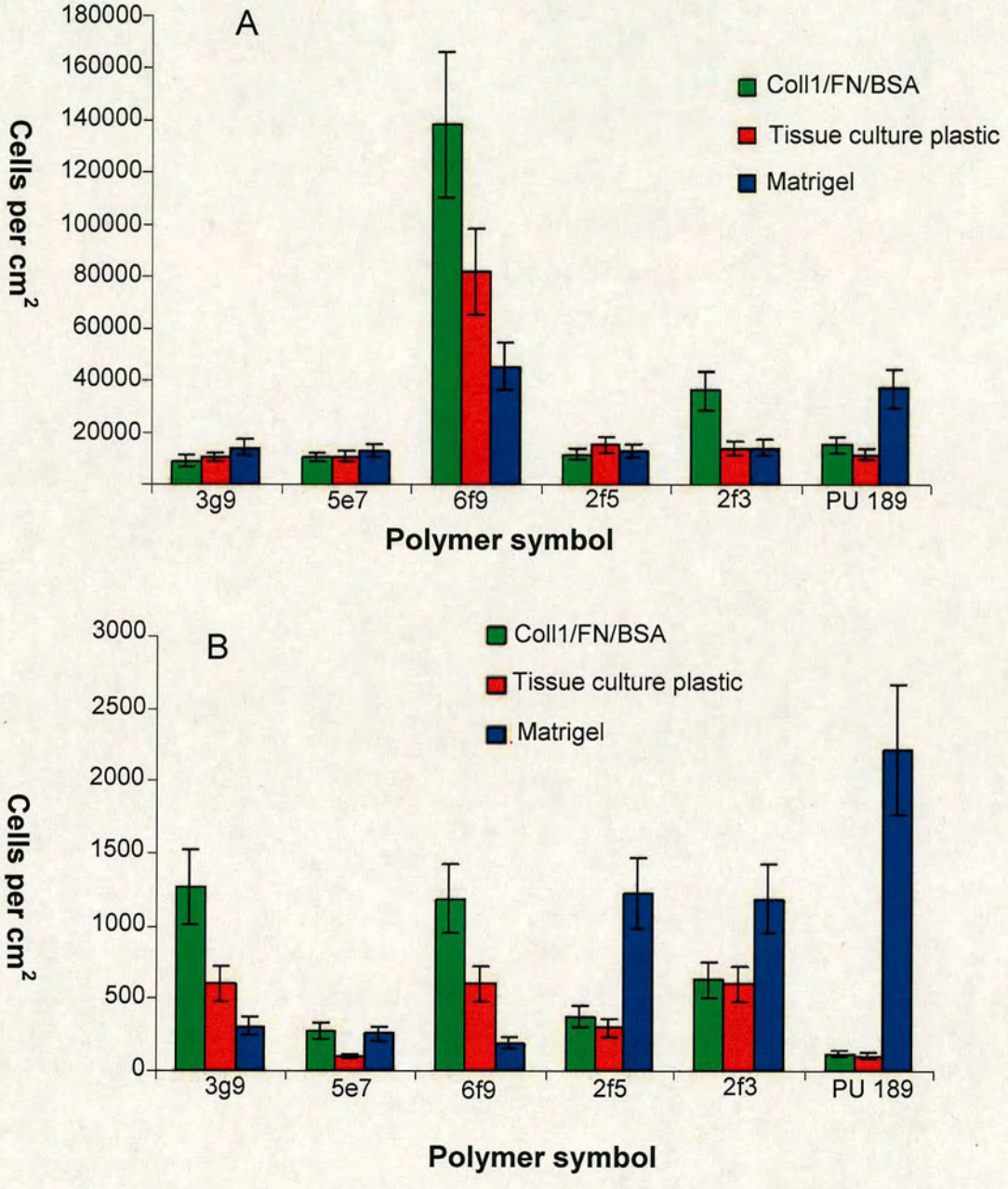

Figure 3.7 *Number of cells per 1 cm$^{2:}$ (A) of limbal – mimicking surface after 24 h transfer; (B) cells left on coverslip after transfer experiment; green bar = cells transferred to Coll1/FN/BSA; red bar = cells transferred to tissue culture plastic; blue bar = cells transferred to Matrigel.*

3.4 Platform for cell transfer - development and tests

The transfer devices were prepared by dip coating of material into a 2% solution of 6f9 in THF. The characteristic shape of an eyeball requires a flexible or pre shaped platform for proper cell delivery. Polymer 6f9 (the best for cell attachment and transfer) was spread over several materials, such as soft contact lenses (PureVision (Balfilcon A) Bausch), polymer clay (Speed Modelina 59018844470019), polystyrene–wool,[153] polystyrene cell cultivation plastic (Nunc Cat. No. 156800), filter paper (Whatman Cat No. 1001 090), polypropylene (Cat No BTR 615106), polyurethane foam (Tytan Euroline Cat No 4455) and a glass coverslip of 23 mm diameter (VWR Cat No. 631-0150, used as a control). Also, pure 6f9 formed in a curved shape was tested. A platform with 6f9 was used in a transfer experiment. (**Figure 3.8**) The limbal - mimicking surface was polystyrene tissue cultivation plastic.

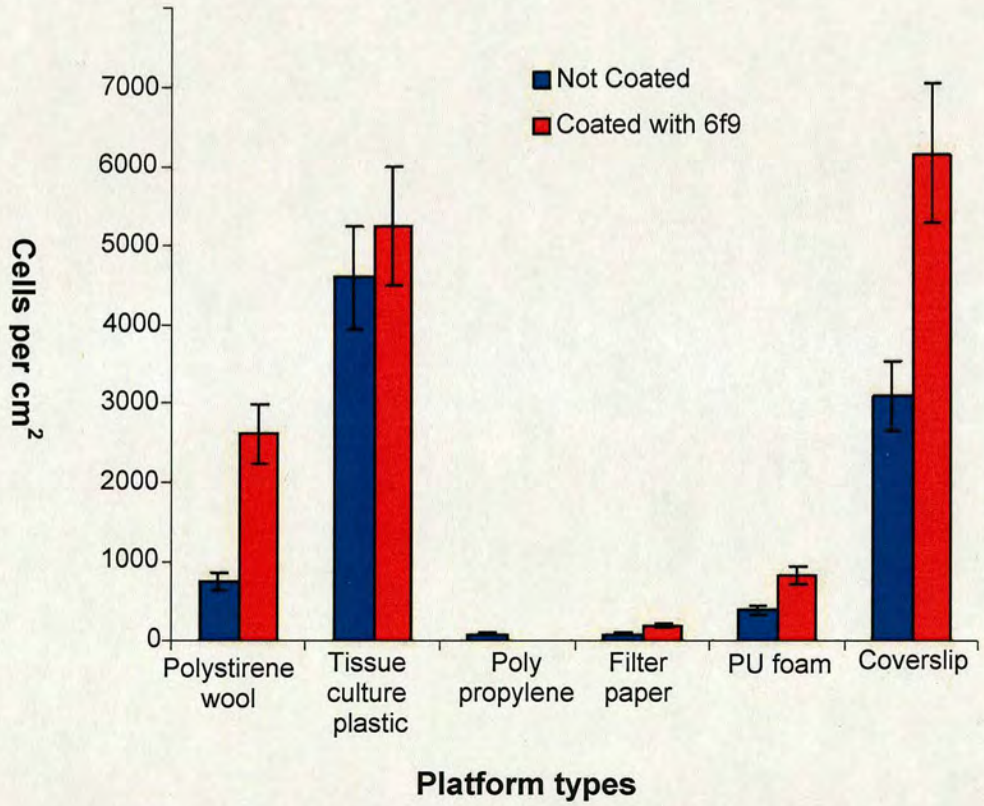

Figure 3.8 *Number of cells per 1 cm^2 of polystyrene tissue cultivation plastic after 24 h transfer. Red bars = transfer from platforms covered with 6f9; blue bars = transfer from platforms not coated with 6f9.*

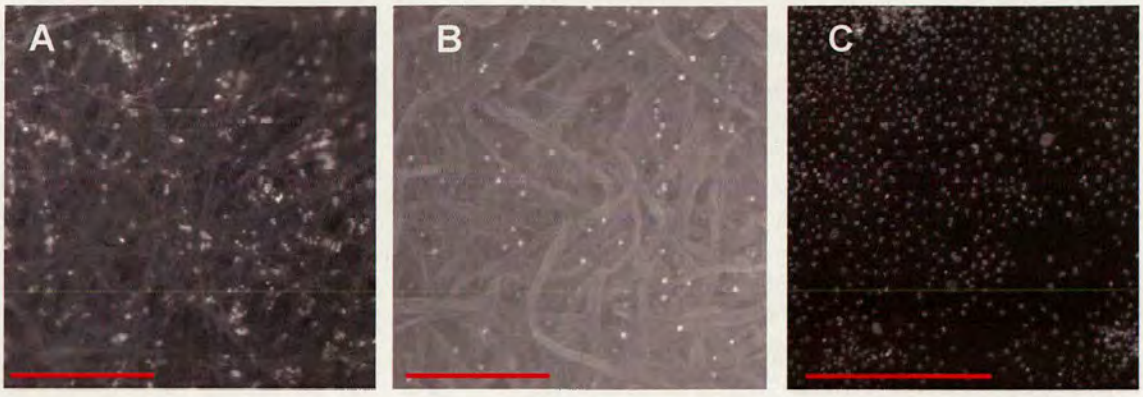

Figure 3.9 *DAPI images of human corneal epithelial cells stained with Hoechst 33342 (nuclei stain) left on platforms covered with 6f9 after transfer: (A) polystyrene wool; (B) filter paper; (C) polystyrene tissue cultivation plastic (scale bars 1 mm).*

The best transfer was observed in the case of polystyrene tissue culture plastic coated with 6f9. (**Figure 3.8**) However polystyrene wool has an important advantage as a transfer device mainly because of its full permeability and ability to fit to any type of curved surface. Also, soft polystyrene fibres are not likely to cause eye damage. (**Figure 3.9 A**)

Platforms, such as the contact lenses, polymeric clay and polypropylene and polyurethanes did not reveal any significant ability to transfer cells with or without 6f9.

3.5 Conclusions

High-throughput polymer screening (including polymer microarray preparation and screening for cell binding) was successfully employed for the identification of active polymers from a library of 252 polymers. The activity of 13 polymers was successfully confirmed by experiment on coverslips leading to the identification of 5 candidates for transfer experiments. Polymer 6f9 was found to be the most effective in its ability for cell transfer. Finally, platforms based on polymer 6f9 were prepared in order to develop medically serviceable devices. The ultimate goal of replacing a fibroblast-type surface for cell transferring by non-animal originating materials was achieved. The obtained results were patented: *Copolymers Suitable for Use in Corneal Bandages WO 2008/047169 A2*

Chapter 4 : Novel substrates for embryonic stem cell culture

4.1 Principles of cellular immobilization

In modern biology, cell adhesion is a widely studied subject. Cell adhesion proteins are crucial for the functioning of organisms, they hold together cells to give tissues and also regulate the function of migrating cells. For example, regulation of cellular adhesion proteins is pivotal during the development of embryos in the process of morphogenesis.[154] Many types of tumour are related to mutations in genes encoding adhesion proteins that result in abnormal cell -cell interactions.[155] Some specific cell adhesion proteins are involved in regulation of synaptic adhesion in the brain which is connected to learning and memory processes.[156] The activity of viruses and bacteria depend on interaction or lack of interaction with adhesion proteins.[157]

In the main, cells do not exist in isolation and tend to interact with non-cellular components of the environment or with other cells. The study of cell adhesion involves the adhesion of protein molecules present at the surface of cells with molecules that they bind with. Generally, three classes of multiprotein complexes are responsible for cell adhesion: the extracellular matrix (ECM) proteins, the cell adhesion molecules/adhesion receptors and cytoplasmic plaque/peripheral membrane proteins.

ECM proteins (including the fibronectins, collagens, laminins and proteoglycans) are large glycoproteins that assemble into complex macromolecular arrays (fibrils, for example). They can be tightly associated with the cell surface due to their ability of binding to cellular adhesion receptors.[157]

The cell adhesion receptors are typically transmembrane glycoproteins which are involved in interactions with the extracellular (EC) surface. They determine the specificity of cell-ECM and cell-cell recognition. They include members of the selectin, cadherin, immunoglobulin, integrin and proteoglycan superfamilies. The cell adhesion receptors at the EC surface recognize and interact either with proteins of the ECM or with other cell adhesion receptors on the neighbouring cells. Cell adhesion receptors located at the intracellular surface of the plasma membrane associate with peripheral membrane proteins or cytoplasmic plaque.[157]

Cytoplasmic plaque proteins link the adhesion systems to the cytoskeleton, thus regulating the functions of the adhesion molecules and transport signals initiated at the cell surface by the adhesion receptors. The biochemical properties of these classes of proteins and the diversity of roles of the various families of adhesion receptors is described in detail in several excellent reviews.[158-164]

A variety of cell adhesion mechanisms determine the overall architecture of the tissue. The cell adhesion systems help to translate the basic genetic information into a complex three-dimensional pattern of cells in tissues. Both dynamic adhesive events (cell arrangement during the tissue development) and stable adhesive interactions (cell adhesion in fully formed tissues) often utilize the same adhesion proteins with the same adhesive mechanisms.[165]

In addition cell adhesion events require cooperation with signalling processes that control the transfer of information between cells. Cell adhesion proteins not only respond to cell signalling events but also moderate signals into the cell. Therefore, controlling physical cell adhesion systems opens the way for intercellular signalling studies. Due to the multiplicity of the cell surface components the principles of immobilisation of cells onto a surface are more complex than the immobilisation of single biomolecules and should be considered as the result of range of a cooperative and dynamic non-covalent interactions between these components and a given substrate.

The immobilisation of cells onto surfaces has been the subject of research for nearly one hundred years.[166] Some of the most significant approaches to this problem are cell immobilization by electrostatic interactions and use of cell specific receptors or cell specific antibodies.

Cell immobilization by electrostatic interactions can be performed using highly positively charged surfaces such as poly-L-lysine, which promotes non-specific immobilisation of cells. A disadvantage of this approach is that cell cycles are disturbed by such strong interactions.[167,168] Biomolecular recognition is based on interactions of proteins present on EC surfaces with complementary biomolecules on the substrate. This is a softer method for cell immobilization and allows for selective cellular binding. Highly cell-specific immobilisation can be achieved *via* interaction between antibodies and a complementary antigen,[169] or integrins and adsorbed extracellular matrix proteins.[170,171]

The research in this chapter is focussed on the phenomenon of cell adhesion to external surfaces, in particular to polymeric surfaces. Many natural product based materials are used for the cell cultivation, for example collagen, fibronectin, albumin or gelatine but they have limitations, *e.g.* can be a source of contamination (such as bovine spongiform encephalitis (BSE)). Because of this, replacing these products with synthetic polymers is crucial for the therapeutic application of cells cultivated *ex vivo*.[172]

Potentially, the most efficient strategy to realise the aims of cell binding on artificial surfaces is to predict the properties of such surfaces, which are required by cells, for binding and subsequently to manufacture them. Recently an advanced application of this methodology was reported by Kohn *et al.*[173] Using advanced software he was able to generate a library of 2000 virtual polymers and "simulate" their binding activity with NIH3T3 cells. It is striking that, to validate results of this simulation, he used a library of 50 real polymers.

Our recent methodology based on HT screening does not predict cell – polymer interactions. In this situation, polymers are screened on the microarray and active ones are selected for a more precise investigation. This strategy was reported before by Turnier,[109] Mizomoto[113] and Langer.[106]

In my opinion, polymers capable of a very strong interaction with cells (covalent or electrostatic interactions) disturb the cell's cycle dramatically. The ideal polymer for cell adhesion should be capable of an efficient absorption of proteins present in medium and those generated by cells in a correct spatial orientation. According to this reasoning, it follows that the act of cell adhesion is an effect of a cell-protein interactions. Due to this, the cells are kept healthy and behave naturally (with no effect on the cell cycle).[174]

4.2 mES cells characteristics

Mouse embryonic stem (mES) cells were chosen over hES cells due to their availability. mES have all the properties characteristic of mammalian embryonic stem cells as, they can be turned into any cell type of the body's tissues. mES cells used in this study were modified by fusion of the gene for GFP to Oct. Oct4 is present in immature undifferentiated cells only,[128] meaning that analysis of GFP allows easy recognition of differentiated and undifferentiated cells (by flow cytometric analysis). Standard protocols used for mES cell monolayer cultivation involves gelatine, which carries all

the disadvantages of natural products (potential sources of viral, bacteria and prion contamination). The ultimate goal of this research was to find an artificial surface which allowed for cell growth and proliferation without using gelatine.

Leukemia inhibitory factor (LIF) is commonly used in the mES cells cultivation for a differentiation prevention. In the presence of this natural product in the media cells remain undifferentiated. This natural product is produced from genetically modified yeast[175] and cultivation without LIF results in rapid differentiation to form ectoderm, endodermal or mesodermal cell types.

4.3 Pre-synthesised polymers screening for mES adhesion

124 Polyacrylates[113,152] and 100 KIT (see section 6.2.5) polymers were printed by contact printing in a microarray format on an agarose-coated slide. An agarose surface was used to prevent the binding of cells outside the deposited spots, resulting in a patterned array of cells. Since cells were only present on the spotted features, the analysis could be conducted at precise and specific positions. Quantitative analysis based on establishing the number of cells per spot and degree of coverage of the spot requires monolayer cellular coverage. However in the case of mES cells a monolayer is very difficult to produce especially on the microarray, due to a very limited binding surface area and a strong tendency for mES cells to form 3D structures. This problem could not be solved by reducing the concentration of the cells or the incubation time or even spot size; an observation that was confirmed when collagen was printed onto a microarray, which acted as a control (**Figure 4.1**). **Figure 4.1 A1** and **A2** show a typical contact printed collagen spot after a 48 h incubation of mES cells (700,000 cells per slide). The entire area of the spot was completely covered with cells. Fluorescent (DAPI) imaging (**Figure 4.1 A2**) showed that cells were not a monolayer. **Figure 4.1 B1** shows a similar collagen spot after a 24 h incubation of mES cells (700,000 cells per slide). The red circle (**Figure B1**) indicates the available binding area and a comparison of **Figure 4.1 B1** and **B2** shows that the mES cells started to form a 3-D layer even before all the available binding area had been covered by cells (cell stacking is preferred, despite the availability of free space). In conclusion monolayers could not be achieved by reducing the cell incubation time.

The same problem was evident when the number of cells was reduced to 300,000 per slide. Cultivation of the cells for 48 h and 24 h on collagen spots led to cells having similar appearances after both time periods. However, for both 24 h and 48 h incubation times the reduction of the number of cells to 300,000 per slide resulted in more than 50% of the spots being completely unoccupied. The reduction in the number of cells used resulted in many spots not being approached by cells at all, which meant that cell proliferation on these spots could not occur.

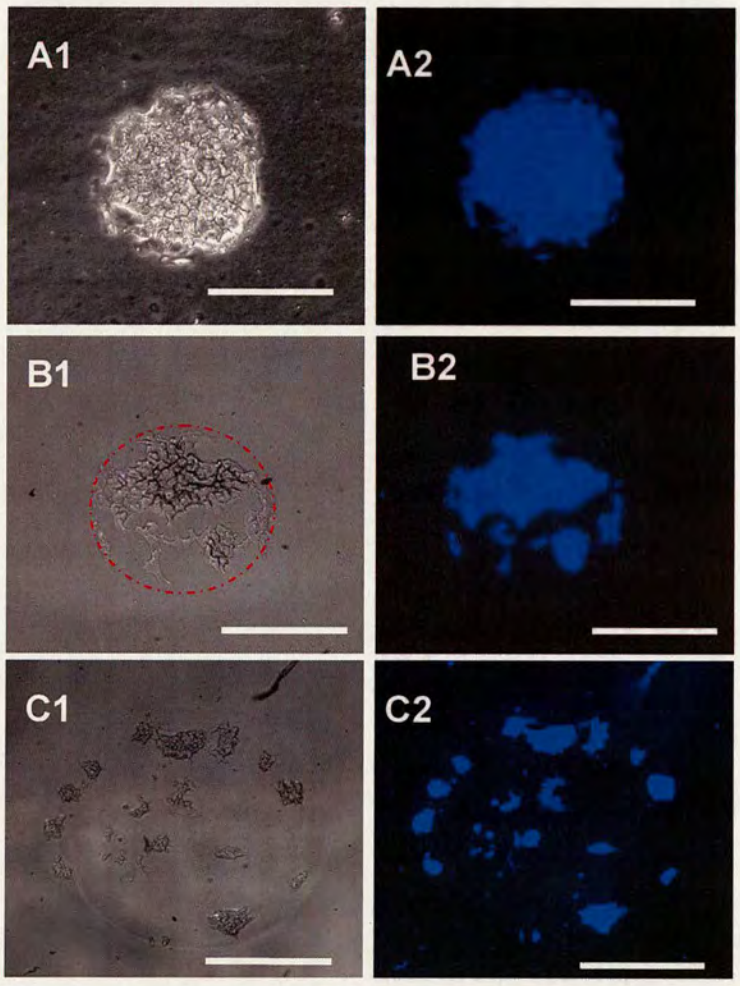

Figure 4.1 *Images of mES-Oct4 on collagen spots printed on agarose coated slides: (A) contact printed collagen spot after 48 h cells incubation, $7x10^5$ mES-Oct4 cells seeded per slide (scale bar 250 μm); (B) contact printed collagen spot after 24 h cells incubation, $7x10^5$ m ES cells seeded per slide (scale bar 250 μm); (C) inkjet printed collagen spot after 48h cells incubation, $7x10^5$ cells seeded per slide (scale bar 500 μm). Images were taken with a Leica microscope using a 5x/0.12 objective after cells fixing and staining (Hoescht 33245); A1-C1 - bright field and A2-C2 - DAPI filter.*

Increasing the sizes of spots up to 600 μm, (*via* inkjet printing of a collagen solution) still did not allow the formation of monolayers. (**Figure 4.1 C1** and **C2**) The preference for 3D mES cell growth was so strong that only a qualitative analysis of cells attached on microarays was performed.

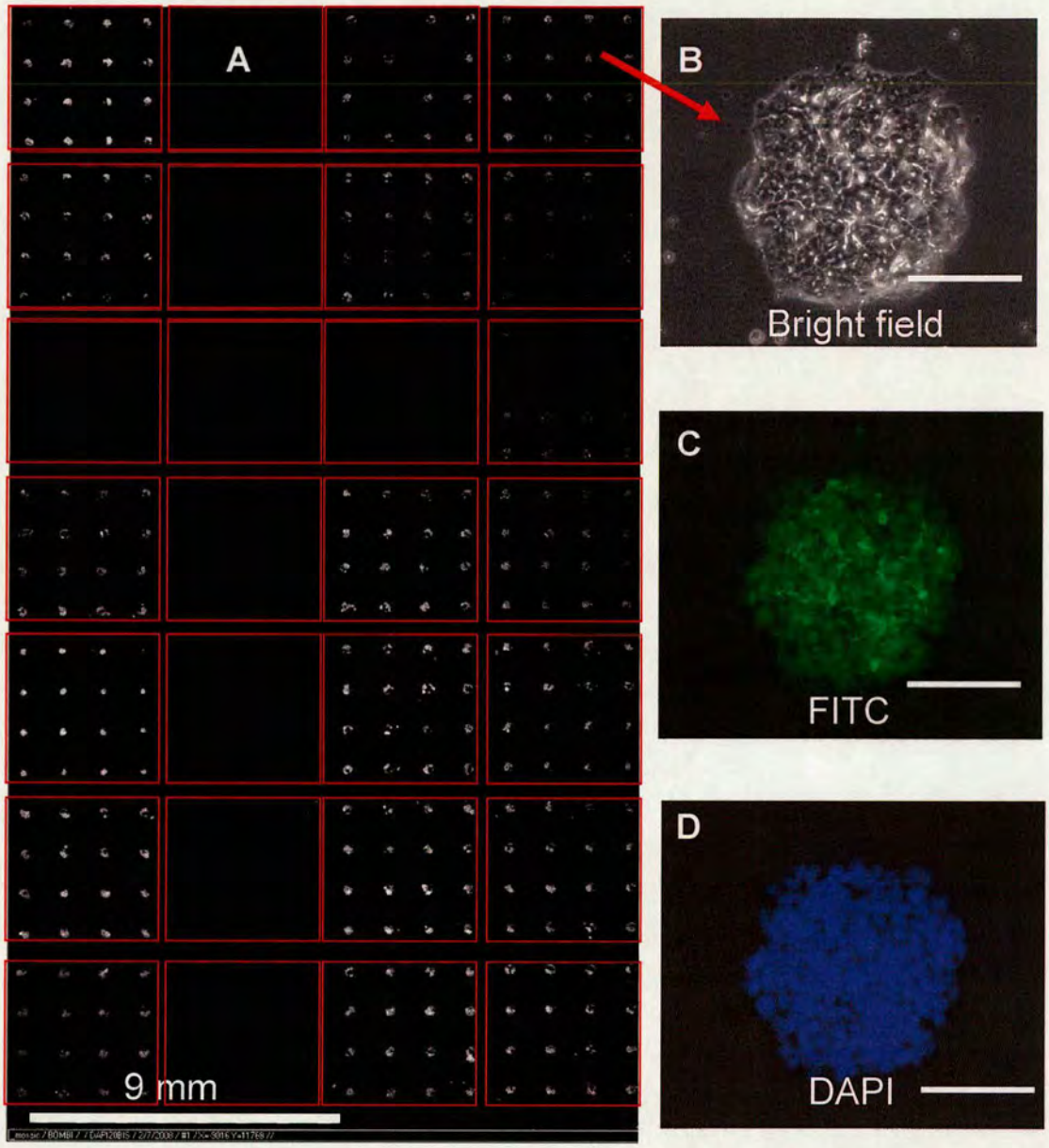

Figure 4.2 *Images of mES-Oct4 cells on a microarray of pre-synthesised polymers printed by contact printing: (A) mosaic of fluorescence images (DAPI filter) of mES-Oct4 cells on polymer spots, red squares represents 16 replications of the same polymer spots (scale bar 9 mm); mES-Oct4 cells on polymer spots; (B) bright field; (C) FITC filter; (D) DAPI filter (scale bar 100 μm). Images were taken with a Nikon microscope using a 10x/0.30 objective, controlled by the Pathfinder software (Imstar) after cell fixing and staining (Hoechst 33342).*

For this reason, quantitative analysis of mES-Oct4 on microarrays was postponed until a later stage (experiments involving coverslips). Polymers collected on the microarrays were classified according to three categories - strong binding - when cell coverage was 100% of each spot area, medium binding - when cell coverage was less than 100% but greater than 50% and non-cell binding polymers.

To be able to distinguish the cells from the polymer, the cells were fixed with formaldehyde (4% wt) and stained with Hoechst 33342 (nuclei stain) (**Figure 4.2**) and fluorescent images were taken with FITC (**Figure 4.2 C**) and DAPI (**Figure 4.2 D**) filters.

4.4 Contact printed polymeric squares for mES cell proliferation

The limited area of the polymeric spots on the microarray was insufficient for observing cell growth and proliferation. Because of this limitation, polymer spots were printed close enough in order for them to merge forming larger squares rather than separate spots. This facilitated the observation that polymers were binding cells and allowing proliferation. The polymers for this experiment (3BG9, 3n9, 2a7, 2BB7, KIT 45, KIT 47, KIT 54, KIT 89, KIT 100) were selected following a primary microarray screening. Squares were generated by contact-printing arrays (16x16) with the distance between individual spots being 160 μm. (**Figure 4.3** and **Table 4.1**)

Imaging of cells on polymer squares during incubation confirmed the binding activity of the hit polymers selected following a primary microarray screening. The preference of 3D mES cell growth was observed once again. After a 48 h incubation period, the cells were growing in stacks rather than in a monolayer, finally after 72 h (due to the expansion of stacked cells) the entire available binding area was occupied.

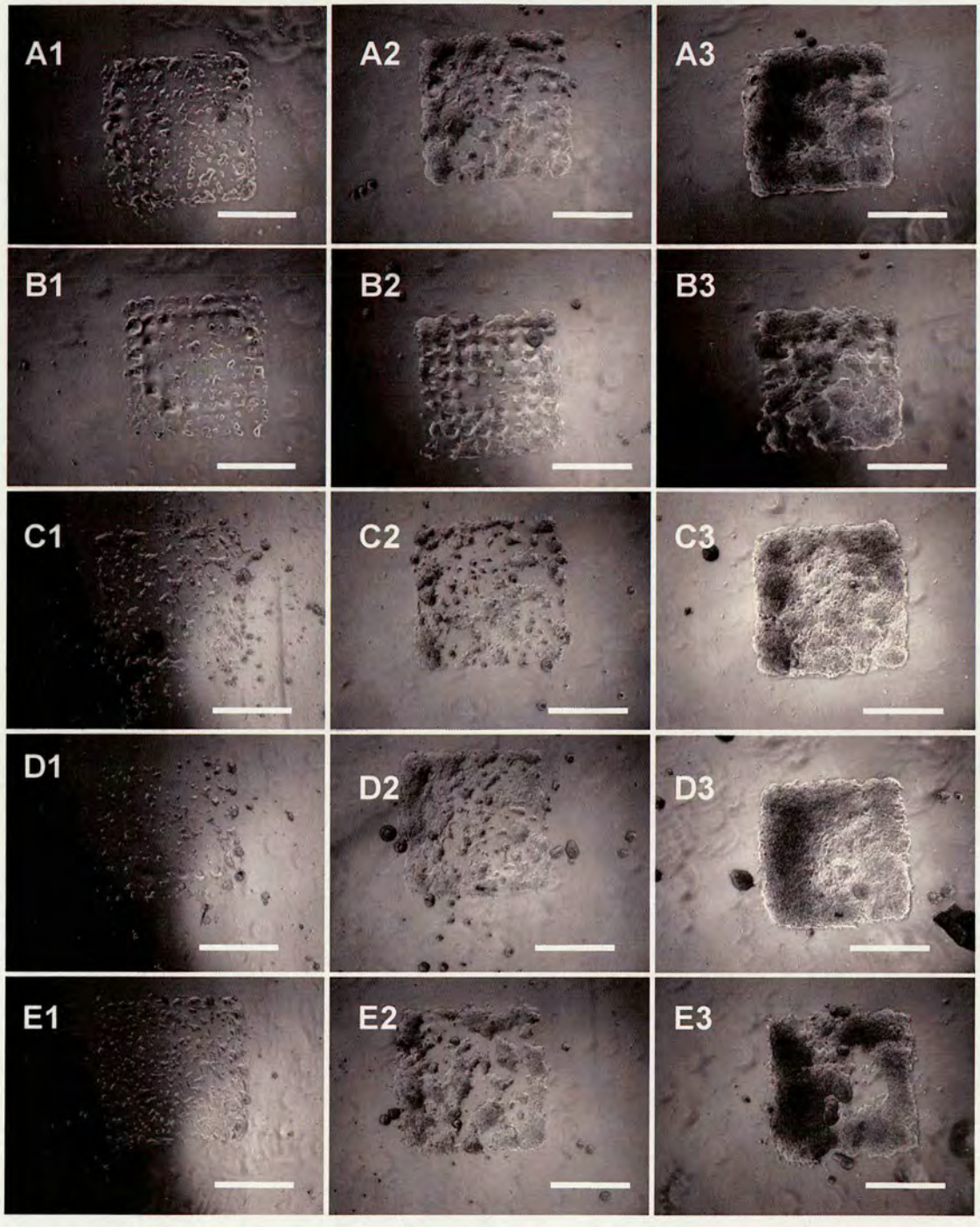

Figure 4.3 *Images of mES cells growing on a polymer microarray (16x16 spots with a distance of 160μm formed square) on an agarose coated glass slide printed with: (A) 2-methoxyethylmethacrylate/ethylene glycol methacrylate phosphate co-polymer (molar ratio 9:1) 3BG9; (B) 2-methoxyethylmethacrylate/N,N-dimethylvinylbenzylamine co-polymer (molar ratio 9:1) 3n9; (C) Polyethylene, chlorosulfonated (KIT polymer 54); (D) Poly(diallyl phthalate) (KIT polymer 45); (E) Zein, purified (KIT polymer 100); (A1-E1) 24 h incubation; (A2-E2) 48 h incubation; (A3-E3) 72 h incubation. (Scale bars 1 mm). Images were taken with a Leica microscope using a 5x/0.12 objective.*

Polyacrylates symbol;monomer 1/monomer 2 (molar ratio %)	
3BG9; MEMA/EGMP-H(90/10)	3n9; MEMA/DMVBA(90/10)
2a7; MMA/DEAA(70/30)	2BB7; MMA/AES-H(70/30)
Symbol definition of monomer	
MMA: methyl methacrylate	MEMA: 2-methoxyethylmethacrylate
DEAA: diethylacrylamide	AES-H: mono-2-(acryloyoxy)ethyl succinate
DMVBA: dimethylvinylbenzylamine	
KIT polymers	
KIT 45 - poly(diallyl phthalate)	
KIT 47 - poly(4,4'-dipropoxy-2,2'-diphenyl propane fumarate)	
KIT 54 - polyethylene, chlorosulfonated	
KIT 89 - styrene/maleic anhydride copolymer, partial methyl ester	
KIT 100 - zein, purified	

Table 4.1 *Symbol definition of mES cell binding polymer.*

4.5 Coverslip experiments

The capacity of polymers for cellular attachment was established by an initial microarray screening and confirmed by performing experiments on cover slips. The first reason for this scale-up is that polymers on microarrays have a specific morphology. For example, the ring effect (which is a problem arising from solvent evaporating from the microarray after printing) which may cause a difference between the cell-polymer interactions at the edge of a polymeric spot compared with those found in the centre of the same spot.

Polymers were deposited onto coverslips (13 mm diameter) as thin uniform layers, which meant that the cell binding activity of each polymer could be confirmed. In order to spread polymers onto coverslips, the polymers had to be dissolved in a low boiling point solvent (such as THF). Solvent evaporated quickly after the polymer solution had been dispersed by spin coating and a uniform polymeric surface was formed on each coverslip.

The binding surfaces were significantly larger than the analogous polymer areas on the microarray – the diameter of cell binding polymeric spots varied from between 0.4 and 1.5 mm. The larger available area for cells meant that experiments investigating proliferation could be carried out, allowing the observation of the growth rates of cells and cell morphology. Another benefit of using a larger binding area was that cells could be attached to surfaces with relatively large distances separating each other. The binding between the external surface of cells and the polymeric surfaces competed with binding

between cells. The result of having larger distances between attached cells was that interactions between the cells and polymeric surfaces was preferred. The final step of experiments involving the cultivation of cells on coverslips was cell detachment and flow cytometry analysis. Flow cytometry analysis measures the fluorescence and number of cells and allows the specificity of interactions between mES and particular polymers to be established.

Three polymers, 2-methoxyethylmethacrylate/ethylene glycol methacrylate phosphate co-polymer (3BG9) (molar ratio 9:1), 2-methoxyethylmethacrylate/N,N-dimethylvinylbenzylamine co-polymer (3n9) (molar ratio 9:1) and polyethylene, chlorosulfonated–(KIT 54) were the best binding polymers. As a reference, a disc of the tissue culture plastic (13 mm diameter) coated with 0.1% gelatine solution was used **Figure 4.4.**

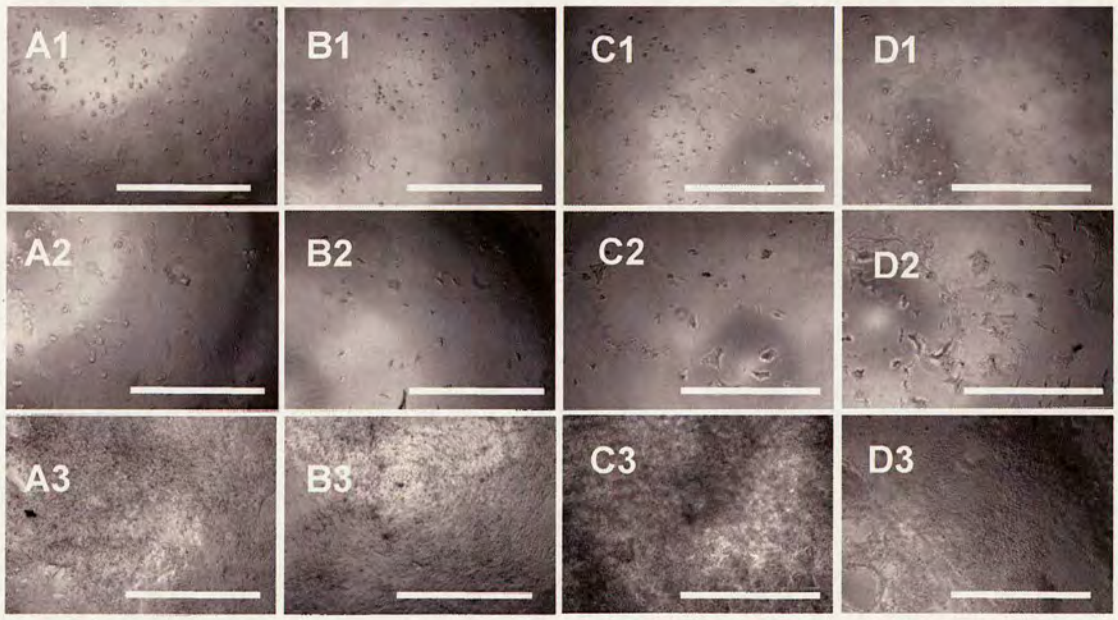

Figure 4.4 *Images of mES-Oct4 cells growing on: (A) a standard tissue culture plastic (disc 13 mm diameter, coated with 0.1% gelatine); a coverslip (13 mm in diameter) coated with (B) 3BG9;(C)KIT 54 ; (D) 3n9 (A1 - D1) bright field image of living cells after 24 h incubation; (A2 - D2) 48 h incubation; (A3 - D3) 8 days incubation showing a layer of cells on polymeric surface; (scale bars 60 μm). Images were taken with a Leica microscope using a 5x/0.12 objective.*

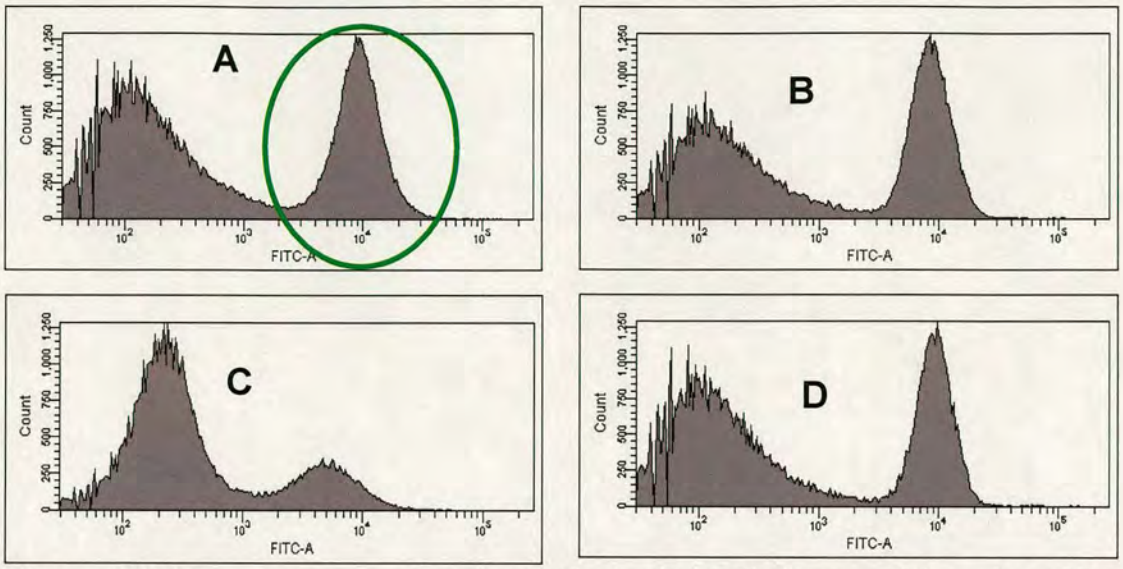

Figure 4.5 *Flow cytometry results of mES-Oct4 cells. Cells harvested from the mES cell population incubated after 8 days (A) on tissue culture plastic disc 13 mm diameter, coated with 0.1% gelatine; (B) 3BG9; (C) polyethylene, chlorosulfonated (KIT 54); (D) 3n9. Green circle indicates fluorescent population of undifferentiated cells.*

Cells were harvested (using trypsin) from the polymer surfaces and analysed by flow cytometry in order to calculate the cell number and look at changes in fluorescence. mES-Oct4 cells have the gene for GFP fused to Oct. Oct4 is present in immature undifferentiated cells only,[128] meaning that analysis of GFP allows easy recognition of differentiated and undifferentiated cells (by flow cytometry). Four independent experiments were run. (**Figure 4.5**)

All samples analysed by flow cytometry were prepared according to the same procedure (see section 6.1.10). The procedure allowed for evaluation of the number of cells present per coverslip. (**Table 4.1**)

Coverslip coated with	**cells/coverslip** [a] **$\times 10^6$**	S.D n=4 **$\times 10^6$**	Non differentiated cells (%)	S.D. n=4
TCP [b], gelatine,	1.14	±0.13	54	±7.5
3BG9 [c]	1.31	±0.33	44	±8.2
54 [d]	1.31	±0.24	22	±3.4
3n9 [e]	1.16	±0.12	35	±6.3

Notes: a) Average number of cells attached on coverslip; b) TCP = tissue culture plastic flask; c) 3BG9 = 2-methoxyethylmethacrylate/ethylene glycol methacrylate phosphate co-polymer (molar ratio 9:1); d) 54 = polyethylene, chlorosulfonated; e) 3n9 = 2-methoxyethylmethacrylate/N,N-dimethylvinylbenzylamine co-polymer (molar ratio 9).

Table 4.2 *FACS results of the differentiation of mES cells under different conditions.*

Results from analysis by flow cytometry of cells attached to coverslips covered with polymers showed that (as found previously), the tissue culture plastic covered with gelatine provided a high protection from cell differentiation. Gelatine provided a culture surface that allowed 55% of cells to remain in undifferentiated state. In contrast, polyethylene, chlorosulfonated promoted the undifferentiated state of only 22% of cells. However polymer 3BG9 was almost as good at preventing differentiation as gelatine. The crucial advantage of artificial polymers is that they are free of bio-contamination.

4.6 Conclusions

Polymer microarrays prepared by printing pre-synthesised polymers were successfully used for pre-selection of mES cell binding polymers. Screening of microarrays with mES cells allowed the selection of 3 polymers which were later tested on a coverslip for comparison of the ability of cell binding with traditional substrates used for mES cultivation. One of these polymers showed binding activity and differentiation prevention similar to tissue culture plastic coated with gelatine.

Chapter 5 : Controlling surface architecture for advance cell patterning

5.1 Cell patterning – introduction

5.1.1 Importance of cell patterning

Cell patterning on a 2D surface or within a 3D scaffold has been broadly applied, for example in the manipulation of cells *in vitro* in attempts to understand cellular responses to the environment[176,177] or to pave the way towards tissue engineering applications.[178] This includes, for example, engineered rat kidney tissue for implantation,[179] skin tissue for repair and regeneration,[180] human neural stem cells for implantation into monkey brains with Parkinson's symptoms for the replacement of the damaged neurons[181] and bone marrow stem cells for liver regeneration.[182]

Research on cell patterning typically focuses on understanding cell-biomaterial interactions in an attempt to understand and influence cell behaviour upon binding to a substrate.[183-187] For example, dendric cell behaviour[188-191] and epithelial cellular migration have been shown to be controlled by substrate rigidity.[192] Moreover polymers have been used to modulate stem-cell differentiation.[193,194] Research on cell-cell signalling has been carried out by controlling the size of microwells and distance between them, to help understand the function of the substrate in mESC colony formation under controlled microenvironmental conditions.[195]

5.1.2 Techniques for cell patterning

Current techniques for cell patterning follow two main strategies. The first uses a modified office-based inkjet printer to pattern living cells directly onto a substrate (with or without gelation of materials) to form 2D or 3D patterned cells,[196,197] while the second is based on patterning biomaterials followed by cell adhesion exclusively onto the designed domains.[198]

5.1.2.1 Direct cell patterning *via* Inkjet printing[196]

Inkjet printing (technology used in desktop printers) is a interesting method of cell patterning because it is simple and avoids contact with the substrate.

This method usually involves modification of consumer printers to replace the paper-feed system with a computer-driven platform to move the sample under the nozzle.[199] (**Figure 5.1**)

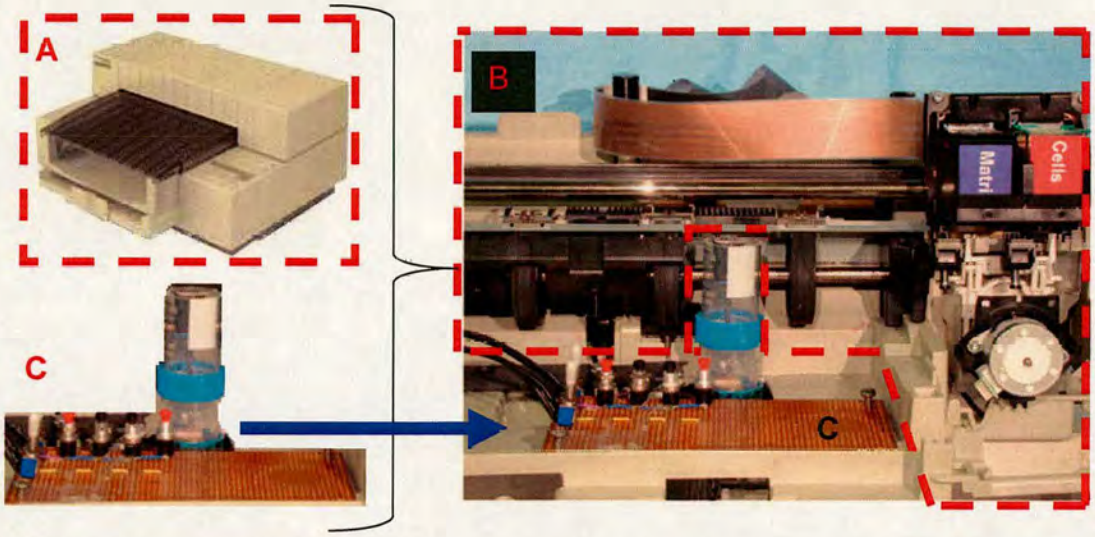

Figure 5.1 *Scheme of HP DeskJet printer modification for direct cell patterning: (A) HP DeskJet 550; (B) modified HP printer; (C) chamber for cell patterning. Reproduced with permission (copyright Elsevier, 2007).*[199]

Due to the size of yeast and bacteria (0.5-5 μm), these can be readily printed, whereas larger animal cells (10-100 μm) vary in their ability to survive printing. Concentrated buffer solution shrinks the cells and so reduces the likehood of damaging the cell in the nozzle. Often a complex growth medium may be crucial for protection of the cells during printing but in this instance viscosity is a limiting factor. Sterility is a major concern for cell viability. Consumer cartridges are difficult to autoclave and must be washed with alcohol instead. In addition, the printing equipment must be used in a sterile environment.

For example, motor neuron cells and Chinese hamster ovary cells were printed in a 3x concentrated phosphate buffer (***Note***: 1x PBS has a concentration of 137 mM NaCl, 10 mM Phosphate and 2.7 mM KCl) with a thermal printer.[200] In the process of ink preparation about 20% of the Chinese hamster ovary cells were dead and, additionally, a few percent were killed during the printing step. For human stem cells, viability was found to be higher when the buffer concentration was lower (x1) and viability dropped

when the buffer concentration increased (x3). The high viability of human stem cells was also achieved using a printing-medium that included glucose glutamine and pyruvate. For comparison, human fibroblasts were piezo inkjet printed with over 98% viability at lower drive voltages (x1 PBS). Immediate use of the ink is important because cells tend to agglomerate and print less well after 20 min storage in printing media.[196] However, the cellular damage during printing is an important limitation of the method.

The surface upon which the cells are deposited is pivotal for the quality of cell patterning. If the surface is dry, cell viability on the patterns drops dramatically, but very wet surfaces allow the cells to float and resolution of printing is limited. Usually the cells are printed in a puddle of medium that allows the cells to survive until further medium is added. Chinese hamster ovary cells were printed upon gel substrates with medium to keep the surface wet.[200] The thickness of the medium layer has also to be carefully optimised to avoid cells floating.

Thus far, there is no reported method to print a single line of cells. Nakamura *et al.* attempted this challenge by printing patterns of single drops consisting of 1-2 cells each. **(Figure 5.2)** With this method the lines (50 μm wide) were generated by printing cells suspended in sodium alginate onto a film of calcium chloride ($CaCl_2$ gels the alginate).[201]

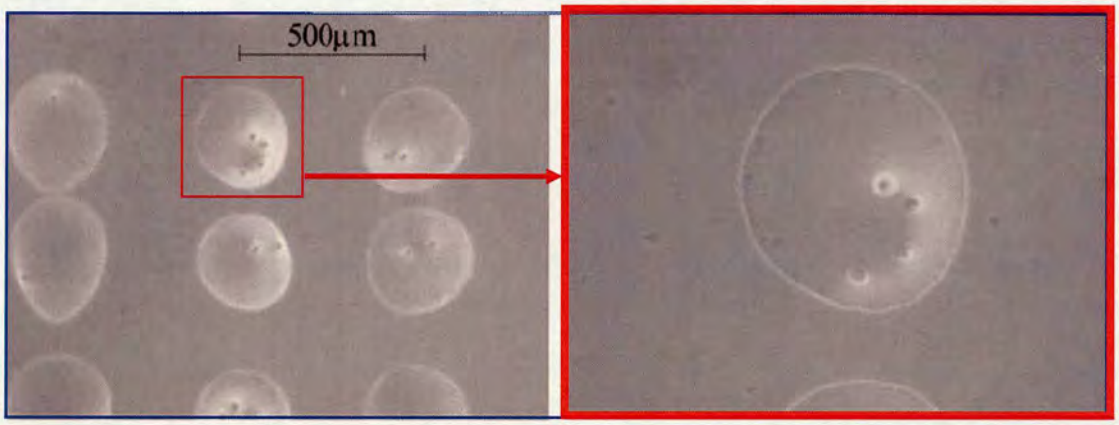

Figure 5.2 *Example of direct cell patterning via inkjet printing Images of printed dots with one to four endothelial cells. Reproduced with permission*[201] *(Mary Ann Liebert, Inc, 2005).*

Inkjet printing was successfully applied for 3D cell patterning. Boland and co-workers[199] used a modified HP DeskJet printer for printing cross-linking agent ($CaCl_2$ solution) premixed with cells (mouse endothelial cells) onto hydrogel (alginate/gelatin). **(Figure 5.3 A)** In contact with $CaCl_2$, alginate/gelatine were instantly crosslinked and micro shells were fabricated as shown in **Figure 5.3.**

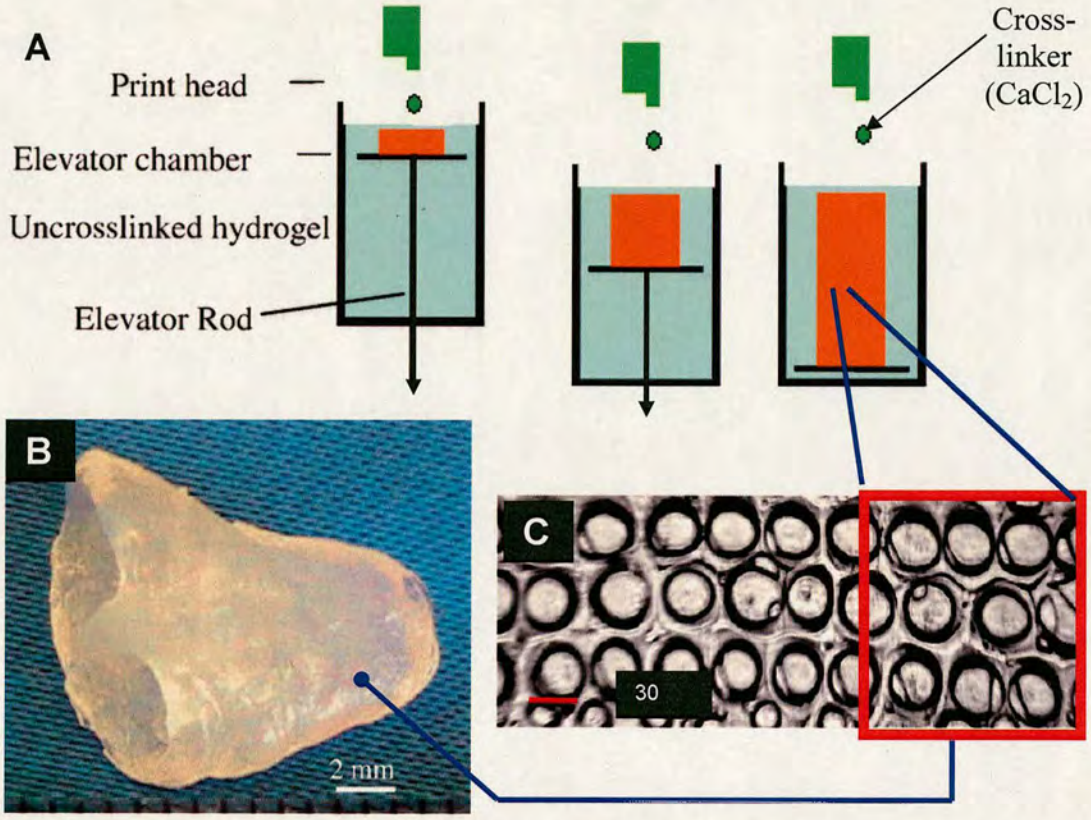

Figure 5.3 *Scheme of three dimensional cell patterning via inkjet printing: (A) scheme of 3D printing; (B) macroscale image of 3D hydrogel structure (containing cells); (C) images of microshells (containing cells) trapped in cross-linked hydrogel. Reproduced with permission (copyright Elsevier, 2007).*[199]

Perspective of development for direct cell patterning via Inkjet printing

According to the opinion of Paul Calvert published in the perspectives section of Science magazine in 2007, there are two obvious directions for the development of inkjet based cell patterning methods,[196] (1) preparation of structures for cell - cell communication studies and (2) building organs for implant.

(1) Cell interaction studies can be performed *via* building layered structures of inkjet printed polymeric films, about 100 nm in thickness. Layers of biopolymer and cells printed into multilayer sandwiches could be used to study the effect of proximity on different cell types, tissue development and development of disease. Accurate cell positioning in the patterns is pivotal for studying the effect of spacing between different cell types on tissue development. For stem cells matrix-mediated-differentiation studies and inkjet cellular patterning could be employed as a method for accurate cell distribution.

(2) Building artificial organs *via* inkjet based cellular patterning remains a significant challenge for the future. The advantage of inkjet printing mediated cell patterning is that it could be easily scalable (submicrometer to hundreds of micrometers). Secondly, not only the cells can be delivered onto developing structures but also other materials, such us precursors of bones (including mineral scaffolds or osteoblast cells), corneas and cartilages. The most promising approach to build a functioning organ is *via* printing a geometrically precise matrix with a few cells that will grow and finally complete the structure. However, these require better understanding of the communication between the cells and between cell and external cellular matrix.[202,203] Another issue that must be solved is the feeding of the cells during organ constructon (before the regular blood supply).

In summary inkjet printing technology offers a way to create artificial organs and 3D bio-structures for studying cell interactions

5.1.2.2 Cell patterning *via* biomaterial deposition[198]

The second strategy for cell patterning that has attracted much attention is based on patterning biomaterials followed by cell adhesion exclusively onto the designed domains.[198] These include techniques such us soft lithography, photo lithography and dip-pen nanolithography.

5.1.2.2.1 Cell patterning via soft lithography[198]

One example of this approach is the use of soft lithography, with soft elastomeric stamps (with patterns designed in PMDS) used to transfer cellular binding materials onto a

substrate in a highly defined pattern.[204-205] Soft lithography includes indirect cellular patterning, direct cellular patterning and negative patterning.

Indirect patterning

Cell patterns were fabricated by attaching cells on a gold or silver-coated surface *via* micro-contact printing of thiol-based molecules. Stamped thiol-based molecules produced geometrically controlled patches of self assembled monolayers. (**Figure 5.4**)

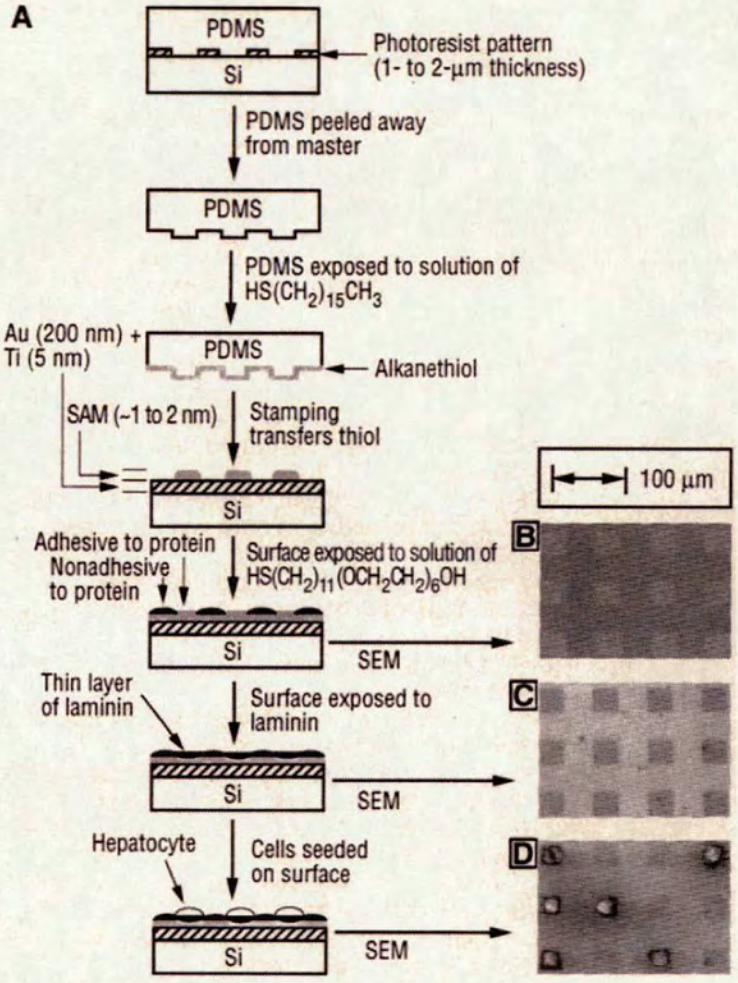

Figure 5.4 *Scheme of indirect cell patterning: (A) indirect printing; (B) SEM images of substrates after printing hexadecanethiol (adhesive regions) and exposure to PEG-terminated alcanethiol (non adhesive region); (C) SEM of laminin coated substrate; (D) SEM images of Rat hepatocytes cells on the laminin coated surface. Reproduced with permission*[206] *(Copyright AAAS, 1994).*

Typically, hydrophobic alkanethiolates are printed on to gold substrates - in that way hydrophobic patterns are fabricated.[206-208] In the next step ethylene–glycol-terminated thiols (cell adhesion inhibitors) are spread over the non-stamped areas. In a third step, the hydrophobic regions are functionalized through the adsorption of fibronectin or other protein enhancing cell attachment.

In another application, Patel[209] coated modified polystyrene surfaces using biotinylated poly-lactic–poly(ethylene glycol) (PLA–PEG). In a second step, the avidin was printed on these modified substrates. The avidin pattern was subsequently functionalized with any biotinylated protein.

Oliva used a micro-contact patterned protein A (cell wall surface protein) on glass substrates. The patterns were functionalized with a chimeric protein. The chimeric protein was constructed with the extracellular domain of the axonal guidance molecule L1 linked to the Fc fragment of immunoglobulins (IgG). The Fc fragment of immunoglobulins was selectively bound to protein A. The surface was backfilled with poly-L-lysine prior to neuron cultivation. As a result, axon growth was found selectively over the patterns, while the dendrites were found over the background. [210]

Direct printing

There are many approaches to directly pattern the substrates with cell adhesion supporting molecules. In the simplest variant, the molecules are physisorbed on the surface. The list of applicable adhesion supporting molecules include different extra-cellular matrix (ECM) proteins and synthetic peptides.[211] **(Figure 5.5)** The type of the printed ECM molecules needed to be optimised for the cellular system used.

In the first reports about protein-printing, Bernard stamped different immunoglobulins and BSA,[212] while James used poly-L-lysine.[213] Many cell types were successfully patterned using fibronectin as the ink.[214-216]

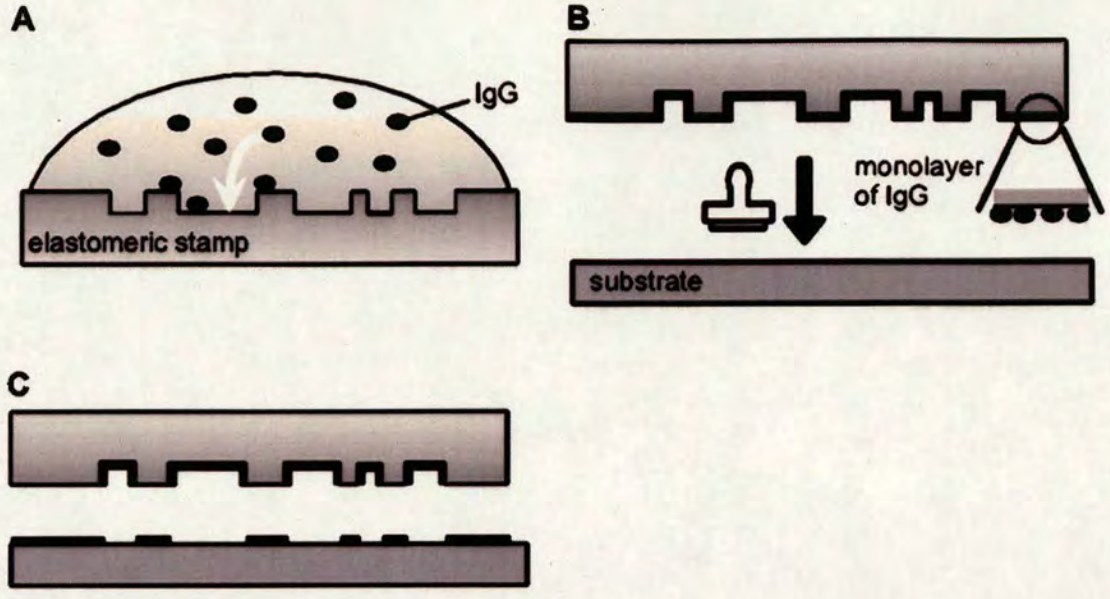

Figure 5.5 *Scheme of direct cell patterning: (A) generation of adhesive protein (IgG) layer on electrometric stamp; (B) placement of stamp on non-adhesive substrate; (C) removing the stamp – a layer of protein is deposited wherever contact occurred. Reproduced with permission[212] (copyright ACS, 1998).*

Neurons were patterned by using synthetic polypeptides containing the cell binding sequences of laminin, [217] polylysine-conjugated laminin,[218] agrin[219] or by using pure laminin.[220] Patterning of *Escherichia coli* was achieved through stamping specific antibodies.[221] The stability of the physisorbed molecular patterns (not covalently attached to the underlying substrate) is not sufficient for longer-term studies and stronger covalent linkage of the stamped molecules to the surface is preferred. Using thiol-based self assembly monolayer chemistry, the synthetic oligopeptides (containing a cell adhesion motif and the thiol residues) were patterned on gold surfaces.[222] Different methods for covalently linked patterns are silanization of glass[223-225] and chemical activation of different polymeric surfaces.[226,227]

Negative patterning[198]

In the majority of the reports, the cell adhesive regions are printed while the background inhibits cell adhesion. Example of the opposite approach include stamping octadecyltricholorosilane (cell attachment inhibitor) onto silicon wafers and backfilling

with N^1[3-(trimethoxysilyl) propyl]diethylenetriamine (DETA) (cell adhesive patches).[228,229] (**Figure 5.6**) Negative patterning approaches are rather rare and an interesting area of scientific exploration.[230]

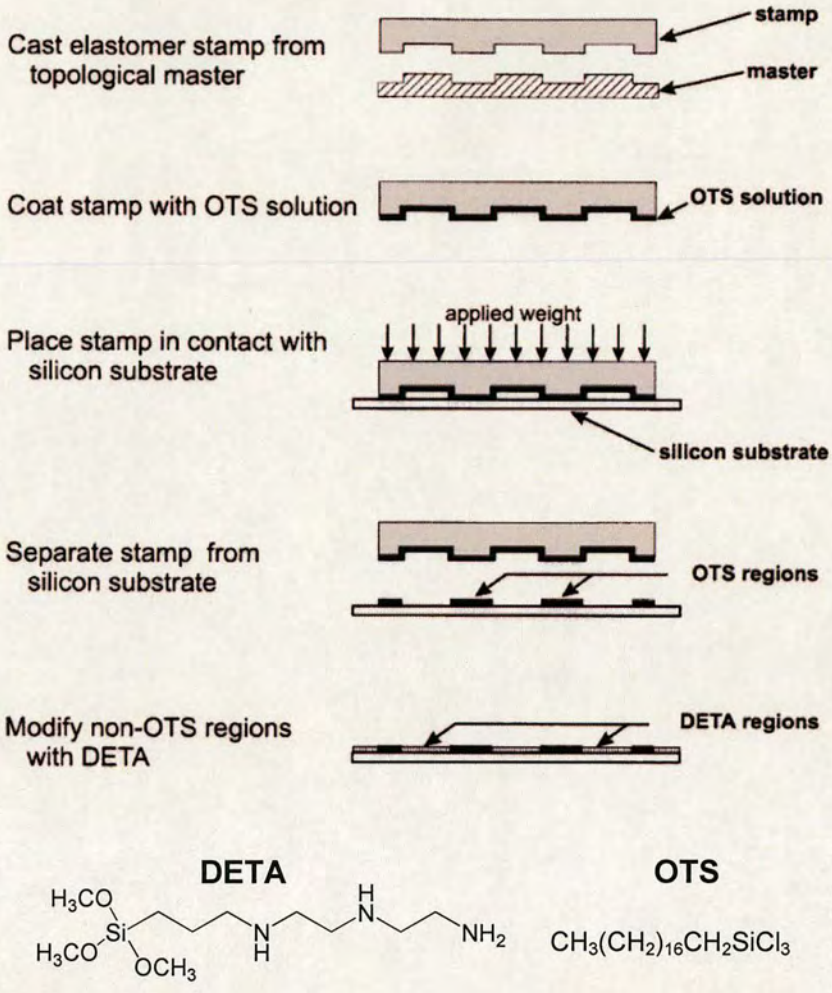

Figure 5.6 *Scheme of negative cell patterning. Reproduced with permission*[228] *(copyright Elsevier, 1999).*

5.1.2.2.2 Cell patterning via photolithography[198]

Another example of a technique utilized for cell patterning is photolithography (UV initiated functionalization through highly defined masks).[198] A mask is typically made of a quartz (glass) plate coated with a non-transparent layer of chromium (with desired geometric features). The design of the mask is prepared using computer-aided design (CAD) software. Quartz/chromium masks allow feature resolution down to 1 μm and

could be replaced by printing the drawn features on a transparent foil using a commercial inkjet printer (feature resolution with a tolerance of 10 μm). (**Figure 2.1**)

For example, Scotchford used chemical vapour deposition (CVD) processes for deposition of the desired metal 1 (covered by native oxide layer). The layer was spin-coated with a UV sensitive polymer.[231] Subsequent to photo-resistant patterning, the whole wafer was coated with metal 2. The last step was a "lift-off" process – removing the photo resistant polymer by dissolution in an organic solvent. As a result, the patterned surface is consisted of metal 1 (background) and metal 2 (pattern). When this strategy was used to generate niobium, titanium or vanadium patches on an aluminium background, cells were able to sense differences between different metal–oxides. After 24 h, the aluminium (covered with Al_2O_3) surface attracted significantly lower number of cells than more cytophilic patches of TiO_2, Nb_2O_5 and V_2O_5.[231]

Kleinfeld reported fabrication of patterns using aminosilane[232] and alkylsilanes.[233] The substrate and the patterned photo-resistant polymer were coated with a hydrophobic alkylsilane, followed by a photo-resistant polymer "lift-off". The area previously protected by the photo-resistant polymer was subsequently coated with a hydrophilic aminosilane. Rat calvaria osteoblasts cells showed a preference for the aminosilane surface compared to the alkylsilane. Interestingly, this cellular behaviour was observed only when cells were incubated with serum. Different affinity of the two silane-terminated surfaces for serum proteins is the reason for preferential cell attachment on the aminosilane surface. Moreover, after 20 days of cell culture the mineralization was restricted to the aminosilane pattern. Experiments performed with human cells showed different outcome. Human osteosarcoma cells were attached and grown on the aminosilane surface in the absence of serum proteins.

Bhatia used a similar approach, with "open windows" fabricated within a photo-resistant polymer for directly immobilised cell binding proteins prior "lift-off" process.[234] Disadvantages of this approach is that the immobilized proteins are exposed to an organic solvent during the "lift-off" process. This can drive partial protein denaturation. However this technique was successfully applied to the production of a two-dimensional co-culture of hepatocytes and 3T3 fibroblasts cells. In the first step hepatocytes cells

were allowed to attach to the pattern under serum-free conditions. In a second step 3T3 cells (with serum) were attached to the glass.

5.1.2.2.3 Cell patterning via dip-pen nanolithography[198]

More exotic approaches include techniques such as dip-pen nanolithography,[235,236] which rely on an AFM tip to deliver cell binding materials to highly defined, specific positions on a surface. This naturally provides tremendous resolution but also has a number of limitations with respect to applicability, scale-up and general accessibility. (**Figure 2.5**)

5.1.3 Indirect cell patterning *via* inkjet printing

In 2004, Boland and co-workers reported cellular patterning by printing a cell binding material (in this case type II collagen)[237] onto an agarose coated surface using a modified Canon Bubble Jet system (BJC-2100, Canon Inc. Tokyo, Japan), thereby allowing smooth muscle cells to be attached in a defined pattern. (**Figure 5.7**)

The novelty of the approach presented here lies in the significant improvement of the complexity of computer aided design of the cellular patterns (see **Figure 5.8**). The complex cellular patterns generated with high accuracy are pivotal for future applications, such as artificial organ development for implants.

The scientific inkjet printer operated in a drop-on-demand mode *via* a piezoelectric firing mechanism, which created droplets with a volume of approximately 380 pL at frequencies between 0 and 2 kHz and used a stroboscopic camera to monitor droplet formation. This allowed accurate control of the volume of the deposited materials by simply varying the number of drops printed in any specific location. The advantages of this kind of printer are that they can control printing of any desired pattern using virtually whatever material is desired and addressed to any specific position on a slide. Recently, this inkjet based approach was used by the Bradley group to prepare, in a high-throughput and highly miniaturised manner, 231 formulations of three independent liquid crystals (in essence converting a conventional 3 component-phase diagram into a rectangular format)[123] and was also used to prepare 1800 polymers on a glass slide by *in situ* nanolitre polymerisation.[124,127]

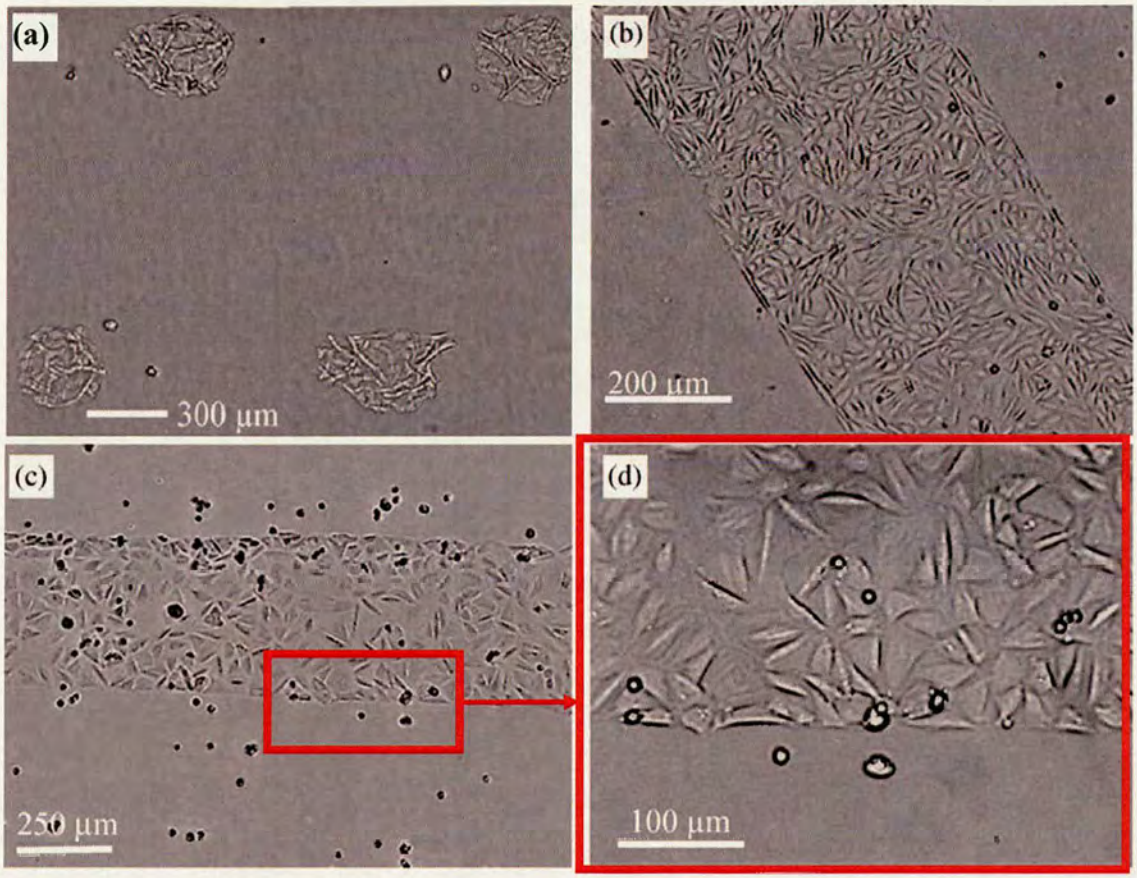

Figure 5.7 *Microscope images of a printed collagen features seeded with smooth muscle cells: (A) spots; (B) line; (C) line after high-density seeding; (D) morphology of the patterned smooth muscle cells. Reproduced with permission*[237] *(copyright Elsevier, 2004).*

5.1.3.1 Pattern design

To demonstrate this approach, a material which could bind a variety of cell lines was an important priority. Collagen was chosen as the patterning material because it is a well known universal cellular binder and widely applied in cell culture.[237] For printing in a defined pattern any desired image or picture was converted from an image file (*e.g.* a bitmap file) into a coordinate file using the software WinDig, which was converted to a macro file suitable for use by the printer using an in-house bitmap converter (see section 6.6.2). This allowed the printer to ink different solutions and print them at the required positions with high accuracy. (**Figure 5.8**)

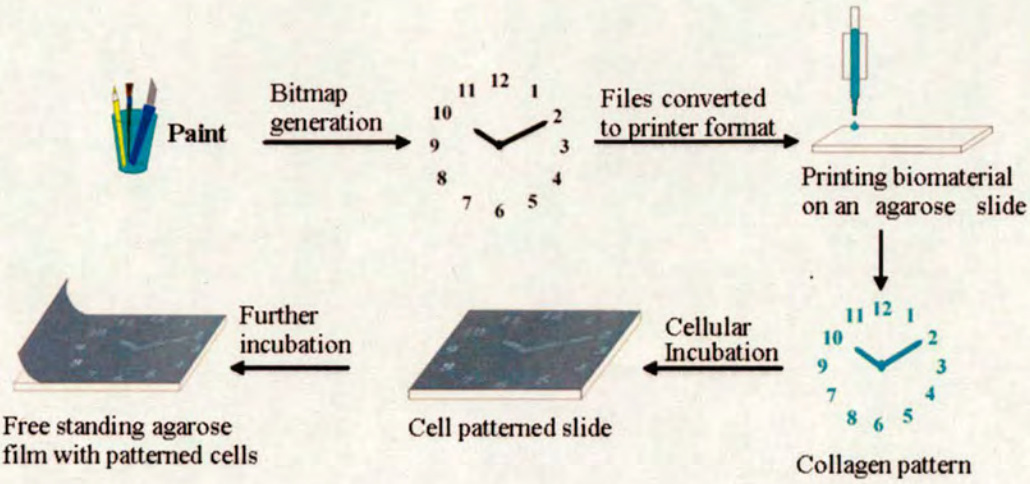

Figure 5.8 *Scheme of generation of an image of a "clock" and its conversion to a file suitable for inject printers. Collagen printing, cellular binding and substrate detachment gave a free-standing film with patterned cells.*

The quality of the printed patterns was controlled by many factors, such as the hydrophobility of the substrate surface, the size of the printing nozzle and the viscosity of the solutions. Different concentrations of collagen solutions were tested, with the printer generating consistent drops with a collagen concentration of 1 mg/mL (in 0.1 M acetic acid). Printing of a second spot on top of the first one after it had been dried gave images with sharp boundaries. The collagen patterned slide was then dried and sterilized before use.

HeLa[238] and mouse embryonic stem cells (mES-Oct4)[128] both adhered and proliferated only on the patterned areas of the slides (**Figure 5.9 and 5.10**). It can be seen (**Figure 5.9**) how sharp the resulting image was, following cellular staining and fixing and shows that the drops of the printed collagen are around 230 μm in diameter, which is thus the limit of patterning fidelity on agarose. The attached HeLa cells, which spread all over the collagen showed a healthy cellular morphology. (**Figure 5.9**)

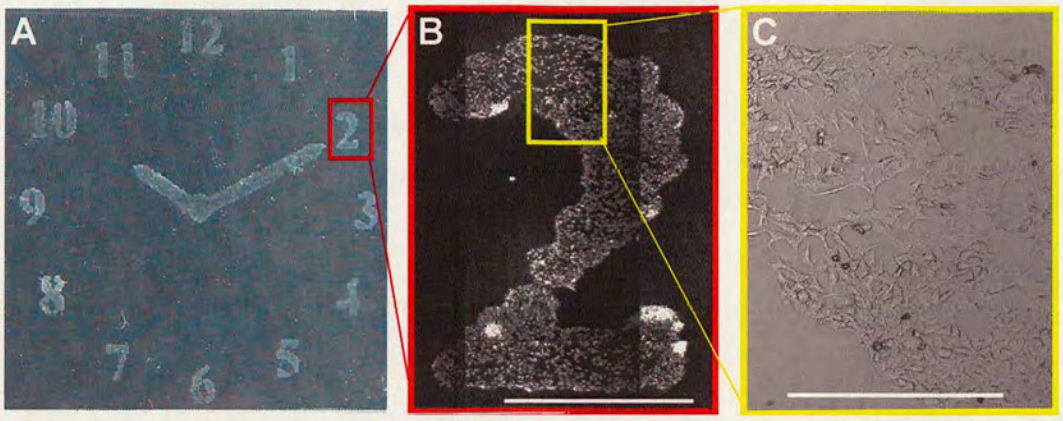

Figure 5.9 *Images of cells patterned via inkjet printing: (A) HeLa cells patterned in the image of a clock via collagen printed onto agarose (square is 26x26 mm); (B) Hoechst 33324 (nuclei staining) images of HeLa cells in a patterned "2" (Scale bar 1 mm); (C) bright light image expansion showing part of the number "2". (Scale bar 0.25 mm).*

The clock image patterned with mEC-Oct4 cells is shown in **Figure 5.10**. mEC-Oct4 cells after 48 h incubation began to develop 3D cellular aggregates on the collagen pattern as shown by the live cell image. **(Figure 5.10)**

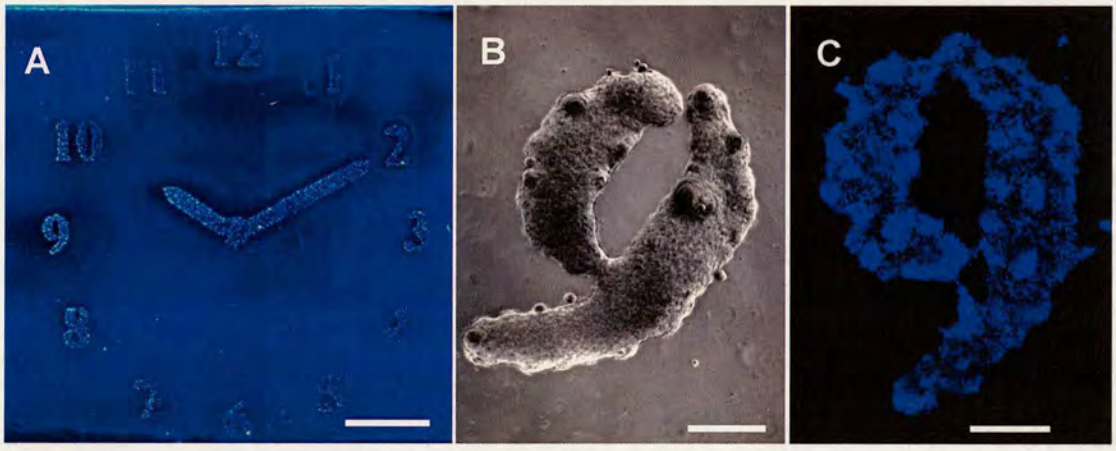

Figure 5.10 *Images of mES-Oct4 cells patterned on: (A) collagen patterns printed on agarose coated glass slide, fixed with formaldehyde (4% w/v) and stained with Hoechst 33324 (nuclei stain),(scale bar 5 mm); (B) live cell imagining of mES-Oct4 cells patterned as a "9" (scale bar 0.5 mm); (C) fixed and stained mES-Oct4 patterned as a "9". Scale bar 0.5 mm.*

5.1.3.2 Cell gradient generation

To print a collagen gradient, collagen was inkjet printed onto the agarose coated slide in a one drop per position mode. During the first pass 100 parallel lines (5 mm long) were printed with a 130 μm gap between two adjacent lines. (**Figure 5.11 B**) With subsequent printings the number of lines was decreased by two lines. Since the distance between two drops was less than 260 μm the printed collagen drops merge together to generate a gradient on the agarose coating. (**Figure 5.11**)

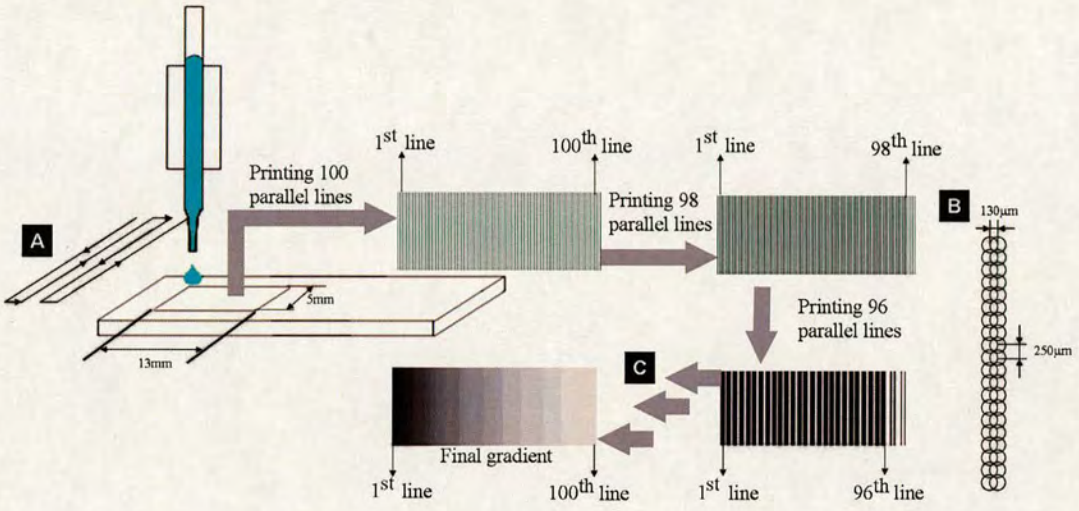

Figure 5.11 *Scheme of generating a collagen gradient: (A) basic pipette motion for generating parallel lines of collagen; (B) printing parameters for two parallel lines of collagen; (C) printing the gradient is a 50 steps process. In the first step 100 lines are printed. In the second 98 and so on up to 50th step when 2 lines only are printed.*

Upon culture, the printed gradients showed a gradual change in affinity for cells. (**Figures 5.12** and **5.13**)

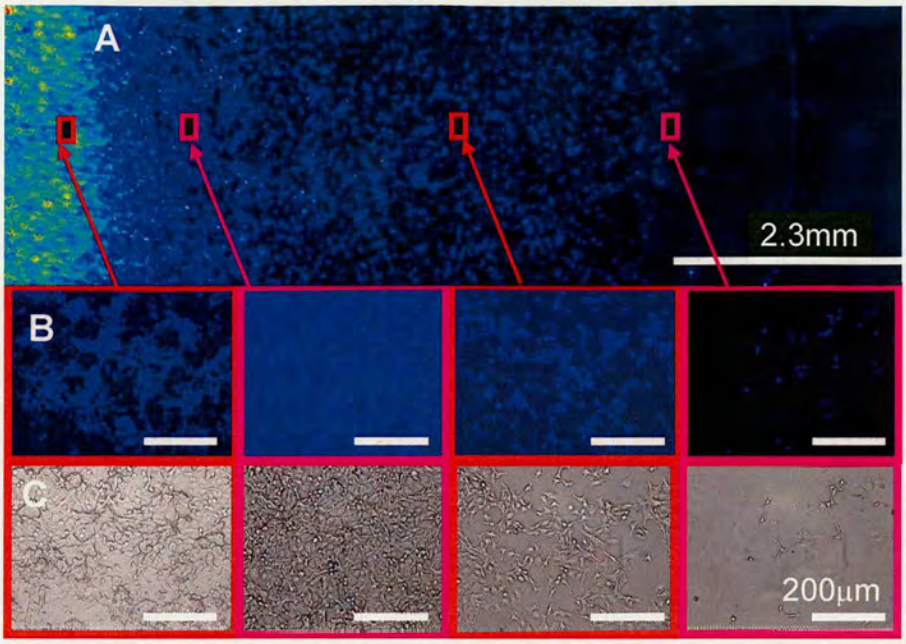

Figure 5.12 *Images of HeLa cell: (A) growing on a collagen gradient printed on an agarose coated glass slide; the cells were stained (Hoechst 33324) and fixed; (B) fluorescent images; (C) brightfield images of regions of the gradient array. The scale bars in the expanded images are 200 μm.*

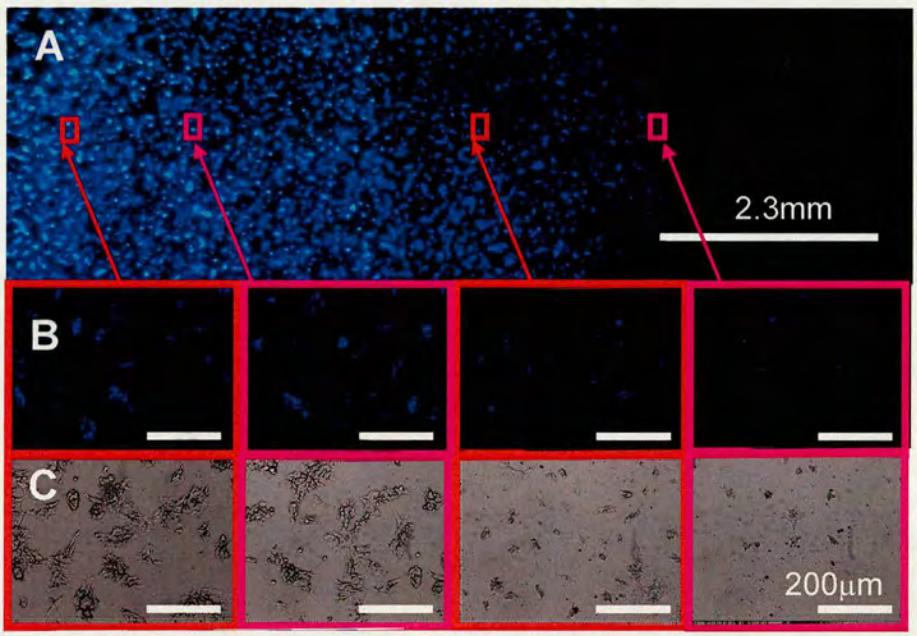

Figure 5.13 *Images of mES-Oct4 cells: (A) growing on a collagen gradient printed on an agarose coated glass slide; the cells were stained (Hoechst 33324) and fixed; (B) fluorescent images; (C) brightfield images of regions of the gradient array. The scale bars in the expanded images are 200 μm.*

In 2004, Boland and co-workers presented a method for generating cellular gradients using collagen printed onto agarose coated slides. The gradient was designed using PowerPoint software (Microsoft, Redmond, WA) and printed using a modified Canon Bubble Jet system (BJC-2100, Canon Inc. Tokyo, Japan).[238] However, their gradient looked significantly different to those presented in this thesis (**Figure 5.14**), with smooth muscle cells in the separate colonies rather than freely spread across the gradient. That could be explained by the specificity of the smooth muscle cell but more likely the significant improvement of gradient uniformity showed in **Figures 5.12 and 5.13** is the result of printing collagen with much better accuracy.

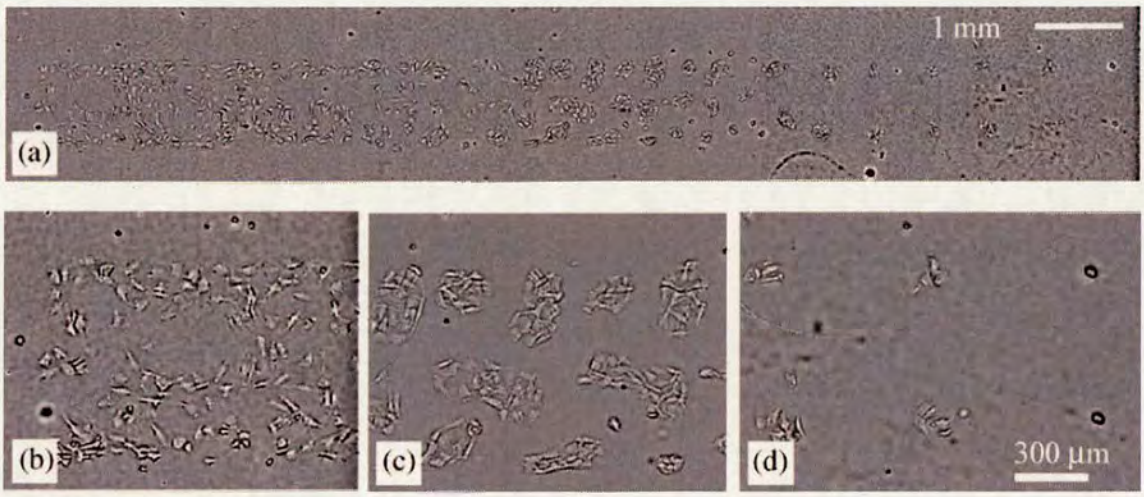

Figure 5.14 *Images of smooth muscle cells gradient pattern after 2 days culture: (A) the overall gradient; enlarged views of (B) head (C) middle and (D) tail of the gradient. Reproduced with permission1*[238] *(copyright Elsevier, 2004).*

5.1.3.3 Free standing hydrogel film with patterned cells

The cell patterned agarose layer could be detached from the glass slide to give a free standing hydrogel film with patterned cells as shown in (**Figure 5.16**). Agarose is well known[238] as a cytophobic material for use in cellular patterning and can effectively prevent the adhesion of most cell types. Slides with varying thickness of dried agarose film (2.3 μm, 9.3 μm and 26 μm, measured *via* SEM) were evaluated. (**Figure 5.15**)

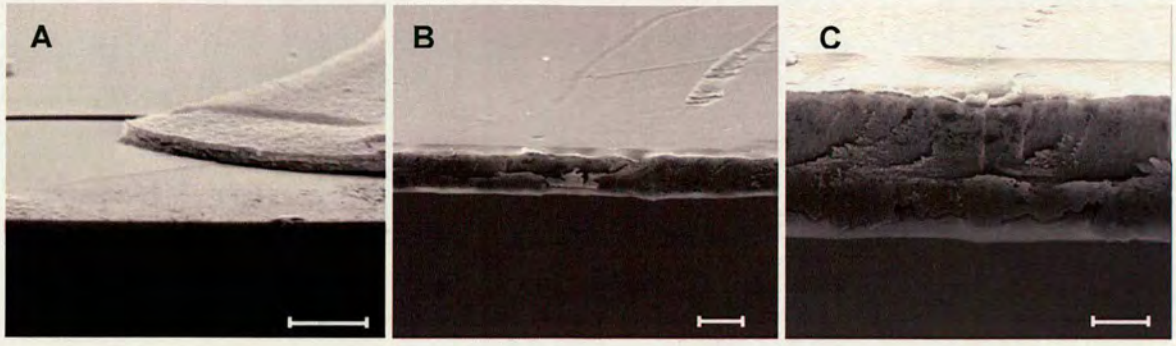

Figure 5.15 *SEM Images of agarose film: (A) 2.3 μm thickness; (B) 9.3 μm thickness; (C) 26 μm thickness (scale bars 10 μm).*

It was observed that 2.3 μm agarose film firmly adhered onto the amino-glass slide (>2 weeks), while the 9 μm and 26 μm agarose films became detached after 24 h. **Figure 5.16** shows a free standing agarose film (26 μm) patterned with HeLa cells (stained and fixed), which came visible after the agarose film was dried. (**Figure 5.16 B**)

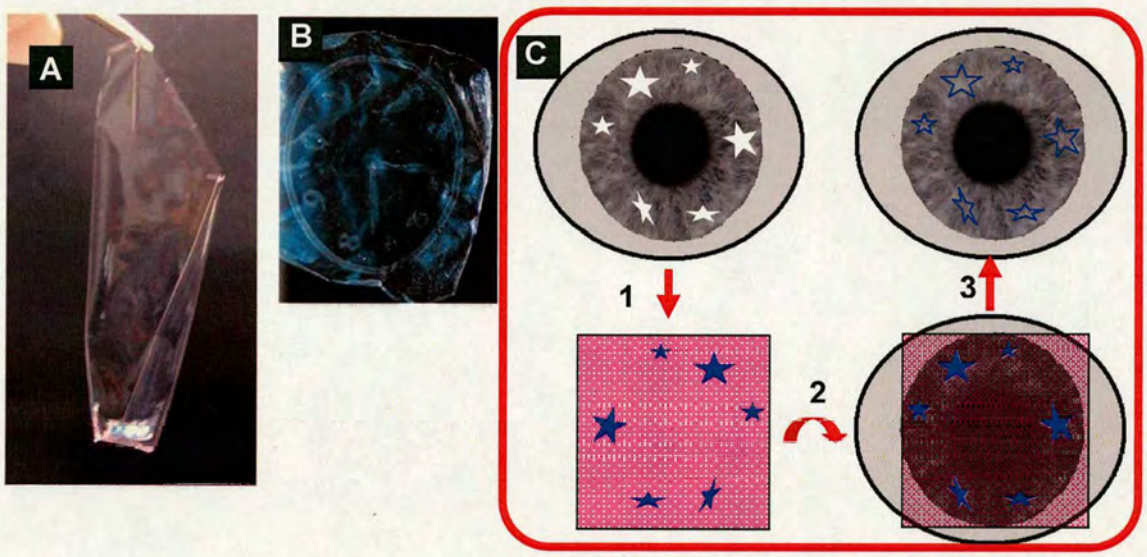

Figure 5.16 *Images of free-standing agarose film (34.4 μm thickness): (A) with patterned HeLa cells (approx 26 mm x 76 mm); (B) the cell patterned clock become visible after the agarose film was dried (26 mm x 26 mm); (C) suggested application of cellular films – for cornea treatment; (1) wound imagining, printing "cell filling" patterns and cell incubation in desired regions of agarose film (blue stars); (2) placing patterned cells on cornea; (3) cell incubation.*

The free-standing agarose films have many applications. For example, the simple imaging of the wounded area of the tissue allows the design of cellular patterns with an exact shape that covers all the wounds, while the permeable agarose film would allow fluid and oxygen exchange to support transfer and growth of the cells.

5.1.3.4 Conclusions

To summarize, a flexible method has been developed to attach and grow cells on agarose coated amino-modified glass slides patterned with collagen using a scientific inkjet printer. Any 2D pattern could be generated and multi-biomaterials could be delivered onto any position on the pattern in a step-wise manner. The free standing agarose film patterned with cells could be applied in tissue engineering. An "organ printing" approach could be envisaged where cell aggregates are placed layer on layer followed by morphing layers into 3D structures.[239] Since non-selective cellular transfer has been previously applied in regenerative medicine, mostly notably in the regeneration of damaged epithelium,[129] it was of interest to investigate this area of research using our cell-patterning technique. As such, I fabricated a free standing film of patterned HeLa cells, whereby the agarose layer could be detached from the glass slide to give a hydrogel film impregnated with cells. Agarose is well known to be a cytophobic material and has been applied extensively in cellular patterning and can effectively prevent the adhesion of most cell types. As such, agarose presented itself as an ideal candidate upon which to develop a free standing cell-patterned hydrogel film.

5.1.4 Exotic cell patterning *via* laser printing

Heat transfer printing is a transfer technique developed over one hundred years ago[240] and has been the main printing technique for printing coloured images, *e.g.* words on T-shirts, caps, bags, ski boards, etc.

5.1.4.1 Pattern design

In the process of cell patterning *via* laser printing two critical phases must be distinguished and described in order to avoid misunderstanding. The ***first phase is glass patterning*** followed by a ***second phase - cell patterning***. The goal of the first phase is to

pattern the glass with material which does not bind cells. The goal of cell patterning is to attach the cells to the unmasked surface, (**Figure 5.17**) thereby giving the desired pattern.

First phase - glass patterning

The pattern desired (**Figure 5.17 A**) was printed onto a colour laser transparency (210x297 mm) using a standard office based laser printer of resolution 600dpi. (**Figure 5.17**) The advantages of this kind of printer are their ready availability and the ease of printing any desired pattern using commercially available toners with different colours. The main components of the laser printer toner are a styrene acrylate copolymer (75-85% wt), wax (5-10% wt) and pigment (1-5% wt), which are not soluble in water or aqueous medium after printing (and show cytophobic effects to cells).[241] Toner was printed onto commonly used transparencies, which were made from polyethylene terephthalate (PET) (see section 6.6.3.6) to give the desired pattern. Patterns placed onto the PET were transfered to the glass *via* heating (175 °C). (**Figure 5.17**) The reason why the toner can be transferred onto the glass slides can be explained according to the theory of offset printing.[242] At about 175 °C, the distance between the molecules of the melted toner and the glass slide becomes very close (~10 Å), which generates a strong adhesion of the melted toner to the glass surface. Therefore, the toner on the PET is readily transferred onto the glass surface. This is the end of the first phase- glass patterning.

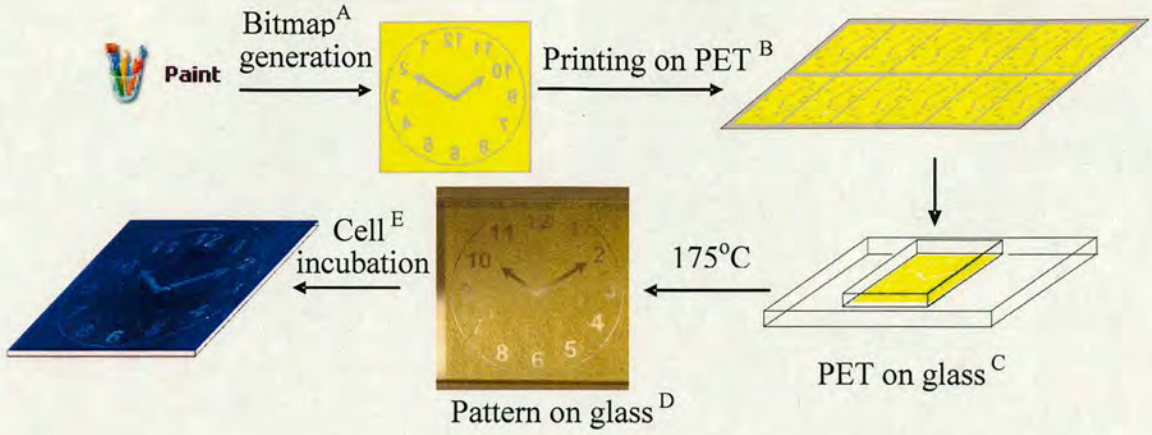

Figure 5.17 *Scheme of cellular patterning via laser printing: (A) an image (for example, a clock face) is generated in reverse to act as a template of the final cellular pattern; (B) the image was then printed onto a transparency (PET) via laser printing; (C) the image on the PET sheet was then placed (face down) onto the glass slide; (D) during heating the laser toner deposited onto PET was transferred onto the glass via heat transfer; (E) cell incubation on the patterned glass slides resulted in cellular patterned glass.*

Second phase - cell patterning

The patterned glass slide (product of the first phase) was used for cell patterning. In the second phase cells were incubated on the patterned glass and after 48 h the cells were observed to be successfully restricted to the unmasked glass surface. (**Figure 5.17**) In this way, cell patterning was performed.

It was found that both HeLa and mES-Oct 4 cells bound and proliferated on the naked glass but not on masked areas of the slide. (**Figure 5.18**) The patterned glass slide was incubated with mES-Oct4 cells (700,000 cells per slide) after sterilizing with irradiation by UV light. The living cell images were taken in order to monitor the changes over time following seeding. (**Figure 5.18**) The images taken after 48 h and 72 h incubation showed that the cells attached and spread only on the unmasked glass surface. In the case of HeLa cells, the slide with attached cells was fixed, stained and fluorescently imaged after 48 h. The result is shown in **Figure 5.18 C**. The expanded arrow of the cell patterned clock indicates that the cells were successfully restricted in the unmasked glass surface and displayed a healthy morphology.

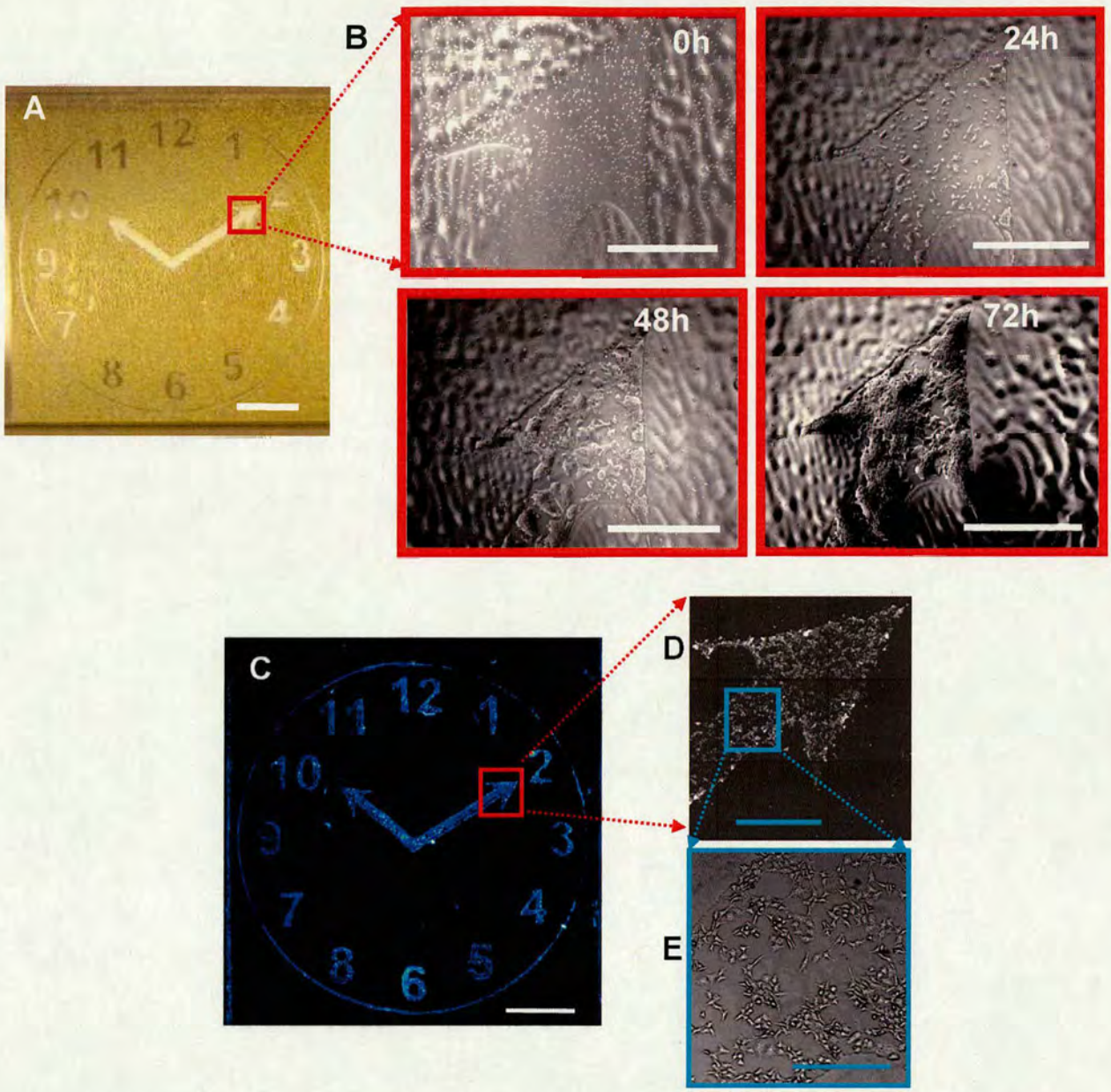

Figure 5.18 *Images of mES-Oct4 and HeLa cell patterning: (A) an image of a clock face on a glass slide before cell incubation, (scale bar 5 mm); (B) image of living mES-Oct4 cells on the "clock hand" taken with a Leica microscope using a 5x/0.12 objective after 0, 24, 48 and 72 h incubation (scale bars 1 mm); (C) a fluorescent image of HeLa cells patterned on the clock face, after the cells were fixed and stained with Hoechst 33342 (nuclei dye), taken using a CCD – based fluorescent imager with a DAPI filter (scale bar 5 mm); (D) fluorescent image of the expanded "clock hand" from the cell patterned clock scanned using a Nikon microscope with a 10x/0.30 objective and a DAPI filter set (scale bar 1 mm); (E) bright light image of a further expanded area with 20x0.30 objective (scale bars 250 μm).*

Patterning of mES-Oct4 cells (**Figure 5.19**) was found to be more challenging because mES cells can form multilayers on the glass surface.

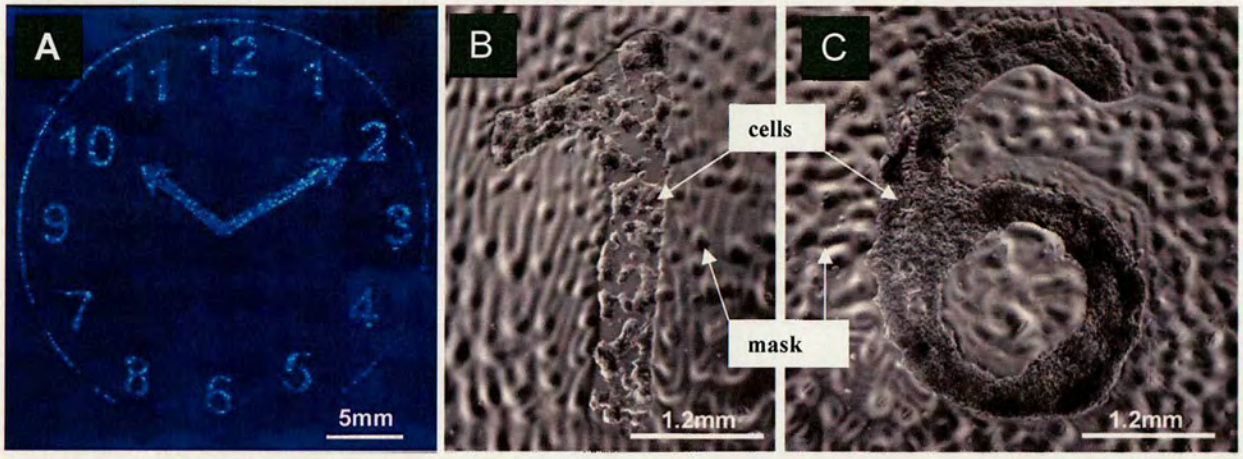

Figure 5.19 *Images of mES- Oct4 cells: (A) patterned as a "clock face". Cells were fixed and stained with Hoechst 33342 before images were taken using a CCD - based fluorescent Bioanalyser (LaVision Biotec) with a DAPI filter; (B) living mES - Oct4 cells patterned as the digit '1' after 48 h incubation; (C) living mES - Oct4 cells patterned as a digit '6' after 72 h incubation. Images were taken with a Leica microscope with 5x objective.*

To illustrate the possible fidelity of the method, images such as cycles, triangles or squares with various dimensions were printed. (**Figures 5.20, 5.21** and **5.22**)

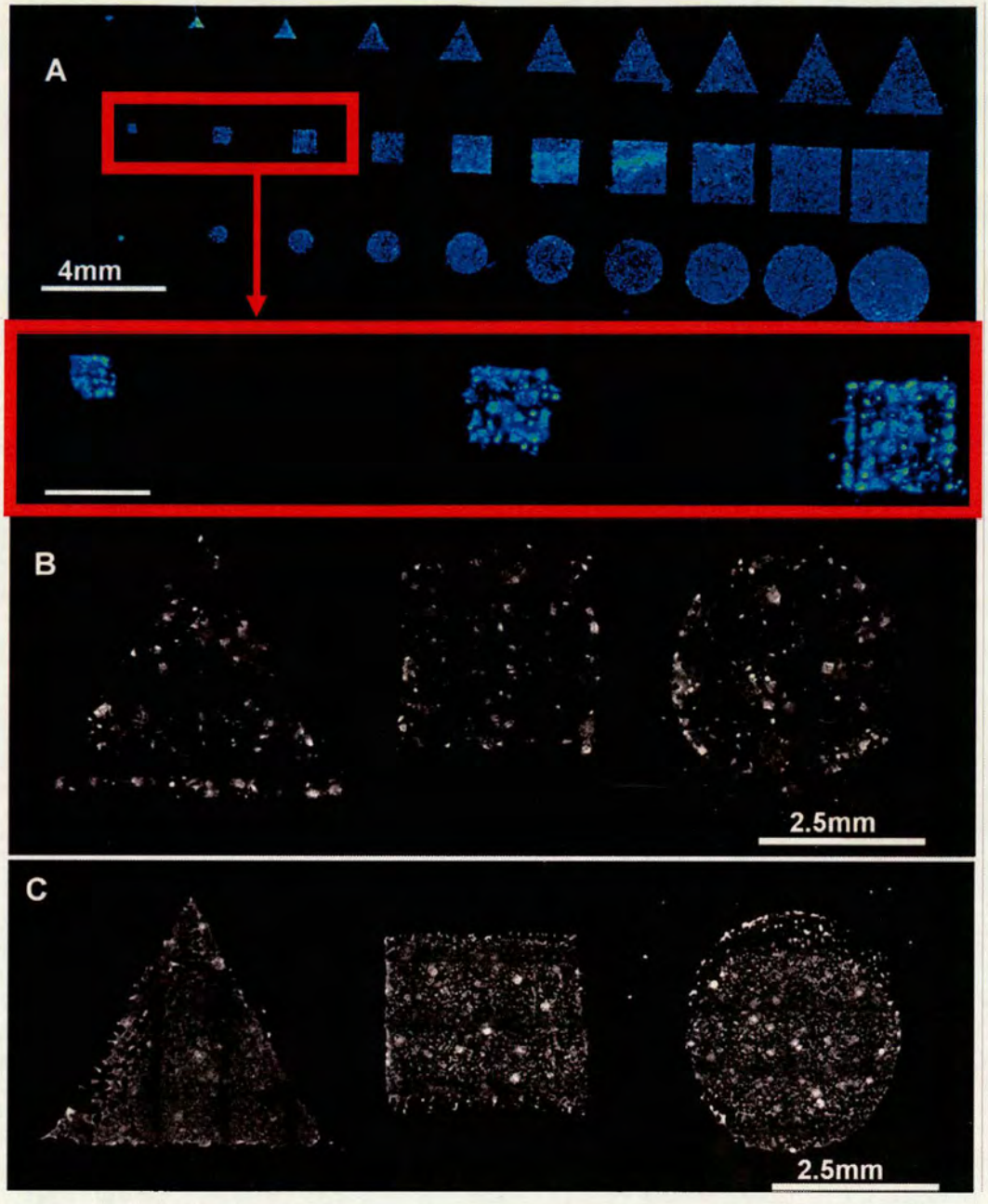

Figure 5.20 *Images of patterned cells on heat transfer printed glass slides: (A) fluorescent image of mES - Oct4 cell patterned on different shaped and sized images; (B) expanded mES- Oct4 cell patterned shape; (C) expanded HeLa cells patterned shape.*

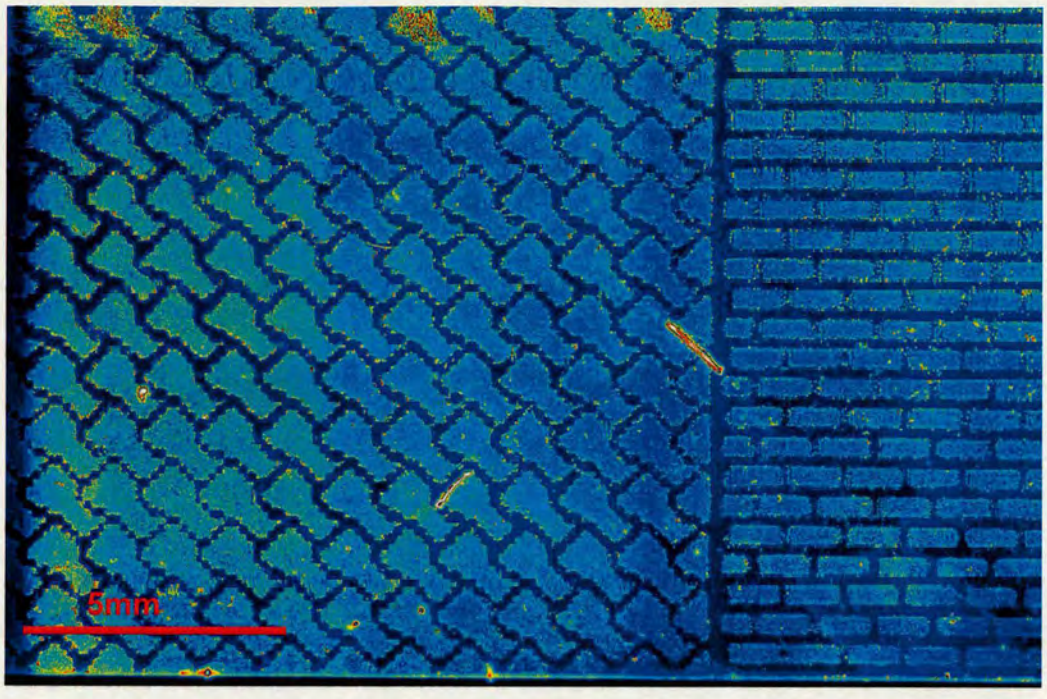

Figure 5.21 *Images of HeLa cells array patterned on one masked glass slides.*

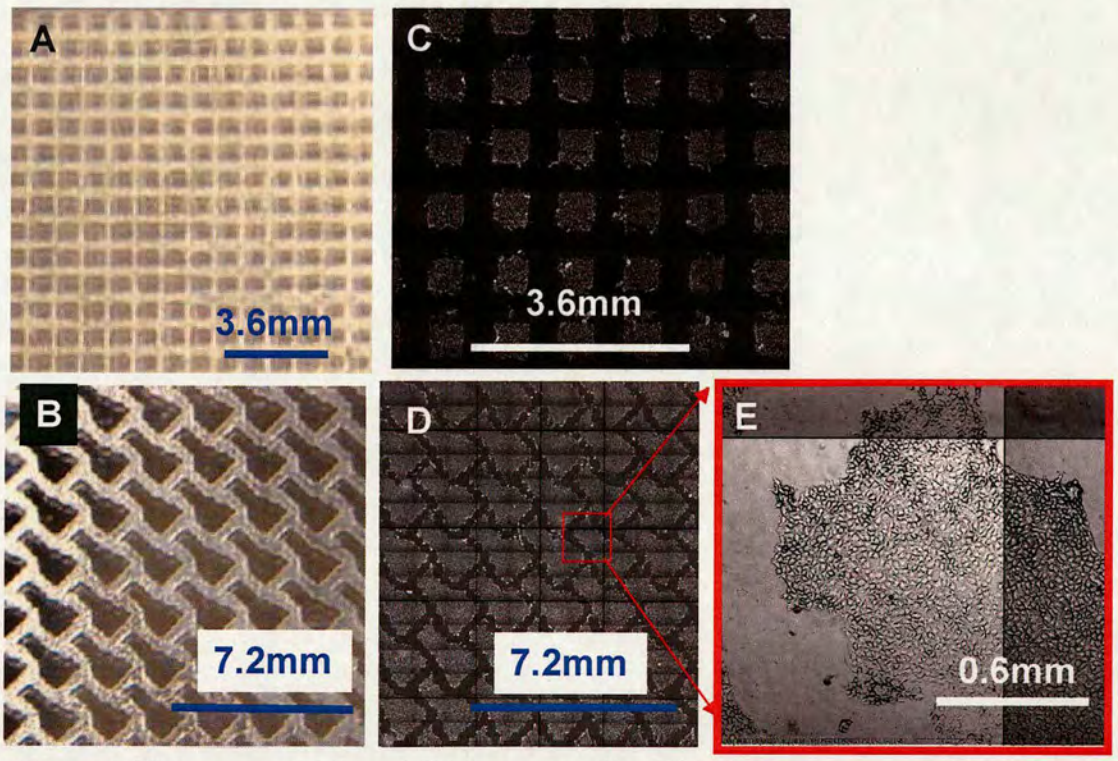

Figure 5.22 *Images of (A) and (B) heat-transfer printed square arrays; (C) (D) and (E) images of HeLa cells growing on the glasses surface, scanned using a Nikon microscope using a 10x/0.30 objective and a DAPI filter set.*

An important feature of cell patterning methodologies is the ability to obtain the smallest feature size possible. To achieve this, lines with a width down to 25 μm were printed allowing single cells to grow and spread along the direction of the lines. (**Figure 5.23**) The patterns were obtained using methods described before (**see Figure 5.17**) but lines were printed in place of clock face patterns. (**Figure 6.6**)

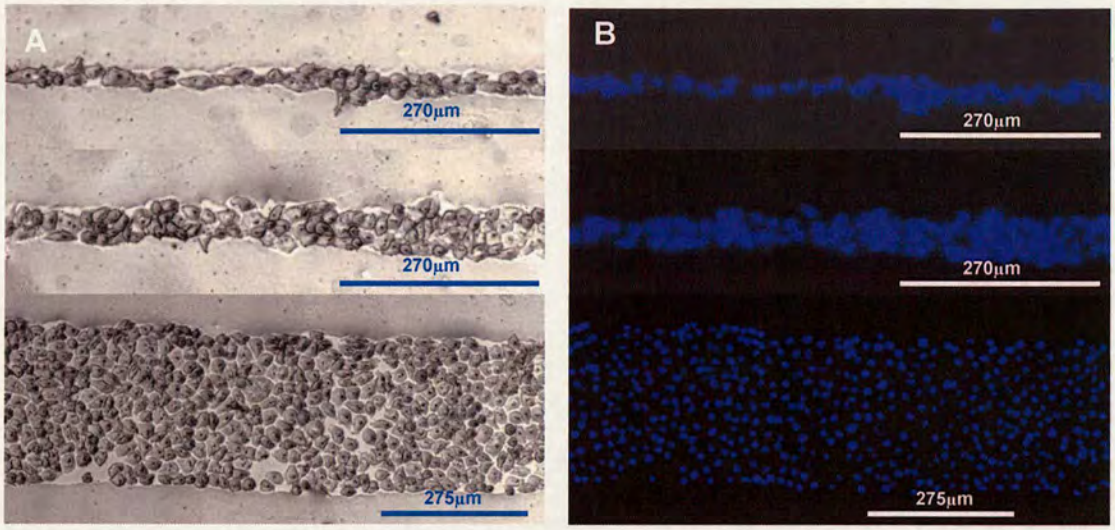

Figure 5.23 *Images of HeLa cells patterned on lines: (A) brightfield images; (B) fluorescent images taken using a Leica microscope with 10x/0.30 objective.*

5.1.4.2 Preparation of free standing cellular clusters

The patterned cells (obtained using the method described before (**Figure 5.17**)) could easily be detached from the patterned glass substrate after 72 h incubation forming shaped stem cell continuums, perhaps for use, in tissue engineering applications.[225] (**Figures 5.24** and **5.25**)

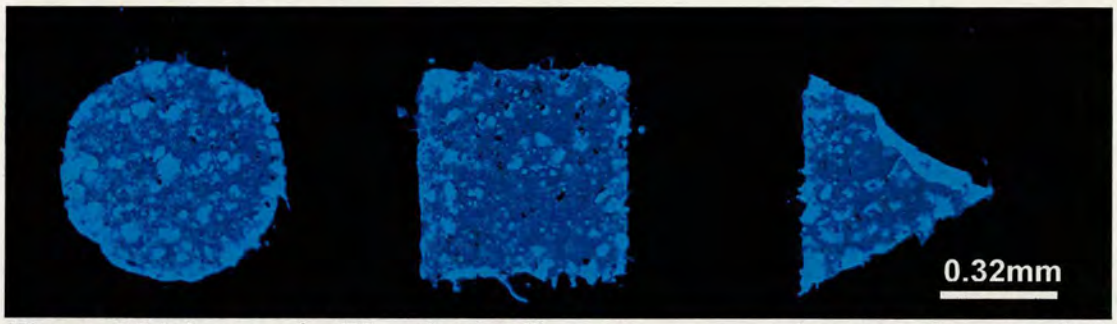

Figure 5.24 *Image of mES – Oct4 cell continuums on a heat-transfer printed glass substrate after 72 h incubation, scanned using a BioAnalizer 4F/4S white light scanner using the DAPI filter.*

The process of moving cell films from the slide is shown in **Figure 6.5**. After 72 h incubations of mES-Oct4 cells on the patterned glass slides (**Figure 6.5 A**) generated cellular continuums weakly attached to the glass. Simply by moving the end of the needle towards the mask borders (**Figure 6.5 A**) the cellular continuums could be detached from the patterned surface and become a free standing cell film. (**Figures 6.5 B** and **5.25 B**) This free standing cell film drifted freely in the media and could be picked by on the end of a pipette. (**Figure 6.5 C**) Moreover, the free standing cell film placed on a tissue culture plastic with medium could attach to the bottom of the dish (**Figure 6.5 D**) and the cells could proliferate. (**Figure 5.25 C**)

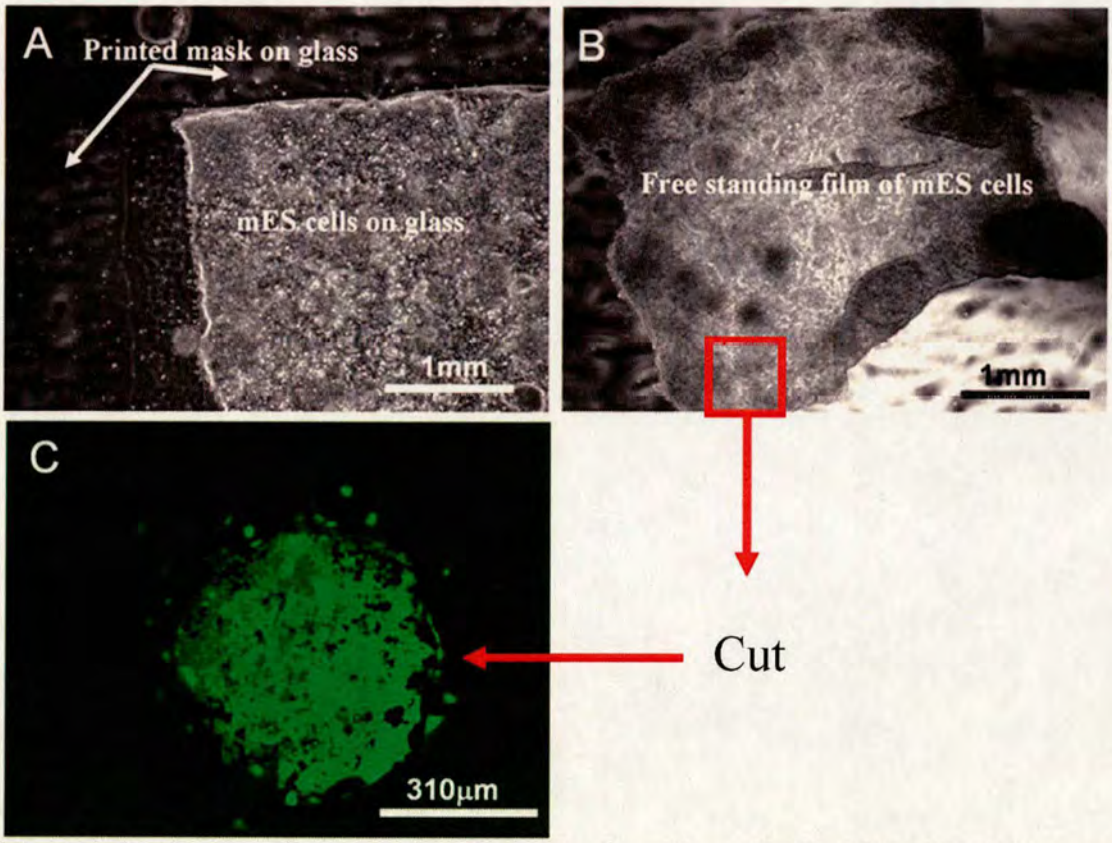

Figure 5.25 *Scheme of preparation of free standing films of mES-Oct4 cells: (A) image of living mES-Oct4 cells attached and proliferating on a patterned surface; (B) image of a free standing film of living mES-Oct4 cells detached by peeling off from the transfer printed glass using a needle after a 72 h incubation. Images were taken using a Leica microscope with 5x objective; (C) the fluorescent images of mES cells after the freestanding film of mES-Oct4 cells was peeled off from the transfer printed glass and cultivated on a tissue culture plastic for 24 h. The mES cells were stained using Celltracker green before images were collected using a Nikon microscope using a 10x/0.30 objective.*

5.1.4.3 Conclusions

In conclusion a heat-transfer printing approach has been developed for the first time for patterning cells. This approach allows any image to be patterned using a commercially available laser printer, with the printed toner on PET sheet successfully transferred onto glass slides. It was found that the toner could prevent the attachment of cells, so that cells were restricted to the defined printed images. The patterned cells (especially mES cells) could be easily detached from these slides to form a free-standing layer of cells.

Chapter 6 : Experimental

6.1 General information

6.1.1 Equipment

QArray^{mini} microarrayer (Genetix).

BioAnalyzer 4F/4S white light scanner and FIPS software (LaVision BioTech).

HCS platform and Pathfinder™ software (IMSTAR).

Biosafety cabinet: HERAsafe KS 18 class II (Heraeus).

Incubator: HERAcell 150 (Heraeus).

Vacuum oven: Vacutherm VT6025 (Heraeus).

Inkjet printer (Microdrop, GmbH, Norderstedt, Germany) equipped with a micro-pipette (AD-K-501, 70 μm diameter nozzle).

^{1}H and ^{13}C NMR spectra were recorded on a Bruker B-ACS-60 (250 and 62.5 MHz, respectively) in the solvents indicated at 300 K. Chemical shifts for proton and carbon spectra are reported on the δ scale in ppm and were referenced to solvent. All coupling constants (*J* values) were measured in Hz.

ES/MS and APCI/ MS analyses were recorded on an Agilent 1100 series systems. Mass spectra were obtained on a VG Platform single Quadrupole mass spectrometer in electrospray positive mode (ES^+) and electrospray negative mode (ES^-).

IR spectra were recorded on a Bruker Tensor 27 FT-IR with a golden SPECAC gate accessory with neat compounds.

6.1.2 Polymers

The polymer poly(urethane),[32] poly(acrylate)[246] libraries, respectively, were synthesised by Jean-Francois Thaburet and Hitoshi Mizomoto as part of a previous project. Most polymer had been previously characterised in terms of molecular weight (by gel permeation chromatography), wettability[40,248] and glass transition temperature (by differential scanning calorimetry). Asset of 100 "KIT" polymers (see section 6.2.5) was purchased from Sigma Aldrich.

6.1.3 Surfaces for cellular adhesion studies

Standard glass microscope slides (Menzel GlaserCat. No. 6311304 size 26x76 mm) were coated with agarose by manually dip-coating the slide into agarose Type I-B (1.0% w/v in deionised water at 65 °C). The coating on the bottom of the slide was removed by wiping with a piece of tissue. After drying for 24 h at room temperature, coated slides were stored at 4 °C or immediately used for printing. This protocol was optimized by Guilhem Tourniaire as part of previous project.[40] Amino functionalized slides (Sigma, Silane Prep Slides Cat.No. S4651-72EA) were replaced here successfully by ordinary glass slides (Menzel GlaserCat. No. 6311304).

6.1.4 Pre- synthesised polymer microarray fabrication

The polymer microarrays were prepared by contact printing (Qarray^{mini}, Genetix) with 32 aQu solid pins (K2785, Genetix) using polymer solutions (10 mg/mL in NMP) located in polypropylene 384-well microplates. The following printing parameters were used on agarose-coated slides, 10 ms stamping time, 5 stampings per spot and 200 ms inking time. The spot to spot distance was 1120 μm and typical spot sizes were 300 μm. Once printed, the slides were dried under vacuum (24 h at 40 °C/200 mbar) and sterilised by exposure to UV irradiation for 20 min prior to use.[40]

6.1.5 Chemicals and solvents

Unless specified, the chemicals and solvents used in all the experiments were obtained from Sigma-Aldrich.

6.1.6 Cell culture media and supplements

Unless specified, all cell culture media were from Sigma-Aldrich and all supplements added to the culture medium were supplied by Gibco, Invitrogen, used as received.

Unless specified, each culture media (**Table 6.1**) was supplemented with 10% v/v heat inactivated fetal calf serum, streptomycin (100 units/mL), penicillin (100 mg/mL) and L-glutamine (4 mM).

Cell line	Culture medium
HCEC	M-EPI
HeLa	RPMI 1640
ESC (Oct4-GFP)	GMEM

Table 6.1 *Name of the cell lines used and the corresponding culture medium: Human Cornea Epithelial Cells (HCEC); Epilife epithelial cell media (M-EPI); Embryonic Stem Cells (ESC); Glasgow's modified Eagle's medium (GMEM); HeLa cells, Dubelcco's modified Eagle's medium (DMEM).*

6.1.7 mES cell cultivation

mES-Oct4 were kindly provided by Dr Josh Brickman, Institute for Stem Cell Research (ISCR), University of Edinburgh.

mES-Oct4 cells were incubated in a Gibco incubator at 37 °C with 5% CO_2 using GMEM growth medium supplemented with heat inactivated fetal calf serum 10% v/v, penicillin (100 units/mL), streptomycin (100 mg/mL) and L-glutamine (2.0 mM), Sodium pyruvate (2.0 mM), 2-mercaptoethanol (0.1 mM), LIF (0.18 units/mL), puromycin (1 μg/mL).

When mES Cell cultivation was performed on a microarray the following protocol was applied. mES-Oct4 cells were used at passage 10 or earlier. The cells were seeded in $7x10^5$ per slide with 7 mL medium in a 4-rectangular well plate (Nunc, Denmark). After 48 h incubation cells attached on the slides were stained with a nuclei stain (Hoescht 33245) for 15 min and then fixed with formaldehyde (4% wt) in PBS pH 7.5 for another 15 min.

6.1.8 Cellular screening of microarrays and grids using mES-Oct4 cells

Microarrays and grids were used for cellular screening according to the following protocol. mES-Oct4 (the 8^{th} passage) cells were seeded at $7x10^5$ cells per slide and then incubated in a Gibco incubator at 37 °C with 5% CO_2 with 7 mL of media per slide in a four-rectangular well plate (Nunc, Denmark) for 48h. The media was GMEM complemented with heat inactivated fetal calf serum 10% v/v, penicillin

(100 units/mL), streptomycin (100 mg/mL), L-glutamine (2.0 mM), Sodium pyruvate (2.0 mM), 2-mercaptoethanol (0.1 mM) and LIF (0.18 units/mL). Cells attached on the slides were fixed with formaldehyde solution (4% wt) in (PBS) pH 7.5 for 15 min (5 mL) and stained with Hoescht 33342 (550 µl, 1 µg/mL) for 15 min then washed with water (20 mL). Fluorescence images of a whole slides were taken with a BioAnalyzer 4F/4S (LaVision BioTech) using a DAPI filter with a 20 µs exposure time. Bright field and fluorescence images of the polymer features and mES cells on polymer features were obtained using a Nikon microscope using a 10x/0.30 objective and fluorescence images a DAPI filter.

6.1.9 mES-Oct4 cell cultivation on coverslips

Coverslips were placed in 12-well plates and cells were seeded into the wells (120000 cells/well in GMEM growth medium) such that the final volume was 2 mL in each well. The medium was GMEM complemented with heat inactivated fetal calf serum 10% v/v, penicillin (100 units/mL), streptomycin (100 mg/mL), L-glutamine (2.0 mM), Sodium pyruvate (2.0 mM), 2-mercaptoethanol (0.1 mM) and LIF (0.18 units/mL). The plates were placed in the incubator at 37 °C, 5% CO_2. After every 24 h the medium was removed and wells were filled with the 2mL GMEM growth medium. 7 changes of media were performed in order to cultivate cells on coverslips for 8 days. Living cell images were taken with a Leica microscope using a 5x/0.12 objective.

6.1.10 Flow cytometry analysis of mES-Oct4 cultivated onto the coverslips

Stem cells were washed in PBS (2x1 mL per coverslip), harvested *via* trypsination (0.25 mL per coverslip) and resuspended in 300 µL of GMEM. The cell pellet was collected *via* centrifugation (1200 rpm, 4 min) and resuspended in 2 mL of 2% fetal bovine serum (FBS) in PBS. 0.1 mL of this solution was placed into a FACS tube and 0.5 mL of 2% FBS in PBS was added. mES-Oct4 GFP cells were analysed on a flow cytometer (FACSAria BD Biosciences) and analysed using the FACSDiva software. Cell samples were excited with a 488 nm (Coherent® Sapphire™ solid state) laser and a 530/30 nm

(Fluorescein) filter was used for fluorescence analysis of the cellular population. The number of cells detected in each sample by FACS [244] was multiplied by a factor of 20 in order to calculate the overall number of cells harvested from each coverslip.

6.1.11 Imaging

Three types of imagining equipment were used:

A BioAnalyzer 4F/4S with a light scanner, equipped with DAPI filter (LaVision Bio Tech) was used for imaging microarrays and girds. The BioAnalyzer was capable of imaging relatively big areas for example a standard microscopy slide (26x76 mm) was analysed in single scan.

A Nikon microscope controlled by the Pathfinder software (Imstar) equipped with a 10x/0.30 objective and a DAPI filter was used to imagining spots on microarrays and chosen areas of girds in order to detect cells presents and cellular morphology. Automatic arranging of the images into mosaic format result in generating high resolution images of girds and microarrays.

A Leica microscope equipped with a selection of objectives and filters (FITC, DAPI) was used for living cell imagining. Fluorescent images were obtained using 350 nm excitation, 460 nm emission filters (DAPI) and 494 nm excitation, 521 nm emission filters (FITC).

6.1.12 Inkjet printing

Materials deposited *via* inkjet printing were printed *via* Autodrop inkjet printing system (Microdrop Technology, Norderstedt, Germany), using (unless specified) the following printing parameters: 120 V, 28 μs and 100 Hz with a AK-501 micropipette (70 μm nozzle).

6.1.13 HeLa / mES cells on slide incubation for cellular patterning

HeLa cells were grown in RPMI 1640 growth medium, supplemented with heat inactivated fetal calf serum 10% v/v, penicillin (100 units/mL), streptomycin (100 mg/mL) and L-glutamine (4.0 mM) at 37 °C with 5% CO_2 (Gibco). mES cells were grown using GMEM growth medium supplemented with heat inactivated fetal calf

serum 10% v/v, penicillin (100 units/mL), streptomycin (100 units/mL) and L-glutamine (2.0mM), Sodium pyruvate (2.0 mM), 2-mercaptoethanol (0.1 mM), LIF (0.18 units/mL), puromycin (1 μg/mL). The patterned slides were placed into a 4-rectangular well-plate and sterilized for 20 min under UV irradiation prior to the addition of cells ($7x10^5$ cells per slide with 7 mL of complete media) into the well plate and incubation. Media was changed every 24 h.

6.1.14 HeLa / mES cells staining and fixing

The well plate medium was removed and the slides washed with PBS three times. Cells attached on the slides were fixed using paraformaldehyde (4% w/v in PBS) for 30 min, stained using Hoechst 33342 (0.50 μg/mL) for 15 min and washed with distilled water.

6.2 Experimental for Chapter 1

6.2.1 Experimental procedures for Chapter 1

Glass slide treatment

Before use, glass slides were rinsed in hexane, dimethylformamide (DMF), acetone and methanol and etched using an oxygen plasma (Europlasma NV Junior System (Frequency: 50 Hz, R_f Power: 100 W)) for 2 min at 27 Pa in on oxygen atmosphere.

Masking glass slide

A 30% w/v sucrose masking solution was prepared by dissolving sucrose (1.5 g) in water (3.5 mL), which was printed on the glass surface *via* an Autodrop inkjet printing system (Microdrop Technology, Norderstedt, Germany), using the following printing parameters 140 V, 28 μs and 200 Hz). An array of 128 (8 x 16) sucrose spots (each spot was 1.5 mm in diameter) was generated by printing 800 drops (0.9 μL) of sucrose onto the desired area of the glass slide.

After printing, the sucrose masked slides were dried in 60 °C for 1 h, and then coated with 4 μL Tridecafluoro-1,1,2,2-tetrahydrooctyl)dimethylchlorosilane (TFCS) per slide using a Control Coater (bar of 4.5 mm diameter and coating speed 2.5 cm/s). Finally, the slides were washed in water (3 x 200 mL) to remove the mask and excess TFCS, and dried under a stream of nitrogen. The result was a hydrophobic patterned slide consisting of an array of 128 (8 x 16) hydrophilic features.

Polymer deposition

Each specific polymer (see sections 6.2.3, 6.2.4 and 6.2.5) was deposited by piezo jet-printing 800 drops (0.9 μL) of each of the polymer solutions printed onto each defined hydrophilic feature using the printing parameters 140 V, 28 μs and 800 Hz. Each slide thus contained an 8 x 16 grid giving a total of 128 polymer spots with the area of each spot approximately 1.76 mm^2.

Small molecule deposition

105 mM and 95 mM solutions of sulfamethoxazole were prepared in methanol and ethanol respectively. A 77.5 mM solution of carbamazepine was prepared in dimethyl sulfoxide (DMSO) and a 56mM solution of ROY was prepared in 1-Methyl-2-

pyrrolidinone (NMP). These solutions were inkjet printed (140 V, 28 μs and 800 Hz) onto the polymer features (800 drops per spot, 0.9 μL, taking 1.5 s per spot).

After solvent evaporation, the crystals remaining on the polymer spots were analysed, initially by optical microscopy (Leica microscope using a 5x/0.12 objective).

Crystal analysis

Analysis of microscope images allowed polymer to be selected which gave "repeatable crystal habits" for the small molecules. Crystals were analysed by Raman spectroscopy using a LAB Ram 300 an Olympus BX 40 microscope equipped with a 632 nm diode laser and a 1800 lines/mm grating, with data collected and analysed using the LabSpec-4.18 software package with calibration using a silicon standard (Raman spectra maximum at 521 cm^{-1}). Spectra were typically collected using an Olympus SLM Plan100 objective and a 150 μm slit.

The Raman spectra obtained from crystals of small molecules were compared with literature data [19,154] and specific polymorphisms were identified and assigned.

6.2.2 ROY synthesis

ROY 2-(2-nitroanilino)-5-methylthiophene-3-carbonitrile was prepared by Phillip Milnes according to United States Patent: 5229382 (publication date 07/20/1993, Lilly Industries Limited).

A solution of 2-amino-5-methylthiophene-3-carbonitrile (1 g) and 2-fluoronitrobenzene (764 μL) in dry tetrahydrofuran (100 mL) was added, drop-wise under nitrogen to a slurry of sodium hydride (347 mg) in dry tetrahydrofuran (20 mL).

The mixture was stirred for 24 h at 25 °C, poured onto cracked ice and extracted into 500 mL dichloromethane (three times). The combined extracts were washed with 2 M hydrochloric acid (2 x 20 mL) and water (2 x 20 mL). The organic extract was dried over magnesium sulphate and the solvent removed under reduced pressure. The residue was crystallised from ethanol to give a yellow/orange/red mixed polymorphic solid (1.09 g) in 58% yield: m.p. 98-103 °C (EtOH), literature 99-102 °C (EtOH); **^{1}H NMR (250 MHz, $CDCl_3$)** 9.54 (s, 1H, 1 x N<u>H</u>), 8.17 (dd, 1H, J = 9Hz, J = 1.5 Hz, Ar<u>H</u>), 7.40-7.49 (m, 1H, 1 x Ar<u>H</u>), 7.12 (dd, 1H, J = 9 Hz, J = 1.5 Hz, 1 x Ar<u>H</u>), 6.86-

6.93 (m, 1H, ArH), 6.71 (m, 1H, 1 x ArH), 2.40 (s, 3H, 3 x CH_3). **^{13}C NMR** ($CDCl_3$, 62.5MHz): 149.3 (C), 141.7 (C), 136.6 (CH), 134.5 (C), 127.1 (CH), 124.3 (CH), 120.3 (CH), 116.5 (CH), 114.1 (C), 105.1 (C), 16.0 (CH_3); **m/z (ES^+)** 282.1 $[M+Na]^+$ (100%), 260.1 $[M+H]^+$ (32%); **(ES^-)** 258.1 $[M-H]^-$ (100%).

6.2.3 Inkjet mediated synthesis of cross linked co - polymers

0.1 mL of cross linker (ethylene glycol dimethacrylate) was added to 0.9 mL of individual monomer before adding 10 mg of photo initiator (2,2-dimethoxy-2-phenylacetophenone). These solutions were printed by piezo jet-printing 800 drops of each of the monomer solutions onto a specific hydrophilic feature of the patterned slide. Slides were placed under a UV light (UV lamp, Black-Ray, Model B 100AP) for 5 min and washed with diethyl ether (2x200 mL) before drying in a vacuum oven at 40 °C for 4-5 h.

Monomers used for *in situ* polymerisation were: methyl methacrylate, *N,N*-dimethylacrylamide, hydroxypropyl methacrylate, 2-(dimethylamino)ethyl methacrylate, *N, N*-diethylaminoethyl acrylate, 2-(tert-butylamino)ethyl methacrylate, 2-hydroxyethyl methacrylate and 2-(methylthio)ethyl methacrylate.

6.2.4 Synthesis of linear co-polymers

A mixture of azobisisobutyronitrile 1% (w/w) (10 mg), monomers 20% (w/w) (0.2 g) and solvent (0.7 g NMP) were purged with nitrogen for 2 h before heating (60°C) overnight under nitrogen. The products were precipitated by drop-wise addition of a diethyl ether (200 mL) to give a solid. Polymers were washed with diethyl ether (50 mL) and n-hexane (50 mL) and re-precipitated (dissolving in NMP (10 mL) and precipitation using diethyl ether (200 mL)) and dried under vacuum at 40 °C for 48 h. 1% w/v polymer solutions were then prepared in NMP. (**Table 6.2**)

Monomer1/Monomer2	Monomer 1 %	Monomer 2 %	Yield %	Solvent
2-hydroxyethylmethacrylate/ 2-(diethylamino)ethyl methacrylate	50	50	50	NMP
hydroxypropylmethacrylate / 2-(dimethylamino)ethyl methacrylate	90	10	30	NMP
2-hydroxyethylmethacrylate / 2-(methylthio)ethyl methacrylate	30	70	44	NMP

Table 6.2 *Monomers used in linear co-polymer synthesis.*

6.2.5 Polymer Kit – dissolution parameters

A polymer kit (102 polymers) was purchased from Scientific Polymer Products, Inc., (catalogue #205). Polymers were dissolved at 1% w/v in the indicated solvent to allow inkjet printing. (Some polymer solutions required reflux heating before getting clear solutions). All the polymer solutions were filtered prior to printing (using glass wool). (**Table 6.3**)

KIT Polymer No.	Polymer	Solvent
1	acrylonitrile/butadiene/styrene resin	DCM/NMP 1:1
2	alginic acid, sodium salt	H_2O
3	butyl methacrylate/isobutyl methacrylate copolymer	NMP
4	cellulose acetate	NMP
5	cellulose acetate butyrate	NMP
6	cellulose propionate	NMP
7	cellulose triacetate	DCM/NMP 1:1 v/v
8	ethyl cellulose	DCM/NMP 1:1 v/v
9	ethylene/acrylic acid copolymer	THF/NMP 1:1 v/v
10	ethylene/ethyl acrylate copolymer	Toluene
11	ethylene/propylene copolymer	Hexane
12	ethylene/vinyl acetate copolymer (14 wt% vinyl acetate)	Toluene
13	ethylene/vinyl acetate copolymer	DCB

	(18 wt% vinyl acetate)	
14	ethylene/vinyl acetate copolymer (28 wt% vinyl acetate)	DCB
15	ethylene/vinyl acetate copolymer (33 wt% vinyl acetate)	Toluene
16	ethylene/vinyl acetate copolymer (40 wt% vinyl acetate)	DCB
17	ethylene/vinyl acetate copolymer (45 wt% vinyl acetate)	DCB/NMP 1:1 v/v
18	hydroxybutyl methyl cellulose	Toluene
19	hydroxypropyl cellulose	NMP
20	hydroxypropyl methyl cellulose	NMP
21	methyl cellulose	Toluene
22	methyl vinyl ether/maleic acid copolymer	NMP
23	2,5-furandione-methyl vinyl ether copolymer	NMP
24	nylon 6	NMP
25	nylon 6/6	NMP
26	nylon 6/9	NMP
27	nylon 6/12	NMP
28	nylon 6(3)T	NMP
29	nylon 11	NMP
30	nylon 12	NMP
31	phenoxy resin045A	NMP
32	Polyacetal	NMP
33	polyacrylamide	H_2O
34	polyacrylamide, carboxyl modified, low carboxyl content	H_2O
35	polyacrylamide, carboxyl modified, high carboxyl content	H_2O
36	poly(acrylic acid)	NMP
37	polyamide resin	Toluene
38	1,2-polybutadiene	NMP
39	poly(1-butene), isotactic	Toluene

40	poly(butylene terephtalate)	NMP
41	poly(n-butyl methacrylate)	NMP
42	polycaprolactone	NMP
43	polycarbonate	NMP
44	poly(diallyl isophthalate)	NMP
45	poly(diallyl phthalate)	NMP
46	poly(2,6-dimethyl-p-phenylene oxide)	DCM
47	poly(4,4'-dipropoxy-2,2'-diphenyl propane fumarate)	NMP
48	poly(ethyl methacrylate)	NMP
49	polyethylene, high density	NMP
50	polyethylene, chlorinated (25 wt% chlorine)	Toluene
51	polyethylene, chlorinated (36 wt% chlorine)	Toluene
52	polyethylene, chlorinated (42 wt% chlorine)	Toluene
53	polyethylene, chlorinated (48 wt% chlorine)	NMP
54	polyethylene, chlorosulfonated	NMP
55	poly(ethylene oxide)	H_2O
56	polyethylene, oxidized	Toluene
57	poly(ethylene terephthalate)	NMP
58	poly(2-hydroxyethyl methacrylate)	NMP
59	Poly(isobutyl methacrylate)	NMP
60	polyisoprene, chlorinated	NMP
61	poly(methyl methacrylate)	NMP
62	poly(4-methyl-1-pentene)	NMP
63	poly-alpha-methylstyrene	NMP
64	poly(p-phenylene ether-sulphone)	NMP
65	Poly(phenylene sulfide)	NMP
66	polypropylene, isotactic, chlorinated	Toluene
67	polypropylene, isotactic	Toluene

68	polystyrene	NMP
69	polysulfone	NMP
70	poly(tetrafluoroethylene)	Not soluble
71	poly(2,4,6-tribromostyrene)	NMP
72	poly(vinyl acetate)	NMP
73	poly(vinyl formal)	NMP
74	poly(vinyl chloride), carboxylated	NMP
75	poly(vinyl butyral)	NMP
76	poly(vinyl chloride)	NMP
77	vinyl chloride-acrylic acid copolymer	NMP
78	poly(vinyl formal)	NMP
79	polyvinylpyrrolidone	NMP
80	poly(vinyl stearate)	Toluene
81	poly(vinylidene fluoride)	NMP
82	styrene/acrylonitrile copolymer	NMP
83	styrene/acrylonitrile copolymer	NMP
84	styrene/allyl alcohol copolymer	NMP
85	styrene/butadiene, ABA block copolymer	NMP
86	styrene/butyl methacrylate copolymer	NMP
87	styrene/ethylene-butylene, ABA block copolymer	Toluene
88	styrene/isoprene, ABA block copolymer	Toluene
89	styrene/maleic anhydride copolymer, partial methyl ester	NMP
90	vinyl alcohol/vinyl butyral copolymer	NMP
91	vinyl chloride/vinyl acetate/maleic acid terpolymer	NMP
92	vinyl chloride/vinyl acetate copolymer (90% vinyl chloride, 10% vinyl acetate)	NMP
93	vinyl chloride/vinyl acetate copolymer (88% vinyl chloride, 12% vinyl acetate)	NMP
94	vinyl chloride/vinyl acetate/maleic acid terpolymer	NMP
95	vinyl chloride/vinyl acetate/vinyl alcohol	NMP

	terpolymer	
96	vinyl chloride/vinyl acetate/hydroxylpropyl acrylate terpolymer	NMP
97	vinylidene chloride/acrylonitrile copolymer	NMP
98	vinylidene chloride/vinyl chloride copolymer	NMP
99	N-vinylpyrrolidone/vinyl acetate copolymer	NMP
100	zein, purified	NMP
101	polyethyleneimin	NMP
102	chitosan	1N HCl (aq)

Table 6.3 *Dissolution solvents for the kit polymers.*

6.2.6 Crystal morphologies obtained on polymers and record of Raman shifts for SMA, CBM and ROY have been provided in the Electronic Data Section.

6.3 Experimental for Chapter 2

6.3.1 Experimental procedures for Chapter 2

Oil layer preparation

0.30 mL of mineral paraffin oil for oil baths (Fisher Scientific, CAS 8012-95-1, density 0.89 g/mL, flesh point 215 °C) was placed onto an agarose coated glass slides (see section 6.1.3) and left for 15 min in order to form a thin layer of oil across whole slide.

Monomer solution

0.5 g of each of the 24 monomers **(see Table 6.6)** were placed into glass vials and 0.5 mL of 10% w/w of 2,2-dimethoxy-2-phenylacetophenone (photo-initiator) in NMP was added. Monomer solutions (35 μl each) were placed into a polypropylene 384 micro-well plate.

Monomer inkjet printing- microarray and grid fabrication

Polymer microarrays were fabricated by printing 50 drops of monomer per feature, with a 1 mm pitch between spots, *via* an inkjet printing system (see section 6.1.12), using the following printing parameters 98 V, 29 μs and 100 Hz. Each monomer was printed 25 times (5x5). Co-polymers were fabricated by printing 25 drops of each monomer. The pipette was cleaned between each monomer to avoid contamination. The cleaning protocol included filling the micropipette with NMP, applying an impulse (12500 Hz) frequency to the micropipette for 5 s and empting the micropipette.

Polymer grids were fabricated by printing drops onto a slide with movement of the piezo-pipette along a linear path (at a constant velocity of 10 mm/s). The distance between lines was 1 mm in the y direction and 2 mm in the x direction, while the lines were approximately 300 μm wide. After printing microarrays (25 min) and grids (10 min) the monomers were polymerised *in situ via* UV irradiation (UV lamp, Black-Ray, Model B 100AP) for 30 min with a 20 cm distance between the slides and the bulb. The oil layer was removed by placing the microarray at the bottom of a beacker containing water (100 mL). Water and oil were discarded from over the slide and traces oil remaining on the slides was removed by ethanol (100 mL).

Cellular screening of microarrays and grids using mES-Oct4 cells

This was performed according to the protocol presented in section 6.1.8.

Coverslip fabrication

A P6708 spin coater (Speedlines Technologies) and coverslips (13 mm diameter VWR Cat No. 631-0150, Menzel-Glaser) were used. 50 μL of poly 2-(methylthio)ethyl methacrylate solution (2% w/v in THF) was placed onto the coverslip and spun for 10 s at 2000 rpm. Coverslips were dried under vacuum 12 h at 45 °C/200 mbar and irradiated with UV light for 20 min for sterilization.

Due to lack of solubility of poly divinylbenzene (cross linked polymer) 100 μL of divinylbenzene solution (50% w/v in NMP) containing 0.5% of 2,2-dimethoxy-2-phenylacetophenone (UV initiator) was placed onto the coverslip and UV irradiated (20 min, UV lamp, Black-Ray, Model B 100AP). Coverslips were washed with water, dried under vacuum (12 h at 45 °C/200 mbar) and irradiated with UV light for 20 min for sterilization.

mES-Oct4 cell cultivation on coverslips

This was performed according to protocol reported in section 6.1.9.

Flow cytometry analysis of mES-Oct4 cultivated onto the coverslips

This was performed according to protocol reported in section 6.1.10.

6.3.2 Localization of polymers on the microarrays prepared via high throughput polymerisation

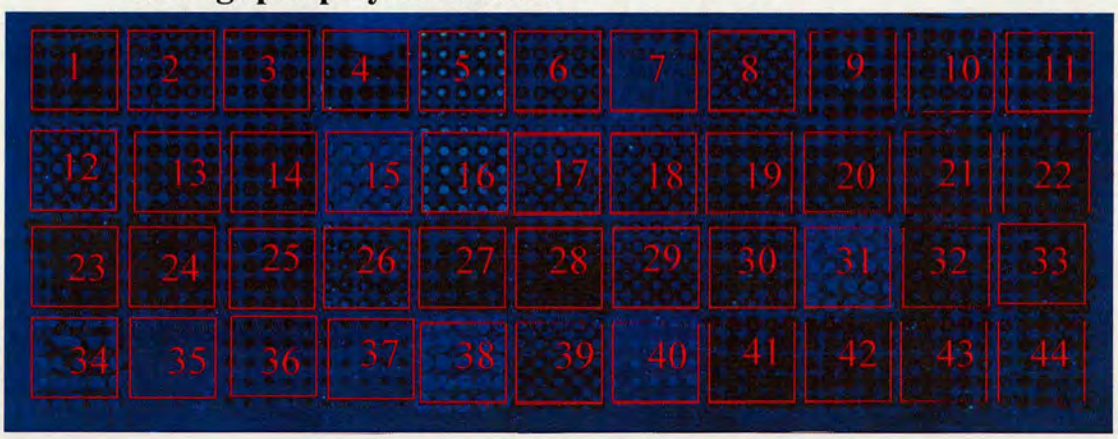

Table 6.4 *Polymer microarray screened with mES-Oct4 cells, red squares represent 25 replications of the same polymer spot.*

1	styrene */tert*-Butyl methacrylate co-polymer	23	poly *tert*-Butyl methacrylate
2	poly 2-vinylpyridine	24	poly ethoxyethyl methacrylate
3	poly 3-(trimethoxysilyl)propyl methacrylate	25	poly N-tert-Butylacrylamide
4	poly N-Isopropylacrylamide	26	poly styrene
5	poly 4-bromostyrene	27	2-vinylpyridine/4-bromostyrene co-polymer
6	ethyl methacrylate/ ethylene glycol methacrylate co-polymer	28	poly 4-hydroxybutyl acrylate
7	poly 4-vinylpyridine	29	poly methyl methacrylate
8	4-bromostyrene/ styrene co-polymer	30	ethyl methacrylate/2-hydroxyethyl acrylate co-polymer
9	N-Isopropylacrylamide/ *tert*-Butyl methacrylate co-polymer	31	poly divinylbenzene
10	poly benzyl methacrylate	32	glycidyl methacrylate/ butyl methacrylate co-polymer
11	2-(methylthio)ethyl methacrylate /styrene co-polymer	33	poly glycidyl methacrylate
12	benzyl methacrylate / styrene co-polymer	34	poly ethyl methacrylate
13	2-vinylpyridine/4-vinylpyridineco-polymer	35	glycidyl methacrylate /N-tert-Butylacrylamide co-polymer
14	poly butyl methacrylate	36	poly methyl acrylate
15	poly 2-(methylthio)ethyl methacrylate	37	Styrene/2-hydroxyethyl acrylate co-polymer
16	methyl acrylate/4-vinylpyridine co-polymer	38	benzyl methacrylate /divinylbenzene co-polymer
17	poly 2-hydroxyethyl acrylate	39	methyl acrylate/ N,N-Dimethylacrylamide co-polymer
18	2-methoxyethyl methacrylate/2-hydroxyethyl acrylate copolymer	40	poly(ethylene glycol) monomethacrylate – Mn 360
19	ethylene glycol methacrylate/2-hydroxyethyl acrylate co-polymer	41	poly ethylene glycol methacrylate
20	poly 2-methoxyethyl methacrylate	42	Styrene /4-hydroxybutyl acrylate co-polymer
21	4-vinylpyridine/ 4-bromostyrene co-polymer	43	N,N-diethylacrylamide / N,N-dimethylacrylamide co-polymer
22	poly N,N-dimethylacrylamide	44	poly N,N-diethylacrylamide

Table 6.5 *List of Co-polymers corresponding to sectors on the microarray.*

6.3.3 Printing of polymer grids

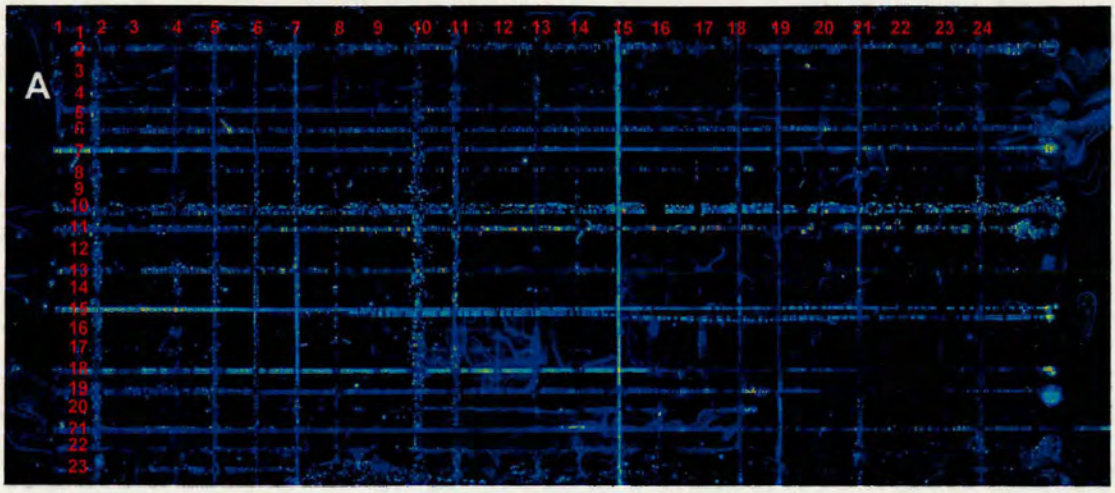

Figure 6.1 *Image of polyacrylate grid fabricated in situ screened with mES-Oct4 cells, line numbers correspond to the polymeric listed below.*

1	polybutyl methacrylate	13	polyglycidyl methacrylate
2	polyethyl methacrylate	14	polyethoxyethyl methacrylate
3	polyN,N-diethylacrylamide	15	polymethyl methacrylate
4	poly4-vinylpyridine	16	polyN-Isopropylacrylamide
5	poly2-vinylpyridine	17	polyN-tert-Butylacrylamide
6	poly2-(methylthio)ethyl methacrylate	18	poly3-(trimethoxysilyl)propyl methacrylate
7	polybenzyl methacrylate	19	poly *tert*-Butyl methacrylate
8	poly2-methoxyethyl methacrylate	20	polyN,N-dimethylacrylamide
9	poly2-hydroxyethyl acrylate	21	poly4-hydroxybutyl acrylate
10	polydivinylbenzene	22	polymethyl acrylate
11	polystyrene	23	polyethylene glycol methacrylate
12	poly(ethylene glycol) monomethacrylate – Mn 360	24	poly4-bromostyrene

Table 6.6 *List of polymers corresponding to lines on grid.*

6.3.4 Comparing micro and macro scale polymerisation

1 mL of each of 24 monomers (**Table 6.6**) was prepared according to the protocol presented in section 6.3.1 - Monomer solution preparation.

Monomer solutions were printed through the oil layer according to protocol described in section 6.3.1 - Monomer inkjet printing. The individual polymer arrays were fabricated by printing 50 drops (per feature) of each monomer solution and 200 features per slide, with a 1 mm pitch between spots. Monomers were polymerised *in situ via* UV irradiation according to the protocol described in section 6.3.1 - Monomer inkjet printing. Polymeric features (loosely attached to the glass surface) were peeled from the surface. 2 mg of each polymer was dissolved in 2 mL of NMP for GPC analysis.

Monomer solutions in the glass vials (0.6 μL each) were polymerised upon UV (UV lamp, Black-Ray, Model B 100AP) irradiation for 30 min. 2 mg of each polymer was dissolved in 2 mL of NMP for GPC analysis.

Results of these GPC analyse are provided in **Table 6.7.**

GPC-SEC analysis (Agilent 1100 series) was carried out on a PLgel 5 μm Mixed-C column (300 mm x 7.5 mm) from Polymer Laboratories. Data was analysed using the ChemStation software (Agilent technologies). Polymer analyses were run using 1-Methyl-2-pyrrolidone (NMP) as the eluent at a flow rate of 0.5 mL/min at 55 °C. The polymer was detected by an refraction index detector. Polystyrenes (Polymer Laboratories) with a peak molecular weight range from 580 to 300,000 g/mol were used as standards.

Monomer	Traditional synthesis Mn ($x10^4$)/Mw ($gmol^{-1}$)	Inkjet based spot synthesis Mn ($x10^4$)/Mw ($gmol^{-1}$)
butyl methacrylate	3.42/1.2	2.68/1.1
ethyl methacrylate	9.28/2.3	8.63/2.3
N,N-diethylacrylamide	23.36/3.4	20.68/3.1
4-vinylpyridine	8.34/4.8	4.09/6.4
2-vinylpyridine	1.70/1.7	8.17/2.9
2-(methylthio)ethyl methacrylate	12.36/4.3	10.84/5.1
benzyl methacrylate	3.89/1.8	3.46/1.7
2-methoxyethyl methacrylate	9.14/4.01	7.38/3.7
2-hydroxyethyl methacrylate	48.42/9.8	11.04/4.2
divinylbenzene	Cross linked product	Cross linked product
styrene	8.90/1.8	6.88/1.5
poly(ethylene glycol) monomethacrylate -Mn 360	Not soluble	Not soluble
glycidyl methacrylate	4.25/1.8	3.53/1.76
ethoxyethyl methacrylate	3.95/1.4	4.37/2.7
methyl methacrylate	9.78/1.8	11.63/2.4
N-isopropylacrylamide	7.23/2.9	2.84/1.8
N-tert-butylacrylamide	9.98/2.5	8.59/2.1
3-(trimethoxysilyl)propyl methacrylate	6.02/3.5	7.54/3.1
tert-Butyl methacrylate	11.30/1.6	6.47/1.7
N,N-dimethylacrylamide	22.86/3.4	19.81/4.3
4-hydroxybutyl acrylate	6.77/1.9	6.98/2.7
methyl acrylate	8.38/1.3	9.62/1.3
ethylene glycol di-methacrylate	Cross linked product	Cross linked product
4-bromostyrene	Not soluble	Not soluble

Table 6.7 *Summary of macro and micro polymerisation.*

6.3.5 Preventing evaporation

Two types of slides were used in this experiment: (a) normal glass slides and (b) glass slides covered with a layer of paraffin oil (see section 6.3.1 - Oil layer preparation). Approximately 7 mg of water was printed on to the slide by inkjet printing (100 spots, 180 drops/spot - printing parameters 120 V; 27 μs; 500 Hz). After printing slides were weighted once per minute for 4 h (repeated 3 times for each type of glass slide).

Mass of water printed onto glass through a layer of oil is constant, therefore the standard deviation can not be estimated. Standard deviation of the mass of water on the *glass slide (no oil layer)* is less than 0.001 mg. (**Table 6.8**)

	Weight of the water let on slide (mg)					
	Run 1		**Run 2**		**Run 3**	
Time after printing (min)	**Glass slide**	**Glass slide covered with a layer of oil**	**Glass slide**	**Glass slide covered with a layer of oil**	**Glass slide**	**Glass slide covered with a layer of oil**
0	6.16	7.01	6.15	7.03	6.14	7.01
1	6.12	7.01	6.11	7.03	6.10	7.01
2	6.01	7.01	6.00	7.03	5.99	7.01
3	5.76	7.01	5.76	7.03	5.75	7.01
4	5.31	7.01	5.32	7.03	5.31	7.01
5	4.73	7.01	4.72	7.03	4.72	7.01
6	4.04	7.01	4.04	7.03	4.03	7.01
7	3.27	7.01	3.26	7.03	3.25	7.01
8	2.46	7.01	2.46	7.03	2.46	7.01
9	1.63	7.01	1.62	7.03	1.63	7.01
10	0.73	7.01	0.72	7.03	0.72	7.01
11	0	7.01	0	7.03	0	7.01
12	0	7.01	0	7.03	0	7.01
13	0	7.01	0	7.03	0	7.01
14	0	7.01	0	7.03	0	7.01
15	0	7.01	0	7.03	0	7.01
16 .../ 240	0	7.01	0	7.03	0	7.01

Table 6.8 *Weight of material deposited on: (A) normal glass slide and (B) a glass slide covered with a layer of paraffin oil.*

6.3.6 Substrates for printing.

Fluorescein solution (NMP, 0.5% w/v) was inkjet printed using the protocol described in section 6.1.2. 1,5,10,20, 30 and 40 drops per feature (30 replications each) were printed onto five types of slides (1) glass slide, (2) amino slides, (3) agarose coated glass slide, (4) hydrophobic patterned slide, and (5) hydrophobic glass slide. (1) (Menzel GlaserCat. No. 6311304 size 26x76 mm) and (2) amino-functionalized slides (Sigma, Silane Prep Slides Cat.No. S4651-72EA) were used as received. (3) fabricated according to the protocol presented in section 6.1.3 (4) fabricated according to protocol presented in section 6.2.1 and (5) fabricated according to protocol presented in section 6.2.1 - with no masking procedure.

To obtain general view of the slides printed with fluorescein in NMP (0.5% w/v) a LaVision Biotech analyser was used. Images were taken with a fluorescence filter with an exposure time of 20 μs. Spot diameter was evaluated by imaging with a Leica microscope. Images were analysed with Supervisor SEMCO T2. (**Table 6.9**) and the diameter of 20 spots (for each number of drop per spot) was measured.

Average diameter (μm) of 20 spots ± SD	**(1) Glass slide**	**(2) Amino slide**	**(3) Agarose slide**	**(4) Hydrophobic pattern**	**(5) Hydrophobic Slides**
1 drops/spot	365.2± 8.5	215± 2.6	342.7± 4.7	59.8± 2.4	199.3± 8.8
5 drops/spot	581± 9.9	255.6± 2.6	614.3± 4.8	102.7± 2.3	249± 9
10 drops/spot	803± 9.5	338.7± 2.7	796.9± 5.8	131.2± 2.9	481.5± 10
20 drops/spot	979.3± 21	464.9± 3.1	929.7± 6.4	315.4± 5.7	597.7± 10
30 drops/spot	1142.5± 43.5	597.7± 4,7	1095.7± 8.2	465± 7	763.7± 11.8
40 drops/spot	1240.4± 70.8	720.5± 6.9	1261.7± 8.5	554.5± 9.4	1128.9± 13.3
50 drops/spot	1374.5± 87	763.7± 8.2	1393.6± 11	574.5± 8.7	1261.7± 14.2

Table 6.9 *Spot diameter (μm) on different type of slides.*

6.4 Experimental for Chapter 3

6.4.1 Experimental procedures for Chapter 3

Polymer microarray fabrication

Solutions of 125 polyurethanes[151] (**Table 6.21**) and 128 polyacrylates[113,152] (**Table 6.20**) were prepared by dissolving 20 mg of polymer in 2 mL of NMP (1% w/v). Polymer solutions (0.35 mL) were added into polypropylene 384-well microplates.

The polymer microarrays were prepared by contact printing using polymer solutions (10 mg/mL in NMP) according to the protocol presented in section 6.1.12.

125 polyurethanes[151] and 128 polyacrylates [113,152] were printed onto two slides (quadruplicates) within a field of 16x32 spots.

Screening polymer microarray using Human Corneal Epithelial Cell

Microarrays of 125 polyurethanes[151] and 128 polyacrylates[113,152] were placed in 90 mm Petri dishes and allowed to soak in Human Corneal Epithelial Cell Line (HCEC) medium (EpiLife) along with the antibiotics penicillin (1000 units/mL), streptomycin (1000 units/mL) and fungizone (1000 units/mL), overnight at room temperature in order to allow sterilisation.

After 24 h, medium was removed, slides were washed once with PBS (10 mL) and the Petri dishes were filled with 15 mL of EpiLife with the antibiotics penicillin (100 units/mL), streptomycin (100 units/mL) and fungizone (100 units/mL). 2 million Human Corneal Epithelial Cells were seeded into the Petri dishes. The cells were incubated at 37 °C, 5% CO_2 for 24 h. The media was removed and slides were washed with PBS (3x5 mL). The cells were fixed by adding 10 mL of 4% formaldehyde for 10 min and washed with PBS (3x5 mL). The cells were stained with Hoescht 33342 (10 mL, 1 μg/mL) in PBS for 10 min, excess Hoescht 33342 was pipetted out and the slides were washed with PBS (3x5 mL). Slides were rinsed with water and left to dry.

Image capture and analysis was carried out using the high resolution HCS platform (20X objective) and Pathfinder™ software. Cell compatibility with the different polymers was determined by counting the number of cells present on each spot using a DAPI filter. Results are presented in **Tables 6.10 and 6.11**.

Focused polymer microarray fabrication and screening

A focused microarray was fabricated using 5 polyurethanes and 8 polyacrylates. (**Table 6.12**) Polymer solutions were printed (section 6.1.12) onto an agarose coated slide with 16 replications of each polymer, within a field of 16x32 spots. Once printed, the slides were dried under vacuum (24 h at 40 °C/200 mbar) and sterilised by exposure to UV irradiation for 20 min prior to use.[108]

Cell cultivation on microarrays were performed according to the same protocol as described above.

Image capture and analysis was carried out using the same protocol as described above. Results are presented in **Table 6.12**.

Scale-up experiment on coverslips

Four polyacrylates (**Table 6.13**) were chosen for the scale-up experiment using coverslips.

A P6708 spin coater (Speedlines Technologies) and coverslips (13 mm diameter VWR Cat No. 631-0150, Menzel-Glaser) were used. Polymer solutions (2% w/v in THF) (50 μL) was placed onto the coverslip and spun for 10 s at 2000 rpm. Coverslips were dried under vacuum for 12 h at 45 °C/200 mbar and sterilized by irradiating with UV light for 20 min.

Polystyrene tissue culture plastic (PS-TCP) and coverslips were coated with solutions (50 μl) of collagen type I (0.03 mg/mL), fibronectin (0.01 mg/mL) and bovine serum albumin (0.01 mg/mL) in PBS as a control.

Coverslips were placed in 12-well plates and the wells were filled with the Human Corneal Epithelial Cell Line (HCEC) medium, EpiLife, along with antibiotics (penicillin (1000 units/mL), streptomycin (1000 units/mL) and fungizone (1000 units/mL) and left overnight at room temperature in order to allow sterilisation.

After 24 h the medium was removed, coverslips were washed with PBS and the wells were filled with 1 mL of EpiLife with antibiotics penicillin (100 units/mL), streptomycin (100 units/mL) and fungizone (100 units/mL). Cells were seeded into the wells (120000 cells/well) such that the final volume was 2 mL in each well. The plates were placed in the incubator at 37 °C, 5% CO_2. After 24 h the media was removed and coverslips were

washed with PBS (3x1 mL). The cells were fixed by adding 1 mL of 4% formaldehyde and leaving aside for 10 min at room temperature. The coverslips were washed 3x with PBS (3x1 mL) and the cells were stained with Hoescht 33342 (550 µl, 1 µg/mL) and left aside for 10 min. The coverslips were washed with PBS (3x1 mL) and water (3x1 mL) and left to dry.

Image capture and analyses were carried out using a high resolution HCS platform (10X objective) and Pathfinder™ software. The microscope imaged areas (1234 µm x 943 µm) were combined to give a mosaic of the whole coverslip. Cell compatibility with the different polymers was determined by automatic counting of the number of the cells present on each coverslip using a DAPI filter and Pathfinder. Results are presented in **Tables 6.13** and **6.14**.

Cell transfer

Three limbal – mimicking surface were fabricated using: tissue culture plastic, tissue culture plastic coated with solution (30 µL) composed of collagen type I (0.03 mg/mL), fibronectin (0.01 mg/mL) and bovine serum albumin (0.01 mg/mL) in PBS, and tissue culture plastic coated with Matrigel (30 µL) = (laminin, collagen type IV, heparan sulphate proteoglycan and entactin). These surfaces were prepared inside a 12-well plate.

4 polyacrylates and 1 polyurethane (**Table 6.15**) were coated onto coverslips by spin coating (according to the protocol described above). Human Cornea Epithelial cells were cultivated on them for 24 h (according to the protocol described above). Coverslips were removed from wells, washed with PBS (1 mL), inverted up-side down and placed onto the cell-receiving surface. After 24 h incubation, cells attached on both cell-receiving surfaces and coverslips were fixed, stained and analysed according to the protocol described above. Results are presented in **Tables 6.15** and **6.16** (number of cells on the receiving surface), **Tables 6.17** and **6.18** (number of cells left on the coverslip after cell transfer).

Transfer devices - fabrication and analysis

The limbal – mimicking surface was polystyrene tissue cultivation plastic - the bottom of the well.

Materials such as Soft contact lenses (PureVision (Balfilcon A) Bausch), polymer clay (Speed Modelina 59018844470019), polystyrene – wool,[153] polystyrene cell cultivation plastic (Nunc Cat. No. 156800), filter paper (Whatman Cat No. 1001 090), polypropylene (Cat No BTR 615106), polyurethane foam (Tytan Euroline Cat No 4455), 13 mm diameter glass coverslip (VWR Cat No. 631-0150) were dip coated in 6f9 solution (2 mL) (2% w/v in THF) and then dried under vacuum for12 h at 45 °C/200 mbar and irradiated with UV light for 20 min. Pure 6f9 was film were formed by evaporation of 1 mL polymer (6f9) solution (2% w/v in THF). (**Table 6.20**)

Human Cornea Epithelial cells were cultivated on the materials for 24 h (according to the protocols described above). Materials were removed from wells, washed in PBS (1 mL) inverted and placed onto the cell-receiving surface. After 24 h incubation cells attached on cell-receiving surfaces were fixed, stained and analysed according to the protocol described above.

Image capture and analysis was carried out using the same procedures as described above. Results are presented in **Tables 6.20**.

6.4.2 Polymer library microarrays analysis

The symbols of polyacrylates and polyurethanes are explained in **Tables 6.20 and 6.21.**

Polymer	Number of cells per spot				AVER	SD
	1	2	3	4		
2f7	303	362	295	335	324	31
2f3	533	548	428	443	488	61
5e5	364	276	355	281	319	47
5e7	671	537	587	713	627	80
3g9	155	182	203	137	169	29
6f9	373	432	398	402	401	24
1a5	67	82	97	59	76	17
2BE7	101	75	84	96	89	10
PU222	40	52	46	53	47	4
PU258	43	42	36	47	42	5
PU189	61	48	49	57	54	5
PU197	18	12	23	11	16	7
PU220	42	35	38	28	36	5
1a7	30	54	15	1	25	23
2a5	0	0	14	3	4	7
2a7	30	69	4	12	29	29
2BB7	44	2	46	18	28	21
3BA7	0	0	112	10	31	55
3BB9	0	0	0	111	28	56
3h7	4	17	24	44	22	17
3h9	15	2	36	74	32	31

Table 6.10 *Table of results for polymer microarrays analysis.*

Screened polyurethanes that do not bind the Human Corneal Epithelial Cells							
3	23	48	79	158	176	195	211
4	24	49	81	159	177	196	212
8	25	50	83	160	179	198	213
9	28	53	85	161	181	199	214
10	29	55	87	162	182	200	215
12	30	57	89	163	183	201	216
13	31	59	93	164	184	202	217
14	33	61	94	165	185	203	218
15	35	63	95	166	186	204	219
16	38	65	96	168	187	205	221
17	41	67	97	169	188	206	223
18	43	69	98	171	190	207	224
19	45	71	99	172	191	208	225
20	46	73	100	174	193	209	226
22	47	77	101	175	194	210	229
Screened polyacrylates that do not bind the Human Corneal Epithelial Cells							
1b7	2g7	3b9	3i9	5AA7	5f9	5x7	7a9
2a9	2g9	3BA5	3j5	5AA9	5h7	5x9	7b5
2b7	2h7	3BB5	3j7	5AB5	5h9	5z5	7b7
2b9	2h8	3BE9	3j9	5AB7	5i5	5z7	7b9
2BA7	3a5	3c5	3l9	5AB9	5i7	5z9	
2BA9	3a7	3c7	3m5	5AC5	5i9	6a5	
2BB9	3a9	3c9	3m7	5AC7	5j5	6a9	
2BC9	3AB 5	3e7	3m9	5AE5	5j9	6b7	
2BE9	3AB 9	3e9	3n9	5AE7	5l5	6b9	
2BG9	3AC 7	3f7	3v7	5AE9	5l7	6c7	
2c5	3AC 9	3f9	3x5	5b7	5m7	6c9	
2c7	3AE 5	3g5	3z5	5b9	5m9	6e9	
2c9	3AE 7	3g7	5a7	5c5	5n7	6g9	
2e9	3AE 9	3i5	5a9	5c7	5v9	7a5	
2f9	3b7	3i7	5AA5	5c9	5x5	7a7	

Table 6.11 *Table of results for polymer microarrays analysis - polymers that did not bind the Human Corneal Epithelial Cells.*

6.4.3 Focused Polymer library microarray analysis

The symbols of polyacrylates and polyurethanes are given in **Tables 6.20 and 7.21.**

Polymer	Number of cells per spot																Average.	SD
	1	2	3	4	5	6	7	8	9	10	11	12	13	14	15	16		
2f7	284	484	404	264	504	344	424	304	464	324	444	364	364	404	333	435	384	72
2f3	432	292	532	302	522	302	522	322	502	392	432	361	463	313	511	392	412	89
5e5	301	346	366	376	336	376	286	426	257	455	336	336	376	411	241	471	356	66
5e7	641	741	531	511	641	570	672	731	506	736	501	711	601	522	720	601	621	90
3g9	152	139	167	166	183	174	202	260	237	193	155	224	221	210	209	116	188	38
6f9	479	474	249	294	344	384	384	374	344	298	434	430	419	309	254	344	364	72
1a5	83	91	87	85	66	93	92	90	89	64	63	73	71	69	67	65	78	12
2BE7	101	102	73	74	63	69	71	103	105	107	75	79	80	96	97	113	88	16
PU222	51	53	50	54	50	54	49	55	51	53	49	55	50	54	51	53	52	2
PU258	57	59	56	60	56	60	55	61	57	59	55	61	56	60	55	61	58	2.2
PU189	65	67	63	69	64	68	63	69	65	67	63	69	64	68	63	69	66	2.4
PU197	27	29	28	28	27	29	28	28	27	29	27	29	27	29	28	28	28	0.8
PU220	41	43	42	42	42	42	42	42	41	43	41	43	42	42	42	42	42	0.3

Table 6.12 *Table of results for focused polymer library microarrays analysis.*

6.4.4 Coverslip analysis

Polymer	Number of cells per coverslip 1cm^2				AVER.	SD
	Coverslip 1	Coverslip 2	Coverslip 3	Coverslip 4		
2f5	11121	10264	15763	14905	13013	2725
5e5	19931	24128	18148	25912	22030	3603
3g9	4239	2861	3052	4047	3550	694
6f9	11561	16939	12754	15747	14250	2513
Coll1/FN/BSA$^{(A)}$ (Control)	9974	9377	8138	7542	8758	1114
PS-TCP$^{(B)}$ (Control)	3541	4727	3362	4905	4134	795

Notes: (A) coverslip coated with Collagen type 1, fibronectin and bovine serum albumin; (B) polystyrene tissue culture plastic.

Table 6.13 *Number of cells per cm^2.*

Half of the coverslips were analysed at The Kroto Research Institute University of Sheffield with cells on each coverslip and were counted using a fluorescent microscope.

Polymer	AVERAGE.	SD (n=4)
2f5	12988	3284
5e7	24140	2563
3g9	3255	589
6f9	14774	2345
Coll1/FN/BSA[(A)](Control)	9578	2015
PS-TCP[(B)] (Control)	4532	894

Notes: (A) coverslip coated with Collagen type 1, fibronectin and bovine serum albumin; (B) polystyrene tissue culture plastic ring (13mm diameter)

Table 6.14 *Number of cells per cm^2. Data obtained from The Kroto Research Institute University of Sheffield (manual counting).*

6.4.5 Results of transfer experiments

The symbols of polyacrylates and polyurethanes are explained in **Tables 6.20 and 6.21.**

Polymer → limbal imitate surface	Number of cells per 1cm^2 of limbal – imitate surface transfer from coverslip				AVER.	SD
	Coverslip 1	Coverslip 2	Coverslip 3	Coverslip 4		
3g9→Coll1/FN/BSA	688	1119	1078	648	883	250
3g9→PS-TCP	1007	1171	882	1298	1090	183
3g9→matrigel	1266	1512	1030	1751	1390	311
5e7→Coll1/FN/BSA	1092	1180	854	768	974	194
5e7→PS-TC	896	1082	782	1197	989	186
5e7→ matrigel	1106	1396	980	1525	1252	252
6f9→Coll1/FN/BSA	11897	11065	16693	15862	13879	2811
6f9→PS-TCP	6353	10137	7421	9070	8245	1685
6f9→matrigel	3904	5162	5490	3578	4534	934
2f5→Coll1/FN/BSA	1270	1012	870	1414	1142	246
2f5→PS-TCP	1341	1886	1687	1143	1514	335
2f5→matrigel	1187	1377	1023	1544	1283	226
2f3→Coll1/FN/BSA	3097	4169	2887	4380	3633	750
2f3→PS-TCP	1129	1641	1113	1659	1386	306
2f3→matrigel	1174	1646	1037	1786	1411	361
PU189→Coll1/FN/BSA	1316	1848	1208	1957	1582	375
PU189→PS-TCP	905	1363	930	1339	1134	251
PU189→matrigel	3262	2947	4320	4636	3791	814

Table 6.15 *Number of cells per 1cm^2 of limbal – imitate surface transfer from coverslip.*

Polymer → limbal imitate surface	AVERAGE	SD (n=4)
3g9→Coll1/FN/BSA	883	251
3g9→PS-TCP	1089	182
3g9→matrigel	1389	310
5e7→Coll1/FN/BSA	973	195
5e7→PS-TC	989	185
5e7→ matrigel	1251	250
6f9→Coll1/FN/BSA	13879	2810
6f9→PS-TCP	8245	1685
6f9→matrigel	4533	935
2f5→Coll1/FN/BSA	1141	245
2f5→PS-TCP	1514	335
2f5→matrigel	1282	225
2f3→Coll1/FN/BSA	3633	750
2f3→PS-TCP	1385	305
2f3→matrigel	1410	360
PU189→Coll1/FN/BSA	1582	375
PU189→PS-TCP	1134	250
PU189→matrigel	3791	812

Table 6.16 *Number of cells per 1cm^2 of limbal – imitate surface transfer from coverslip Data obtained from The Kroto Research Institute University of Sheffield.*

After 24 h coverslips were removed and cells left on the cell-receiving surface were fixed, stained and counted. (**Tables 6.17** and **6.18**)

Polymer → limbal imitate surface	**Number of cells per 1cm^2 of coverslip left behind, after transfer**				**AVER.**	**SD**
	Coverslip 1	**Coverslip 2**	**Coverslip 3**	**Coverslip 4**		
3g9→Coll1/FN/BSA	1134	1443	1024	1553	1289	250
3g9→PS-TCP	512	487	713	738	613	131
3g9→matrigel	232	283	341	391	312	69
5e7→Coll1/FN/BSA	334	293	218	257	276	50
5e7→PS-TC	96	117	101	112	107	10
5e7→ matrigel	305	213	311	221	263	53
6f9→Coll1/FN/BSA	1044	1358	956	1447	1201	238
6f9→PS-TCP	521	714	498	736	617	125
6f9→matrigel	168	207	135	239	187	45
2f5→Coll1/FN/BSA	289	462	336	414	375	77
2f5→PS-TCP	224	381	284	320	302	66
2f5→matrigel	1038	1413	977	1473	1225	254
2f3→Coll1/FN/BSA	552	749	533	767	650	125
2f3→PS-TCP	546	743	517	771	644	131
2f3→matrigel	1025	1382	976	1432	1204	236
PU189→Coll1/FN/BSA	104	119	99	125	112	12
PU189→PS-TCP	95	112	92	114	103	11
PU189→matrigel	1752	2775	2028	2502	2264	460

Table 6.17 *Number of cells per 1cm^2 of coverslip left behind, after transfer.*

Polymer → limbal imitate surface	AVERAGE	SD (n=4)
3g9→Coll1/FN/BSA	1328	263
3g9→PS-TCP	629	142
3g9→matrigel	312	71
5e7→Coll1/FN/BSA	277	54
5e7→PS-TC	113	13
5e7→ matrigel	282	48
6f9→Coll1/FN/BSA	1191	241
6f9→PS-TCP	681	135
6f9→matrigel	177	49
2f5→Coll1/FN/BSA	395	68
2f5→PS-TCP	312	72
2f5→matrigel	1258	247
2f3→Coll1/FN/BSA	643	136
2f3→PS-TCP	655	141
2f3→matrigel	1184	252
PU189→Coll1/FN/BSA	122	18
PU189→PS-TCP	112	14
PU189→matrigel	2384	422

Table 6.18 *Number of cells per 1mm^2 of coverslip left behind after transferring the human corneal epithelial cells. Data obtained from The Kroto Research Institute University of Sheffield.*

6.4.6 Platforms for direct HCE cell transfer

The symbols of polyacrylates and polyurethanes are explained in **Tables 6.20** and **6.21.**

Platform	Number of cells per 1cm^2 of limbal –platform transferred				AVER	SD
	Coverslip 1	Coverslip 2	Coverslip 3	Coverslip 4		
PS-wool	724	655	896	827	776	107
PS-wool coated with 6f9	2350	3053	2384	3019	2702	387
PS-Petridish	4328	5150	4020	5456	4739	675
PS-Petridish coated with 6f9	4798	5960	6129	4627	5379	775
PP	76	97	73	101	87	14
PP coated with 6f9	0	0	0	0	0	0
Filter paper	80	101	86	96	91	10
Filter paper coated with 6f9	173	158	216	200	187	26
PU foam	362	342	352	461	379	55
PU foam coated with 6f9	703	974	827	849	838	111
coverslip	2657	3694	3376	2975	3176	454
coverslip coated with 6f9	7014	5591	5433	7172	6303	917

Table 6.19 *Number of cells per 1cm^2 of limbal –platform transferred.*

6.4.7 Human Corneal Epithelial Cell culture and Cell cultivation on coverslips

Human corneal epithelial cells (kindly provided by Professor Sheila MacNeil from The Kroto Research Institute University of Sheffield) were grown in serum free Epilife epithelial cell media (M-EPI-500-CA 500 mL from Cascade Biologics), supplemented with Human Corneal Growth Supplement (5 mL) and antibiotics penicillin (100 units/mL), streptomycin (100 units/mL) and fungizone (100 units/mL). For attachment and growth the tissue culture plastic was coated with BSA, fibronectin, and collagen I (BSA Sigma A7030) 0.01 mg/mL in PBS, fibronectin (Sigma F4759)

0.01 mg/mL in PBS (Sigma), and Rat tail Collagen I (Sigma) 0.03 mg/mL (in acetic acid 0.1 M).

6.4.8 Polyacrylates used [113,152]

Polyacrylates symbol;monomer 1/monomer 2 (molar ratio%)	
1a5;St/DEAA(50/50)	3n9; MEMA/DMVBA(90/10)
1a7;St/DEAA(70/30)	3v7; MEMA/VAA (70/30)
1b7;St/DMAA(70/30)	3x5;MEMA/VI(50/50)
2a5; MMA/DEAA(50/50)	3z5;MEMA/ VPNO(50/50)
2a7; MMA/DEAA(70/30)	5a7;HEMA/DEAA(70/30)
2a9; MMA/DEAA(90/10)	5a9;HEMA/DEAA(90/10)
2b7; MMA/DMAA(70/30)	5AA5;HEMA/VP-4(50/50)
2b9; MMA/DMAA(90/10)	5AA7;HEMA/VP-4(70/30)
2BA7;MMA/A-H(70/30)	5AA9; HEMA/ VP-4(90/10)
2BA9;MMA/A-H(90/10)	5AB5; HEMA/ VP-2(50/50)
2BB7;MMA/AES-H(70/30)	5AB7; HEMA/ VP-2(70/30)
2BB9;MMA/AES-H(90/10)	5AB9; HEMA/ VP-2(90/10)
2BC9;MMA/MA-H(90/10)	5AC5; HEMA/ DAAA(50/50)
2BE7;MMA/AAG-H(70/30)	5AC7; HEMA/ DAAA(70/30)
2BE9;MMA/AAG-H(90/10)	5AE5; HEMA/ MNPMA(50/50)
2BG9; MMA/ EGMP-H(90/10)	5AE7; HEMA/ MNPMA(70/30)
2c5; MMA/PAA(50/50)	5AE9; HEMA/ MNPMA(90/10)
2c7; MMA/PAA(70/30)	5b7; HEMA/ DMAA(70/30)
2c9; MMA/PAA(90/10)	5b9; HEMA/ DMAA(90/10)
2f3;MMA/DMAEMA(30/70)	5c2; HEMA/PAA(20/80)
2f5;MMA/DMAEMA(50/50)	5c5; HEMA/PAA(50/50)
2f7;MMA/DMAEMA(70/30)	5c7; HEMA/PAA(70/30)
2f9;MMA/DMAEMA(90/10)	5c9; HEMA/PAA(90/10)
2g7;MMA/DEAEA(70/30)	5f9; HEMA/ DMAEMA(90/10)
2g9;MMA/DEAEA(90/10)	5h7; HEMA/ DMAEA(70/10)
2h7;MMA/DMAEA(70/30)	5h9; HEMA/ DMAEA(90/10)
2h8;MMA/DMAEA(80/20)	5i5; HEMA/ MTEMA(50/50)
3a5; MEMA/DEAA(50/50)	5i7; HEMA/ MTEMA(70/30)
3a7; MEMA/DEAA(70/30)	5i9; HEMA/ MTEMA(90/10)
3a9; MEMA/DEAA(90/10)	5j5; HEMA/ BAEMA(50/50)
3AB5; MEMA/VP-2(50/50)	5j9; HEMA/ BAEMA(90/10)
3AB9; MEMA/ VP-2(90/10)	5l5;HEMA/DMAPMAA(50/50)
3AC7; MEMA/DAAA(70/30)	5l7;HEMA/DMAPMAA(70/30)
3AC9; MEMA/DAAA(90/10)	5m7;HEMA/BACOEA(70/30)
3AE5;MEMA/MNPMA (50/50)	5m9;HEMA/BACOEA(90/10)

3AE 7;MEMA/MNPMA(70/30)	5n5;HEMA/DMVBA(50/50)
3AE 9;MEMA/MNPMA(90/10)	5v9;HEMA/VAA(90/10)
3b7;MEMA/DMAA(70/30)	5x5;HEMA/VI(50/50)
3b9;MEMA/DMAA(90/10)	5x7;HEMA/VI(70/30)
3BA5;MEMA/A-H(50/50)	5x9; HEMA/ VI(90/10)
3BA7; MEMA/A-H(70/30)	5z5; HEMA/ VPNO(50/50)
3BB5; MEMA/AES-H (50/50)	5z7; HEMA/ VPNO(70/30)
3BB9; MEMA/AES-H (90/10)	5z9; HEMA/ VPNO(90/10)
3BE9; MEMA/AAG-H (90/10)	6a5; HPMA/DEAA(50/50)
3c5;MEMA/PAA(50/50)	6a9; HPMA/DEAA(90/10)
3c7;MEMA/PAA(70/30)	6b7; HPMA/ DMAA(70/30)
3c9; MEMA/PAA(90/10)	6b9; HPMA/ DMAA(90/10)
3f7; MEMA/ DMAEMA(70/30)	6c7; HPMA/PAA(70/30)
3f9; MEMA/ DMAEMA(90/10)	6c9; HPMA/PAA(90/10)
3g5; MEMA/ DEAEA(50/50)	6f9; HPMA/DMAEMA(90/10)
3g7; MEMA/ DEAEA(70/30)	6g9; HPMA/DEAEA(90/10)
3g9; MEMA/ DEAEA(90/10)	7a5; HBMA/DEAA(50/50)
3h7; MEMA/ DMAEA(70/30)	7a7; HBMA/DEAA(70/30)
3h9; MEMA/ DMAEA(90/10)	7a9; HBMA/DEAA(90/10)
3i5; MEMA/MTEMA (50/50)	7b5;HBMA/DMAA(50/50)
3i7; MEMA/MTEMA (70/30)	7b7;HBMA/DMAA(70/30)
3i9; MEMA/MTEMA (90/10)	7b9; HBMA/DMAA(90/10)
3j5; MEMA/ BAEMA(50/50)	3e5;MEMA/DEAEMA(50/50)
3j7; MEMA/ BAEMA(70/30)	3e7;MEMA/DEAEMA(70/30)
3j9; MEMA/ BAEMA(90/10)	3e9;MEMA/DEAEMA(90/10)
3l9;MEMA/DMAPMAA(90/10)	5e5;HEMA/DEAEMA(50/50)
3m5; MEMA/ BACOEA(50/50)	5e7;HEMA/DEAEMA(70/30)
3m7; MEMA/ BACOEA(70/30)	2e9; MMA /DEAEMA(90/10)
3m9; MEMA/ BACOEA(90/10)	6e9; HPMA/DEAEMA(90/10)

Table 6.20 *List of polyacrylate on the microarrays.*

6.4.8.1 Structure of monomers used for synthesis polyacrylates

MMA

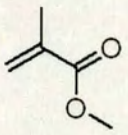

MEMA

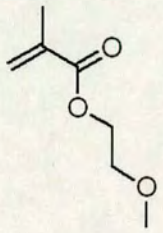

MEA

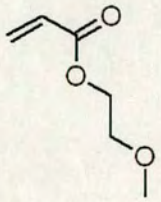

DEAEMA

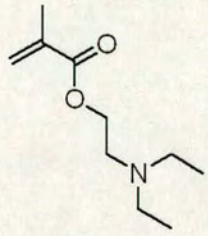

HEMA

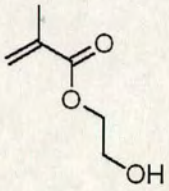

HBMA

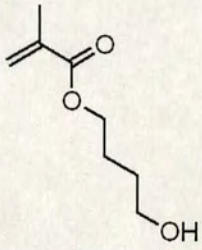

HPMA

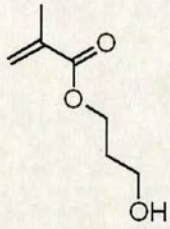

DEAEA

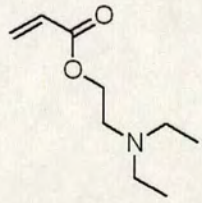

MTEMA

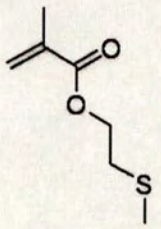

BAEMA

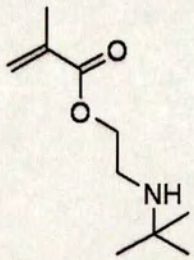

AAG-H

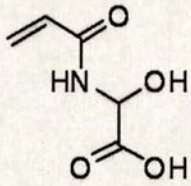

MA-H

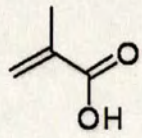

AES-H

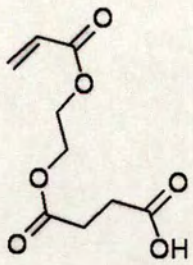

A-H

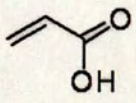

VPNO

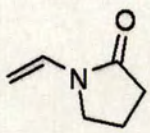

VI

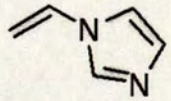

VP-2

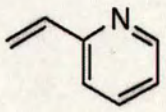

VP-4

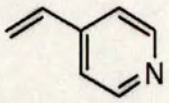

MNPMA

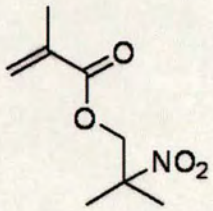

DEAA

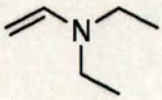

DMAEMA

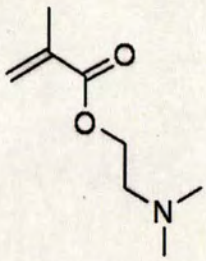

DMAEA

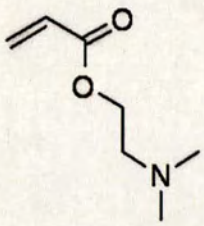

VAA

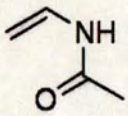

DMAA

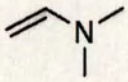

DAAA

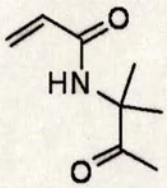

BACOEA

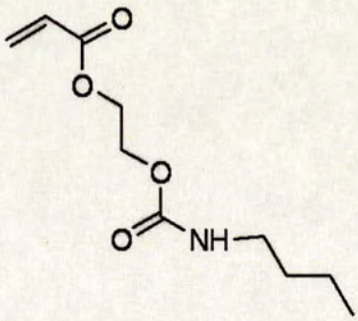

NIPAAm

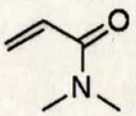

St

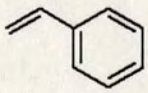

6.4.8.2 List of monomers used for synthesis polyacrylates

MEMA: 2-methoxyethylmethacrylate
MEA: 2-methoxyethylacrylate
HEMA: 2-hydroxyethylmethacrylate
HPMA: hydroxypropylmethacrylate
HBMA: hydroxybutylmethacrylate
MMA: methyl methacrylate
EMA: ethyl methacrylate
BAEMA: 2-(tert-butylamino)ethyl methacrylate
BACOEA: 2-[[(butylamino)carbonyl]oxy]ethyl acrylate
MNPMA: 2-methyl-2-nitropropyl methacrylate
DEAA: diethylacrylamide
DMAA dimethylacrylamide
NIPAA: *N*-isopropylacrylamide
DAAA diacetone acrylamide(*N*-(1,1-dimethyl-3-oxobutyl)-acrylamide)
DMAPMAAm: *N*-[3-(dimethylamino)propyl]acrylamide
DEAEMA: 2-(diethylamino)ethyl methacrylate
DMAEMA: 2-(dimethylamino)ethyl methacrylate
DEAEA: 2-(diethylamino)ethyl acrylate
DMAEA: 2-(dimethylamino)ethyl acrylate
MTEMA: 2-(methylthio)ethyl methacrylate
VAA: *N*-vinylacetamide
VI: 1-vinylimidazole
VPNO: 1-vinyl-2-prrolidinone
VP-4: 4-vinylpyridine
VP-2: 2-vinylpyridine
A-H: acrylic acid
AES-H: mono-2-(acryloyoxy)ethyl succinate
MA-H: methacrylic acid
AAG-H: 2-acrylamidoglycolic acid
EGMP-H: ethylene glycol methacrylate phosphate
DEAEA: 2-(diethylamino)ethyl acrylate
DEAEMA: 2-(diethylamino)ethyl methacrylate
St styrene

6.4.9 Polyurethanes used [151]

PU-	Polymer structure				ratio (mol)		
	Diol	Mn	DIS	Extender			
					mon (1)	mon (2)	x
222	PHNAD	900	BICH	OFHD	0.25	0.52	0.23
258	PTMG	1000	BICH	OFHD	0.17	0.52	0.33
220	PHNAD	900	MDI	DMAPD	0.25	0.52	0.23
197	PTMG	650	BICH	DHM	0.25	0.52	0.23
189	PPG	1000	BICH	OFHD	0.17	0.52	0.33
3	PEG	400	HDI	none	48.5	51.5	0
4	PPG	2000	HDI	none	48.5	51.5	0
8	PEG	400	BICH	none	48.5	51.5	0
9	PPG	2000	BICH	none	48.5	51.5	0
10	PTMG	2000	BICH	none	48.5	51.5	0
12	PEG	900	TDI	none	48.5	51.5	0
13	PEG	400	TDI	none	48.5	51.5	0
14	PPG	2000	TDI	none	48.5	51.5	0
15	PTMG	2000	TDI	none	48.5	51.5	0
16	PEG	2000	MDI	none	48.5	51.5	0
17	PEG	900	MDI	none	48.5	51.5	0
18	PEG	400	MDI	none	48.5	51.5	0
19	PPG	2000	MDI	none	48.5	51.5	0
20	PTMG	2000	MDI	none	48.5	51.5	0
22	PEG	900	PDI	none	48.5	51.5	0
23	PEG	400	PDI	none	48.5	51.5	0
24	PPG	2000	PDI	none	48.5	51.5	0
25	PTMG	2000	PDI	none	48.5	51.5	0
28	PEG	400	HMDI	none	48.5	51.5	0
29	PPG	2000	HMDI	none	48.5	51.5	0
30	PTMG	2000	HMDI	none	48.5	51.5	0
31	PEG	2000	HDI	BD	0.25	0.52	0.23
33	PEG	900	HDI	BD	0.25	0.52	0.23
35	PEG	400	HDI	BD	0.25	0.52	0.23
38	PPG	2000	HDI	ED	0.25	0.52	0.23
41	PEG	2000	BICH	BD	0.25	0.52	0.23
43	PEG	900	BICH	BD	0.25	0.52	0.23
45	PEG	400	BICH	BD	0.25	0.52	0.23
46	PEG	400	BICH	ED	0.25	0.52	0.23

47	PPG	2000	BICH	BD	0.25	0.52	0.23
48	PPG	2000	BICH	ED	0.25	0.52	0.23
49	PTMG	2000	BICH	BD	0.25	0.52	0.23
50	PTMG	2000	BICH	ED	0.25	0.52	0.23
53	PEG	900	TDI	BD	0.25	0.52	0.23
55	PEG	400	TDI	BD	0.25	0.52	0.23
57	PPG	2000	TDI	BD	0.25	0.52	0.23
59	PTMG	2000	TDI	BD	0.25	0.52	0.23
61	PEG	2000	MDI	BD	0.25	0.52	0.23
63	PEG	900	MDI	BD	0.25	0.52	0.23
65	PEG	400	MDI	BD	0.25	0.52	0.23
67	PPG	2000	MDI	BD	0.25	0.52	0.23
69	PTMG	2000	MDI	BD	0.25	0.52	0.23
71	PEG	2000	PDI	BD	0.25	0.52	0.23
73	PEG	900	PDI	BD	0.25	0.52	0.23
77	PPG	2000	PDI	BD	0.25	0.52	0.23
79	PTMG	2000	PDI	BD	0.25	0.52	0.23
81	PEG	2000	HMDI	BD	0.25	0.52	0.23
83	PEG	900	HMDI	BD	0.25	0.52	0.23
85	PEG	400	HMDI	BD	0.25	0.52	0.23
87	PPG	2000	HMDI	BD	0.25	0.52	0.23
89	PTMG	2000	HMDI	BD	0.25	0.52	0.23
93	PTMG	650	BICH	BD	0.485	0.515	0
94	PTMG	1000	BICH	BD	0.485	0.515	0
95	PTMG	650	MDI	BD	0.485	0.515	0
96	PTMG	1000	MDI	BD	0.485	0.515	0
97	PHNGAD	1800	BICH	DMAPD	0.25	0.52	0.23
98	PHNGAD	1800	BICH	DEAPD	0.25	0.52	0.23
99	PTMG	650	HDI	DMAPD	0.25	0.52	0.23
100	PTMG	1000	HDI	DMAPD	0.25	0.52	0.23
101	PTMG	650	BICH	DMAPD	0.25	0.52	0.23
158	PTMG	250	MDI	OFHD	0.25	0.52	0.23
159	PTMG	250	MDI	BD	0.25	0.52	0.23
160	PTMG	250	MDI	EG	0.25	0.52	0.23
161	PTMG	650	MDI	EG	0.25	0.52	0.23
162	PTMG	1000	MDI	EG	0.25	0.52	0.23
163	PTMG	2000	MDI	EG	0.25	0.52	0.23
164	PTMG	250	MDI	PG	0.25	0.52	0.23
165	PTMG	650	MDI	PG	0.25	0.52	0.23

166	PTMG	1000	MDI	PG	0.25	0.52	0.23
168	PTMG	250	BICH	none	48.5	51.5	0
169	PTMG	650	BICH	none	48.5	51.5	0
171	PTMG	250	HDI	none	48.5	51.5	0
172	PTMG	650	HDI	none	48.5	51.5	0
174	PTMG	250	MDI	none	48.5	51.5	0
175	PTMG	650	MDI	none	48.5	51.5	0
176	PTMG	1000	MDI	none	48.5	51.5	0
177	PTMG	250	HDI	NMPD	0.25	0.52	0.23
179	PTMG	2000	HDI	NMPD	0.25	0.52	0.23
181	PTMG	2000	BICH	NMPD	0.25	0.52	0.23
182	PTMG	650	MDI	NMPD	0.25	0.52	0.23
183	PTMG	1000	MDI	NMPD	0.25	0.52	0.23
184	PTMG	2000	MDI	NMPD	0.25	0.52	0.23
185	PHNAD	900	MDI	OFHD	0.17	0.52	0.33
186	PTMG	650	BICH	OFHD	0.25	0.52	0.23
187	PTMG	1000	BICH	OFHD	0.25	0.52	0.23
188	PTMG	2000	BICH	OFHD	0.25	0.52	0.23
190	PTMG	650	HDI	OFHD	0.25	0.52	0.23
191	PTMG	1000	HDI	OFHD	0.25	0.52	0.23
193	PPG	1000	MDI	DMAPD	0.17	0.52	0.33
194	PTMG	650	MDI	OFHD	0.25	0.52	0.23
195	PTMG	1000	MDI	OFHD	0.25	0.52	0.23
196	PTMG	2000	MDI	OFHD	0.25	0.52	0.23
198	PTMG	1000	BICH	DHM	0.25	0.52	0.23
199	PTMG	2000	BICH	DHM	0.25	0.52	0.23
200	PTMG	650	HDI	DHM	0.25	0.52	0.23
201	PTMG	1000	HDI	DHM	0.25	0.52	0.23
202	PTMG	2000	HDI	DHM	0.25	0.52	0.23
203	PTMG	650	MDI	DHM	0.25	0.52	0.23
204	PTMG	1000	MDI	DHM	0.25	0.52	0.23
205	PTMG	2000	MDI	DHM	0.25	0.52	0.23
206	PPG	1000	HDI	OFHD	0.25	0.52	0.23
207	PPG	1000	BICH	OFHD	0.25	0.52	0.23
208	PPG	1000	MDI	OFHD	0.25	0.52	0.23
209	PPG	1000	HDI	PG	0.25	0.52	0.23
210	PPG	1000	BICH	PG	0.25	0.52	0.23
211	PPG	1000	MDI	PG	0.25	0.52	0.23
212	PHNAD	900	HDI	PG	0.25	0.52	0.23

213	PHNAD	900	BICH	PG	0.25	0.52	0.23
214	PHNAD	900	MDI	PG	0.25	0.52	0.23
215	PHNAD	900	HDI	BD	0.25	0.52	0.23
216	PHNAD	900	BICH	BD	0.25	0.52	0.23
217	PHNAD	900	MDI	BD	0.25	0.52	0.23
218	PHNAD	900	HDI	DMAPD	0.25	0.52	0.23
219	PHNAD	900	BICH	DMAPD	0.25	0.52	0.23
221	PHNAD	900	HDI	OFHD	0.25	0.52	0.23
223	PHNAD	900	MDI	OFHD	0.25	0.52	0.23
224	PHNAD	900	HDI	none	48.5	51.5	0
225	PHNAD	900	BICH	none	48.5	51.5	0
226	PHNAD	900	MDI	none	48.5	51.5	0
229	PPG-PEG	1900	MDI	none	48.5	51.5	0

Table 6.21 *List of monomers used in the synthesis of the poly(urethanes).*

6.4.9.1 List of compounds used for synthesis polyurethanes

Chain Extender (Ext.):

EG: ethylene glycol
ED: ethylene diamine
PG: propylene glycol
BD: 1,4-butanediol
DMAPD: 3-dimethylamino-1,2-propanediol
DEAPD: 3-diethylamino-1,2-propanediol
DHM: diethyl bis(hydroxymethyl)malonate
NMPD: 2-nitro-2-methyl-1,3-propanediol
OFHD: 2,2,3,3,4,4,5,5-octafluoro-1,6-hexanediol

Diisocyanate (Dis.):

BICH: 1,3-bis(isocyananatomethyl)cyclohexane
MDI: 4,4'-methylenebis(phenylisocyanate)
HMDI: 4,4'-methylenebis(cyclohexylisocyanate)
HDI: 1,6-diisocyanohexane
PDI: 1,4-diisocyanobenzene
TDI: 4-methyl-1,3-phenylene diisocyanate

Polyol:

PPG: poly(propylene glycol)
PTMG: poly(tetramethylene glycol)
PEG: poly(ethylene glycol)
PHNAD: poly[1,6-hexanediol/neopentyl glycol-*alt*-(adiptic acid)]diol
PHNGAD: poly[1,6-hexanediol/neopentyl glycol/diethylene glycol-*alt*-(adiptic acid)]diol

6.5 Experimental for Chapter 4

6.5.1 Experimental procedures for Chapter 4

Polymer microarray fabrication

The polymer microarrays were fabricated according to procedure presented in section 6.1.4. 124 Polyacrylates [113,152] and 100 KIT polymers were printed on two slides in quadruplicate (for focused library in 16 repetitions) within field 16x32 spots (KIT polymers were dissolved according to conditions described in section 6.2.5).

mES cell cultivation

mES-Oct4 cell cultivation was performed according to procedures described in section 6.1.7.

mES cells staining and fixing

mES-Oct4 cell staining and fixing was performed according to procedures described in section 6.1.14.

Imagining

Imagining of mES-Oct4 cell attached on slides after staining and fixing was performed according to procedures described in section 6.1.11.

Polymer coating on coverslips

P6708 spin coater (Speedlines Technologies) and coverslips (13 mm diameter VWR Cat No. 631-0150, Menzel-Glaser) were used. 50 μL of polymer solution (2% w/v in THF) was placed onto the coverslip and spun for 10 s at 2000 rpm. Coverslips were dried under vacuum (12 h at 45 °C/200 mbar) and irradiated with UV light for 20 min for sterilization.

Flow cytometry

mES-Oct4 GFP cells were analysed on a flow cytometer according to procedure presented in section 6.1.10 .

6.5.2 Screening (with mES-Oct4 cells) microarrays prepared *via* printing pre-synthesised polymers

Polymers KIT (**Table 6.3**) and polyacrylates[113,152] (**Table 6.20**) collected on the microarrays were screened with mES-Oct4 cells and classified according to three

categories: strongly binding (✓) – when cell coverage was 100% of each spot area, medium binding (~) – when cell coverage was less than 100% but greater than 50% and non-cell binding polymers (✗).The symbols of KIT polymers are explained in section 6.2.4.

KIT polymers							
1	✗	26	✗	51	✓	76	✗
2	✗	27	✗	52	✓	77	✗
3	✗	28	~	53	✗	78	✗
4	✗	29	✗	54	✓	79	✗
5	✗	30	✗	55	✗	80	✗
6	✗	31	✗	56	✓	81	✗
7	✗	32	✗	57	~	82	✗
8	✗	33	✗	58	✗	83	✗
9	✗	34	✗	59	✗	84	✗
10	✗	35	✗	60	✗	85	✗
11	✗	36	✗	61	✓	86	~
12	~	37	✗	62	✗	87	✓
13	✗	38	✗	63	✗	88	✗
14	✗	39	✗	64	✗	89	✓
15	✗	40	✗	65	✓	90	~
16	✗	41	✗	66	~	91	✗
17	✗	42	✗	67	✗	92	✗
18	✗	43	✗	68	~	93	✗
19	✗	44	~	69	✗	94	✗
20	✗	45	✓	70	✗	95	✗
21	✗	46	✓	71	✗	96	✗
22	✗	47	✓	72	✓	97	~
23	✗	48	✗	73	✗	98	✗
24	✗	49	✗	74	✗	99	✗
25	✗	50	~	75	✗	100	~

Table 6.22 *Immobilisation of mES Oct4 on KIT polymer microarrays.*

Polyacrylates symbol;monomer 1/monomer 2 (molar ratio%)			
3e5;MEMA/DEAEMA (50/50) ✓	3AC9;MEMA/DAAA(90/10) ✓	3n7;MEMA/DMVBA(70/30) ✓	5g7;HEMA/DEAEA(70/30) ✗
3e9;MEMA/DEAEMA (90/10) ✗	3b5;MEMA/DMAA(50/50) ✗	3n9;MEMA/DMVBA(90/10) ✓	5g9;HEMA/DEAEA(90/10) ✗
5e7;HEMA/DEAEMA (70/30) ✗	3b7;MEMA/DMAA(70/30) ✗	3x5;MEMA/VI(50/50) ✗	5h5;HEMA/DMAEA(50/50) ✗
5e9;HEMA/DEAEMA(90/10) ✗	3BA7;MEMA/A-H(70/30) ✓	3x7; MEMA/VI(70/30) ~	5h9; HEMA/ DMAEA(90/10) ✗
7e7;HBMA/DEAEMA(70/30) ✗	3BA9; MEMA/A-H(90/10) ✓	3x9; MEMA/VI(90/10) ✓	5i5; HEMA/ MTEMA(50/50) ✗
2a5; MMA/DEAA(50/50) ✓	3BB7; MEMA/ AES-H(70/30) ✓	4a5; MEA/DEAA(50/50) ✗	5i7; HEMA/ MTEMA(70/30) ~
2a7; MMA/DEAA(70/30) ✓	3BB9; MEMA/ AES-H(90/10) ✗	4a7; MEA/DEAA(70/30) ✗	5i9; HEMA/ MTEMA(90/10) ~
2b5; MMA/DMAA(50/50) ✗	3BB5; MEMA/ AES-H(50/50) ✗	4a9; MEA/DEAA(90/10) ✗	5j5; HEMA/ BAEMA(50/50) ✗
2b9; MMA/DMAA(90/10) ✗	3BC5; MEMA/ MA-H(50/50) ✓	4b5; MEA/ DMAA(50/50) ✗	5j9; HEMA/ BAEMA(90/10) ✗
2BA5; MMA/A-H(50/50) ✗	3BC7; MEMA/MA-H(70/30) ✗	4b7;MEA/DMAA(70/30) ✗	5m5;HEMA/BACOEA(50/50) ✗
2BA5;MMA/A-H(50/50) ✗	3BC9;MEMA/MA-H(90/10) ✗	4b9;MEA/DMAA(90/10) ✗	5m7;HEMA/BACOEA(70/30) ✗
2BA7;MMA/A-H(70/30) ✗	3BE9;MEMA/AAG-H(90/10) ✓	4c7;MEA/PAA(70/30) ✗	5n5;HEMA/DMVBA(50/50) ✓
2BB7;MMA/AES-H(70/30) ✓	3BG5;MEMA/EGMP-H(50/50) ✗	4c9;MEA/PAA(90/10) ✗	5n7;HEMA/DMVBA(70/30) ✓
2BC7;MMA/MA-H(70/30) ~	3BG7;MEMA/EGMP-H(70/30) ✓	5a7;HEMA/DEAA(70/30) ✗	5n9;HEMA/DMVBA(90/10) ✓
2BC9;MMA/MA-H(90/10) ✗	3BG9;MEMA/EGMP-H(90/10) ✗	5a9;HEMA/DEAA(90/10) ✗	5v5;HEMA/VAA(50/50) ✗
2BE5;MMA/AAG-H(50/50) ✓	3c5;MEMA/PAA(50/50) ✓	5AA5;HEMA/VP-4(50/50) ~	5v7;HEMA/VAA(70/30) ✗
2BE3;MMA/AAG-H(30/70) ✗	3c7;MEMA/PAA(70/30) ✗	5AA7;HEMA/VP-4(70/30) ~	5x7;HEMA/VI(70/30) ~
2BE7;MMA/ AAG-H(70/30) ✓	3c9; MEMA/PAA(90/10) ✓	5AA9; HEMA/ VP-4(90/10) ~	5x9; HEMA/ VI(90/10) ✗
2BE9; MMA/ AAG-H(90/10) ~	3f5; MEMA/ DMAEMA(50/50) ✓	5AB5; HEMA/ VP-2(50/50) ✗	5z5; HEMA/ VPNO(50/50) ✗
2BG5; MMA/ EGMP-H(50/50) ✓	3f7; MEMA/ DMAEMA(70/30) ✓	5AB7; HEMA/ VP-2(70/30) ✗	5z7; HEMA/ VPNO(70/30) ✗
2BG7;MMA/EGMP-H(70/30) ✗	3f9; MEMA/ DMAEMA(90/10) ~	5AB9; HEMA/ VP-2(90/10) ✗	5z9; HEMA/ VPNO(90/10) ✗

2BG9; MMA/ EGMP-H(90/10) ✓	3g5; MEMA/ DEAEA(50/50) ✓	5AC5; HEMA/ DAAA(50/50) ✗	6b5; HPMA/ DMAA(50/50) ~
2c5; MMA/PAA(50/50) ✗	3g3; MEMA/ DEAEA(30/70) ✗	5AC7; HEMA/ DAAA(70/30) ✗	6b7; HPMA/ DMAA(70/30) ✗
2c7; MMA/PAA(70/30) ✗	3g7; MEMA/ DEAEA(70/30) ✗	5AC9; HEMA/ DAAA(90/10) ✗	6b9; HPMA/ DMAA(90/10) ✗
3a5; MEMA/DEAA(50/50) ✗	3g6; MEMA/ DEAEA(60/40) ~	5AE7; HEMA/ MNPMA(70/30) ~	6BB9; HPMA/ AES-H(90/10) ~
3a7; MEMA/DEAA(70/30) ✓	3g9; MEMA/ DEAEA(90/10) ~	5AE9; HEMA/ MNPMA(90/10) ✗	6c5; HPMA/PAA(50/50) ~
3a9; MEMA/DEAA(90/10) ✓	3g9; MEMA/DEAEA(90/10) ~	5AE5; HEMA/ MNPMA(50/50) ~	6c7; HPMA/PAA(70/30) ~
3AA5; MEMA/ VP-4(50/50) ✓	3h5; MEMA/ DMAEA(50/50) ✓	5b7; HEMA/ DMAA(70/30) ✗	6c9; HPMA/PAA(90/10) ~
3AA7; MEMA/ VP-4(70/30) ✗	3h6; MEMA/ DMAEA ✗	5c5; HEMA/PAA ✗	7a5; HBMA/DEAA(50/50) ✓
3AA9; MEMA/VP-4(90/10) ✓	3h7; MEMA/ DMAEA(70/30) ✗	5c7; HEMA/PAA(70/30) ✗	7a7; HBMA/DEAA(70/30) ~
3AB5; MEMA/ VP-2(50/50) ✓	3h9; MEMA/ DMAEA(90/10) ✓	5c9; HEMA/PAA(90/10) ✗	7a9; HBMA/DEAA(90/10) ✗
3AB7; MEMA/VP-2(70/30) ~	3j7; MEMA/ BAEMA(70/30) ✗	5f5; HEMA/ DMAEMA(50/50) ✗	7AA5; HBMA/ VP-4(50/50) ✓
3AB9; MEMA/ VP-2(90/10) ~	3m7; MEMA/ BACOEA(70/30) ✓	5f5; HEMA/ DMAEMA(50/50) ~	7AA7; HBMA/ VP-4(70/30) ✓
3AC5; MEMA/DAAA(50/50) ✗	3m9; MEMA/ BACOEA(90/10) ✓	5f7; HEMA/ DMAEMA(70/30) ✗	7AA9; HBMA/ VP-4(90/10) ~
7z5; HBMA/VPNO(50/50) ✗	7z7;HBMA/VPNO(70/30) ✗	7z9 HBMA/VPNO(90/10) ✗	

Table 6.23 *Immobilisation of mES Oct4 on polyacrylates microarrays. List of monomers used for synthesis polyacrylates and structure are presented in section 6.4.8.*

6.5.3 Localization of polymers on the microarrays prepared *via* printing pre-synthesised polymers

mES-Oct4 cells on a microarray of pre-synthesised polymers printed by contact printing. (**Table 6.24**) The symbols of KIT polymers and polyacrylates are given in sections 6.2.5 and 6.4.8 respectively.

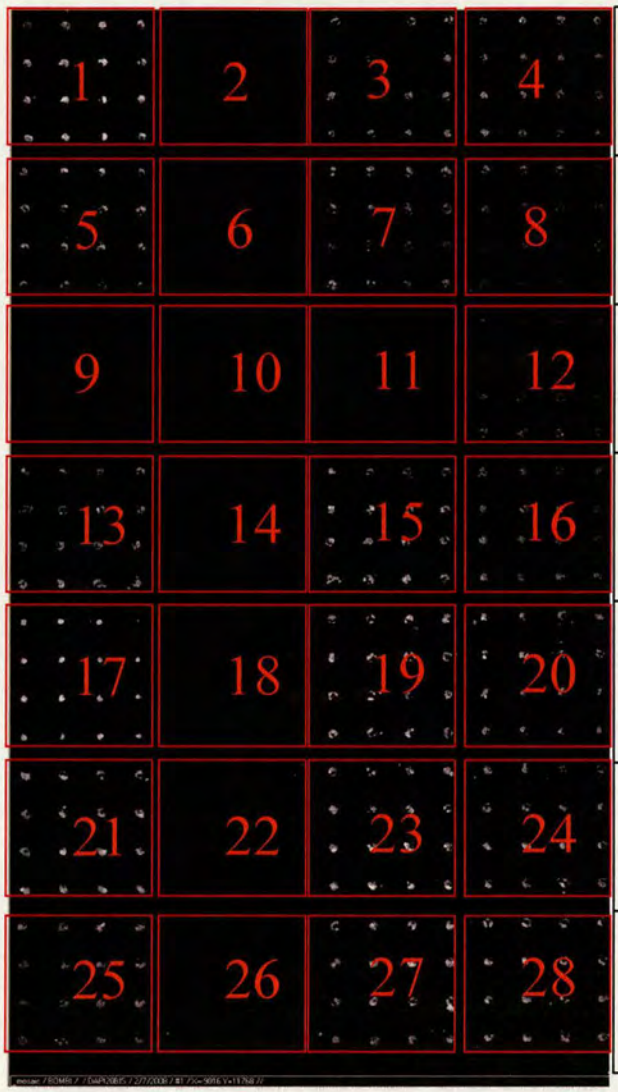

3BG9	3z7	1e7	5e5
KIT 54	3i7	7n7	2a9
5AC5	7a9	5e9	6f9
2a5	3f5	KIT 90	KIT 23
3n9	1c7	KIT 89	Colla gen
2a7	6a5	KIT 45	KIT 47
3a9	5j5	KIT 100	2BB7

Table 6.24 *Microarray of pre-synthesised polymers screened with mES-Oct4 cells: (left panel) mosaic of fluorescence images (DAPI filter) of mES-Oct4 cells on polymeric spot, red squares represents 16 replications of the same polymer spots (scale bar 9 mm) and (right panel) decoding table: polymer names corresponding to the microarray sectors.*

6.6 Experimental for chapter 5

6.6.1 Cell patterning *via* inkjet printing – general procedure

6.6.1.1 Preparation of the coated glass slides

Slides were prepared according to protocol described in section 6.1.3. The thickness of dried agarose coating was 2.34 μm (measured by SEM).[243] Thicker agarose coatings, 9 μm and 26 μm thickness respectively, were obtained by spreading 1 mL and 2.5 mL of 1% agarose solutions onto the glass slides. (**Figure 6.2**)

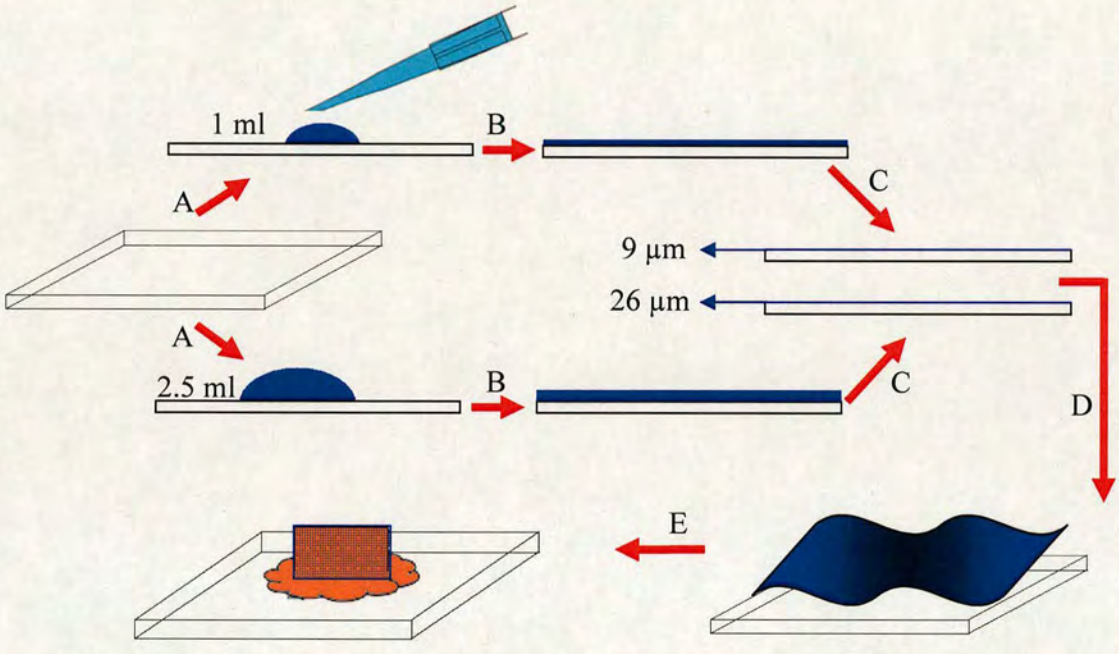

Figure 6.2 *Scheme of agarose layer fabrication: (A) agarose solution (1% w/w in water) deposition onto glass slide at 60 °C); (B) agarose solution spontaneously spread across the slide prior gelation; (C) 24 h drying at R.T; (D) 48 h slide incubation at 37 °C in water- agarose layer detachment; (E) "free standing" agarose film (0.5 x3 cm) was fixed onto slide prior SEM analysis.*

6.6.1.2 Collagen patterning

The collagen patterns were fabricated using an inkjet printer (Microdrop, GmbH, Norderstedt, Germany) using a micro-pipette (AD-K-501) with a 70 μm diameter nozzle. The typical printing parameters were: 140 V, impulse duration 29 μs, and frequency 100 Hz. 0.1% wt of collagen in 0.1 M acetic acid aqueous solution was

prepared and filled in a 96-well plate as the ink source for the printer. The collagen pattern was obtained by double printing in a one spot-one drop mode, which generated spots of 200 μm in diameter.

6.6.1.3 Cell culture

HeLa and mES cells were cultivated according to the protocols described in section 6.1.13. Cells were stained and fixed according to the protocol described in section 6.1.14.

6.6.1.4 Visualisation of patterned slides

Patterned, fixed, cells on slides were analysed using the equipment described in section 6.1.11.

6.6.2 Conversion processes of files of images or pictures into inkjet printer compatible files.

1) Software packages such as Paint or Microsoft Office Picture Manager were used to transform jpg or other picture files into bitmap image files.
2) WinDig - Free Data Digitizer (Copyright 1994-1996, created by D. Lovy) – was used to transform the Bitmap image files into X, Y coordinate files. The WinDig 2.5 file was downloaded from : http://www.unige.ch/sciences/chifi/cpb/windig.html
3) The X,Y coordinate files were transformed into printer macro files by running the application script (created by Dr Andy Turner from Research Computing Office, School of Chemistry, University of Edinburgh) on Perl5.8.8 (available at http://www.perl.com).

Application script:

```
#!/usr/bin/perl
#
use Cwd;
```

```
$path = cwd;

$infile = $ARGV[0];
$outfile = $ARGV[1];
open(input, "<$infile");

$nfile = 1;
open(output, ">$outfile$nfile.mmf");
$i = 0;
while ($line = <input>) {
 if ($i == 50) {
  $nfile++;
  print output "include, c:\\$outfile$nfile.mmf\n";
  close(output);
  open(output, ">$outfile$nfile.mmf");
  $i = 0;
 }
 chomp($line);
 @cart = split(/ +/, $line);
 $x = $cart[1];
 $y = $cart[2];

 $xs = sprintf("%.3f", $x);
 $ys = sprintf("%.3f", $y);

 print output "set,dis,2,$xs,$ys,37,1,1,1,1,0,3,0,1\n";
 print output "dis\n";
 $i++;
}
close(output);
```

close(input);

exit;

An example of the converted files of the patterns for the Microdrop inkjet printer and a "step by step" illustrated manual for bitmap conversion have been provided in the Electronic Data Section.

6.6.3 Cell patterning *via* laser printing- general procedure

6.6.3.1 Glass slide patterning

Negative patterns and images (**Figure 6.3 A**) were printed on PET transparencies at 600 dpi using an HP Color LaserJet 4600DN with a yellow print cartridge C9722A. (**Figure 6.3 B**)

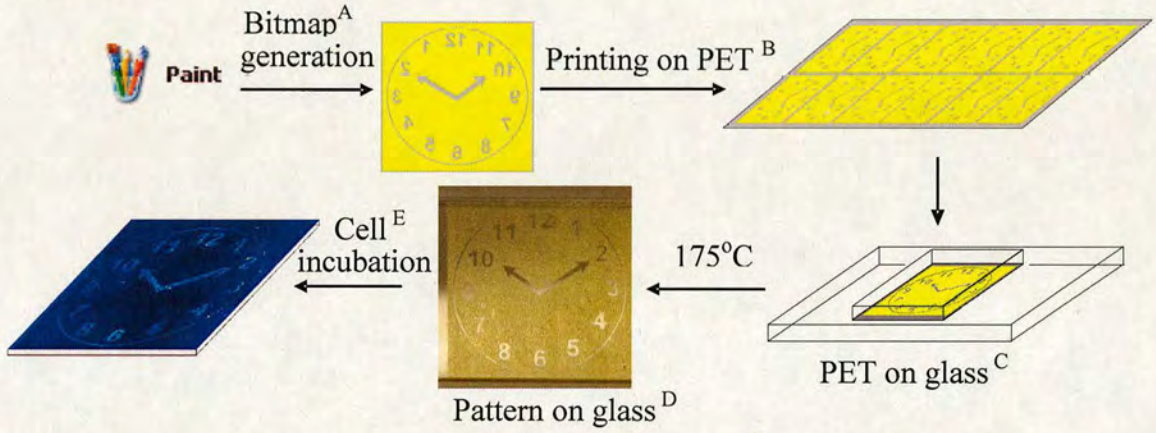

Figure 6.3 *Scheme of patterning via laser printing: (A) image ("clock face" as an example) is the negative of final cellular patterns; (B) image was printed on the transparencies (PET) via laser printer; (C) image on PET sheet was placed (face down) onto the glass slide; (D) during heating toner deposited on the PET was transferred to the glass (heat transfer); (E) cell incubation on the patterned glass slides resulted in cellular patterns placed on the glass.*

Printed images or patterns (26x26 mm) were cut from the A4 PET sheet (**Figure 6.3 C**) and placed face down onto a microscope glass slides, heated at 175 °C for 2 min (hot plate) and pressed using a metal stripe to ensure good contact between the PET film and the glass slide. The PET film was peeled off and the slides annealed for 10 min at

200 °C to give the "masked" glass slides. **Figure 6.4** shows the difference between the printed images before and after the annealing.

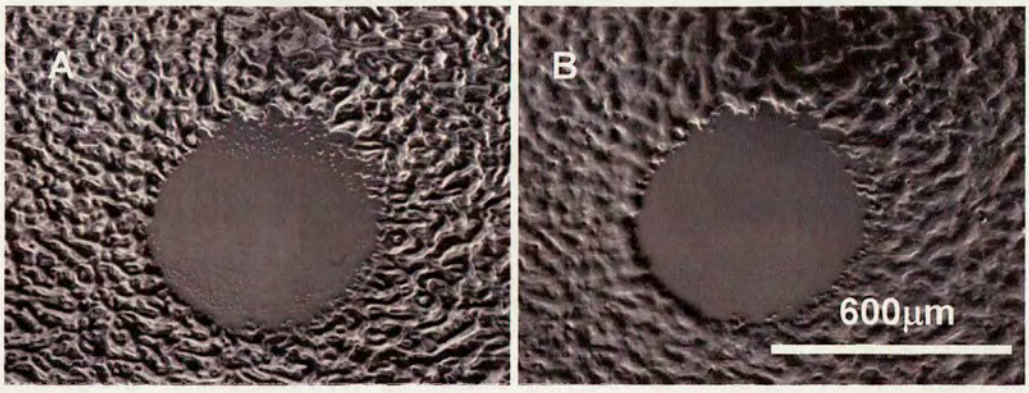

Figure 6.4 *Bright light image of a heat-transfered image: (A) pre-annealing (200 °C, 10 min); (B) post-annealing.*

6.6.3.2 Cell cultivation and staining

HeLa and mES cells were cultivated according to the protocol described in section 6.1.13. Cells were stained and fixed according to the protocol described in section 6.1.14.

6.6.3.3 Visualisation of patterned slides

Patterned fixed cells were analysed using the equipment described in section 6.1.11.

6.6.3.4 Preparation of free standing cellular clusters

The free standing cellular cluster was fabricated using mES-Oct4 cells according to the protocol described in section 6.6.3.1 and 6.6.3.2. After 72h incubation, the mES-Oct4 cellular cluster was harvested from the slide and located on the tissue culture plastic for further incubation. (**Figure 6.5**)

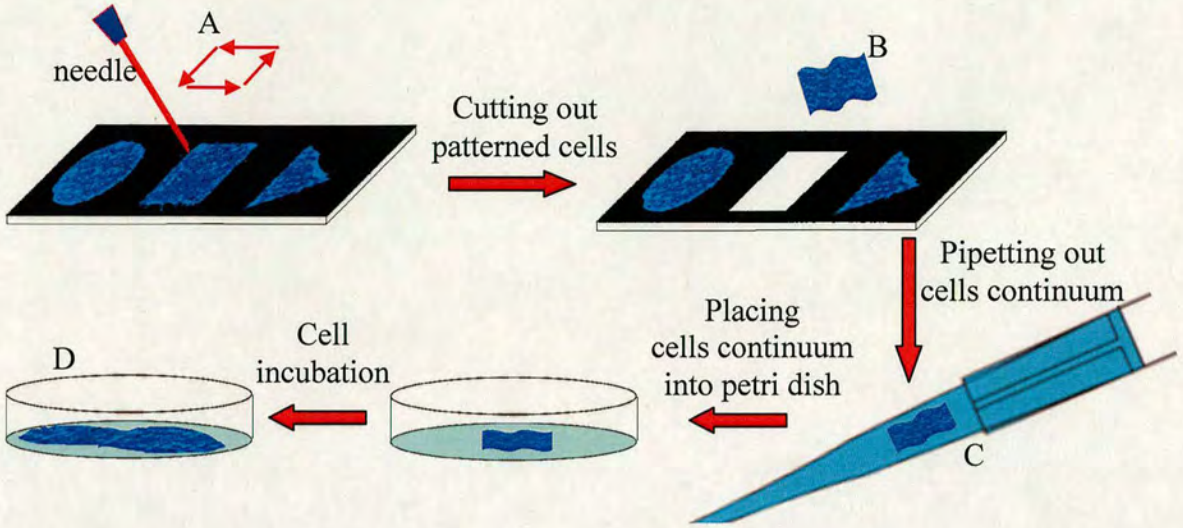

Figure 6.5 *Scheme of preparation of free standing cellular clusters: (A) needle's end motion for separation of cellular continuum from the patterned surface; (B) free standing cell film drifting freely inside the medium; (C) free standing cell film inside pipette tip; (D) proliferation of cells continuum after locating on tissue culture plastic.*

6.6.3.5 HeLa cells patterning on lines

Line of the HeLa cells were fabricated according to the protocol described in section 6.6.3.1 and 6.6.3.2 using mask shown in **Figure 6.6.** Imaging of patterned HeLa cells was performed according to the protocol presented in section 6.11 after 48 h incubation.

Figure 6.6 *Scheme of mask design for patterning HeLa cells in lines. Original white areas were replaced by black colour for better visualisation "pt" = weight unit in PowerPoint software, 1 pt ≈0.355 mm.*

6.6.3.6 Materials for cell patterning *via* laser printing

PET film - A4 Colour Laser Transparencies (210x297 mm) from Supplies Team ® (West Yorkshire UK). 4-rectangular well plates made from PS with non-treated surface and a volume of 22 mL/well from Nunc (Langenselbold, D).

Chapter 7 : General conclusion

In **Chapter 1**, a high-throughput method for studying polymorphism in small molecules has been presented. This approach uses arrays of polymers to generate or trigger different polymorphic forms. The crystal habit forms of the small molecule solids were found to be a poor indicator of polymorphic form, but Raman spectroscopy was a very successful technique that could be used to characterize different polymorphic forms. Powder X-ray Diffraction was not a suitable analysis technique because of the small scale of the high-throughput method. Many of the polymers were selective in terms of triggering specific polymorphic forms and a few were very selective and specific, demonstrating the role of these polymers in determining the crystallisation process. The method is clearly an attractive alternative to the screening processes previously reported.[54] This method allowed three different small molecules to be screened for crystallisation (in triplicate) with 128 polymers, requiring just milligram quantities of each molecule and 27 μg of each polymer per array, while generating large numbers of polymorphic forms. Polymers triggered different polymorphic forms of small molecules in a very subtle manner and although the materials on which crystals grow are important, as demonstrated here, there are many other influences including solvent type and control of evaporation.[55] Therefore, no correlation between the structure of the polymer and the triggering of specific polymorphic growth could be identified during the screening of these 128 polymers. Nevertheless, it was established that all the polymers that gave repeatable crystal habits of carbamazepine were soluble in DMSO. As DMSO was used as a crystallisation solvent this could indicate the importance of polymer mediated slowdown of solvent evaporation or polymer solubility. In the case of poly(2,6-dimethyl-p-phenylene oxide), which allowed for selective growth of orange needles of ROY, the solubility in NMP was low. Therefore, in this instance, the polymer could act as a heteronucleation source.

This method could readily be used by the pharmaceutical industry, for whom early establishment of the polymorphism of drugs is crucial for a successful and complete patent claim. Moreover, the reported method can be applied to the high throughput

crystallisation of proteins, since crystallisation on a small scale facilitates the ability to perform a large number of independent experiments.

In **Chapter 2**, the fabrication of arrays of polymers generated either as spot-based microarrays or as grids, *via* inkjet printing through oil, has been demonstrated. This allows the generation of large arrays of co-polymers in a highly miniaturized, automated and highly reproducible manner, giving polymers with excellent spot morphology (on the micro-array platform). These arrays of polymers were used to identify polymers for selective mES cells binding. Polymer microarrays prepared by high-throughput polymerisation have proven to be useful tools for the selection of cell binding polymers. Screening of microarrays with mES cells allowed the selection of 2 polymers which were later tested on coverslips for comparison of their ability for mES cell cultivation compared to traditional substrates used for this purpose. The most important achievement was increasing the experimental efficiency of the preparation of polymer microarrays by *in situ* polymerisation instead of traditional gram scale polymer synthesis.[127] This approach will be applicable in many research areas, such as cellular immobilisation, identification of cell specific polymers, controlling stem cell differentiation and fate, protein trapping and the development of plastic electronics and biosensing layers as it allows the properties of many polymers to be investigated without having to resort to large-scale synthesis.

In **Chapter 3** high-throughput polymer screening (including polymer microarray preparation and screening for cell binding) was successfully employed for the identification of active polymers from a library of 252 polymers for cell transfer in order to develop medically serviceable devices. The activity of 13 polymers was successfully confirmed by experiment on coverslips leading to the identification of 5 candidates for transfer experiments. Polymer 6f9 was found to be the most effective in its ability for cell transfer. Finally, platforms based on polymer 6f9 were prepared in order to develop medically serviceable devices. The ultimate goal of replacing a fibroblast-type surface for cell transferring by non-animal originating materials was achieved. The obtained

results were patented: *Copolymers Suitable for Use in Corneal Bandages WO 2008/047169 A2.*

This strategy is important, as it can be employed to transfer specific types of cells to specified places in the body for applications in tissue engendering and regenerative medicine, especially for skin muscle repair, nerve reconstruction and vascularisation enhancing.

In **Chapter 4,** polymer microarrays prepared by printing pre-synthesised polymers were successfully used for pre-selection of mES cell binding polymers. Screening of microarrays with mES cells allowed the selection of 3 polymers which were later tested on a coverslip for comparison of the ability of cell binding with traditional substrates used for mES cultivation. It was shown that in the case of mES cells a monolayer is very difficult to produce, especially on the microarray, due to a very limited binding surface area and a strong tendency for mES cells to form 3D structures. This problem could not be solved by reducing the concentration of the cells or the incubation time or even the spot size. Results from analysis (by flow cytometry) of cells attached to coverslips covered with polymers showed that (as found previously), tissue culture plastic covered with gelatine provided the highest protection from cell differentiation, allowing 55% of cells to remain in the undifferentiated state. By contrast, chlorosulfonated polyethylene promoted the undifferentiated state in only 22% of cells. However polymer 3BG9 was almost as good at preventing differentiation as gelatine. The crucial advantage of artificial polymers is that they are free of bio-contamination.

The strategy described here can readily be used to produce surfaces for controlling stem cell differentiation and fate. This could be achieved by employing a wider polymer library and using fluorescent labels to distinguish the type of cells within a population of differentiated cells.

In **Chapter 5,** a flexible method for inkjet mediated patterning of biomolecules and cells has been developed, by attaching and growing cells on agarose coated amino-modified glass slides patterned with collagen using a scientific inkjet printer. Any 2D pattern

References List

(1) Sumner, J. in: *American Household Botany: A History of Useful Plants 1620-1900*, Sumner, J. (ed.), Chapter 4, p146. Cambridge: Timber Press, **2004**.

(2) Dubos, R. J.; Dubos R. in: *Pasteur and Modern Science*, Dubos, R. J.; Dubos R., Brock, T. D. (eds.), Chapter 2, p 14. Washington DC: ASM Press, **1998**

(3) Bernstein, J. in: *Polymorphism in Molecular Crystals*, Bernstein, J. (ed.), Chapter 1.2, pp 2 Calaredon: Oxford University Press, 2007.

(4) Schorlemmer, C. in: *A Manual of the Chemistry of the Carbon Compounds or organic chemistry*, Schorlemmer, C (ed.). London: MacMillan&Co, **1874**.

(5) Senechal, M. in: *Historical atlas of crystallography*, de Faria, J. L. (ed.), Chapter 2, pp 43-59. Dordrecht: Kluwer Academic Publishers, **1990**.

(6) Toma, P. H.; Kelley, M. P.; Borochardt, T. B., Byrn, S. R.; Kahr, B. Chem. *Mater.* **1994**, *6*, 1317-1324.

(7) Groth P. H. R. in: *An Introduction to Chemical Crystallography*, Engelemann, W. (ed.). London: John Wiley & Sons, **1917.**

(8) Kutzke, H.; Al-Mansour, M.; Klapper, H. *J. Mol. Struct.* **1996,** *374*, 129-135.

(9) Day, G. M.; Trask, A. V.; Motherwell, W. D. S.; Jones, W. *Chem. Commun.* **2006**, *1*, 54-56.

(10) Vishweshwar, P.; McMahon, J. A.; Paterson, M. L.; Zawratko, M. J. *J. Am. Chem. Soc.* **2005**, *127*, 16802-16803.

(11) McCrone, W. C. in: *Physics and chemistry of the organic solid State*, Fox, D. (ed.), Chapter 5, pp. 726-767. New York: John Wiley & Sons, Inc., **1965**.

(12) Findlay A. F. in: *The phase rule and its applications,* Cambell, A. N.; Smith, N. O. (eds.), pp 7-19. New York: Dover Publications.

(13) Buerger, M. J.; Bloom, M. C. *Z. Kristallogr.* **1937**, *96*, 182-200

(14) Sirota, N. N. *Cryst. Res. Technol.* **1982**, *17*, 661-191.

(15) Bernstein, J. in: *Polymorphism in Molecular Crystals*, Bernstein, J. (ed.), Chapter 1.3, pp. 8-10. Calaredon: Oxford University Press, **2007**.

(16) McPherson, A. in: *Preparation and analysis of protein crystals*, McPherson, A (ed.), Chapter 5, pp 127-159. New York: Wiley, **1982**.

(17) Yu, L. X.; Furness, M. S.; Raw, A.; Woodland Outlaw, K. P.; Nashed, N. E.; Ramos, E.; Miller, S. P. F.; Adams, R. C.; Fang, F.; Patel, R. M.; Holcombe, F. O., Jr.; Chiu, Y.; Hussain, A. S. *Pharm. Res.* **2003**, *20*, 531-536.

(18) Yu, L. X.; Ellison, C. D.; Hussain, A. S. in: *Applications of pharmacokinetic principles in drug development*, Krishna, R. (ed.), Chapter 3, pp 53-75. New York: Springer, **2003.**

(19) (a) Price, C. P.; Grzesiak, A. L.; Matzger, A. J. *J. Am. Chem. Soc.* **2005**, *127*, 5512-5517. (b) Li, H.; Stowell, J. G.; Borchardt, T. B.; Byrn, S. R. *Crystal Growth & Design* **2006**, *6*, 2469-2474. (c) Ruedas-Rama, M. J.; Lopez-Sanchez, M.; Ruiz-Medina, A.; Molina-Diaz, A.; Ayora-Canada, M. J. *Analyst* **2005**, *130*, 1617-1623.

(20) Dunitz, J. D.; Bernstein, J. *Acc. Chem. Res.* **1995**, *28*, 193-200.

(21) Aizenberg, J.; Black, A. J.; Whitesides, G. M. *J. Am. Chem. Soc.* **1999**, *121*, 4500-4509.

(22) Han, Y.; Wysocki, L. M.; Thanawala, M. S.; Siegrist, T.; Aizenberg, J. *Angew. Chem., Int. Ed.* **2005**, *44*, 2386-2390.

(23) Ichikawa, K.; Shimomura, N.; Yamada, M.; Ohkubo, N. *Chem. Eur. J.* **2003**, *9*, 3235-3241.

(24) Aizenberg, J.; Black, A. J.; Whitesides, G. M. *Nature* **1999**, *398*, 495-498.

(25) Lang, M.; Grzesiak, A. L.; Matzger, A. J. *J. Am. Chem. Soc.* **2002**, *124*, 14834-14835.

(26) Stupp, S. I.; Braun, P. V. *Science* **1997**, *277*, 1242-1248.

(27) Mann, S.; Ozin, G. A. *Nature* **1996**, *382*, 313-318.

(28) Feng, S.; Bein, T. *Science* **1994**, *265*, 1839-1841.

(29) Berman, A.; Ahn, D. J.; Lio, A.; Salmeron, M.; Reichert, A.; Charych, D. *Science* **1995**, *269*, 515-518.

(30) Aksay, I. A.; Trau, M.; Manne, S.; Honma, I.; Yao, N.; Zhou, L.; Fenter, P.; Eisenberger, P. M.; Gruner, S. M. *Science* **1996**, *273*, 892-898.

(31) Rodrı´guez-Hornedo, N.; Murphy, D. *J. Pharm. Sci.* **1999**, *88*, 651-660.

(32) Cantor, P. *Heterogeneous nucleation and adsorption* **2003**, *361*, 409-417.

(33) (a) Al-Zoubi, N.; Koundourellis, J. E.; Malamataris, S. *J. Pharm. Biomed. Anal.* **2002**, *29*, 459-467. (b) Moynihan, H. A., O'Hare, I. P., *Int. J. Pharm.* **2002**, *247*, 179-185.

(34) Cabeza, A. J. C.; Day, G. M.; Motherwell, W. D.; Jones, W. *Chem. Commun.* **2007**, *16*, 1600-1602.

(35) Kogermann, K.; Aaltonen, J.; Strachan, C. J.; Pöllänen, K.; Veski, P.; Heinämäki, J.; Yliruusi, J.; Rantane, J. *J. Pharm. Sci.* **2007**, *96*, 1802-1820.

(36) Wyttenbach, N.; Alsenz, J.; Grassmann, O. *Pharm. Res.* **2007**, *24*, 888-898.

(37) Tian, F.; Sandler, N.; Aaltonen, J.; Lang, C.; Saville, D. J.; Gordon, K. C.; Strachan, C. J.; Rantanen, J.; Rades, T. *J. Pharm. Sci.* **2007**, *96*, 584-594.

(38) Kipouros, K.; Kachrimanis, K.; Nikolakakis, I.; Tserki, V.; Malamataris, S. *J. Pharm. Sci.* **2006**, *95*, 2419-2431.

(39) Rama, M. J. R.; López-Sánchez, M.; Ruiz-Medina, A.; Molina-Díaz, A.; Ayora-Cañada, M. J. *Analyst* **2005**, *130*, 1617-1623.

(40) Takasuka, M.; Nakai, H. *Vib. Spectrosc.* **2001**, *25*, 197-204.

(41) Karthikeyan, G.; Mohanraj, K.; Elango, K. P.; Girishkumar, K. *Russ. J. Coord. Chem.* **2006**, *32*, 380-385.

(42) Göbel, A.; Thomsen, A.; Mcardell, C. S.; Joss, A.; Giger, W. *Environ. Sci. Technol.* **2005**, *39*, 3981-3989.

(43) Zhang, C.-L.; Wang, F.-A.; Wang, Y. *J. Chem. Eng. Data* **2007**, *52*, 1563-1566.

(44) McKinnon, J. J.; Fabbiani, F. P. A.; Spackman, M. A. *Cryst. Growth Des.* **2007**, *7*, 755-769.

(45) Li, H.; Stowell, J. G.; Borchardt, T. B.; Byrn, S. R. *Cryst. Growth Des.* **2006**, *6*, 2469-2474.

(46) Smith, J. R.; Xu, W.; Raftery, D. *J. Phys. Chem. B* **2006**, *110*, 7766-7776.

(47) Chen, S.; Xi, H.; Yu, L. *J. Am. Chem. Soc.* **2005**, *127*, 17439-17444.

(48) Dunitz, J. D.; Gavezzotti, A. *Cryst. Growth Des.* **2005**, *5*, 2180-2189.

(49) Chen, S.; Guzei, I. A.; Yu, L. J. *Am. Chem. Soc.* **2005**, *127*, 9881-9885.

(50) Grzesiak, A. L.; Lang, M.; Kim, K.; Matzger, A. J. *J. Pharm. Sci.* **2003**, *92*, 2260-2271.

(51) (a) Tian, F.; Zeitler, J. A.; Strachan, C. J.; Saville, D. J.; Gordon, K. C.; Rades, T. *J. Pharm. Biomed. Anal.* **2006**, *40*, 271-280. (b) O'Brien, L. E.; Timmins, P.; Williams, A. C.; York, P. *J. Pharm. Biomed. Anal.* **2004**, *36*, 335-340.

(52) Lang, M.; Kampf, J. W.; Matzger, A. J. *J. Pharm. Sci.* **2002**, *91*, 1186-1190.

(53) Momany, F. A.; Sessa, D. J.; Lawton, J. W.; Selling, G. W.; Hamaker, S. A. H.; Willett, J. L. *J. Agric. Food Chem.* **2006**, *54*, 543-547.

(54) Morissette, S. L.; Almarsson, Ö.; Peterson, M. L.; Remenar, J. F.; Read, M. J.; Lemmo, A. V.; Ellis, S.; Cima, M. J.; Gardner, C. R. *Adv. Drug Delivery Rev.* **2004**, *56*, 275-300.

(55) Liberski, A. R.; Tizzard, G. J.; Diaz-Mochon, J. J.; Hursthouse, M. B.; Milnes, P.; Bradley, M. *Journal of Combinatorial Chemistry* **2008**, *10*, 24-27.

(56) Nie, Z.; Kumacheva, E. *Nature Materials* **2008**, *7*, 277-290.

(57) Théry, M.; Racine, V.; Pépin, A.; Piel, M.; Chen, Y.; Sibarita J.-B.; Bornens M. *Nature Cell Biol.* **2005**, *7*, 947-953.

(58) Théry, M.; Racine, V.; Piel, M.; Pépin, A.; Dimitrov, A.; Chen, Y.; Sibarita J.-B.; Bornens M. *Proc. Natl. Acad. Sci. USA* **2006**, *103*, 19771-19776.

(59) Hollister, S. J. *Nature Materials* **2005**, *4*, 518-524.

(60) Shimoda, T.; Morii, K.; Seki, S.; Kiguchi, H. *Mater. Res. Soc. Bull.* **2003**, *28*, 821-827.

(61) Ruiz, R.; Breyta, G.; Cheng, J. Y.; Colburn, M. E.; Guarini, K. W.; Kim, H.-C.; Zhang, Y. *IBM J. Res. Dev.* **2007**, *51*, 605-633.

(62) Singh, T. B.; Sariciftci, N. S. *Annu. Rev. Mater. Res.* **2006**, *36*, 199-230.

(63) Kane, R. S.; Cohen, R. E; Silbey, R. *Chem. Mater.* **1996**, *8*, 1919-1924.

(64) Park, M.; Harrison, C.; Chaikin, P. M.; Register, R. A.; Adamson, D. H. *Science* **1997**, *276*, 1401-1404.

(65) Campbell, M.; Sharp, D. N.; Harrison, M. T.; Denning, R. G.; Turberfield, A. J. *Nature* **2000**, *404*, 53-56.

(66) Valkama, S.; Kosonen, H.; Ruokolainen, J.; Haatainen, T.; Torkkeli, M.; Serimaa, R.; Ten Brinke, G.; Ikkala, O. *Nature Materials* **2004**, *3*, 872-876.

(67) Moon, J. H.; Ford, J.; Yang, S. *Polym. Adv. Technol.* **2006**, *17*, 83-93.

(68) Bloomstein, T. M.; Rothschild, M.; Kunz, R. R.; Hardy, D. E.; Goodman, R. B.; Palmacci S. T. *J. Vac. Sci. Technol.* **1998**, *B 16*, 3154-3157.

(69) Bloomstein, T. M.; Marchant, M. F.; Deneault, S.; Hardy, D. E.; Rothschild, M. *Opt. Express* **2006**, *14*, 6434-6443.

(70) Cheng, J. Y.; Ross, C. A.; Chan, V. Z.-H.; Thomas, E. L.; Lammertink, R. G. H.; Vancso, G. J. *Adv. Mater.* **2001**, *13*, 1174-1178.

(71) Chou, S. Y.; Krauss, P. R.; Zhang, W.; Guo, L. J.; Zhuang, L. J. *Vac. Sci. Technol. B* **1997**, *15*, 2897-2904.

(72) Hua, F.; Sun, Y.; Gaur, A.; Meitl, M. A.; Bilhaut, L.; Rotkina, L.; Wang, J.; Geil, P.; Shim, M.; Rogers, J. A. *Nano Lett.* **2004**, *4*, 2467-2471.

(73) Schmid, G. M. et al. *J. Vac. Sci. Technol. B* **2006**, *24*, 1283-1291.

(74) Kumar, A.; Whitesides, G. M. *Appl. Phys. Lett.* **1993**, *63*, 2002-2004.

(75) Hui, C. Y.; Jagota, A.; Lin, Y. Y.; Kramer, E. J. *Langmuir* **2002**, *18*, 1394-1407.

(76) Sharpe, R. B. A.; Burdinski, D.; van der Marel, C.; Jansen, J. A. J.; Huskens, J.; Zandvliet, H. J. W.; Reinhoudt, D. N.; Poelsema, B. *Langmuir* **2006**, *22*, 5945-5951.

(77) Workman, R. K.; Manne, S. *Langmuir* **2004**, *20*, 805-815.

(78) Zhou, F.; Zheng, Z. J.; Yu, B.; Liu, W. M.; Huck, W. T. S. *J. Am. Chem. Soc.* **2006**, *128*, 16253-16258.

(79) Park, J.; Kim, Y. S.; Hammond, P. T. *Nano Lett.* **2005**, *5*, 1347-1350.

(80) Yan, L.; Huck, W. T. S.; Zhao, X. M.; Whitesides, G. M. *Langmuir* **1999**, *15*, 1208-1214.

(81) Shah, R. R.; Merreceyes, D.; Husemann, M.; Rees, I.; Abbott, N. L.; Hawker, C. J.; Hedrick, J. L.; *Macromolecules* **2000**, *33*, 597-605.

(82) Zhou, F.; Chen, M.; Liu, W.; Liu, J.; Liu, Z.; Mu, Z. *Adv. Mater.* **2003**, *15*, 1367-1370.

(83) Jiang, X. P.; Clark, S. L.; Hammond, P. T. *Adv. Mater.* **2001**, *13*, 1669-1673.

(84) Kumar, G.; Wang, Y. C.; Co, C.; Ho, C. C. *Langmuir* **2003**, *19*, 10550v10556.

(85) Lin, C. C.; Co, C. C.; Ho, C. C. *Biomaterials* **2005**, *26*, 3655-3662.

(86) Gates, B. D.; Xu, Q.; Stewart, M.; Ryan, D.; Willson, C. G.; Whitesides, G. M.; *Chem. Rev.* **2005**, *105*, 1171-1196.

(87) Nyffenegger, R. M.; Penner, R. M. *Chem. Rev.* **1997,** *97*, 1195-1230.

(88) Piner, R. D.; Zhu, J.; Xu, F.; Hong, S. H.; Mirkin, C. A. *Science* **1999**, *283*, 661-663.

(89) Woodfield, T. B. F.; Malda, J.; de Wijn, J.; Péters, F.; Riesle, J.; van Blitterswijk, C. A.; *Biomaterials* **2004**, *25*, 4149-4161.

(90) Vozzi, G.; Previti, A.; De Rossi, D.; Ahluwalia, A. *Tissue Eng.* **2002**, *8*, 1089-1098.

(91) Vozzi, G.; Flaim, C.; Ahluwalia, A.; Bhatia, S. *Biomaterials* **2003**, *24*, 2533-2540.

(92) Geng, L.; Feng, W.; Hutmacher, D. W.; Wong, Y. S.; Loh, H. T.; Fuh, J. Y. H. *Rapid Prototyping J.* **2005**, *11*, 90-97.

(93) Landers, R.; Hubner, U.; Schmelzeisen, R.; Mulhaupt, R. *Biomaterials* **2002**, *23*, 4437-4447.

(94) Gratson, G. M.; Xu, M. J.; Lewis, J. A. *Nature* **2004,** *428*, 386-386.

(95) Therriault, D.; White, S. R.; Lewis, J. A. *Nature Materials* **2003**, *2*, 265-271.

(96) Xu, M. J.; Gratson, G. M.; Duoss, E. B.; Shepherd, R. F.; Lewis, J. A. *Soft Matter* **2006**, 2, 205-209.

(97) Gratson, G. M.; García-Santamaría, F.; Lousse, V.; Xu, M.; Fan, S.; Lewis, J. A.; Braun, P. V. *Adv. Mater.* **2006**, *18*, 461-465.

(98) Hutmacher, D. W. *Biomaterials* **2000**, *21*, 2529-2543.

(99) Sirringhaus, H.; Kawase, T.; Friend, R. H.; Shimoda, T.; Inbasekaran, M.; Wu, W.; Woo, E. P. *Science* **2000**, *290*, 2123-2126.

(100) Bonaccurso, E.; Butt, H. J.; Hankeln, B.; Niesenhaus, B.; Graf, K. *Appl. Phys. Lett.* **2005**, *86*, id. 124101 (3 p).

(101) Sele, C. W.; von Werne, T.; Friend, R. H.; Sirringhaus, H. *Adv. Mater.* **2005**, *17*, 997-1001.

(102) Park, J. U.; Hardy, M.; Kang, S. J.; Barton, K.; Adair, K.; Mukhopadhyay, D. K.; Lee, C. Y.; Strano, M. S.; Alleyne, A. G.; Georgiadis, J. G.; Ferreira, P. M.; Rogers, J. A. *Nature Materials* **2007**, 6, 782-789.

(103) Christanti, Y.; Walker, L. M. J. *Non-Newtonian Fluid Mech.* **2001**, *100*, 9-26.

(104) Cartera, J. C.; Alvisa, R. M.; Browna, S. B.; Langrya, K. C.; Wilsona, T. S.; McBridea, M. T.; Myrickb, M. L.; Royall Coxc, W.; Grovec, M. E.; Colstona, B. W.; *Biosens. Bioelectron.* **2006**, *21*, 1359-1364.

(105) Roth, E. A.; Xu, T.; Das, M.; Gregory, C.; Hickman, J. J.; Boland, T.; *Biomaterials* **2004**, *25*, 3707-3715.

(106) Anderson, D. G.; Levenberg, S.; Langer, R. *Nat. Biotechnol.* **2004**, *22*, 863-866.

(107) Anderson, D. G.; Putnam, D.; Lavik, E. B.; Mahmood T. A.; Langer, R. *Biomaterials* **2005**, *26,* 4892-4897.

(108) Tourniaire, G. *Polymer Microarrays- Development and Applications.* **2006**, PhD thesis, University of Edinburgh, Edinburgh, UK.

(109) Tourniaire, G.; Collins, J.; Campbell, S.; Mizomoto, H.; Ogawa, S.; Thaburet, J. F.; Bradley, M. *Chem. Commun.,* **2006**, *20*, 2118-2120.

(110) Mant, A.; Tourniaire, G.; Diaz-Mochon, J. J.; Elliott, T. J.; William, A. P.; Bradley, M. *Biomaterials* **2006**, *27*, 5299-5306.

(111) Pernagallo, S.; Unciti-Broceta, A.; Diaz-Mochon, J. J.; Bradley, M. *Biomed. Mater.* **2008**, *3*, 034112 (6pp).

(112) Pernagallo, S.; Diaz-Mochon, J. J.; Bradley, M. *Lab Chip* **2009**, *9*, 397-403.

(113) Mizomoto, H. *The synthesis and screening of polymer libraries using a high throughput approach.* **2004**, PhD thesis, University of Southampton, Southampton, UK.

(114) Schmatloch, S.; Bach, H.; van Benthem, R. A. T. M.; Schubert, U. S. *Macromol. Rapid Commun.* **2004**, *25*, 95-107.

(115) de Gans, B.-J.; Kazancioglu, E.; Meyer, W.; Schubert, U. S. *Macromol. Rapid Commun.* **2004**, *25*, 292-296.

(116) de Gans, B.-J.; Schubert, U. S. *Langmuir* **2004**, *20*, 7789-7793.

(117) Tekin, E.; de Gans, B.-J.; Schubert, U. S. *J. Mater. Chem.* **2004**, *14*, 2627-2632.

(118) de Gans, B.-J.; Xue, L.; Agarwal, U. S.; Schubert, U. S. *Macromol. Rapid Commun.* **2005**, *26*, 310-314.

(119) Marin, V.; Holder, E.; Wienk, M. M.; Tekin, E.; Kozodaev, D.; Schubert, U. S. *Macromol. Rapid Commun.* **2005**, *26*, 319-324.

(120) Tekin, E.; Holder, E.; Marin, V.; de Gans, B.-J.; Schubert, U. S. *Macromol. Rapid Commun.* **2005**, *26*, 293-297.

(121) van den Berg, A. M. J.; de Laat, A. W. M.; Smith, P. J.; Perelaer, J.; Schubert, U. S. *J. Mater. Chem.* **2007**, *17*, 677-683.

(122) de Gans, B.-J.; Hoeppener, S.; Schubert U. S. *J. Mater. Chem.* **2007**, *17*, 3045-3050.

(123) Cull, T. R.; Goulding, M. J.; Bradley, M. *Adv. Mater.* **2007**, *19*, 2355-2359.

(124) Zhang, R.; Liberski, A.; Khan, F.; Diaz-Mochon, J. J.; Bradley, M. *Chem. Commun.* **2008**, *11*, 1317-1319.

(125) Microdrop-Dispenser Heads, http://www.microdrop.de/wDeutsch/products/AD_Pipettes_e_0707.pdfHeads.pdf. Accessed the 02th Nov. 2008.

(126) Microdrop-Dispenser Camera, http://www.microdrop.de/wDeutsch/products/Camera_System_e_0707.pdf Accessed the 02th Nov. 2008.

(127) Liberski, A.; Zhang, R.; Bradley, M.; *Chem. Commun.* **2009**, 334-336.

(128) Wurmser, A. E.; Gage, F. H. *Nature* **2002**, *416*, 485-487.

(129) Notara, N.; Daniels, J. T. *Cell Tissue Res.* **2008**, *331*, 135-143.

(130) Stepp, M. A.; Zieske, J. D. *Ocular Surf.* **2005**, *3*, 15-26.

(131) Dua, H. S.; Shanmuganathan, V. A.; Powell-Richards, A. O.; Tighe, P. J.; Joseph, A. *Brit. J. Ophth.* **2005**, *89*, 529-532.

(132) Daniels, J. T.; Dart, J. K. G.; Tuft, S. J.; Khaw, P. T. *Wound Rep. Regen.* **2001**, *9*, 483-494.

(133) Tseng, S. C. G. *Mol. Biol. Rep.* **1996**, *23*, 47-58.

(134) Spelsberg, H.; Sundmacher, R. *Klin. Monatsbl. Augenheilkd.* **2005**, *222*, 905-909.

(135) Ilari, L.; Daya, S. M. *Ophthalmology* **2002**, *109*, 1278-1284.

(136) Solomon, A.; Ellies, P.; Anderson, D. F.; Touhami, A.; Grueterich, M.; Espana, E. M.; Ti, S. E.; Goto, E.; Feuer, W. J.; Tseng, S. C. *Ophthalmology* **2002**, *109*, 1159-1166.

(137) Holland, E. J.; Djalilian, A. R.; Schwartz, G. S. *Ophthalmology* **2003**, *110*, 125-130.

(138) Niederer, R. L.; Perumal, D.; Sherwin, T.; McGhee, C. N. *Invest. Ophthalmol. Vis. Sci.* **2007**, *48*, 621-626.

(139) Rao, G. N.; John, T.; Ishida, N.; Aquavella, J. V. *Ophthalmology* **1985**, *92*, 1408-1411.

(140) Mathers, W. D.; Jester, J. V.; Lemp, M. A. *Arch. Ophthalmol.* **1988**, *106*, 210-211.

(141) Pellegrini, G.; Traverso, C.E.; Franzi, A. T.; Zingirian, M.; Cancedda, R.; De Luca, M. *Lancet* **1997**, *349*, 990-993.

(142) Higham, M. C.; Dawson, R.; Szabo, M.; Short, R.; Haddow, D. B.; MacNeil, S. *Tissue Eng.* **2003**, *9*, 919-930.

(143) Schwab, I. R. *Trans. Am. Ophthalmol. Soc.* **1999**, *97*, 891-986.

(144) Daya, S. M.; Watson, A.. Sharpe, J. R.; Giledi, O.; Rowe, A.; Martin, R.; James, S. E. *Ophthalmology* **2005**, *112*, 470-477.

(145) Nakamura, T.; Inatomi, T.; Sotozono, C.; Ang, L. P. K.; Koizumi, N.; Yokoi, N.; Kinoshita, S. *Ophthalmology* **2006**, *113*, 1756-1772.

(146) Rama, P.; Bonini, S.; Lambiase, A.; Golisano, O.; Paterna, P. De Luca, M.; Pellegrini, G. *Transplantation* **2001**, *72*, 1478-1485.

(147) Borrás, C.; Esteve, J. M.; Viña, J. R.; Sastre, J.; Viña, J.; Pallardó, F. V. *J. Biol. Chem.* **2004**, *279*, 34332-34335.

(148) Arora, R.; Mehta, D.; Jain, V. *Eye* **2005** *19*, 273-278.

(149) Tsai, R. J.-F.; Li, L.-M.; Chen, J.-K. *N. Engl. J. Med.* **2000**, *343*, 86-93.

(150) Nishida, K.; Yamato, M.; Hayashida, Y.; Watanabe, K; Maeda, N.; Watanabe, H.; Yamamoto, K.; Nagai, S.; Kikuchi, A.; Tano, Y.; Okano, T. *Transplantation* **2004**, *77*, 379-385.

(151) Jose, A. J. *Synthesis and screening of biocompatible polymers using a*

multiparallel approach. **2005**, PhD thesis, University of Southampton, Southampton, UK.

(152) Thaburet, J. F. O.; Mizomoto, H.; Bradley, M. *Macromol. Rapid Commun.* **2004**, *25*, 366-370.

(153) Baker, S. C.; Atkin, N.; Gunning, P. A.; Granville, N.; Wilson, K.; Darren Wilson, D.; Southgate, J. *Biomaterials* **2006**, *27*, 3136-3146.

(154) Gilbert, S. F., in *Developmental Biology,* Gilbert, S. F (ed.), Chapter3, pp.324. Massachusetts: Sinauer Associates, **2000**.

(155) Brüning, A.; Runnebaum, I. B. *Gene Ther.* **2003**, *10*, 198-205.

(156) Solomonia, R. O.; Kiguradze, T.; McCabe, B. J.; Horn, G. *Neuroreport*, **2000**, *11*, 3139-3143.

(157) Thoulouze, M.-I.; Lafage, M.; Schachner, M.; Hartmann, U.; Cremer, H.; Lafon, M. *Journal of Virology*, **1998**, *72*, 7181-7190.

(158) Bernfield, M. R.; Hinkes M. T.; Gallo, R. L. *Development* **1993**, *119*, 205-212.

(159) Gumbiner, B. M. *Neuron* **1993**, *11*, 551-564.

(160) Hynes, R. O. *Cell* **1992**, *69*, 11-25.

(161) Hynes, R. O.; Lander, A.D. *Cell* **1992**, *68*, 303-322.

(162) Mosher, D. F.; Sottile, J.; Wu, C.; McDonald, J. A. *Curr. Opin. Cell. Biol.* **1992**, *4*, 810-818.

(163) Springer, T. A. *Cell* **1994**, *76*, 301-314.

(164) Turner, C. E.; Burridge, K. *Curr. Opin. Cell. Biol.* **1991**, *3*, 849-853.

(165) Gumbiner, B. M. *Cell* **1996**, *84*, 345-357.

(166) Harrison, R. *J.Exp.Zool.* **1914**, *17*, 521-544.

(167) Ranaldi, G.; Marigliano, I.; Vespignani, I.; Perozzi, G.; Sambuy, Y. *J.Nutr.Biochem.* **2002**, *13*, 157-167.

(168) Allen, L. T.; Tosetto, M.; Miller, I. S.; O'Connor, D. P.; Penney, S. C.; Lynch, I.; Keenan, A. K.; Pennington, S. R.; Dawson, K. A.; Gallagher, W. M. *Biomaterials* **2006**, *27*, 3096-3108.

(169) Liu, A. Y. *Cancer Res.* **2000**, *60*, 3429-3434.

(170) Kuschel, C.; Steuer, H.; Maurer, A. N.; Kanzok, B.; Stoop, R.; Angres, B. *Biotechniques* **2006**, *40*, 523-531.

(171) Flaim, C. J.; Chien, S.; Bhatia, S. N. *Nat. Methods* **2005**, *2*, 119-125.

(172) Ziauddin, J.; Sabatini, D. M. *Nature* **2001**, *411*, 107-110.

(173) Kholodovych, V.; Gubskaya, A. V.; Bohrer, M.; Harris, N.; Knight, D.; Kohn, J.; Welsh, W. J. *Polymer* **2008**, *49,* 2435-2439.

(174) Alberts, B.; Johnson, A.; Lewis, J.; Raff, M.; Roberts, K.; Walter, P. in: *Molecular biology of the Cell*, Gibbs, S. (ed.), Chapter 19, pp1104. New York: Taylor&Francis Group, **2002**.

(175) Gough, N. M.; Gearing, D. P.; King, J. A.; Willson, T. A.; Hilton, D. J.; Nicola, N. A.; Metcalf, D. *Proc. Natl. Acad. Sci. U S A* **1988**, *85*, 2623-2627.

(176) Shin, H. *Biomaterials* **2007**, *28*, 126-133.

(177) El-Ali, J.; Sorger, P. K.; Jensen, K. F. *Nature* **2006**, *442*, 403-411.

(178) Vacanti, J. P.; Langer, R. *Mol. Med.* **1999**, *354*, 32-34.

(179) Rosines, E.; Sampogna, R. V.; Johkura, K.; Vaughn, D. A.; Choi, Y.; Sakurai, H.; Shah, M. M.; Nigam, S. K. *Proc. Natl. Acad. Sci.* **2007**, *104*, 20938-20943.

(180) Metcalfe A. D.; Ferguson, M. W. J. *Biomaterials* **2007**, *28*, 5100-5113.

(181) Redmond, D. E.; Bjugstad, K. B.; Teng, Y. D.; Ourednik, V.; Ourednik, J.; Wakeman, D. R.; Parsons, X. H.; Gonzalez, R.; Blanchard, B. C.; Kim, S. U.; Gu, Z.; Lipton, S. A.; Markakis, E. A.; Roth, R. H.; Elsworth, J. D.; Sladek, J. R.; Sidman, R. L.; Snyder, E. Y. *Proc. Natl. Acad. Sci.* **2007**, *104*, 12175-12180.

(182) Furst, G.; Esch, J. S. A.; Poll, L. W.; Hosch, S. B.; Fritz, L. B.; Klein, M.; Godehardt, E.; Krieg, A.; Wecker, B.; Stoldt, V.; Stockschlader, M.; Eisenberger, C. F.; Modder, U.; Knoefel, W. T. *Radiology* **2007**, 243, 171-179.

(183) Chen, C. S.; Mrksich, M.; Huang, S.; Whitesides, G. M.; Ingber, D. E. *Science* **1997**, *276*, 1425-1428.

(184) Monchaux, E.; Vermette, P. *Biomacromolecules* **2007**, *8*, 3668-3673.

(185) Tan, J. L.; Tien, J.; Pirone, D. M.; Gray, D. S.; Bhadriraju, K.; Chen, C. S. *Proc. Natl. Acad. Sci.* **2003**, *100*, 1484-1489.

(186) Flemming, R. G.; Murphy, C. J.; Abrams, G. A.; Goodman, S. L.; Nealey, P. F. *Biomaterials* **1999**, *20*, 573-588.

(187) Petty, R. T.; Li, H-W.; Maduram, J. H.; Ismagilov, R.; Mrksich, M. *J. Am. Chem. Soc.* **2007**, *129*, 8966-8967.

(188) Mant, A.; Tourniaire, G.; Diaz-Mochon, L. J.; Elliott, T. J.; William, A. P.; Bradley, M. *Biomaterials* **2006**, *27*, 5299-5306.

(189) Tourniaire, G.; Collins, J.; Campbell, S.; Mizomoto, H.; Ogawa, S.; Thaburet, J. F.; Bradley, M. *Chem. Commun.* **2006**, *20*, 2118-2120.

(190) Pernagallo, S.; Unciti-Broceta, A.; Díaz-Mochón, J. J; Bradley, M. *Biomed. Mater.* **2008**, *3*, 034112 (6pp).

(191) Unciti-Broceta, A.; Díaz-Mochón, J. J.; Mizomoto, H.; Bradley, M. *J. Comb. Chem.* **2008**, *10*, 179-184.

(192) Saez, A.; Ghibaudo, M.; Buguin, A.; Silberzan, P.; Ladoux, B. *Proc. Natl. Acad. Sci.* **2007**, *104*, 8281-8286.

(193) Gerecht, S.; Burdick, J. A.; Ferreira, L. S.; Townsend, S. A.; Langer, R. *Proc. Natl. Acad. Sci.* **2007**, *104*, 11298-11303.

(194) G. Tourniaire, *Polymer Microarray-Development and Applications* **2006**, PhD thesis, University of Edinburgh, Edinburgh, UK.

(195) Rosenthal, A.; Macdonald, A.; Voldman, J. *Biomaterials*, **2007**, *28*, 3208-3216.

(196) Calvert, P. *Science* **2007**, *318*, 208-209.

(197) Chen, C. Y.; Barron, J. A.; Ringeisen, B. R. *Appl. Surf. Sci.* **2006**, *252*, 8641-8645.

(198) Falconnet, D.; Csucs, G.; Grandin, H. M.; Textor, M. *Biomaterials* **2006**, *27*, 3044-3063.

(199) Boland, T., Tao, X.; Damon, B. J.; Manley, B.; Kesari, P.; Jalota, S.; Bhaduri, S. *Mat. Sci. Eng. C* 2007, *27*, 372-376.

(200) Xu, T.; Jin, J.; Gregory, C.; Hickman, J. J.; Boland, T. *Biomaterials* **2005**, *26*, 93-99.

(201) Nakamura, M.; Kobayashi, A.; Takagi, F.; Watanabe, A.; Hiruma, Y.; Ohuchi, K.; Iwasaki, Y.; Horie, M.; Morita, I.; Takatani S.; Nakamura, M. *Tissue Eng.* **2005**, *11*, 1658.

(202) Mironov, V.; Prestwich, G.; Forgacs, G. F. *J. Mat. Chemistry* **2007**, *17*, 2054.

(203) Nelson, C. M.; VanDuijn, M. M.; Inman, J. L.; Fletcher, D. A.; Bissell, M. J. *Science* **2006**, *314*, 298-300.

(204) Xia, Y. N.; Whitesides, G. M. *Ann. Rev. Mater. Sci.* **1998**, *28*, 153-184.

(205) Kane, R. S.; Takayama, S.; Ostuni, E.; Ingber, D. E.; Whitesides, G. M. *Biomaterials* **1999**, *20*, 2363-2376.

(206) Singhvi, R.; Kumar, A.; Lopez, G. P.; Stephanopoulos, G. N.; Wang, D. I.; Whitesides G. M.; *Science* **1994**, *264*, 696-698.

(207) Mrksich, M.; Dike, L. E.; Tien, J.; Ingber, D. E.; Whitesides, G. M. *Exp. Cell. Res.* **1997**, *235*, 305-313.

(208) Chen, C. S.; Mrksich, M.; Huang, S.; Whitesides, G. M.; Ingber, D. E.; *Biotechnol. Prog.* **1998**, *14*, 356-363.

(209) Patel, N.; Bhandari, R.; Shakesheff, K. M.; Cannizzaro, S. M.; Davies, M. C.; Langer, R. *J. Biomater. Sci.-Polym. Ed.* **2000**, *11*, 319-331.

(210) Oliva, A.; James, C. D.; Kingman, C. E.; Craighead, H. G.; Banker, G. A. *Neurochem. Res.* **2003**, *28*, 1639-1648.

(211) Graber, D. J.; Zieziulewicz, T. J.; Lawrence, D. A.; Shain, W.; Turner, J. N. *Langmuir* **2003** *19*, 5431-5434.

(212) Delamarche, B. E.; Schmid, H.; Michel, B.; Bosshard, H. R.; Biebuyck, H. *Langmuir* **1998**, *14*, 2225-2229.

(213) Davis, J. R. C.; Kam, L.; Craighead, H. G.; Isaacson M.; Turner, J. N. *Langmuir* **1998**, *14*, 741-744.

(214) Kam, L.; Boxer, S. G. *J. Biomed. Mater. Res.* **2001**, *55*, 487-495.

(215) Csucs, G.; Michel, R.; Lussi, J. W.; Textor, M.; Danuser, G. *Biomaterials* **2003**, *24*, 1713-1720.

(216) Lehnert, D.; Wehrle-Haller, B.; David, C.; Weiland, U.; Ballestrem, C.; Imhof, B. A. *J. Cell. Sci.* **2004**, *117*, 41-52.

(217) Klein, C. L.; Scholl M.; Maelicke, A. *J. Mater. Sci.-Mater. Med.* **1999**, *10*, 721-727.

(218) Kam, L.; Shain, W.; Turner, J. N.; Bizios, R.; *Biomaterials* **2001**, *22*, 1049-1054.

(219) Cornish, T.; Branch, D. W.; Wheeler, B. C.; Campanelli, J. T. *Mol. Cell. Neurosci.* **2002**, *20*, 140-153.

(220) Lauer, L.; Klein, C.; Offenhausser, A. *Biomaterials* **2001**, *22*, 1925-1932.

(221) St. John, P. M.; Davis, R.; Cady, N.; Czajka, J.; Batt, C. A.; Craighead, H. G. *Anal. Chem.* **1998**, *70*, 1108-1111.

(222) Zhang, S. G.; Yan, L.; Altman, M.; Lassle, M.; Nugent, H.; Frankel, F. *Biomaterials* **1999,** *20*, 1213-1220.

(223) Cornish, T.; Branch, D. W.; Wheeler, B. C.; Campanelli, J. T. *Mol. Cell. Neurosci.* **2002**, *20*, 140-153.

(224) Wheeler, B. C.; Corey, J. M.; Brewer, G. J.; Branch, D. W. *J. Biomech. Eng.-Trans. ASME* **1999**, *121*, 73-78.

(225) M. Scholl, C. Sprossler, M. Denyer, M. Krause, K. Nakajima and A. Maelicke *J. Neurosci. Methods* **2000**, *104*, 65-75.

(226) J. Lahann, M. Balcells, T. Rodon, J. Lee, I.S. Choi and K.F. Jensen *Langmuir* **2002**, *18*, 3632-3638.

(227) Graber, D. J.; Zieziulewicz, T. J.; Lawrence, D. A.; Shain, W.; Turner, J. N. *Langmuir* **2003**, *19*, 5431-5434.

(228) Kam, L.; Shain, W.; Turner, J. N.; Bizios, R. *Biomaterials* **1999**, *20*, 2343-2350.

(229) St. John, P. M.; Kam, L.; Turner, S. W.; Craighead, H. G.; Issacson, M. Turner, J. N. *J. Neurosci. Methods* **1997**, *75*, 171-177.

(230) Csucs, G.; Michel, R.; Lussi, J. W.; Textor, M.; Danuser, G.; *Biomaterials* **2003**, *24*, 1713-1720.

(231) C.A. Scotchford, M. Ball, M. Winkelmann, J. Vörös, C. Csucs and D.M. Brunette *Biomaterials* **2003**, *24*, 1147-1158.

(232) Kleinfeld, D.; Kahler, K. H.; Hockberger, P. E.; *J. Neurosci* .**1988**, *8*, 4098-4120.

(233) Healy, K. E.; Thomas, C. H.; Rezania, A.; Kim, J. E.; McKeown P. J.; Lom, B.; *Biomaterials* **1996**, *17*, 195-208.

(234) Bhatia, S. N.; Yarmush, M. L.; Toner, M. *J. Biomed. Mater. Res.* **1997,** *34*, 189-199.

(235) Lee, K.; Park, S.; Mirkin, C.; Smith, J. C.; Mrksich, M. *Science* **2002**, *295*, 1702-1705.

(236) Wilson, D. L.; Martin, R.; Hong, S.; Cronin-Golomb, M.; Mirkin, C. A.; Kaplan, D. L. *Proc. Natl. Acad. Sci.* **2001**, *98*, 13660-13664.

(237) Roth, E. A;. Xu, T.; Das, M.; Gregory, C.; Hickman, J. J.; Boland, T. *Biomaterials* **2004**, *25*, 3707-3715.

(238) Masters, J. R. *Nat. Rev. Cancer* **2002**, *2*, 315-319.

(239) Mironov, V.; Prestwich, G.; Forgacs, G. *J. Mater. Chem.* **2007**, 2054-2060.

(240) Fan, Z.; Ho, J. C.; Jacobson, Z. A.; Yerushalmi, R.; Alley, R. L.; Razavi, H.; Javey, A. *Nano Lett.* **2008**, *8*, 20-25.

(241) Material Safety Data Sheet: http://www.hp.com/hpinfo/globalcitizenship/environment/productdata/pdf/lj_c9722a_us_eng_v4.pdf Accessed the 05th Feb. 2008.

(242) Liu, F.; Shen, W. *Coll. Surf. A: Physicochem. Eng. Aspects* **2008**, *316*, 62-69.

(243) Ferdous, K.; Rahul, T.; Richard, O.; Bradley, M. *Angew. Chem. Int. Ed.* **2009**, *48*, 978-982.

(244) Di Fabio, S.; Corrias, F.; Monardo, F.; Titti, F.; *Journal of Immunological Methods* **2004**, *284*, 7-14.

Appendix I: Publications

Screening for Polymorphs on Polymer Microarrays

Albert R. Liberski,[†] Graham J. Tizzard,[‡] Juan J. Diaz-Mochon,[†] Michael B. Hursthouse,[‡] Phillip Milnes,[†] and Mark Bradley*[,†]

School of Chemistry, The University of Edinburgh, West Mains Road, Edinburgh EH9 3JJ, U.K., and School of Chemistry, University of Southampton, University Road, Highfield, Southampton SO17 1BJ, U.K.

Received June 29, 2007

Introduction. The way in which compounds crystallize has been the subject of study for many centuries with perhaps the most classical example relating to tartaric acid. A current focal point in this area is the phenomenon of polymorphism. This arises because of two main considerations; first in terms of patent law, new crystal forms of a solid compound can be considered as innovations and can be protected as intellectual property (this crucial issue has promoted the intense search for new polymorphs). Second, and of more practical consideration, is the fact that specific crystal forms can alter the dissolution rate of a compound,[1] and thus, the pharmokinetics of any drug are partially determined by the specific crystal form, an issue that also supports the patentability of a polymorph.[2,3]

Many polymorphs have been discovered serendipitously, but traditional methods of discovery and selection of polymorphic forms usually involve the variation of crystallization parameters such as temperature and solvent,[4] and current high-throughput screens generally rely on variation of these parameters. Examples of well-known compounds for which new polymorphic forms have been discovered, after many years of work, include maleic acid (120 years after it was first crystallized)[5] and aspirin,[6] confirming McCrone's often quoted pronouncement.[7] However, fewer than 5% of compounds in the Cambridge Structural Database are reported to be polymorphic,[8] whereas it is known from other studies that do not provide a full structure (e.g., spectroscopic, thermal, and microscopy studies) that more than 35% of known compounds show polymorphic behavior. Therefore new developments in high-throughput platforms[9] for primary polymorph screening would be a valuable tool for the discovery of, as yet, uncharacterized forms.

The substrates upon which crystals grow play a pivotal role in allowing selective growth. For example, calcium carbonate crystal growth can be easily "tuned" by interaction with different surfaces,[10–12] allowing a range of specific structures to be generated. Organic compounds, however, are typically difficult to tune because their "packing" is much more temperamental.[4,13] In the approach presented here, control over specific factors involved in the crystallization processes such as concentration and temperature were used, but the main variable was the surface upon which crystallization occurred. It is well-known that polymers can support the growth of specific types of crystals.[4,13] However, the nature of the interactions between the polymer and the compound under investigation are not understood, and it is not possible to predict the specific polymorphic form generated by crystallization on a specific polymeric support. The technique described here provides a tool to better understand these types of interactions, as well as to reduce the amount of material needed to carry out a "full-polymorphic screen". The approach developed, related to that described by Kazarian,[14] used polymer microarrays onto which solutions of small-molecules were applied and allowed to crystallize, which because of the size of the arrays, required only tiny amounts of solution. The resultant crystals underwent direct characterization on the microarray by optical and Raman microspectroscopy (Raman spectroscopy has been proven to be a valid tool to differentiate between polymorphic forms.).[4] It should be noted that even though different crystal habit forms were found within the array these did not always correspond to different polymorphic forms according to Raman shifts. In general, organic materials tend to crystallize in less symmetric space groups than inorganic materials, a phenomenon which makes crystal habit a less efficient indicator of different polymorphic forms in organic materials than it is for inorganic materials.

The first step in the process consisted of fabrication of the polymer microarrays. This approach consisted of hydrophobic patterning of a glass slide into three grids, each consisting of 8 × 16 hydrophilic "features". A specific polymer was then deposited by piezo jet-printing 800 drops of each of the polymer solutions onto a specific hydrophilic feature (each drop was ~30 μm in diameter, and therefore, ~0.9 μL of a 1% polymer solution was deposited, equating to approximately 9 μg of polymer per spot). The polymers used in this study were synthesized or obtained commercially (see Supporting Information for full experimental details). Two solvents were used for inkjet printing: NMP and toluene. NMP was the dominant solvent used because it efficiently dissolved the majority of the library of polymers, whereas toluene was used for the more hydrophobic polymers (see Supporting Information). Each slide thus contained three 8 × 16 grids giving a total of 128 polymer spots with the area of each spot approximately 1.76 mm^2.

Three well-known and broadly studied small molecules were used in this study: carbamazepine,[15–19] sulfamethoxazole,[20–24] and 2-[(2-nitrophenyl)amino]-3-thiophenecarbonitrile[25–29] (often termed ROY (red/orange/yellow) from the well-known colors of the different polymorphic forms).[30] This choice was the result of the large number of polymorphic studies previously carried out on these compounds, which allowed us to compare our approach to previous reports.[4,31,32] Mother liquors of the small molecules were printed onto the polymer

* To whom correspondence should be addressed. Phone: +44(0) 131 650 4820. Fax: +44 (0) 131 650 6453. E-mail: Mark.bradley@ed.ac.uk.
[†] University of Edinburgh.
[‡] University of Southampton.

10.1021/cc700107x CCC: $40.75
Published on Web 01/01/2008

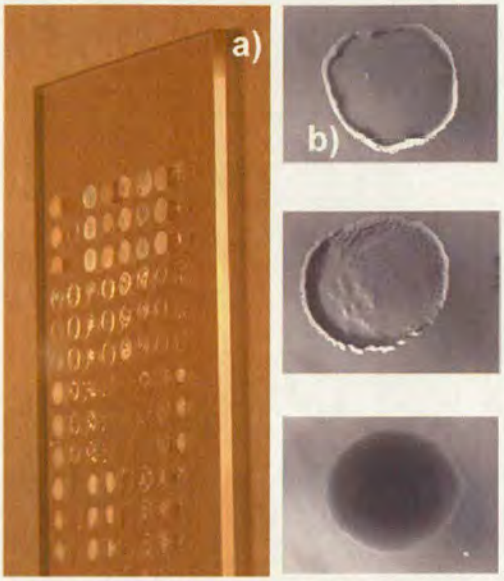

Figure 1. (a) Optical image of a polymer microarray, printed on a masked 27 × 75 mm glass slide, used for polymorph seeding. (b) Image of a single polymer feature (~1.5 mm in diameter).

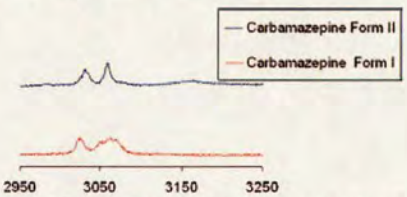

Figure 2. Analytical bands found in Raman spectra corresponding to carbamazepine (Raman details × 100 objective).

features (again 800 drops per spot, 0.9 μL, taking 1.5 s), and after solvent evaporation, the crystals remaining on the polymer spots were analyzed, initially by optical microscopy (40 min for the analysis of 128 polymers). The solvent can play two roles, passively acting as a carrier for the small molecule, or it can also play more of a role by co-dissolving the polymer. Solvent choice dictates also the evaporation rate, which also influences crystallization. Raman spectroscopy gave excellent results (Figure 2), with 10 Raman spectra (16 scans per spectra) recorded per feature (in triplicate) to ensure robust data reproducibility (with five Raman spectra recorded per minute).

The first compound analyzed was carbamazepine. There are four known polymorphic forms of carbamazepine reported in the Cambridge Structural Database, although to our knowledge form IV of carbamazepine has not been characterized by Raman spectroscopy.[33,34] Following the protocol described above, polymer spots containing specific and repeatable crystal habit forms (Figures 2 and 3) were identified using Raman spectroscopy.

In the case of carbamazepine (printed in DMSO), most of the polymers supported specifically polymorphic form I, for

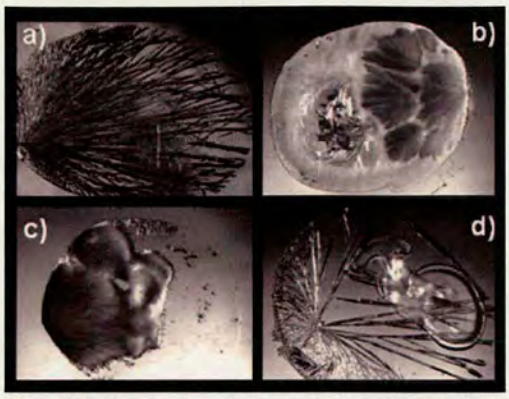

Figure 3. Carbamazepine crystals generated on different polymer features (a) form II on 2,5-furandione−methyl vinyl ether copolymer, (b) form I on poly(vinyl butyral), (c) form I on poly(*n*-butyl methacrylate), and (d) form II on vinyl chloride−acrylic acid copolymer.

example poly-*N*-butyl methacrylate. Vinyl chloride−acrylic acid copolymer and 2,5-furandione−methyl vinyl ether copolymer supported selectively and specifically form II. Additional characterization of the crystals obtained was undertaken using thermomicroscopy with analysis of the crystals on a hot-stage, while heating at 10 °C/min, confirming the interpretation of the Raman spectra and matching previous reports.[31] These results obtained confirmed the interpretation of the Raman spectra and matched those previously reported.[31] In these studies, only 27 μg of each polymer and 6.5 mg of carbamazepine were used, and two different polymorphic forms were detected.

According to the Cambridge Structural Database, four forms of sulfamethoxazole have been discovered to date and all of them have characteristic Raman shifts.[4] In this case the 128 polymers were screened in triplicate under two different experimental conditions (ethanol or methanol) giving rise to 768 crystallization experiments!

With ethanol as a solvent, excellent control of crystal habit could be achieved (see Supporting Information). However closer analysis by Raman spectroscopy revealed all of the crystals were polymorphic form I, again confirming that in the case of organic compounds, crystal habit is rarely correlated with polymorphic form. If methanol was used, the results were significantly different. Raman measurements showed that on most of polymers, mixtures of form I and II were present (Figure 4). However, ethyl cellulose supported specifically form II of sulfamethoxazole, while on hydroxybutyl methyl cellulose most of the spot area was occupied by polymorphic form II, but with form I appearing on the polymer edge. Butyl methacrylate/isobutyl methacrylate copolymer and α-Zein[35] supported the formation of only form I (see Supporting Information for full set of results).

Finally a challenging small-molecule, from a polymorphic study point of view, 5-methyl-2-[(2-nitrophenyl)amino]-3-thiophenecarbo-nitrile (ROY), was analyzed. According to the Cambridge Structural Database, six forms of ROY have been reported to date, all of which have characteristic Raman

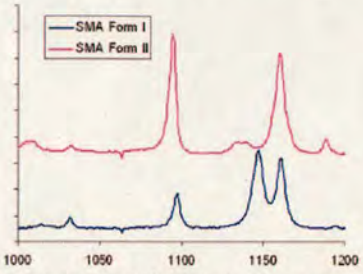

Figure 4. Analytical bands found in the Raman spectrum corresponding to polymorphs of sulfamethoxazole. Two polymorphs were found on the polymer array.

shifts. After a solution of ROY (in NMP/acetone) was printed onto the polymer array (see Supporting Information.) Polymorphic forms could be readily detected by bright field microscopy because the different forms of ROY have different colors. From the six known polymorphic forms, four of them were found within the array (yellow needles (YN), yellow prisms (YP), red prisms (RP), and orange needles (ON), Figure 5. For instance, acrylic acid−ethene copolymer and cellulose hydroxypropyl ether supported four polymorphic forms. Other polymers supported three types of crystals, such as poly(ethyl methacrylate) (yellow prisms, red prisms, and orange needles). Selectivity, in the case of the polymer polyacrylamide carboxyl, was better with just two forms (yellow prisms and orange needles). More selective polymers were also discovered. Thus, poly(isobutyl methacrylate) supported almost exclusively orange needle generation, but in small regions, perfectly shaped yellow prisms were detected, confirming that the polymer impact was rather subtle (see Figure 5d). One of the most selective polymers was poly(2,6-dimethyl-*p*-phenylene oxide), which supported the growth of only orange needles. These results were confirmed by Raman spectroscopy demonstrating the reliability of the method.

Attempts were made to characterize each of the samples using powder X-ray diffraction (PXRD), but because of the scale of the method, the PXRD response was inadequate (Figure 6).

In conclusion, a high-throughput method for studying polymorphism in small molecules has been presented. The approach uses arrays of polymers to generate or trigger different polymorphic forms. The crystal habit forms of the small molecule solids were demonstrated to be a poor indicator of polymorphic form, and Raman was a very successful technique that was used to characterize different polymorphic forms. PXRD was not suitable because of the small scale of the HT method. While the hydrophilic glass surface (control) yielded just amorphic forms in all three of the compounds studied, many of the polymers were selective in terms of triggering specific polymorphic forms and a few were very selective and specific, demonstrating the role of polymers in the crystallization process. The method is clearly an attractive alternative to screening processes previously reported.[36] This method allowed three different small molecule compounds to be screened (in triplicate) with 128 polymers and required

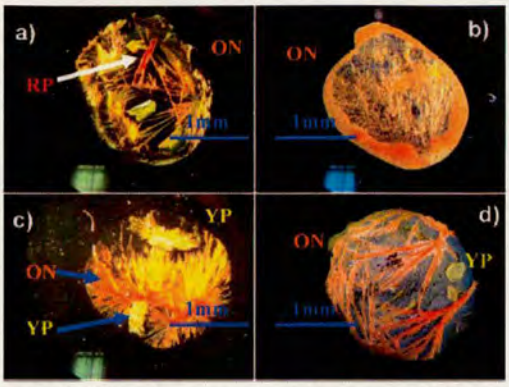

Figure 5. ROY crystals generated on different polymer SP (a) three polymorphic forms, red prisms, yellow prisms, and orange needles, on hydroxypropyl cellulose, (b) a single polymorph, orange needles, on poly(2,6-dimethyl-p-phenylene oxide), (c) two polymorphic forms, orange needles and yellow prisms, on polyacrylamide, carboxyl-modified, low carboxyl content, and (d) two polymorphic forms, orange needles and yellow prisms, on poly(isobutyl methacrylate).

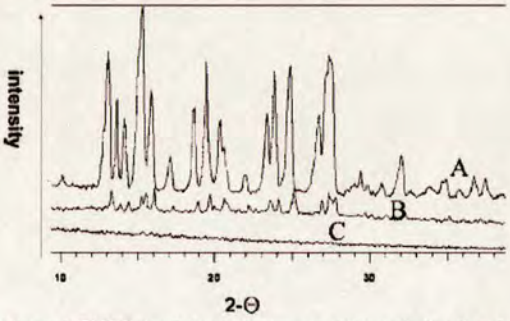

Figure 6. PXRD signals for carbamazepine (data collection time 3 min): (A) 12 mm spot diameter, (B) 6 mm spot diameter, and (C) 2 mm spot diameter.

just milligram quantities of compound and 27 μg of each polymer per array, while generating large numbers of polymorphic forms. Polymers triggered different polymorphic forms of small molecules in a very subtle manner, and although the materials on which crystals grow are important, as demonstrated here, there are many other influences such as solvent and control of evaporation.

Acknowledgment. We would like to thank the EPSRC and Ilika Technologies.

Supporting Information Available. Details of polymer microarray preparation, polymer synthesis, Raman data, crystal habit forms obtained, ROY preparation, PXRD sample analysis, and crystal thermal analysis. This information is available free of charge via the Internet at http://pubs.acs.org.

References and Notes

(1) Morissette, S. L.; Soukasene, S.; Levinson, D.; Cima, M. J.; Almarsson, Ö. *Proc. Natl. Acad. Sci.* **2006**, *100*, 2180–2184.

(2) Yu, L. X.; Furness, M. S.; Raw, A.; Woodland Outlaw, K. P.; Nashed, N. E.; Ramos, E.; Miller, S. P. F.; Adams, R. C.; Fang, F.; Patel, R. M.; Holcombe, F. O., Jr.; Chiu, Y.; Hussain, A. S *Pharm. Res.* **2003**, *20*, 531–536.
(3) Yu, L. X.; Ellison, C. D.; Hussain, A. S. Predicting human oral bioavailability using in silico models. In *Applications of Pharmacokinetic Principles in Drug Development*; Krishna, R. Ed.; Springer: New York, 2003; pp 53–75
(4) Price, C. P.; Grzesiak, A. L.; Matzger, A. J. *J. Am. Chem. Soc.* **2005**, *127*, 5512–5517.
(5) Day, G. M.; Trask, A. V.; Motherwell, W. D. S.; Jones, W. *Chem. Commun.* **2006**, *1*, 54–56.
(6) Vishweshwar, P.; McMahon, J. A.; Paterson, M. L.; Zawratko, M. J. *J. Am. Chem. Soc.* **2005**, *127*, 16802–16803.
(7) McCrone's often quoted pronouncement is "The number of forms known for a given compound is proportional to the time and money spent in research on that compound." See: McCrone, W. C. Polymorphism. In *Physics and Chemistry of the Organic Solid State*; Fox, D., Ed.; John Wiley & Sons, Inc.: New York, 1965; pp. 726–767.
(8) Dunitz, J. D.; Bernstein, J. *Acc. Chem. Res.* **1995**, *28*, 193–200.
(9) Peterson, M. L.; Morissette, S. L.; McNulty, C.; Goldsweig, A.; Shaw, P.; LeQuesne, M.; Monagle, J.; Encina, N.; Marchionna, J.; Johnson, A.; Gonzalez-Zugasti, J.; Lemmo, A. V.; Ellis, S. J.; Cima, M. J.; Almarsson, Ö. *J. Am. Chem. Soc.* **2002**, *124*, 10958–10959.
(10) Aizenberg, J.; Black, A. J.; Whitesides, G. M. *J. Am. Chem. Soc.* **1999**, *121*, 4500–4509.
(11) (a) Han, Y.; Wysocki, L. M.; Thanawala, M. S.; Siegrist, T.; Aizenberg, J. *Angew. Chem., Int. Ed.* **2005**, *44*, 2386–2390. (b) Ichikawa, K.; Shimomura, N.; Yamada, M.; Ohkubo, N. *Chem.—Eur. J.* **2003**, *9*, 3235–3241.
(12) Aizenberg, J.; Black, A. J.; Whitesides, G. M. *Nature* **1999**, *398*, 495–498.
(13) Lang, M.; Grzesiak, A. L.; Matzger, A. J. *J. Am. Chem. Soc.* **2002**, *124*, 14834–14835.
(14) Chan, K. L. A.; Kazarian, G. *J. Comb. Chem.* **2005**, 185–189.
(15) Cabeza, A. J. C.; Day, G. M.; Motherwell, W. D.; Jones, W. *Chem. Commun.* **2007**, *16*, 1600–1602.
(16) Kogermann, K.; Aaltonen, J.; Strachan, C. J.; Pöllänen, K.; Veski, P.; Heinämäki, J.; Yliruusi, J.; Rantane, J. *J. Pharm. Sci.* **2007**, *96*, 1802–1820.
(17) Wyttenbach, N.; Alsenz, J.; Grassmann, O. *Pharm. Res.* **2007**, *24*, 888–898.
(18) Tian, F.; Sandler, N.; Aaltonen, J.; Lang, C.; Saville, D. J.; Gordon, K. C.; Strachan, C. J.; Rantanen, J.; Rades, T. *J. Pharm. Sci.* **2007**, *96*, 584–594.
(19) Kipouros, K.; Kachrimanis, K.; Nikolakakis, I.; Tserki, V.; Malamataris, S. *J. Pharm. Sci.* **2006**, *95*, 2419–2431.
(20) Rama, M. J. R.; López-Sánchez, M.; Ruiz-Medina, A.; Molina-Díaz, A.; Ayora-Cañada, M. J. *Analyst* **2005**, *130*, 1617–1623.
(21) Takasuka, M.; Nakai, H. *Vib. Spectrosc.* **2001**, *25*, 197–204.
(22) Karthikeyan, G.; Mohanraj, K.; Elango, K. P.; Girishkumar, K. *Russ. J. Coord. Chem.* **2006**, *32*, 380–385.
(23) Göbel, A.; Thomsen, A.; Mcardell, C. S.; Joss, A.; Giger, W. *Environ. Sci. Technol.* **2005**, *39*, 3981–3989.
(24) Zhang, C.-L.; Wang, F.-A.; Wang, Y. *J. Chem. Eng. Data* **2007**, *52*, 1563–1566.
(25) McKinnon, J. J.; Fabbiani, F. P. A.; Spackman, M. A. *Cryst. Growth Des.* **2007**, *7*, 755–769.
(26) Li, H.; Stowell, J. G.; Borchardt, T. B.; Byrn, S. R. *Cryst. Growth Des.* **2006**, *6*, 2469–2474.
(27) Smith, J. R.; Xu, W.; Raftery, D. *J. Phys. Chem. B* **2006**, *110*, 7766–7776.
(28) Chen, S.; Xi, H.; Yu, L. *J. Am. Chem. Soc.* **2005**, *127*, 17439–17444.
(29) Dunitz, J. D.; Gavezzotti, A. *Cryst. Growth Des.* **2005**, *5*, 2180–2189.
(30) Chen, S.; Guzei, I. A.; Yu, L. J. *Am. Chem. Soc.* **2005**, *127*, 9881–9885.
(31) Grzesiak, A. L.; Lang, M.; Kim, K.; Matzger, A. J. *J. Pharm. Sci.* **2003**, *92*, 2260–2271.
(32) Tian, F.; Zeitler, J. A.; Strachan, C. J.; Saville, D. J.; Gordon, K. C.; Rades, T. *J. Pharm. Biomed. Anal.* **2006**, *40*, 271–280.
(33) Lang, M.; Kampf, J. W.; Matzger, A. J. *J. Pharm. Sci.* **2002**, *91*, 1186–1190.
(34) O'Brien, L. E.; Timmins, P.; Williams, A. C.; York, P. *J. Pharm. Biomed. Anal.* **2004**, *36*, 335–340.
(35) Momany, F. A.; Sessa, D. J.; Lawton, J. W.; Selling, G. W.; Hamaker, S. A. H.; Willett, J. L. *J. Agric. Food Chem.* **2006**, *54*, 543–547.
(36) Morissette, S. L.; Almarsson, Ö.; Peterson, M. L.; Remenar, J. F.; Read, M. J.; Lemmo, A. V.; Ellis, S.; Cima, M. J.; Gardner, C. R. *Adv. Drug Delivery Rev.* **2004**, *56*, 275–300.

CC700107X

Inkjet fabrication of hydrogel microarrays using *in situ* nanolitre-scale polymerisation†

Rong Zhang, Albert Liberski, Ferdous Khan, Juan Jose Diaz-Mochon and Mark Bradley*

Received (in Cambridge, UK) 20th November 2007, Accepted 19th December 2007
First published as an Advance Article on the web 11th January 2008
DOI: 10.1039/b717932d

Polymer hydrogel microarrays were fabricated by inkjet printing of monomers and initiator, allowing up to 1800 individual polymer features to be printed on a single glass slide.

Hydrogels, due to their intrinsic hydration properties have huge potential, with applications in the area of tissue engineering,[1–3] and cellular attachment/release.[4,5] These flexible gels have also been applied as thermally responsive micropumps/valves,[6] as components in sensors,[7,8] as surface actuators[9] and for drug release.[10]

A multitude of techniques such as photolithography,[11] soft lithography,[12–14] electron-beam lithography,[15] nanolithography[16] and reactive ion etching[17] have been used to generate hydrogel patterns using for example crosslinked poly(2-hydroxyethyl methacrylate) (pHEMA), poly(polyethylene glycol)-methacrylate and polyacrylamides, as well as non-synthetic polymers such as collagen, with feature resolutions ranging from nm's to μm's.

A key aspect in all these processes is the generation of the hydrogel with photo-initiated polymerisation being perhaps the most widely applied approach. This is typically achieved by the irradiation of mixtures of monomers or oligomers with initiators, often through a photomask or *via* the polymerisation of pre-stamped materials,[2,3,5,6,11,13] although other polymerisation methods such as ATRP,[18] plasma polymerization[4] and redox initiated polymerization[8,14] have all been reported.

These methods are generally used to fabricate patterns *en masse* using single, well defined materials. Patterning tens, hundreds or thousands of different materials on a single glass slide remains a huge challenge. Langer and co-workers[19] approached this problem by printing pre-mixed formulations of different monomers on glass slides (coated with pHEMA), using a DNA contact printer, which were then polymerised by UV irradiation, the rapid evaporation of small droplets (printed on the slides) necessitating the use of non-volatile monomers. Our group used an alternative approach *via* the contact printing of pre-formed polymers onto cytophobic (agarose coated) slides to generate well defined polymer microarrays.[20]

Recently an inkjet printing approach was used by our group to prepare, in a high-throughput and highly miniaturised manner, 231 formulations of three independent liquid crystals.[21] Here we report the use of an inkjet based approach for the rapid preparation of patterned hydrogel microarrays on glass slides, through the use of *in situ* pico-nano litre-scale polymerisation (see Scheme 1).‡

The approach used an inkjet printer to rapidly print (independently) both an initiator (ammonium persufate (APS)) and monomers that contained the reductant *N,N,N′,N′*-tetramethylethylenediamine (TEMED) onto glass slides at highly defined positions, with specific numbers of drops printed in any defined position on the array. This APS/TEMED redox system is well established and is able to initiate polymerisation and gelation of many water-soluble acrylamides and acrylates under a range of conditions.[22]

To prepare arrays of polymers the glass slide was initially treated with 3-(trimethoxysilyl)methacrylate in order to provide an anchor for the hydrogel during polymerisation (see ESI† for details). Arrays were prepared in two ways. Firstly, 37 pre-generated mixtures of monomers (Fig. 1) were printed and polymerised (20 copies of each feature were printed) giving 740 features in total (see ESI,† Fig. S1). Polymerisation gave excellent spot morphologies due to the non-contact nature of the deposition (see Fig. 2).

In this array dimethylacrylamide was the major monomer copolymerised with a range of other monomers bearing amino groups with various crosslinkers with different chain length, potentially allowing the amino group to be used as handles for further chemistry.[23] These hydrogel arrays were analysed dry

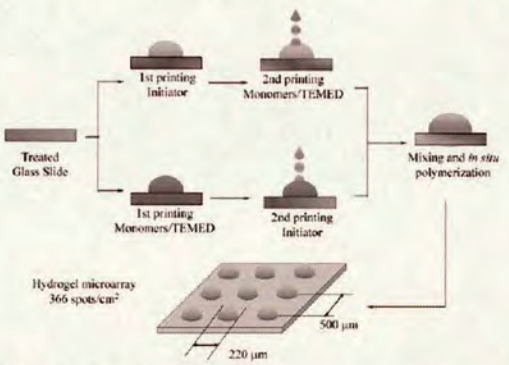

Scheme 1 The two approaches used for inkjetting hydrogel microarray *in situ* pico–nano litre polymerisation.

EaStCHEM, School of Chemistry, King's Building, University of Edinburgh, Edinburgh, UK EH9 3JJ. E-mail: mark.bradley@ed.ac.uk; Fax: 0131 650 6453; Tel: 0131 650 4820
† Electronic supplementary information (ESI) available: Experimental section. See DOI: 10.1039/b717932d

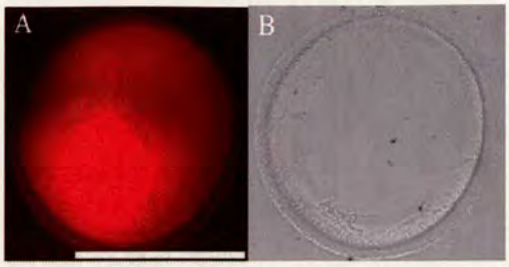

Fig. 5 An image of a hydrogel feature prepared by co-printing 25 drops of a 1% w/w APS aqueous solution with 12 drops of a mixture of DMA, AAm and $PEG_{12}DA$ (ratio 6.1 : 1.7 : 1, 19.5% w/w). (A) Fluorescent microscopic image taken using a Nikon Eclipse 50i microscope with a rhodamine filter and (B) a white-light phase contrast image of the same spot after washing.

Table 1 Molecular weight analysis of linear polymers prepared by nanolitre synthesis on a glass slide compared to those prepared under analogous solution conditions in vials. PDI is the polydispersity index of the polymers

	APS (% w/w)	0.50	0.99	2.90	4.76
Inkjet based spot synthesis	M_n ($\times 10^4$)	7.71	5.72	6.16	9.33
	M_w ($\times 10^4$)	52.29	43.51	37.72	82.37
	PDI	6.78	7.61	6.13	8.83
Traditional synthesis	M_n ($\times 10^4$)	10.25	8.11	9.36	10.21
	M_w ($\times 10^4$)	33.42	35.87	80.39	98.35
	PDI	3.30	4.45	8.59	9.76

spot morphology and size control. This approach allows access to a broad ranges of new polymers in a highly miniaturised manner and will be applicable to many research areas, such as cellular immobilisation, identification of cell specific hydrogels, or protein trapping, while allowing the properties of many polymers to be investigated without having to resort to large-scale synthesis.[24]

We thank the EPSRC and BBSRC for financial support.

Notes and references

‡ The inkjet printer used in this experiment was an autodrop system (Microdrop, GmbH, Norderstedt, Germany) with a AK-501 micropipette operating in drop-on-demand mode *via* a piezoelectric firing mechanism.[21] This printer created droplets with a volume of approximately 380 pL at frequencies between 0 and 2 kHz using a stroboscopic camera to monitor droplet formation, allowing accurate control of the volume of the printed solutions by simply varying the number of drops printed in any specific or defined location. This was controlled by use of an in-house macro.

1 M. C. Cushing and K. S. Anseth, *Science*, 2007, **316**, 1133–1134.
2 D. R. Albrecht, G. H. Underhill, T. B. Wassermann, R. L. Sah and S. N. Bhatia, *Nat. Methods*, 2006, **3**, 369–375.
3 V. A. Liu and S. N. Bhatia, *Biomed. Microdevices*, 2002, **4**, 257–266.
4 S. Bouaidat, C. Berendsen, P. Thomsen, S. G. Peterson, A. Wolff and J. Jonsmann, *Lab Chip*, 2004, **4**, 632–637.
5 H. Liu and Y. Ito, *Lab Chip*, 2002, **2**, 175–178.
6 D. Kuckling, J. Hoffmann, M. Plotner, D. Ferse, K. Kretschmer, H.-J. P. Adler, K.-F. Arndt and R. Reichelt, *Polymer*, 2003, **44**, 4455–4462.
7 Y. Kang, J. J. Walish, T. Gorishnyy and E. L. Thomas, *Nat. Mater.*, 2007, **6**, 957–960.
8 Z. Hu, Y. Chen, C. Wang, Y. Zheng and Y. Li, *Nature*, 1998, **393**, 149–152.
9 A. Sidorenko, T. Krupenkin, A. Taylor, P. Fratzl and J. Aizenberg, *Science*, 2007, **315**, 487–490.
10 R. Yoshida, K. Omata, K. Yamaura, M. Ebata, M. Tanaka and M. Takai, *Lab Chip*, 2006, **6**, 1384.
11 S. J. Bryant, K. D. Hauch and B. D. Ratner, *Macromolecules*, 2006, **39**, 4395–4399.
12 M. D. Tang, A. P. Golden and J. Tien, *Adv. Mater.*, 2004, **16**, 1345–1348.
13 T. Yu, Q. Wang, D. S. Johnson, M. D. Wang and C. K. Ober, *Adv. Funct. Mater.*, 2005, **15**, 1303–1309.
14 F. Chiellini, R. Bizzarri, C. K. Ober, D. Schmaljohann, T. Yu, R. Solaro and E. Chiellini, *Macromol. Rapid Commun.*, 2001, **22**, 1284–1287.
15 T. Schmidt, J. I. Monch and K.-F. Arndt, *Macromol. Mater. Eng.*, 2006, **291**, 755–761.
16 (*a*) D. Wouters and U. S. Schubert, *Angew. Chem., Int. Ed.*, 2004, **43**, 2480–2495; (*b*) P. Xu, H. Uyama, J. E. Whitten, S. Kobayashi and D. L. Kaplan, *J. Am. Chem. Soc.*, 2005, **127**, 11745–11753.
17 P. Bhatnagar, A. D. Strickland, I. Kim, G. G. Malliaras and C. A. Batt, *Appl. Phys. Lett.*, 2007, **90**, 144107.
18 H. Ma, D. Li, X. Sheng, B. Zhao and A. Chilkoti, *Langmuir*, 2006, **22**, 3751–3756.
19 D. G. Anderson, S. Levenburg and R. Langer, *Nat. Biotechnol.*, 2004, **22**(7), 863–866.
20 (*a*) A. Mant, G. Tourniaire, L. J. Diaz-Mochon, T. J. Elliott, A. P. William and M. Bradley, *Biomaterials*, 2006, **27**, 5299–5306; (*b*) G. Tourniaire, J. Collins, S. Campbell, H. Mizomoto, S. Ogawa, J. F. Thaburet and M. Bradley, *Chem. Commun.*, 2006, **20**, 2118–2120; (*c*) S. Pernagallo, A. Unciti-Broceta, J. J. Diaz-Mochón and M. Bradley, *Biomed. Mater.*, 2008, in press; (*d*) A. Unciti-Broceta, J. J. Diaz-Mochón, H. Mizomoto and M. Bradley, *J. Comb. Chem.*, DOI: 10.1021/cc7001556; (*e*) A. R. Liberski, C. J. Tizzard, J. J. Diaz-Mochon, M. B. Hursthouse, P. Milnes and M. Bradley, *J. Comb. Chem.*, DOI: 10.1021/cc700107x.
21 T. R. Cull, M. J. Goulding and M. Bradley, *Adv. Mater.*, 2007, **19**, 2355–2359.
22 (*a*) J. Bo and Y. Zhang, *Eur. Polym. J.*, 1993, **29**, 1251–1254; (*b*) V. I. Lozinsky, R. V. Ivanov, E. V. Kalinina, G. I. Timofeeva and A. R. Khokhlov, *Macromol. Rapid Commun.*, 2001, **22**, 1441–1446.
23 M. Zourob, J. E. Gough and R. V. Ulijn, *Adv. Mater.*, 2006, **18**, 655–659.
24 T. Ono, T. Sugimoto, S. Shinkai and K. Sada, *Nat. Mater.*, 2007, **6**, 429–433.

CREATED USING THE RSC COMMUNICATION TEMPLATE (VER. 3.1) - SEE WWW.RSC.ORG/ELECTRONICFILES FOR DETAILS

ARTICLE TYPE www.rsc.org/xxxxxx | XXXXXXXX

Inkjet Fabrication of Polymer Microarrays and Grids - Solving the Evaporation Problem

Albert Liberski,[a,b] Rong Zhang[a] and Mark Bradley[a,b]*

Received (in XXX, XXX) Xth XXXXXXXXX 200X, Accepted Xth XXXXXXXXX 200X
First published on the web Xth XXXXXXXXX 200X
DOI: 10.1039/b000000x

Polymer microarrays, consisting of either discrete features or a matrix of inter-crossed lines were directly fabricated *in situ* by inkjet printing individual monomers or initiator solutions in organic solvents through a film of oil, thereby allowing the rapid generation of a broad range of co-polymers, while solving the problem of selective monomer evaporation.

Patterning polymers on surfaces is a very attractive approach to enable the modification or tailoring of the properties of a substrate for a specific application.[1] Examples include the patterning of surfaces with alternate strips of fibronectin and poly(ethylene glycol) (PEG) using micro-contact printing (μCP) for investigation of cellular adhesion;[2] surfaces patterned with responsive polyacrylamide gels which can switch on and off displayed images thermally;[3] and surfaces patterned with ligand functionalised co-polymers as platforms for the reversible binding of histidine-tagged proteins.[4] The physical approaches used for surface patterning, include μCP,[5] photolithography,[6] phase segregation[7] and even direct nano-scale patterning on a surface using an AFM cantilever as an 'ink' delivering system[8] although these approaches have typically involved the printing of single, well defined, polymers. Flexibly patterning tens or hundreds of different polymers on a substrate for polymer-screening is however a much more complex undertaking and a number of micro-scale direct printing approaches have been developed. Langer[9] for example achieved this by contact printing pre-mixed solutions of non-volatile monomers on poly(hydroxyethyl methacrylate) (pHEMA) coated glass slides with polymerisation via UV irradiation, while the Bradley group has developed two approaches. Firstly, contact printing pre-formed polymer solutions; from a polymer library; onto agarose coated glass slides to generate so-called polymer microarrays[10] and secondly, *in situ* fabrication, through pico-nano litre-scale mixing, of inkjet printed water soluble monomers and initiators that were deposited onto a slide under conditions of high humidity (to prevent monomers evaporation). This approach allowing over 1800 polymer features to be generated on a single microscope glass slide, but was restricted to hydrogels and water compatible polymerisations.[11]

Herein we report an inkjet printing approach that broadens considerable the monomers that can be used and allows a much broader ranges of polymers to be generated, as well as using inkjet printing to generate a new type of microarray, composed of a matrix of inter-crossed polymers. The approach developed used an inkjet printer to print (independently) both a photo-initiator (2,2-dimethoxy-2-phenylacetophenone) (PI) and monomers (or a mixture of initiator and monomers) onto agarose coated glass slides,[12] which had been pre-coated with a thin layer of mineral paraffin oil (see ESI). Once printed the monomer droplets sank and settled onto the agarose layer where they were polymerised (see Scheme 1 (all the monomers were dissolved in 1-methyl-2-pyrrolidinone (NMP) at a concentration of 50%

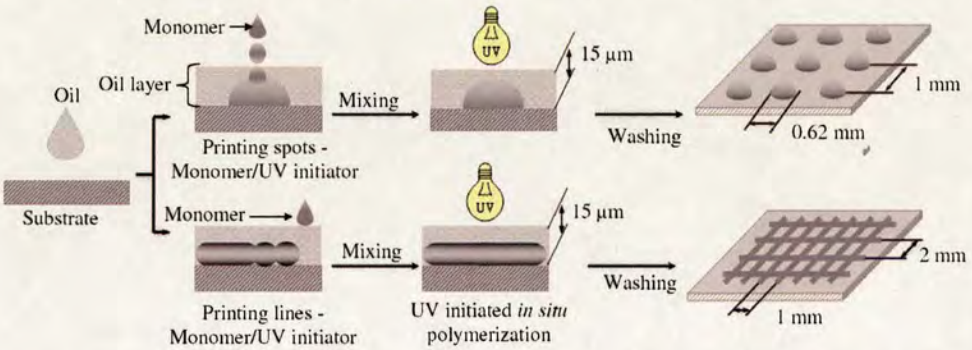

Scheme 1. The two approaches used to prepare polyacrylate microarrays. An oil film was used to prevent evaporation of the nanolitre volumes of the printed monomer solutions while maintaining the pattern on the glass surface. Following UV photo-polymerisation and removal of the oil film the polyacrylate library was left attached on the slide.

(w/v) (Table 1-SI)). The polymer microarrays here were fabricated by printing 50 drops (per feature) of each monomer solution including the photo-initiator (5% w/w) with a 1 mm pitch between spots and exposure to irradiation for 30 min (UV lamp, Black-Ray, Model B 100AP) before removal of the oil layer, but any numbers of drops of any desired monomer can be printed. Using this approach a polymer microarray of 1100 polymers was fabricated *in situ* on a single microscope glass slide with feature sizes of ~0.62 mm and a density of 100 spots/cm^2 (Fig. 1), (see Fig. 2-SI for details of the co-polymers on each spot).

The thickness of the oil layer and its density was crucial for accurate fabrication of the polymer microarray. The path a monomer droplet travels through the oil should be as short as possible so that the drops could be spotted at defined positions during the printing processes, while the oil layer has to be thick enough to cover the whole slide uniformly to prevent evaporation from the printed spots before polymerisation. A 15 µm layer of oil (density 0.89 g/ml) was optimal and using water drops (instead of monomers) it was found that there was no evaporation from the printed droplets even after 4 hours (see Fig. 1-SI). The transparent oil film also allowed *in situ* polymerisation upon UV irradiation for extended periods of time (up to 1-2 hours) while ensuring excellent spot morphology. The use of agarose coated slides as a substrate, provided excellent polymer adherence during polymerization and prevented non-specific cell binding during cellular screening applications and the oil layer could be removed subsequently by washing with ethanol.

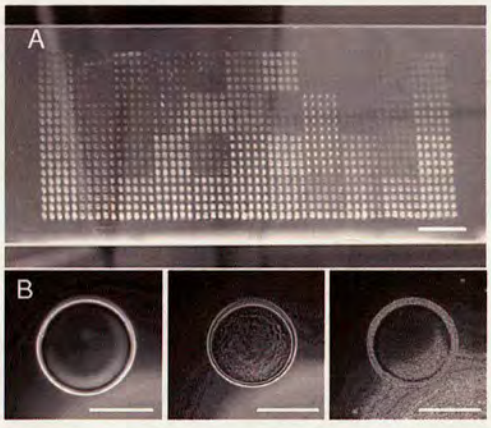

Figure 1. (A) Polymer microarray consisting of 1100 polymer features with 25 (5×5) identical spots for each polymer fabricated by *in situ* polymerisation followed by removal of the oil film (scale bar 5 mm); (B) Bright field images of three typical polymer spots: Top: poly(2-(methylthio)ethyl methacrylate), middle: poly(divinylbenzene), bottom: poly(2-methoxyethyl methacrylate) (scale bar 0.5 mm).

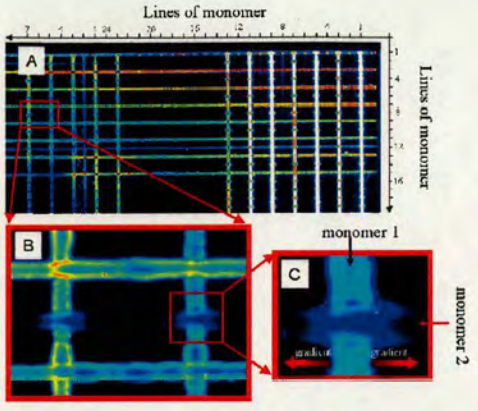

Fig. 2. Fluorescence image of a polymer grid fabricated *in situ*. Fluorescein was mixed with some of the monomers to allowing imaging of the grid. The distance between lines was 1 mm in the y direction and 2 mm in x direction, while the lines are approximately 300 µm wide. The numbers next to axes are monomer numbers in Table 1-SI.

Most of the polymers prepared via this microarray approach had identical molecular weights to those prepared using more conventional conditions [50% w/v monomer solutions with 5% (w/w) initiator were mixed and polymerised in a glass vial with UV initiation for 30 min (see SI)] as analysed by GPC (see Table 2-SI), except 2-vinylpyridine which had a much higher molecular weight (82KDa) when prepared using the inkjet printing approach (17KDa); while 2-hydroxylethyl methacrylate gave the opposite result (11kDa on the array versus 48 KDa conventionally).

The same approach was used to prepare polymer grids. Thus the 24 monomer solutions in NMP (Table 1-SI) were printed in a grid format on an oil covered slide, so that copolymers were obtained at the cross points of the lines of otherwise homo-polymers (Fig. 2). In this case lines were generated by printing drops onto a slide with movement of the piezo-pipette along a linear path at a constant velocity (10 mm/s) and a constant printing frequency (100Hz).

To illustrate the presence of gradients at the cross points some of monomers were mixed with fluorescein so that the concentration changes along the lines were clearly visible via microscopy (Fig. 2). The extent of this mixing can be controlled by the variation in the allowed mixing and photopolymerisation times.

Both polymer microarray and polymer grids were used to identify polymers suitable for mouse embryonic stem cell (mESC) binding and growth (See SI for details).

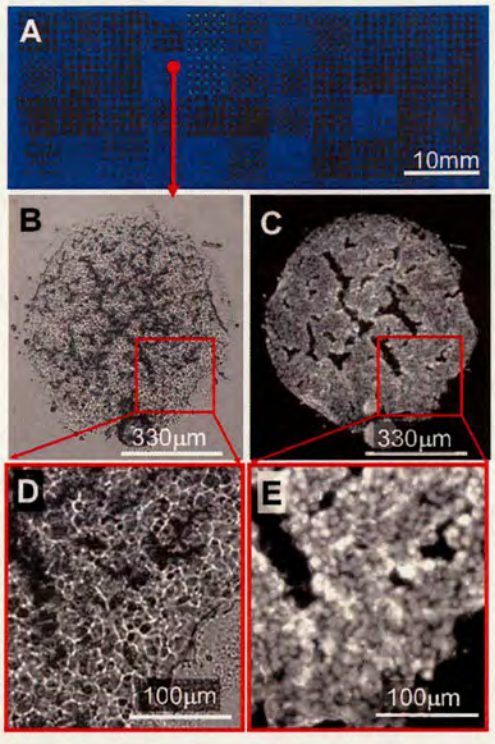

Fig. 3 mES cells grown for 48 h on an *in situ* fabricated polymer microarry. Cells were fixed (4% w/w formaldehyde) and treated with Hoescht 33245 (nuclei stain)). (A) Fluorescence image of the whole slide taken with a BioAnalyzer 4F/4S (LaVision BioTech) using DAPI filter. Images of mES cells on poly 2-(methylthio)ethyl; (B) and (D) Bright field; (C) and (E) are fluorescence images were obtained using a Nikon microscope using a 10x/0.30 objective and a DAPI filter.

After incubation on the array cells were fixed and stained (Fig. 3) and poly(ethyl methacrylate), poly (2-(methylthio)ethyl methacrylate) (pMTEMA), benzyl methacrylate /divinylbenzene co-polymer (1:1 weight ratio), polydivinylbenzene (pDVB), poly(benzyl methacrylate) were identified as polymers that allowed mES cells attachment and proliferation.

Importantly, in terms of reproducibility and compatability of the two platfoms the mES cells grew on identical polymers (see Fig. 3-SI) on both the "grid" and "spot" based microarrays.

In conclusion, the fabrication of arrays of polymers generated either as spot-based microarrays or as grids, via inkjet printing through oil, has been demonstrated allowing the generation of large arrays of co-polymers in a highly miniaturized, automated and highly reproducible manner, giving polymers with excellent spot morphology (on the micro-array platform). These arrays of polymers could be used to identify polymers for selective mES cells binding.

We thank the EPSRC and Ilika Technologies Ltd for financial support.

Notes and references

[a] EaStCHEM, School of Chemistry, King's Building, University of Edinburgh, Edinburgh, EH9 3JJ, UK. Fax: 0131 650 6453; Tel: 0131 650 4820; E-mail: mark.bradley@ed.ac.uk
[b] Ilika Technologies Ltd, Kenneth Dibben House, Enterprise Road, University of Southampton Science Park, Chilworth, Southampton, SO16 7NS, UK.

† Electronic Supplementary Information (ESI) available: Experimental, Table 1-SI, Figure 1-SI, Figure 2-SI, Figure 3-SI. See DOI: 10.1039/b000000x/

‡The inkjet printer used in this experiment was an Autodrop system (Microdrop, GmbH, Norderstedt, Germany) with a AK-501 micropipette (70 μm in diameter) operating in drop-on-demand mode via a piezoelectric firing mechanism. This printer created droplets with a volume of approximately 380 pL at frequencies between 0 and 2 kHz using a stroboscopic camera to monitor droplet formation, allowing accurate control of the volume of the printed solutions by simply varying the number of drops dispensed on desire position.

1 Z. Nie and E. Kumacheva, *Nat. Mater.*, 2008, **7**, 277-290.
2 C. L. Feng, A. Embrechts, I. Bredebusch, J. Schnekenburger, W. Domschke, G. J. Vancso and H. Schonherr, *Adv. Mater.*, 2007, **19**, 286-290.
3 Z. Hu, Y. Chen, C. Wang, Y. Zheng and Y. Li, *Nature*, 1998, **393**, 149-152.
4 G. Zhen, D. Falconnet, E. Kuennemann, J. Voros, N. D. Spencer, M. Textor and S. Zurcher, *Adv. Func. Mater.*, 2006, **16**, 243-251.
5 D. I. Rozkiewicz, Y. Kraan, M. W. T. Werten, F. A. de Wolf, V. Subramaniam, B. J. Ravoo and D. N. Reinhoudt, *Chem. Eur. J.*, 2006, **12**, 6290-6297; M. Thery, V. Racine, A. Pepin, M. Piel, Y. Chen, J.-B. Sibarita and M. Bornens, *Nat. Cell Biol.*, 2005, **7**, 947-U29.
6 S. J. Bryant, K. D. Hauch and B. D. Ratner, *Macromolecules*, 2006, **39**, 4395-4399.
7 S. H. Kim, M. J. Misner, T. Xu, M. Kimura and T. P. Russell, *Adv. Mater.*, 2004, **16**, 226-231.
8 D. Wouters and U. S. Schubert, *Angew. Chem., Int. Ed.*, 2004, **43**, 2480–2495; P. Xu, H. Uyama, J. E. Whitten, S. Kobayashi and D. L. Kaplan, *J. Am. Chem. Soc.*, 2005, **127**, 11745–11753
9 D. G. Anderson, S. Levenburg and R. Langer, *Nat. Biotech.*, 2004, 22(7), 863-866.
10 A. Mant, G. Tourniaire, L. J. Diaz-Mochon, T. J. Elliott, A. P. William and M. Bradley, *Biomaterials*, 2006, **27**, 5299–5306; A. R. Liberski, G. J. Tizzard, J. J. Diaz-Mochon, M. B. Hursthouse, P. Milnes, and M. Bradley, *J. Comb. Chem.*, 2008, **10**, 24-27; A. Unciti-Broceta, J. J. Díaz-Mochón, H. Mizomoto and M. Bradley, *J. Comb. Chem.*, 2008, **10**, 179-184; S. Pernagallo, J. J. Díaz-Mochón and M. Bradley, *Lab Chip*, 2008, in press; H. Mizomoto, Ph.D. thesis, University of Edinburgh, 2004.
11 R. Zhang, A., Liberski, F., Khan, J. J. Diaz-Mochon and M. Bradley, *Chem. Commun.*, 2008, **11**, 1317–1319.
12 G. Tourniaire, J. Collins, S. Campbell, H. Mizomoto, S. Ogawa, J. F. Thaburet and M Bradley, *Chem. Comm.*, 2006, **20**, 2118-2120.

Journal of the Association for Laboratory Automation (JALA) accepted

In situ Nanolitre-Scale Polymer Fabrication for Exotic Cell Patterning

By *Albert Liberski, Rong Zhang and Mark Bradley**

[*] Prof. M. Bradley

EaStCHEM, School of Chemistry,

King's Building, University of Edinburgh,

Edinburgh, UK EH9 3JJ.

E-mail: mark.bradley@ed.ac.uk;

Fax: 0131 650 6453

Tel: 0131 650 4820

Mr. A. Liberski and Dr. R. Zhang

EaStCHEM, School of Chemistry,

King's Building, University of Edinburgh,

Edinburgh, UK EH9 3JJ.

KEYWORDS

Cell patterning, software for inkjet printing, mES cells, biomaterials, nL scale - *in situ* polymerization, synthetic cell binders.

ABSTRACT

A new way of controlling scientific inkjet printer is presented to allow for a new highly flexible approach towards cellular patterning. The inkjet printing was used to perform *in situ* polymerization directly on agarose coated slide, allowing synthetic materials to replace collagen during cells patterning. Using a scientific inkjet printer to form a clock shape allowing cells (HeLa and mouse embryonic stem cells) to be incubated and attached to the defined pattern in a highly specific manner. Advantages of this type of scientific printer are that they can be controlled to print any desired pattern using virtually whatever material is desired and addressed to any specific position on a slide.

INTRODUCTION

Cell patterning on a 2D surface or within a 3D scaffold has been broadly applied (Shin, 2007) for example in the manipulation of cells *in vitro* in attempt to understand cellular responses to the environment (El-Ali et al., 2006) or to pave the way towards tissue engineering applications, and has attracted much attention (Vacanti et al., 1999). This includes, for example, engineered rat kidney tissue for implantation (Rosines et al., 2007), skin repair and regeneration (Metcalfe et al., 2007), human neural stem cells implanted into monkey's brain with Pakinson's symptoms for replacement of the damaged neurons (Redmond Jr. et al., 2007) and bone marrow stem cells for liver regeneration (Fürst et al., 2007).

General research on cell patterning is focused on understanding cell-biomaterial interactions in attempt to understand and influence cell behaviour upon binding to a substrate (Chen et al., 1997; Monchaux et al., 2007; Tan et al., 2003; Flemming et al., 1999; Petty et al., 2007). For

example dendric cell behaviour (Mant et.al, 2006; Tourniaire et al., 2006; Pernagallo et al., 2008; Unciti-Broceta et al., 2008) and epithelial cellular migration have been shown to be controlled by substrate rigidity (Saez et al., 2007), polymers have been used to or modulate stem-cell differentiation (Gerecht et al., 2007; Tourniaire et al., 2006). Also research on cell-cell signalling by controlling the size of microwells and distance between them to help understand the role of the substrate in mES cells colony formation under controlled microenvironment conditions was studied (Rosenthal et al., 2007).

Current techniques for cell patterning follow two main strategies: first is using a modified office-based inkjet printer to pattern living cells directly onto a substrate (with or without gelation materials) to form 2D or 3D patterned cells (Calvert, 2007; Chen et al., 2006) and the second is based on patterning biomaterials followed by cell adhesion exclusively onto the designed domains (Falconnet et al., 2006).

The second strategy has attracted much attention and includes a number of techniques. One example of this approach is the use of soft lithography, with soft elastomeric stamps (with designed patterns in PMDS) used to transfer cellular binding materials onto a substrate in a highly defined pattern (Co et al, 2005; Jiang et al., 2003; Kane et al., 1999). Another example is photolithography (UV initiated polymerisation through highly defined masks) (Liu et al., 2002). More exotic approaches include techniques such as dip-pen nanolithography (Lee et al. 2002; Wilson et al., 2001) which rely on an AFM tip to deliver cell binding materials to highly defined, specific positions on a surface. This naturally provides a tremendous resolution but also has a number of limitations with respect to applicability, scale-up and general accessibility. Modified office-based inkjet printers have also been used to print biomaterials on substrates (Campbell et al., 2005; Roth et al, 2004; Ilkhanizadeh et al., 2007; Sanjana et al, 2004).

In this research a solution to problems involved in the development of practical, flexible and scaleable cellular patterning techniques is proposed. Besides printing complex images using

collagen solution on slides, a novel approach has been presented here for the first time showing that monomers can be directly printed on a slide and polymerised *in situ* for cellular patterning.

MATERIALS AND METHODS

Materials

All materials were purchased from Sigma-Aldrich unless otherwise state. Mouse embryonic stem cell (mES-Oct4) was kindly provided by Josh Brickman from the Institute for Stem Cell Research (ISCR), University of Edinburgh.

Preparation of the coated glass slides

1.0% w/v of agarose (Type I- B) was dissolved in deionised water at 100°C, and then aminoalkylsilane glass slides were dip-coated with agarose solution at 65°C. The coated slides were dried in open air before use. The coating on the bottom side was removed by wiping through a piece of tissue before gelation. After drying for 24h at room temperature, the coated slides were ready for printing. The thickness of dried agarose coating was 2.34 μm (measured by SEM). Thicker agarose coatings, 9.34 μm and 26 μm thickness respectively, were obtained by spreading 1 mL and 2.5 mL of 1% agarose solutions onto the glass slides.

Polymer patterning by *in situ* polymerization

Clock shape patterns were fabricated by printing monomers: divinyl benzene solution (DVB) or 2-(methylthio)ethyl methacrylate) (MTEMA) solution (all 50% w/w in DMSO) mixed with the initiator AIBN (0.1 w/v in monomer solution) onto agarose coated slides covered with a thin layer of paraffin oil (15 μm thick). The drops of monomer solutions sank and settled down on the agarose layer due to higher densities of monomer solutions than oil. The oil layer successfully prevented the evaporation of monomers from the printed slides during the 15h incubation in an oven at 60 C° for polymerization *in situ*. The oil layer was easily removed by washing with water and ethanol respectively.

Collagen Patterning

The collagen patterns were fabricated using an inkjet printer (Microdrop, GmbH, Norderstedt, Germany) equipped with a micro-pipette (AD-K-501, 70μm diameter nozzle). The typical printing parameters were: 140 V voltage, 29 μs pulse and 100 Hz frequency. 0.1% w/v of collagen in 0.1M acetic acid aqueous solution was prepared and used as ink for the printer. The collagen pattern was obtained by printing two drops per spot in a cyclic mode which generated spots of 200 μm in diameter.

Cell culture

HeLa cells were used at passage 10 while mES-Oct4 were used at passage 8. The cells were seeded in $7x10^5$ per slide and then incubated in a Gibco incubator at 37°C with 5% CO_2 with 7 mL medium per slide in a four-rectangular well plate (Nunc, Denmark). The medium for HeLa cells was RPMI 1640 complemented with heat inactivated fetal calf serum 10% v/v, penicillin (100 units/mL), streptomycin (100 mg/mL) and L-glutamine(2.0 mM). The medium for mES-Oct4 was GMEM complemented with heat inactivated fetal calf serum 10% v/v, penicillin (100 units.mL^{-1}), streptomycin (100 mg/mL), L-glutamine (2.0 mM), Sodium pyruvate (2.0 mM), 2- mercaptoethanol (0.1 mM) and LIF (0.18 units/mL). Cells attached on the slides were stained with a nuclei dye (Hoescht 33245) for 15 min and then fixed with formaldehyde solution (4% w/v) in phosphorous buffer saline (PBS) pH 7.5 for another 15 min.

RESULTS AND DISCUSSION

The scientific inkjet printer operated in a drop-on-demand mode *via* a piezoelectric firing mechanism which created droplets of a volume of approximately 380 pL at frequencies adjustable in range between 0 and 2 kHz. A stroboscopic camera was used to monitor droplet formation. This allowed for accurate control of the volume of the deposited materials by simply varying the number of drops printed in any specific location. The advantages of this

kind of printer are that they can be set to print any desired pattern using virtually any desired material and addressed to any specific position on a slide. Recently, this inkjet based approach was used to prepare 231 formulations of three independent liquid crystals in a high-throughput and highly miniaturised manner (in essence converting a conventional 3 component-phase diagram into a rectangular format (Cull et al., 2007)), also for preparing 1800 polymers on a glass slide by in situ nanolitre polymerization (Zhang et al., 2008).
In the process of printing any desired image or picture was converted from bitmap into a coordinate file by WinDig 2.5 software (Lovy, 1996) and then to a macro file using an in-house bitmap converter, which was subsequently read by Microdrop ink-jet printer, (for details see Table 1). This allowed the printer to ink different solutions and print them at the required positions with high accuracy (Scheme 1). Collagen was chosen as the patterning material for the control because it is a well known universal cellular binder and widely applied in cell culture (Roth et al., 2004).The quality of the printed patterns was controlled by the size of the printing nozzle and the viscosity of the solutions. Different concentrations of monomers and collagen solutions were tested, with the printer generating consistent drops when using monomer solution 50% w/w in DMSO and collagen solutions (0.1-1g collagen per mL). The oil layer successfully prevented the evaporation of monomers from the printed slides during the 15h incubation in an oven at 60 C^{o} for polymerization *in situ*. The oil layer was easily removed by washing with water and ethanol respectively. Both collagen and polymer patterned slides were dried and sterilized under UV for half hour before use. HeLa (Masters, 2002) and mouse embryonic stem cells (mES-Oct4) (Camara-Clayette et al., 2006) both adhered and proliferated only on the patterned areas of the slides. Cell adhesion can be seen in Figures 1-4 (the sharpness of the clock upon cellular staining and fixing). Figures 1B and C also show that the drops of the printed collagen are around 230μm in diameter, which is thus the limit of the patterning fidelity. The attached HeLa cells which spread all over the pMTEMA, pDVB (Figure 3) and collagen (Figure 1) show a healthy cellular morphology.

The clock image patterned with mEC-Oct4 cells is shown in at Figure 2A and Figure 4A. mEC-Oct4 cells after 48 hours incubation began to develop 3D cellular aggregates on both polymer and collagen pattern as shown by the live cell image (Figure 2 B,C and Figure 4 B,C).

To print a collagen gradient, the initial collagen solution was diluted 50-fold (0.002 % w/v collagen solution) and inkjet printed onto the agarose coated slide in one drop per position mode. During the first pass 100 parallel lines (5 mm long) were printed with a 130μm gap between every two adjacent lines, with each subsequent printings the number of lines were decremented by two lines. Since the distance between two drops was less than 230μm the printed collagen drops merged together to generate a gradient on the agarose coating. Upon culture the printed gradients showed a linear change of affinity for cells (Figure 5, the gradient of mES-Oct4 cells was shown in Figure 6).

The cell patterned agarose layer could be detached from the glass slide to give a free standing hydrogel film with patterned cells as shown in Figure 7. Agarose is well known (Tourniaire et al., 2006) as a cytophobic material for use in cellular patterning, and can effectively prevent the adhesion of most cell types. Free standing agarose hydrogel films with patterned cells were obtained on a coated agarose layer (Figure 7). Slides with varying thickness of dried agarose film (2.34 μm, 9.34 μm and 26 μm, measured via SEM) were evaluated. It was observed that the thinner agarose film firmly adhered onto the amino-glass slide (>2 weeks), while the 9.34 μm and 26 μm agarose films became detached after 24h. Figure 7A shows a free standing agarose film (26 μm) patterned with HeLa cells (stained and fixed), which become visible after the agarose film was dried (Figure 7B).

To summarize, a flexible method has been developed to attach and grow cells on agarose coated amino-modified glass slides patterned with collagen and *in situ* generated polymers using a scientific inkjet printer. Any 2D pattern could be generated and multi-biomaterials

could be delivered onto any position on the pattern in a step-wise progress. The free standing agarose film patterned with cells could be applied in regenerative medicine applications (Notara et al., 2007). Further experiments designed to develop 3D cellular patterns using a layer by layer mode and bio-degradable substrates are underway.

ACKNOWLEDGMENTS

We thank Ilika Technologies and the EPSRC for funding and Dr Andy Turner for generating the bitmap converter.

COMPETING INTERESTS STATEMENT

The authors declare no competing interests.

REFERENCES

Calvert, P. (2007) Printing Cells. Science. 318, 208-209.

Camara-Clayette, V., Le Pesteur, F., Vainchenker, W., Sainteny, F. (2006) Quantitative Oct4 Overproduction in Mouse Embryonic Stem Cells Results in Prolonged Mesoderm Commitment During Hematopoietic Differentiation In Vitro. Stem Cells. 24, 1937-1945.

Campbell, P.G., Miller, E.D., Fisher, G.W., Walker, L.M., Weiss, L.E. (2005) Engineered spatial patterns of FGF-2 immobilized on fibrin direct cell organization. Biomaterials. 26, 6762-6770.

Chen, C.S., Mrksich, M., Huang, S., Whitesides, G.M., Ingber, D.E. (1997) Geometric Control of Cell Life and Death. Science. 276, 1425-1428.

Chen, C.Y., Barron, J.A., Ringeisen, B.R. (2006) Cell patterning without chemical surface modification: Cell–cell interactions between printed bovine aortic endothelial cells (BAEC) on a homogeneous cell-adherent hydrogel. Appl. Surf. Sci. 252, 8641-8645.

Co, C.C., Wang, Y., Ho, C. (2005) Biocompatible Micropatterning of Two Different Cell Types. J. Am. Chem. Soc. 127, 1598-1599.

Cull, T.R., Goulding, M.J., Bradley, M. (2007) Liquid Crystal Libraries - Ink-jet Formulation and High-Throughput Analysis. Adv. Mater. 19, 2355–2359.

El-Ali, J., Sorger, P.K., Jensen, K.F. (2006) Cells on chips. Nature. 442, 403-411.

Vacanti, J.P., Langer, R. (1999) Tissue engineering: the design and fabrication of living replacement devices for surgical reconstruction and transplantation. Lancet. 354, SI32-34.

Falconnet, D., Csucs, G., Grandin, H.M., Textor, M. (2006) Surface engineering approaches to micropattern surfaces for cell-based assays. Biomaterials. 27, 3044-3063.

Flemming, R.G., Murphy, C.J., Abrams, G.A., Goodman, S.L., Nealey, P.F. (1999) Effects of synthetic micro- and nano-structured surfaces on cell behavior. Biomaterials. 20, 573-588.

Fürst, G., am Esch, J.S., Poll, L.W., Hosch, S.B., Fritz, L.B., Klein, M., Godehardt, E., Krieg, A., Wecker, B., Stoldt, V., Stockschläder, M., Eisenberger, C.F., Mödder, U., Knoefel, W.T (2007) Portal Vein Embolization and Autologous CD133+ Bone Marrow Stem Cells for Liver Regeneration: Initial Experience. Radiology. 24, 171-179.

Gerecht, S., Burdick, J.A., Ferreira, L.S., Townsend, S.A., Langer, R. (2007) Hyaluronic acid hydrogel for controlled self-renewal and differentiation of human embryonic stem cells. PNAS. 104, 11298-11303.

Ilkhanizadeh, S., Teixeira, A.I., Hermanson, O. (2007) Inkjet printing of macromolecules on hydrogels to steer neural stem cell differentiation. Biomaterials. 28, 3936-3943.

Jiang, X., Ferrigno, R., Mrksich, M., Whitesides, G.M. (2003) Electrochemical Desorption of Self-Assembled Monolayers Noninvasively Releases Patterned Cells from Geometrical Confinements. J. Am. Chem. Soc. 125, 2366-2367.

Kane, R.S., Takayama, S., Ostuni, E., Ingber, D.E., Whitesides, G.M. (1999) Patterning proteins and cells using soft lithography. Biomaterials. 20, 2363-2376.

Lee, K., Park, S., Mirkin, C., Smith, J.C., Mrksic,. M. (2002) Protein Nanoarrays Generated By Dip-Pen Nanolithography. Science. 295, 1702-1705.

Liu, V.A., Jastromb, W.E., Bhatia, S.N. (2002) Engineering protein and cell adhesivity using PEO-terminated triblock polymers. J. Biomed. Mater Res. 60, 126-134.

Lovy, D. (1996) WinDig - Free Data Digitizer –. WinDig 2.5 file was downloaded from:

http://www.unige.ch/sciences/chifi/cpb/windig.html

Mant, A., Tourniaire, G., Diaz-Mochon, J.J., Elliott, T.J., William, A.P., Bradley, M. (2006) Polymer microarrays: Identification of substrates for phagocytosis assays. Biomaterials. 27, 5299-5306.

Masters, J.R. (2002). HeLa cells 50 years on: the good, the bad and the ugly. Nat. Rev. Cancer. 2, 315-319.

Metcalfe, A.D., Ferguson, M.W.J. (2007) Bioengineering skin using mechanisms of regeneration and repair. Biomaterials. 28, 5100-5113.

Monchaux E., Vermette, P. (2007) Bioactive Microarrays Immobilized on Low-Fouling Surfaces to Study Specific Endothelial Cell Adhesion. Biomacromolecules. 8, 3668-3673.

Notara, M., Bullet, N.A., Deshpande, P., Haddow, D.B., MacNeil, S., Daniels, J.T. (2007) Plasma polymer coated surfaces for serum-free culture of limbal epithelium for ocular surface disease. J. Mater. Sci: Mater Med. 18, 29-338.

Pernagallo, S., Unciti-Broceta, A., Díaz-Mochón, J.J., Bradley, M. (2008) Biomed. Mater. in press.

Petty, R.T., Li, H-W., Maduram, J.H., Ismagilov, R., Mrksich, M. (2007) Attachment of Cells to Islands Presenting Gradients of Adhesion Ligands. J. Am. Chem. Soc. 129, 8966-8967.

Redmond Jr., D.E., Bjugstad, K.B., Teng, Y.D., Ourednik, V., Ourednik, J., Wakeman, D.R., Parsons, X.H., Gonzalez, R., Blanchard, B.C., U. Kim, S.U., Gu, Z., Lipton, S.A., Markakis, E.A., Roth, R.H., Elsworth, J.D., Sladek, Jr., J.R., Sidman, R.L., Snyder, E.Y. (2007) Behavioral improvement in a primate Parkinson's model is associated with multiple homeostatic effects of human neural stem cells. PNAS. 3, 12175-12180.

Rosenthal, A., Macdonald, A., Voldman, J. (2007) Cell patterning chip for controlling the stem cell microenvironment. Biomaterials. 28, 3208-3216.

Rosines, E., Sampogna, R.V., Johkura, K., Vaughn, D.A., Choi, Y., Sakurai, H., Shah, M.M., Nigam, S.K. (2007) Staged in vitro reconstitution and implantation of engineered rat kidney tissue. PNAS. 104, 20938-20943.

Roth, E.A., Xu, T., Das, M., Gregory, C., Hickman, J.J., Boland, T. (2004) Inkjet printing for high-throughput cell patterning. Biomaterials. 25, 3707-3715.

Saez, A., Ghibaudo, M., Buguin, A., Silberzan, P., Ladoux, B. (2007) Rigidity-driven growth and migration of epithelial cells on microstructured anisotropic substrates. PNAS. 104, 8281-8286.

Sanjana, N.E., Fuller, S.B. (2004) A fast flexible ink-jet printing method for patterning dissociated neurons in culture. J. Neurosci. Methods. 136, 151-163.

Shin, H. (2007) Fabrication methods of an engineered microenvironment for analysis of cell–biomaterial interactions. Biomaterials. 28, 126-133.

Tan, J.L., Tien, J., Pirone, D.M., Gray, D.S., Bhadriraju, K., Chen, C.S. (2003) Cells lying on a bed of microneedles: An approach to isolate mechanical force. PNAS. 100, 1484-1489.

Tourniaire, G., Collins, J., Campbell, S., Mizomoto, H., Ogawa, S., Thaburet, J.F., Bradley, M. (2006) Polymer microarrays for cellular adhesion. Chem. Commun. 20, 2118-2120.

Tourniaire, G. Polymer Microarray-Development and Applications. PhD thesis. University of Edinburgh. 2006.

Unciti-Broceta, A., Díaz-Mochón, J.J., Mizomoto, H., Bradley, M. (2008) Combining Nebulization-Mediated Transfection and Polymer Microarrays for the Rapid Determination of Optimal Transfection Substrates. J. Comb. Chem. 10, 179-184.

Wilson, D.L., Martin, R., Hong, S., Cronin-Golomb, M., Mirkin, C.A., Kaplan, D.L. (2001) Surface organization and nanopatterning of collagen by dip-pen nanolithography. PNAS. 98, 13660-13664.

Zhang, R., Liberski, A., Khan, F., Diaz-Mochon, J.J., Bradley, M. (2008) Inkjet fabrication of hydrogel microarrays using in situ nanolitre-scale polymerisation. Chem. Commun. 11, 1317-1319.

FIGURES AND TABEL LEGEND

Scheme 1. The generation of printer files for a clock pattern followed by collagen patterning (synthetic polymers alternativly), cellular binding and substrate detaching to obtain a free-standing film with patterned cells.

Figure 1. Cell patterning via inkjet printing: (A) HeLa cells patterned in a clock shape on collagen inkjet printed onto agarose (26 mm x 26 mm). (B) Hoeshest 33342 (for nuclei staining) images of HeLa cells in a patterned "2" (Scale bar 1 mm). Images were scanned using a Nikon microscope controlled by the Pathfinder software (Imstar) using a 10x/0.30 objective and a DAPI filter. (C) Bright light image expansion showing part of the number "2" (Scale bar 0.25 mm).

Figure 2. Patterned mES-Oct4 cells on: (A) collagen patterns printed on agarose coated glass slide, fixed with formaldehyde (4% w/v) and stained with Hoescht 33245 (nuclei stain). The image (scale bar 5mm) was taken with a BioAnalyzer 4F/4S with a light scanner (LaVision Bio Tech); (B) Living mES-Oct4 cells patterned "9", on collagen inkjet printed on to an agarose layer. Images were taken with a Leica microscope using a 5x/0.12 objective, before fixing and staining (scale bar 0.5mm); (C) Fixed and stained "9" with mES-Oct4 cells (scale bar 0.5mm).

Figure 3. Patterned HeLa cells on polymeric patterns (A) poly DVB, (B) poly MTEMA , *in situ* polymerized via printing on agarose coated glass slide, fixed with formaldehyde (4% w/v) and stained with Hoescht 33245 (nuclei stain). The image (26 mm x 26 mm) was taken with a BioAnalyzer 4F/4S with a light scanner (LaVision Bio Tech) (scale bars 0.5 cm).
Living HeLa cells patterned "2" and "7", on *in situ* prepared polymers by inkjet printing on to an agarose layer, (C)-cells on poly DVB after 24h incubation,(D)-cells on poly DVB after 48h incubation,(F)- cells on poly MTEMA after 24h incubation,(G)- cells on poly MTEMA after 48h incubation. (scale bars 0.5mm). Images were taken with a Leica microscope using a 5x/0.12 objective, before fixing and staining.
Fixed and stained "2" and "7" with HeLa cells, (E)- poly DVB after 48h incubation (H)- poly MTEMA after 48h incubation. (scale bars 0.5cm) Images were taken with a Leica microscope using a 5x/0.12 and DAPI filter

Figure 4. Patterned mES-Oct4 cells on (A) poly DVB patterns printed on agarose coated glass slide, fixed with formaldehyde (4% w/v) and stained with Hoescht 33245 (nuclei stain). The image (26 mm x 26 mm) was taken with a BioAnalyzer 4F/4S with a light scanner (LaVision Bio Tech) (scale bars 0.5cm);
Living mES-Oct4 cells patterned "3", on *in situ* prepared polymers by inkjet printing on to an agarose layer. (B)-cells on poly DVB after 24h incubation,(C)-cells on poly DVB after 48h incubation, (scale bars 0.5 mm) Images were taken with a Leica microscope using a 5x/0.12 objective, before fixing and staining; (D) Fixed and stained "3" with mES-Oct4 cells, images were taken with a Leica microscope using a 5x/0.12 and DAPI filter.

Figure 5. HeLa cells growing on a collagen gradient printed on an agarose coated glass slide. The cells were stained (Hoeshest 33342) and fixed. (A). Fluorescent images were taken using a CCD–based fluorescent Bioanalyser (LaVision Biotec) with a DAPI filter. (B). Fluorescent

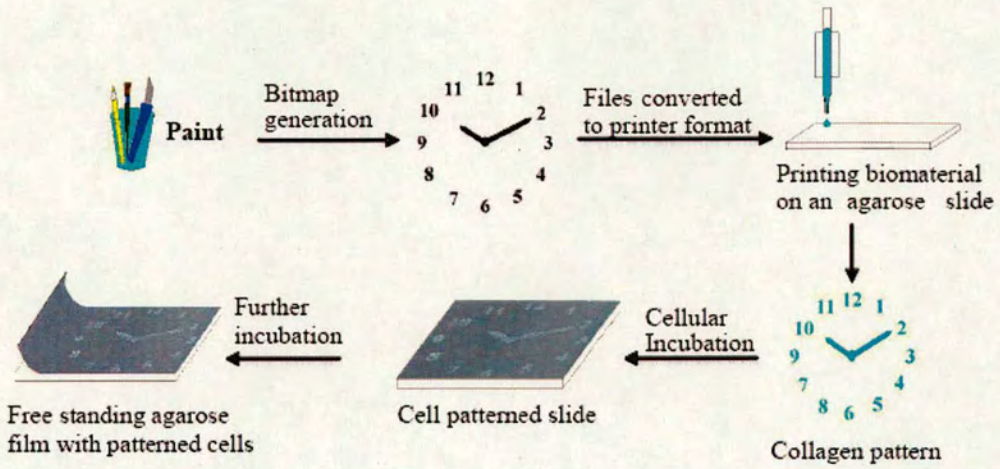

Scheme 1.

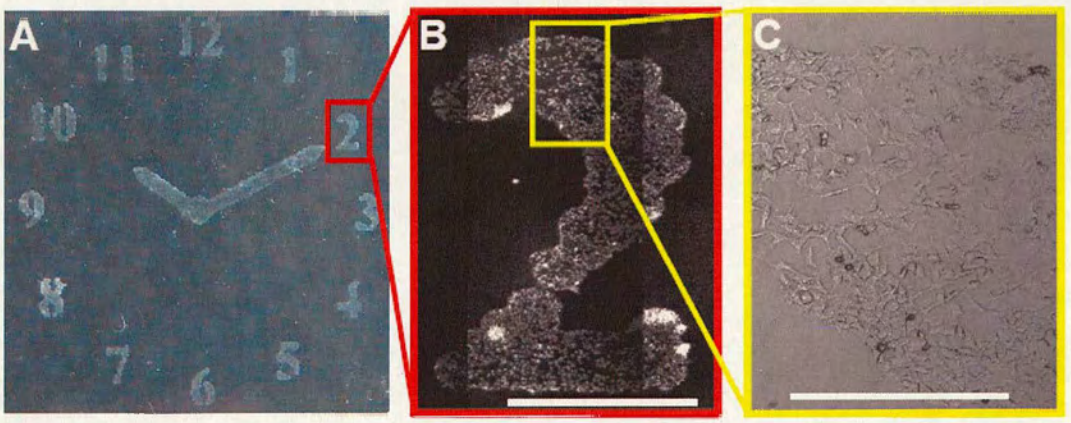

Figure 1.

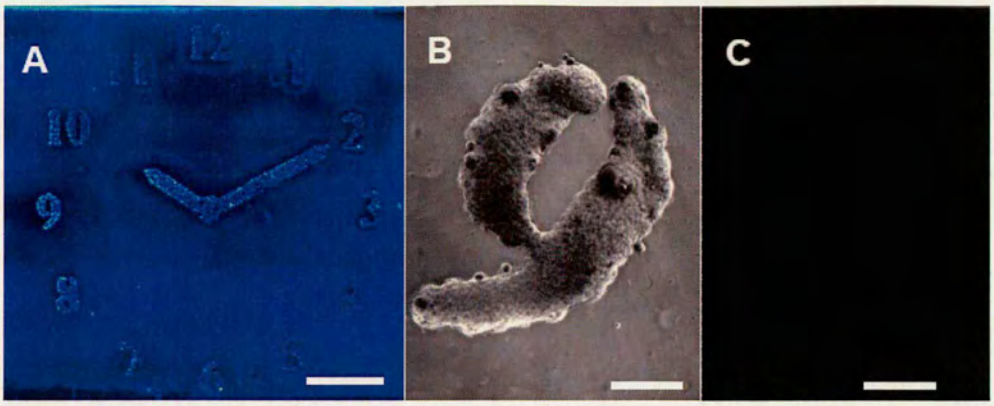

Figure 2.

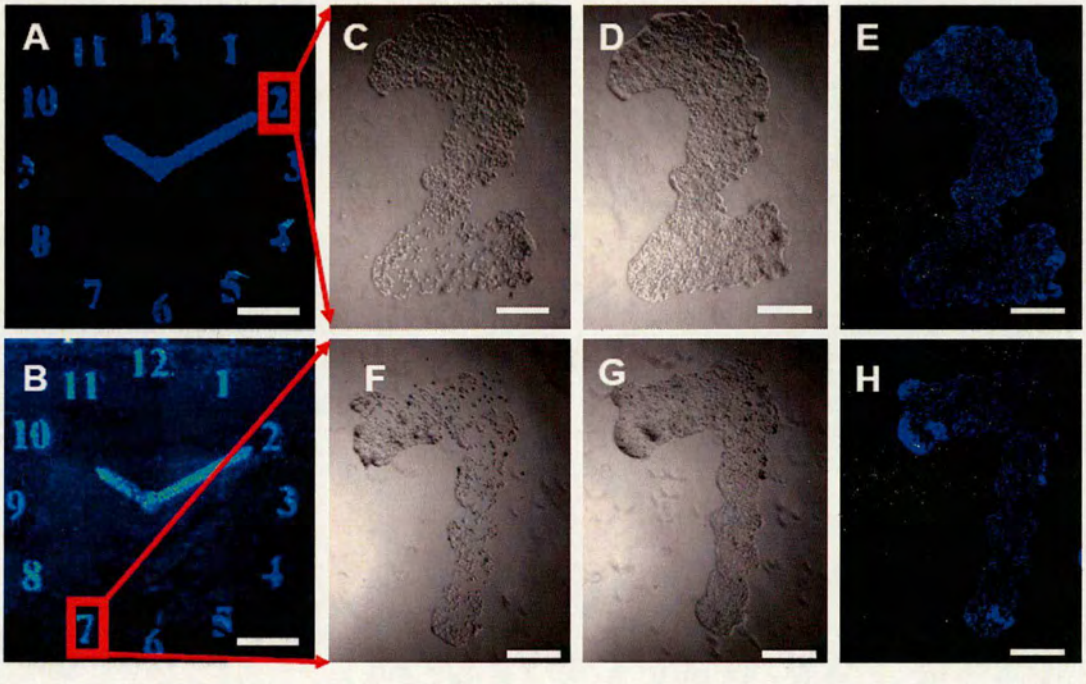

Figure 3.

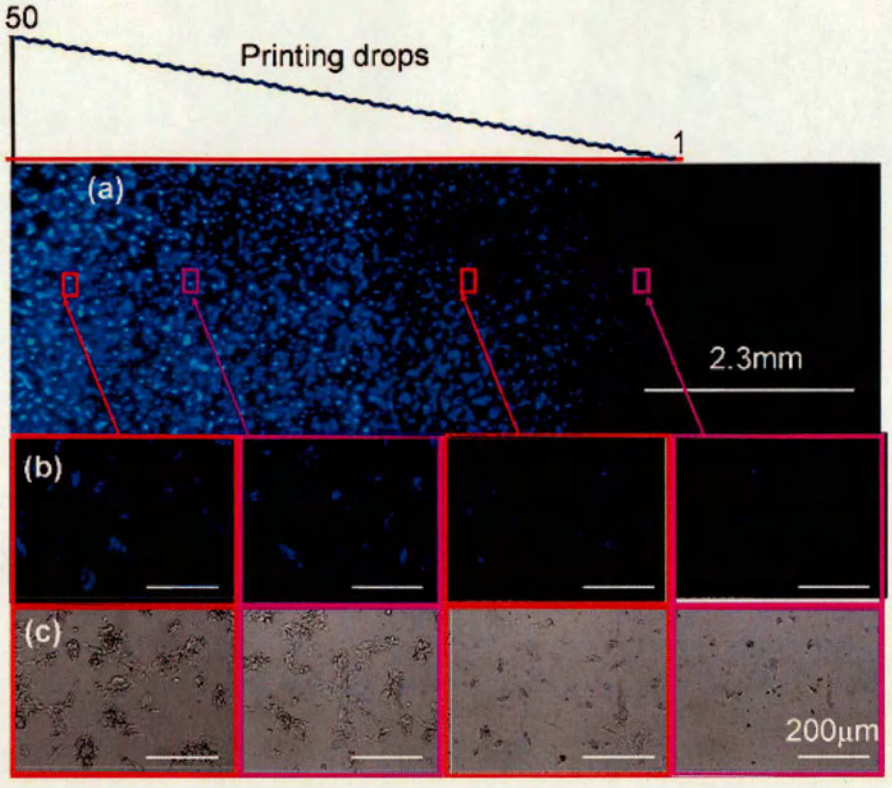

Figure 6.

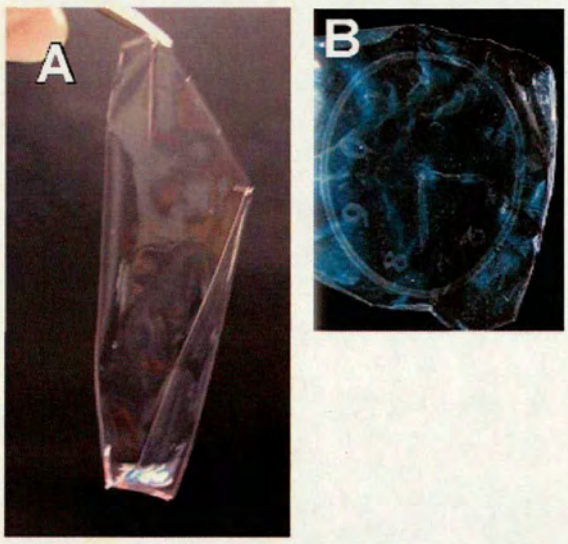

Figure 7.

Table 1.

```
#!/usr/bin/perl
#
use Cwd;
$path = cwd;

$infile = $ARGV[0];
$outfile = $ARGV[1];
open(input, "<$infile");

$nfile = 1;
open(output, ">$outfile$nfile.mmf");
$i = 0;
while ($line = <input>) {
 if ($i == 50) {
  $nfile++;
  print output "include, c:\\$outfile$nfile.mmf\n";
  close(output);
  open(output, ">$outfile$nfile.mmf");
  $i = 0;
 }
 chomp($line);
 @cart = split(/ +/, $line);
 $x = $cart[1];
 $y = $cart[2];

 $xs = sprintf("%.3f", $x);
 $ys = sprintf("%.3f", $y);

 print output "set,dis,2,$xs,$ys,37,1,1,1,1,0,3,0,1\n";
 print output "dis\n";
 $i++;
}
close(output);
close(input);
exit;
```

the application script runs on Perl5.8.8 (available at

http://www.perl.com).

Appendix II : Publications in submission

Pre-submitted to Nature (accepted 19th Nov 07, manuscript NBT-PI18100)

Submitted to Biotechniques – 26 October 2008

Exotic Cell Patterning via Laser Printing

By *Albert Liberski, Rong Zhang and Mark Bradley**

(*) Prof. M. Bradley

EaStCHEM, School of Chemistry,

King's Building, University of Edinburgh,

Edinburgh, UK EH9 3JJ.

E-mail: mark.bradley@ed.ac.uk;

Fax: 0131 650 6453

Tel: 0131 650 4820

Mr. A. Liberski and Dr. R. Zhang

EaStCHEM, School of Chemistry,

King's Building, University of Edinburgh,

Edinburgh, UK EH9 3JJ.

Word count for Abstract: 144

Word count for the body of the manuscript: 1835

KEYWORDS

Cell patterning, laser printing, heat transfer printing, mES cells, free standing cellular layers

ABSTRACT

A method for cell patterning using commonly available tools is presented. A heat-transfer printing approach has been developed for the first time for patterning cells on slides. This approach can be used to pattern any image (including microarrays) using a commercially available laser printer with the printed inks on polyethylene terephthalate (PET) sheets successfully transferred onto glass slides. It is shown that the inks could prevent the attachment of HeLa and mES cells restricting cells to areas where the glass surface intrudes, producing shapes. Importantly, mES cells growing on the patterned glass slides were induced to undergo differentiation more rapidly than those growing on non-patterned glass surfaces. The patterned cells, especially mES cells, could be detached from these slides to give a free-standing layer of cells with designed shapes which could be subsequently re-cultivated.

INTRODUCTION

Cell patterning has become a very important tool in biological research and has found a variety of applications ranging from cellular microarray development (1) to tissue engineering (2). The range of those applications includes deposition of cells in a specific part of biosensors allowing collection data about cell responses to drugs (3), substrate and microenvironment triggered stem cell differentiation (4), engineered rat kidney tissue for implantation (5), skin repair and regeneration (6), human neural stem cell implanted into monkey's brain with Pakinson's symptoms for replacement of the damaged neurons (7) and bone marrow stem cells for liver regeneration (8).

Many different techniques have been used to achieve complex cellular patterning on surfaces (9). The majority of these approaches are based on the preparation of

surfaces fabricated with materials to which cells adhere preferentially rather than other due to different factors such as surface free energy or presence of specific extracellular proteins (10). The main approaches for surface patterning include soft lithography and the preparation of a stamp (usually from polydimethylsiloxane) to deliver cell binding materials onto a surface (11); photolithography (12); dip-pen nanolithography for higher resolution patterning using a AFM tip (13) and inkjet printing to deliver biomaterials (14) or cells (15) onto an appropriate surface using a modified office based inkjet printer (16). However, these techniques need special equipments and are time consuming, expensive and applicable to small surfaces. Recently, transfer printing methods were applied to the preparation of microelectronic devices using elastomeric stamps to transfer semiconductor materials to substrates to form the required microdevice (17-19). Heat transfer is a printing technique for printing coloured images onto variety of substrates, such as T-shirts, caps, bags, ski boards, etc. The advantages of this printing approach are its practicality, its efficient, cheapness and most importantly its scalability. In this paper we report a related approach for fabricating surfaces for patterning mammalian cells , including mouse embryonic stem (mES) cells, derived from the heat transfer printing method allowing generation of any desired pattern for cells on a 2D surface (e.g. glass or polystyrene).

MATERIALS AND METHODES

PET film - A4 Colour Laser Transparencies (210×297 mm) from Supplies Team ® (West Yorkshire UK). Four rectangular well-plates made from PS with non-treated surface and a volume of 22 ml/well from Nunc (Langenselbold, GE).

All other materials were purchased from Sigma-Aldrich.

Mouse embryonic stem cell (mES-Oct4) were kindly provided by Dr Josh Brickman, Institute for Stem Cell Research (ISCR), University of Edinburgh.

Glass slide patterning

Negative patterns and images (see Scheme 1[A])were printed on PET transparencies at 600dpi using an HP Color LaserJet 4600DN with a yellow print cartridge C9722A (see Scheme 1[B]).

PET sheets (10×26 mm) with printed images or patterns (see Scheme 1[C]) were placed face down onto a microscope glass slides, heated at 175°C for 2 min and pressed using a metal stripe to ensure good contact between the foil sheet and the glass slide. The foil was peeled off and the slides annealed for 10 min at 200 °C to give the "masked" glass slides (Figure SI-1 shows the difference between the printed images before and after the annealing).

Cell cultivation and staining

HeLa cells were grown in RPMI 1640 growth medium, supplemented with heat inactivated fetal calf serum 10% v/v, penicillin (100 units/mL), streptomycin (100mg/mL) and L-glutamine (4.0mM) at 37 °C with 5% CO_2 (Gibco). mES cells were grown using GMEM growth medium supplemented with heat inactivated fetal calf serum 10% v/v, penicillin (100units/mL), streptomycin (100units/mL) and L-glutamine (2.0mM), Sodium pyruvate (2.0mM), 2-mercaptoethanol (0.1mM), LIF (0.18 units/mL), puromycin (1μg/mL). The patterned slides were placed into a 4-rectangular well-plate and sterilized for 20 min under UV irradiation prior to the addition of cells ($7x10^5$ cells per slide with 7mL of complete media) into the well-plate and incubation. Media was changed every 24h.

Cells staining and fixing

Medium in the well plate was removed and the slides with PBS three times. Cells were fixed using paraformaldehyde (4%w/v in PBS) for 30 min, stained using Hoechst 33342 (0.50 µg/ml) for 15 min and washed with distilled water.

Visualisation of patterned slides

Patterned fixed cells were analysed using a Nikon microscope controlled by Pathfinder (Imstar, France) using a 10x/0.30 objective and a DAPI filter set. Bright field phase images were taken using the same microscope.

The microscope imaged areas (1234µm×943µm) were combined to give a mosaic of the whole slide. Cell numbers were determined automatically using the Pathfinder™ software. Living cell images were taken with a Leica microscope using a 5x/0.12 objective. Overviews of the slides were performed using a BioAnalizer 4F/4S white light scanner using a DAPI filter.

Flow Cytometry

mES-Oct4 GFP cells were analyzed on a flow cytometer (FACSAria (BD Biosciences and analyzed using the FACSDiva software with a total of 100,000 events per sample). Stem cells were washed in PBS, harvested via trypsination and resuspended in 300 µL of GMEM media. The cell pellet was collected via centrifugation (1200 rpm, 4 minutes) and resuspended in PBS with 2% FBS. Cell samples were excited with a 488nm (Coherent® Sapphire™ solid state) laser and a 530/30 nm (Fluorescein) filter was used for fluorescence analysis of the cellular population. mES-Oct4 GFP cells cultivated on tissue culture plastic and cells cultivated on standard glass slides were used as controls. That control was used to demonstrate the impact of the patterned substrate on the attached mES-Oct4 cells.

RESULTS AND DISCUSSION

Whatever pattern was desired (see Scheme 1[A]) was printed onto an A4 sheet of PET using a standard office based laser printer (see Scheme 1[B]). In this study, all the patterns were printed as non-transparency images to ensure sufficient toner was printed onto the PET to enable transfer. After printing, the image on the PET sheet was transferred onto the glass slide by heating the slides to 175 °C (see Scheme 1[C,D]). Toners with different colours such as black, yellow, blue and red could all be used. Of importance here was that the main components of the laser printer toner were a styrene acrylate copolymer (75-85% wt), wax (5-10%wt) and pigment (1-5%wt) (20), which are neither soluble in water or aqueous medium after printing nor show toxic effects when the printed images are incubated with cells.

The reason of the heated toner can be transferred to glass slides could be explained according to the study on the offset printing (21). At about 175°C, the distance between the molecules of the melted toner and the glass slide becomes very close (~10Å), which generates much stronger adhesion strength than the splitting force of the melted toner. Therefore the toner on the PET could be readily transferred onto the glass surface.

To demonstrate the flexibility of this approach, images of clock faces were printed onto glass slides, followed by cellular incubation. It was found that the inks could prevent the attachment of HeLa and mES cells restricting cells to these areas where the glass surface intrudes; producing shapes (Figure 1 and SI-2 for mES cell patterned clock). Figure 1A is an image of transfer printed clock face on a glass slide using yellow toner. The slide was then incubated with mES-Oct4 GFP cells (700,000 cells per slide) after sterilizing with UV light and the living cells images were taken using a

microscope to monitor the changes over time following seeding (Figure 1B). The images taken after 24,48 and 72 hours incubation showed that the cells attached and spread only on the glass surface intrudes the patterned area.

In the case of HeLa cells the slide with attached cells were fixed and stained and fluorescently imaged after 48h incubation. The result are shown in Figure 1C. The expanded arrow of the cell patterned clock indicates that the cells were successfully restricted to the unmasked glass surface (Figure 1D) and displayed a healthy morphology (Figure 1E).

The printed images kept their shape without significant distortion when the dimensions of the features such as cycles, triangles or squares were more than 300μm in diameter (See Figure SI- 3). Figure 2 shows two examples of patterned HeLa cells on printed glass slide using this approach with dimension of about 500μm, which could be very useful for drug discovery (22) and cell co-culture research.(23). However, lines with a width down to 25μm were also printed, which could allow single cell to grow and spread along the direction of the lines (Figure 3).

The patterned cells could be easily detached from the glass after 72h incubation forming shaped stem cell continuums, perhaps could be used in tissue engineering applications (Figure 4, Figure SI-4 and Scheme SI-1). The cell film was then moved to a Petri-dish and incubated for another 24h showing that the stem cells were still alive and healthy (Fig SI-4C).

To demonstrate the impact of the patterned substrate on the attached mES-Oct4 cells, the cells were harvested after 72 hours incubation and analysed by flow cytometery (Table 1). mES-Oct4 cells only express green fluorescent protein when they are undifferentiated. FACS analysis indicated that more mES-Oct4 cells incubated on the

patterned substrate were differentiated in comparison to cells incubated on the normal glass slide.

Cultivation condition	**cells/cm^2** [a]	Undifferentiated cells (%)	S.D. n=4
TCP, gelatine, LIF Puromycin[b] (control)	**22,000**	76.5	±9.7
Glass microscope slide (not masked)	**36,000**	42.8	±7.9
Patterned glas slide	**219,000**	26.2	±2.4
Patterned glas slide	**36,000**	36.8	±2.6

Notes: a) Average number of cells seeded into a container over the cytophilic surface area. b) TCP is the tissue culture plastic flask. Gelatine, LIF and puromycin are factors to prevent mES cell from differentiation.

Table 1 FACS data of the differentiation of mES cells under different conditions (See Experimental part Figure SI-5 for original FACS plots)

In conclusion a heat-transfer printing approach has been developed for patterning cells on glass slides. This approach could pattern any image using a commercially available laser printer. The printed inks on PET sheet were successfully transferred onto glass slides and applied for cellular patterning. It was found that the inks prevented attachment of HeLa and mES cells so that these cells were restricted into the shapes with only glass surfaces. Importantly, mES-Oct4 cells growing within the patterned glass slides were induced to differentiated state quicker than those growing on non-patterned glass surface. The patterned cells especially mES cells could be easily detached from these slides to form a free-standing layer of cells with special shapes which could be very useful in tissue engineering.

ACKNOWLEDGMENTS

We thank Ilika Technologies and the EPSRC for funding.

COMPETING INTERESTS STATEMENT

The authors declare no competing interests.

REFERENCES

1. **Baird, I.S., A.Y. Yau, and B.K. Mann.** 2008. Mammalian cell-seeded hydrogel microarrays printed via dip-pin technology. BioTechniques *44*:249-256.

2. **Khademhosseini, A., R. Langer, J. Borenstein, and J.P. Vacanti.** 2006. Microscale technologies for tissue engineering and biology. PNAS *103*:2480-2487.

3. **Asphahani, F., and M. Zhang.** 2007. Cellular impedance biosensors for drug screening and toxin detection. Analyst *132*:835-841.

4. **Gerecht, S., J.A. Burdick, L.S. Ferreira, S.A. Townsend, and R. Langer.** 2007. Hyaluronic acid hydrogel for controlled self-renewal and differentiation of human embryonic stem cells. PNAS *104*:11298-11303.

5. **Rosines, E., R.V. Sampogna, K. Johkura, D.A. Vaughn, Y. Choi, H. Sakurai, M. M. Shah, and S.K. Nigam.** 2007. Staged in vitro reconstitution and implantation of engineered rat kidney tissue. PNAS *104*:20938-20943.

6. **Metcalfe, A.D., and M.W.J. Ferguson**. 2007. Bioengineering skin using mechanisms of regeneration and repair. Biomaterials *28:*5100-5113.

7. **Redmond, D.E., K.B. Bjugstad, Y.D. Teng, V. Ourednik, J. Ourednik, D.R. Wakeman, X.H. Parsons, R. Gonzalez, et al.** 2007. Behavioral improvement in a primate Parkinson's model is associated with multiple homeostatic effects of human neural stem cells. PNAS *3*:12175-12180.

8. **Furst, G., J.S.A. Esch, L.W. Poll, S.B. Hosch, L.B. Fritz, M. Klein, E. Godehardt, A. Krieg, et al.** 2007. Portal Vein Embolization and Autologous CD133+ Bone Marrow Stem Cells for Liver Regeneration: Initial Experience. Radiology *243*:171-179.

9. **Falconnet, D., G. Csucs, H.M. Grandin, and M. Textor.** 2006. Surface engineering approaches to micropattern surfaces for cell-based assays. Biomaterials *27*:3044-3063.

10. **Bao, S., and R. Cagan.** 2005. Preferential Adhesion Mediated by Hibris and Roughest Regulates Morphogenesis and Patterning in the *Drosophila* Eye. Develop. Cell 8:925-935.

11. **Co, C.C., Y.Wang, and C. Ho.** 2005. Biocompatible Micropatterning of Two Different Cell Types. J. Am. Chem. Soc. *127*:1598-1599.

12. **Liu, V.A., W.E. Jastromb, and S.N. Bhatia.** 2002. Engineering protein and cell adhesivity using PEO-terminated triblock polymers. J. Biomed. Mater Res. *60*:126-134.

13. **Lee, K., S. Park, C. Mirkin, J.C. Smith, and M. Mrksich.** 2002. Protein Nanoarrays Generated By Dip-Pen Nanolithography. Science *295*:1702.

14. **Campbell, P.G., E.D. Miller, G.W. Fisher, L.M. Walker, and L.E. Weiss.** 2005. Engineered spatial patterns of FGF-2 immobilized on fibrin direct cell organization. Biomaterials *26*:6762-6770.

15. **Calvert, P.** 2007. Printing Cells. Science. *318*:208-209.

16. **Xu, T., J. Jin, C. Gregory, J. J. Hickman and T. Boland.** 2005. Inkjet printing of viable mammalian cells. Biomaterials .*26*:93-99.

17. **Meitl, M.A., Z.-T. Zhu, V. Kumar, K.J. Lee, X. Feng, Y.Y. Huang, I. Adesinda, R.G. Nuzzo, and J. A. Rogers.** 2006. Transfer printing by kinetic control of adhesion to an elastomeric stamp. Nat. Mater. *5*:33-38.

18. **Ahn, J.-H., H.-S. Kim, K.J. Lee, S. Jeon, S.J. Kang, Y. Sun, R.G. Nuzzo, and J.A. Rogers.** 2006. Heterogeneous Three-Dimensional Electronics by Use of Printed Semiconductor Nanomaterials. Science *314*:1754-1757.

19. **Fan, Z., J.C. Ho, Z.A. Jacobson, R. Yerushalmi, R.L. Alley, H. Razavi, and A. Javey.** 2008. Wafer-Scale Assembly of Highly Ordered Semiconductor Nanowire Arrays by Contact Printing. Nano Lett. *8*:20-25.

20. Hp material safety data sheet.

21. **Liu F., and W. Shen.** 2008. Forced wetting and dewetting of liquids on solid surfaces and their roles in offset printing. Coll. Surf. A: Physicochem. Eng. Aspects. *316*:62-69.

22. **Castel, D., A. Pitaval, M.-A. Debily, and X. Gidrol.** 2006. Cell microarrays in drug discovery. Drug Discovery Today *11*:616-622.

23. **Barrett, D.G., and M.N. Yousaf.** 2007. Rapid Patterning of Cells and Cell Co-Cultures on Surfaces with Spatial and Temporal Control through Centrifugation. Angew. Chem. Int. Ed. *46*:7437-7439.

FIGURES AND SCHEME

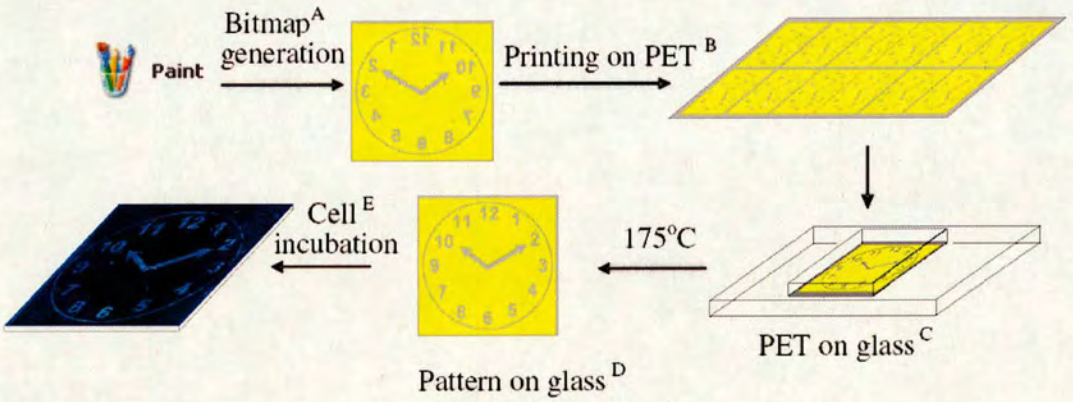

Notes: (A) Image ("clock face" as an example) is the negative of final cellular patterns; (B) Image was printed on transparencies (PET) via laser printer; (C) Image on PET sheet was placed (face down) onto the glass slide; (D) During the heating toner deposited on PET was transferred to glass (heat transfer); (E) Cells incubation on so patterned glass slides results in cellular patterns placed within uncovered glass.

Scheme 1. Cellular Patterning via laser printing.

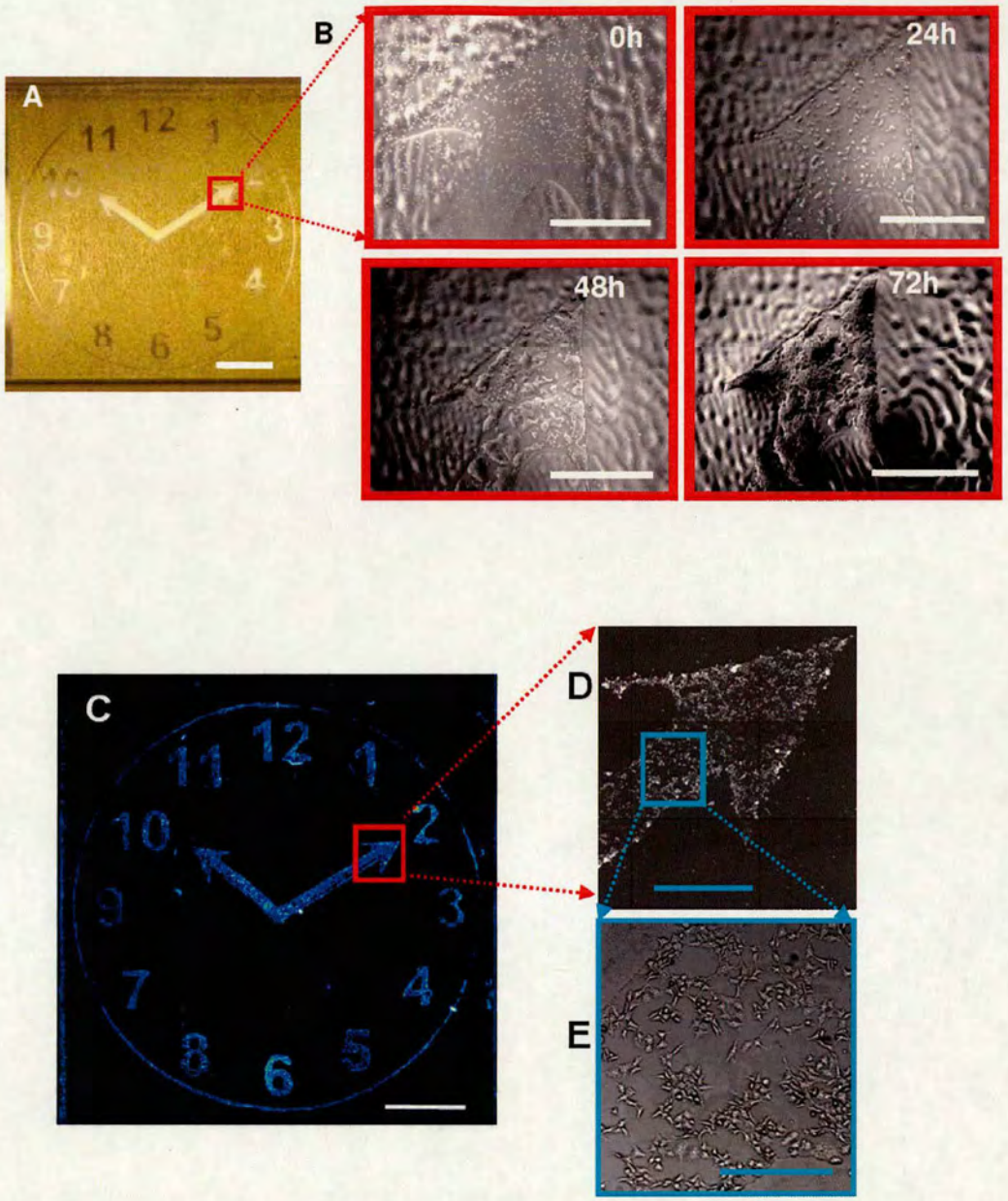

Figure1. mES-Oct4 GFP cell and HeLa cells patterning. (A) An image of clock face before cell incubation, (scale bar 5mm); (B) Image of living mES-Oct4 GFP cell on the "clock hand" taken with a Leica microscope using a 5×/0.12 objective after cells seeding for 0, 24, 48 and 72 hours incubation (scale bars 1mm); (C) A fluorescent

(Bioanalyser -LaVision Biotec) with a DAPI filter (scale bar 5mm); (D) Fluorescent image of the expanded "clock hand" from the cell patterned clock scanned using a Nikon microscope with a 10×/0.30 objective and a DAPI filter set (scale bar 1mm); (E) Bright light image of a further expanded area with 20×0.30 objective (scale bars 250 µm).

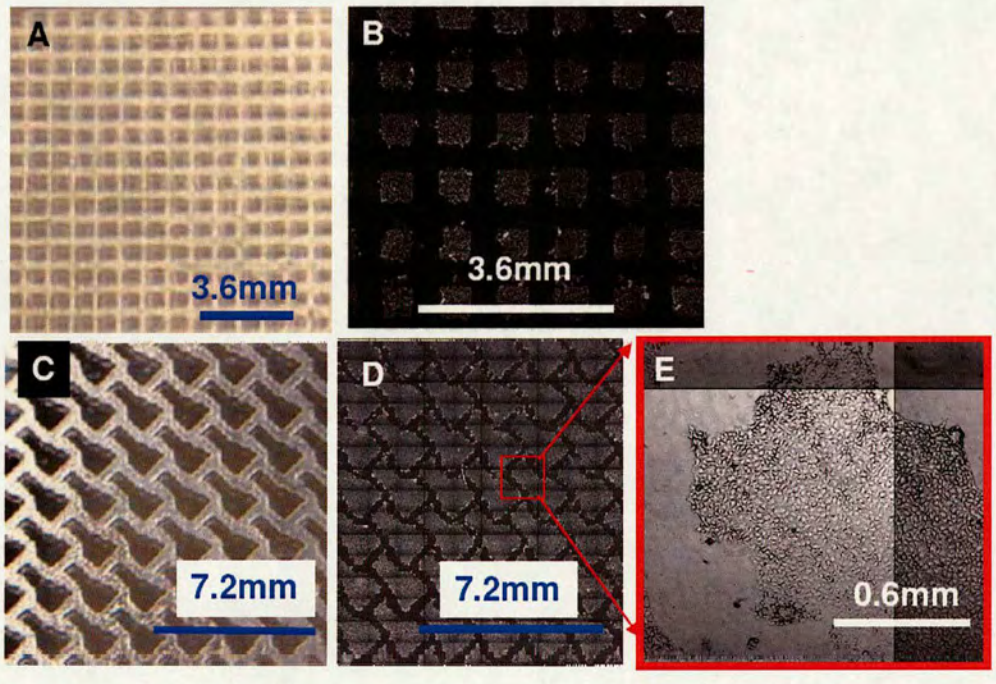

Figure 2 (A) and (C) Heat-transfer printed features arrays; (B) and (D) images of HeLa cells growing on the unmasked glasses surface, scanned using a Nikon microscope using a 10×/0.30 objective and a DAPI filter set. (E) Magnification of array with HeLa cells after 24h incubation.

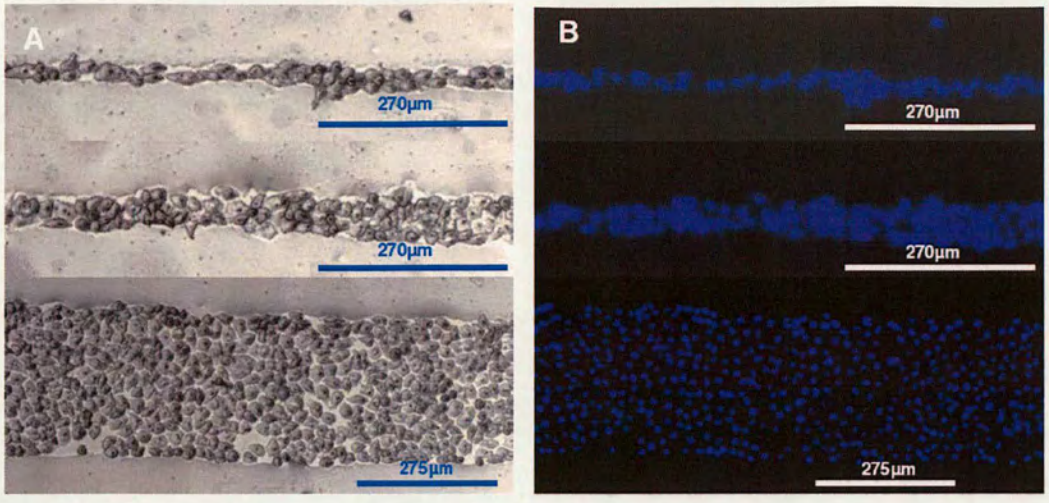

Figure 3 HeLa cells patterned on lines. (A) bright light images and (B) fluorescent images taken using a Leica microscope with 10×/0.30 objective.

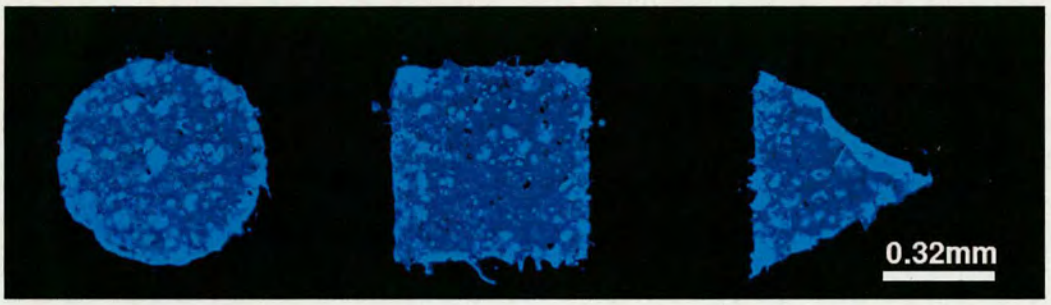

Figure 4 Various images of "mES-Oct4 GFP cell continuums" on a heat-transfer patterned microscope glass slide after 72h incubation, scanned using a BioAnalizer 4F/4S white light scanner using the DAPI filter.

Appendix III: List of Presentations

Oral presentations:

- Advan. in Microarray Technology 1 st-3 th November 2006, Amsterdam (NL).
- Ilika project meeting, 1st March 2007, Southampton (UK).
- Ilika project meeting, 5th April 2008, Southampton (UK).
- Chemistry Innovation 3 th September 2008, Leicester (UK).
- Bradley group presentation, 6th August 2005, Edinburgh (UK).
- Bradley group presentation, 12th March 2006, Edinburgh (UK).
- Bradley group presentation, 16th April 2007, Edinburgh (UK).
- Bradley group presentation, 26th February 2008, Edinburgh (UK).
- Postgraduate Research Seminars 3th October 2006, Edinburgh (UK).
- Postgraduate Research Seminars 11th November2007, Edinburgh (UK).
- Institute of Stem Cell Research (ISCR), 2nd March 2008, Edinburgh (UK).

Appendix IV: Posters 28 May 2008 – Sunday, 1 June 2008

- 8th World Biomaterials Congress, 28th May 2008, Amsterdam (NL).

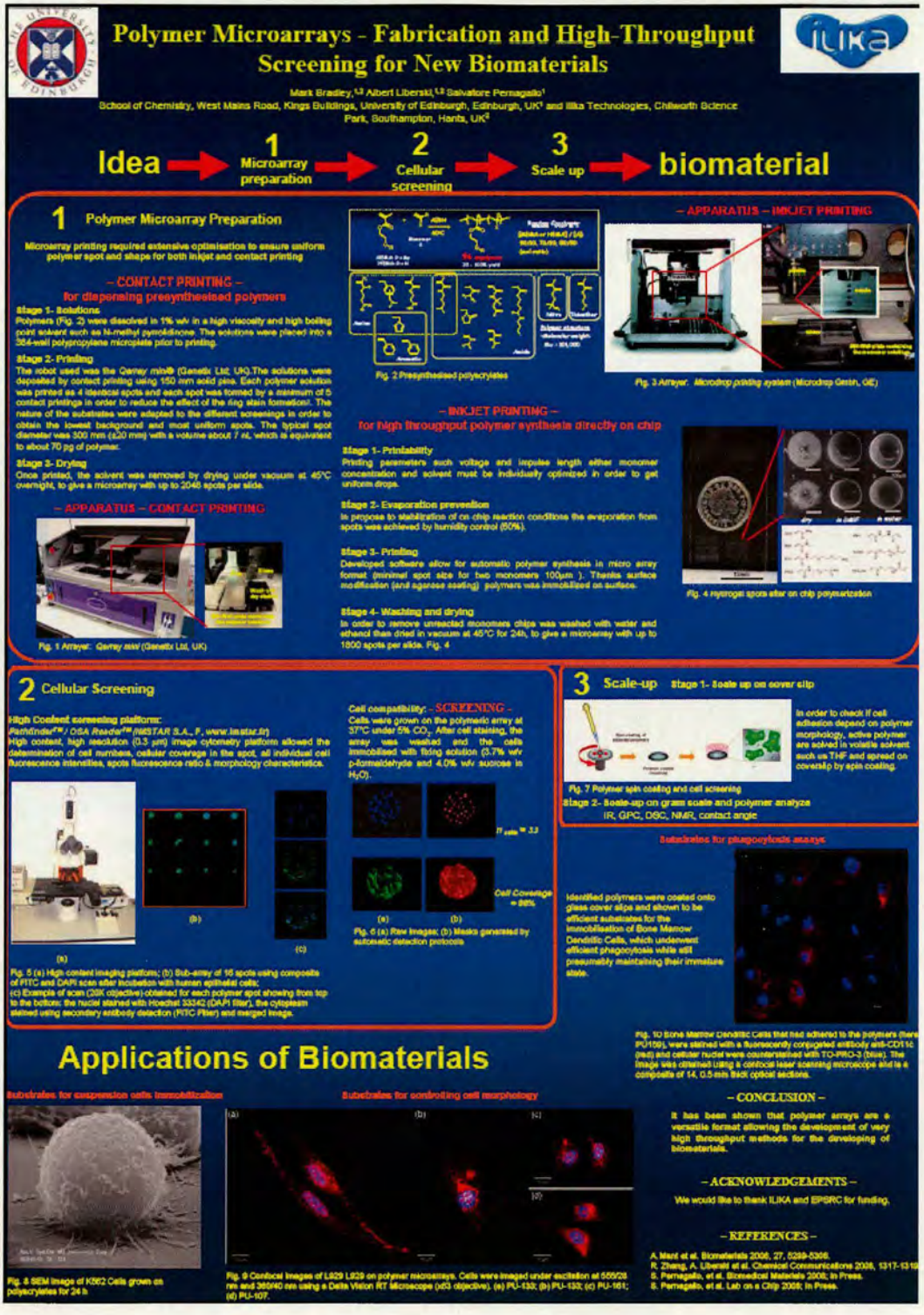

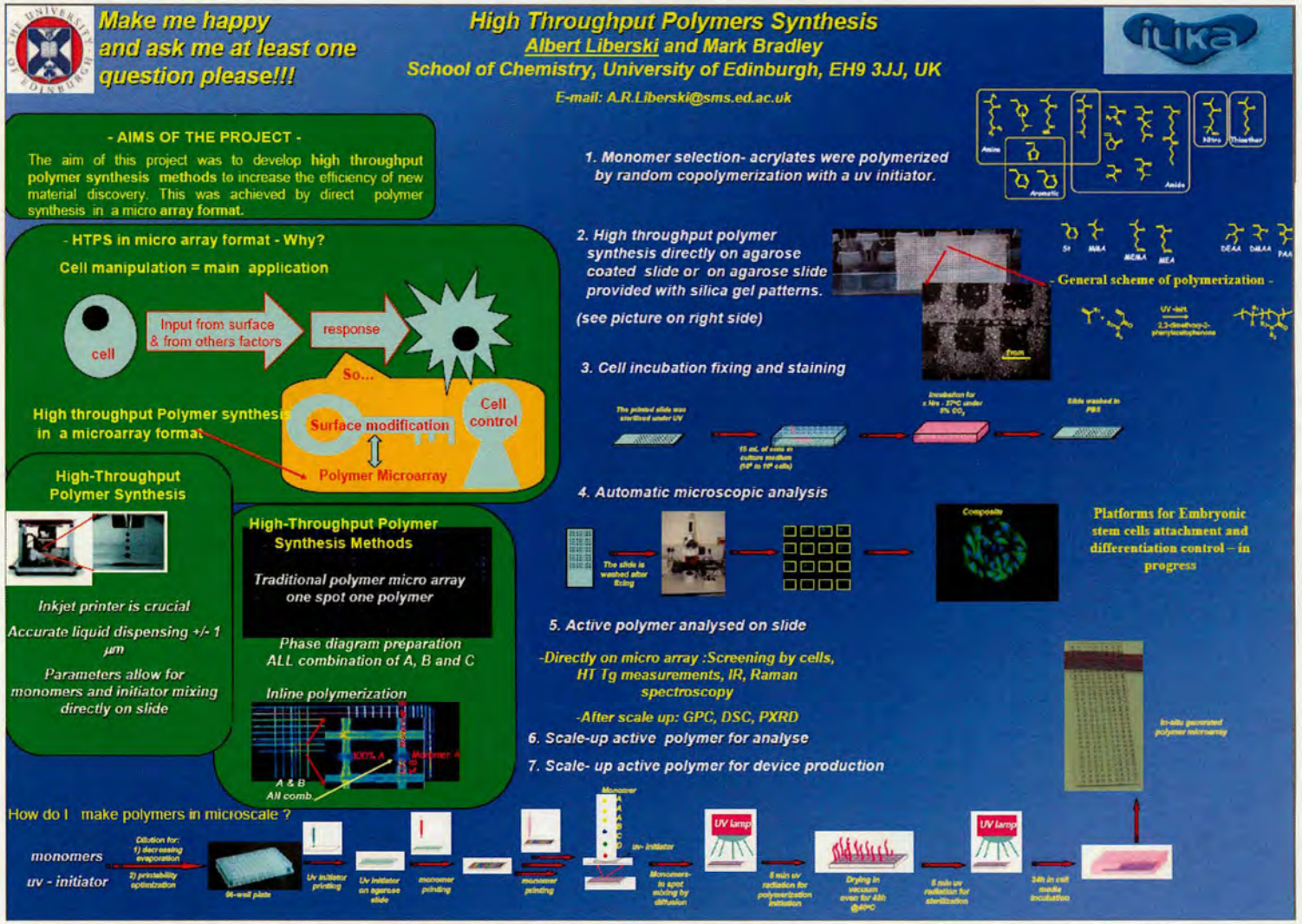
Make me happy and ask me at least one question please!!!
High Throughput Polymers Synthesis
Albert Liberski and Mark Bradley
School of Chemistry, University of Edinburgh, EH9 3JJ, UK
E-mail: A.R.Liberski@sms.ed.ac.uk
- AIMS OF THE PROJECT -
The aim of this project was to develop high throughput polymer synthesis methods to increase the efficiency of new material discovery. This was achieved by direct polymer synthesis in a micro array format.
- HTPS in micro array format - Why?
Cell manipulation = main application
cell
Input from surface & from others factors
response
So...
Surface modification
Cell control
Polymer Microarray
High throughput Polymer synthesis in a microarray format
High-Throughput Polymer Synthesis
Inkjet printer is crucial
Accurate liquid dispensing +/- 1 μm
Parameters allow for monomers and initiator mixing directly on slide
High-Throughput Polymer Synthesis Methods
Traditional polymer micro array one spot one polymer
Phase diagram preparation ALL combination of A, B and C
Inline polymerization
How do I make polymers in microscale ?
monomers
uv - initiator
1. Monomer selection- acrylates were polymerized by random copolymerization with a uv initiator.
2. High throughput polymer synthesis directly on agarose coated slide or on agarose slide provided with silica gel patterns.
(see picture on right side)
- General scheme of polymerization -
3. Cell incubation fixing and staining
4. Automatic microscopic analysis
Platforms for Embryonic stem cells attachment and differentiation control – in progress
5. Active polymer analysed on slide
-Directly on micro array :Screening by cells, HT Tg measurements, IR, Raman spectroscopy
-After scale up: GPC, DSC, PXRD
6. Scale-up active polymer for analyse
7. Scale- up active polymer for device production